VÂNIA SOFIA SERRÃO DE SOUSA

DEVELOPMENT OF DRINKING WATER TREATMENT PROCESSES FOR NANOPARTICLES REMOVAL

UAlg FCT
UNIVERSIDADE DO ALGARVE
FACULDADE DE CIÊNCIAS E TECNOLOGIA

2019

VÂNIA SOFIA SERRÃO DE SOUSA

DEVELOPMENT OF DRINKING WATER TREATMENT PROCESSES FOR NANOPARTICLES REMOVAL

Doutoramento em Ciências do Mar, da Terra e do Ambiente

Ramo Ciências e Tecnologias do Ambiente

Especialidade em Gestão de Água

Trabalho realizado sob a orientação da

Professora Doutora Maria Margarida da Cruz Godinho Ribau Teixeira

UAlg FCT
UNIVERSIDADE DO ALGARVE
FACULDADE DE CIÊNCIAS E TECNOLOGIA

2019

Declaração de autoria de trabalho

DEVELOPMENT OF DRINKING WATER TREATMENT PROCESSES FOR NANOPARTICLES REMOVAL

Declaro ser a autora deste trabalho, que é original e inédito. Autores e trabalhos consultados estão devidamente citados no texto e constam da listagem de referências incluída.

_____

This thesis was supported by

PhD Grant (SFRH/BD/100402/2014) from the Portuguese Foundation of Science and Technology, trough the *European Social Found* from European Union.

CENSE – Center for Environmental and Sustainability Research which financed by national funds FCT/MCTES (UID/AMB/04085/2019).

Para a minha avó Isaura

Acknowledgments

I would like to gratefully acknowledge my supervisor Professor Margarida Ribau Teixeira for giving me constant encouragement, support and unabridged availability, and especially for always listening my ideas, even when they are a little “out of the box”. During these years her scientific advisement was crucial, with fruitful ideas and suggestions, productive discussions and high standards set for my work.

I also want to address special thanks to Professor Maria João Bebianno for her support and the availability of the laboratory and equipment whenever necessary, to Professor Ana Costa for the kind assistance on several chemical materials characterisation and to Professor Luís Nunes for the precious knowledge on the statistical and modelling fields.

Special thanks are also addressed to my former colleague Claudia Corniuc for the contribution to this thesis labwork, to Paulo Pedro for the uncountable AAS analyses performed, crucial to this thesis, to Filomena Rita for all the laboratory help and support, and also to Paula Caboz for the precious support with all the paperwork.

I also express my sincere acknowledgments to Águas do Algarve, S.A., in particular to Helena Lucas, Rui Sancho, Rosário Coelho, Rita Batista and Isabel de Sousa and to Águas do Alentejo, S.A. in particular to Olga Martins.

To my closest friends a special thanks all the moments shared together.

Finally, I am very grateful to my entire family, specially my parents Irene and José and grandparents Isaura (*in memoriam*) and Hermínio for the unconditional love and support. To my husband, Ricardo, a very special thanks for always believe in me, supporting every single step in my professional journey and for those long days at the laboratory. As also, for all the support, patience, dedication and, especially, love during this emotional ride.

ABSTRACT

The ability of drinking water treatments (DWT) to remove ENPs from water is crucial to ensure the safety of public water supply. This thesis assessed the removal of three commercial metal-based nanoparticles, titanium dioxide (TiO_2), silver (Ag) and copper oxide (CuO) in DWT, exploring and comparing the potential of conventional and advanced processes. To understand the removal mechanisms, individual ENPs and mixtures of the three ENPs, dispersed in synthesised and natural surface waters were used. Conventional coagulation/ flocculation/ sedimentation (C/F/S) process alone and enhanced with powdered activated carbon (PAC) were studied, and the advanced membrane filtration processes, ultrafiltration (UF) and nanofiltration (NF), were integrated with conventional C/F/S (hybrid water treatment) or used alone (NF). These technologies were evaluated under typical DWT operational conditions. Overall, results show that optimised treatments are able to remove ENPs, without hampering other DWT target compounds. Residual turbidity, dissolved organic carbon, specific UV absorbance and aluminium were below the guidelines and similar to those found in actual DWTP. C/F/S removed 93% and 98% of the tested ENPs, depending on water characteristics. C/F/S+PAC and C/F/F→UF treatments improved the removal of single and multiple ENPs in approximately 10% compared with C/F/S alone, with Ti and Cu undetected in the C/F/S→UF treated water. However, due to AgNPs dissolution, residual Ag concentrations were present in the C/F/S→UF treated water. Using NF, the dissolved Ag was eliminated from treated water to undetectable values (depending on water characteristics). The main mechanisms responsible for the removal were charge neutralisation (C/F/S), size exclusion (UF and NF), adsorption and complexation with salts and adsorption on NOM (PAC and NF). This study contributes to the advancement of knowledge on the removal of emerging contaminants from drinking water, demonstrating that the processes optimisation for the ENPs removal is a key factor to ensure safe water, reducing the potential hazards associated to the ingestion of these contaminants and meeting the drinking water quality guidelines.

Keywords: Engineered nanoparticles, surface water, drinking water treatment, metal-based, conventional water treatment, advanced water treatment.

RESUMO ALARGADO

A capacidade de controlar e manipular a forma e o tamanho de estruturas à escala nanométrica veio revolucionar diversas áreas industriais, possibilitando a criação de produtos adaptáveis, mais eficientes e de baixo custo através da integração de nanomateriais manufaturados, especialmente nanopartículas (NPs). Contudo, o crescimento exponencial de produtos do quotidiano contendo NPs leva à introdução destas nanoestruturas no meio aquático, originando potenciais riscos toxicológicos tanto para o ambiente como para a saúde humana. As características intrínsecas das NPs, tais como tamanho reduzido, forma variada, área superficial elevada, assim como as suas capacidades de agregação e dissolução, proporcionam uma maior reatividade, podendo ampliar o seu efeito tóxico e tornando-as responsáveis por efeitos nocivos nos organismos vivos.

A introdução de NPs manufaturadas em águas superficiais utilizadas para a produção de água para consumo apresenta um elevado risco para a saúde humana, uma vez que pode levar à exposição direta às NPs através da ingestão de água contaminada. A ingestão de NPs pode causar efeitos adversos à saúde humana, tais como problemas renais, inflamações gastrointestinais, implicações ao nível do sistema neurológico e doenças cancerígenas. Embora ainda existam algumas dúvidas relacionadas com a toxicidade destas nanoestruturas, algumas NPs já foram identificadas como tóxicas para a saúde humana, nomeadamente as de origem metálica, onde se incluem as NPs de TiO_2, Ag e CuO. Atualmente, já foram detetadas NPs em águas superficiais, águas para consumo humano e em água da torneira com concentrações entre os ng/L e os µg/L.

Embora o tratamento de água seja uma das principais estratégias para evitar a exposição humana às NPs através da ingestão, os poucos estudos existentes descrevem os tratamentos convencionais como sendo ineficientes na sua remoção. Estes estudos, para além de mostrarem uma elevada variabilidade nas eficiências de remoção, foram maioritariamente realizados usando elevadas concentrações de NPs dispersas em água ultrapura, da torneira ou soluções sintéticas, sem considerarem a complexidade das águas superficiais naturais.

Assim sendo, este trabalho pretendeu estudar a capacidade dos tratamentos de água convencionais e avançados para remover nanopartículas de águas superficiais. Para tal, a remoção de NPs de origem metálica foi explorada e avaliada usando diversas estratégias de tratamento, de modo a garantir uma eficiente remoção de NPs e de iões provenientes da sua dissolução. Os tratamentos propostos tiveram também por base a minimização do impacte da

requalificação das estações de tratamento de águas para consumo humano recuperando os processos mais utilizados na produção de água potável. Para os ensaios foram escolhidas nanopartículas manufaturadas disponíveis comercialmente, TiO_2, Ag e CuO, com base na sua elevada produção e aplicação em produtos do quotidiano. De modo a compreender os mecanismos de remoção, as NPs foram usadas individualmente e em conjunto dispersas em águas sintéticas (águas modelo) e águas naturais provenientes de barragens (Alentejo e Algarve) atualmente utilizadas para a produção de água para consumo humano. Em todas as opções de tratamento estudadas, os processos foram sempre otimizados tendo em vista a maximização da remoção das NPs, aplicando condições operacionais típicas em contexto real de tratamento de água. O tipo e doses de coagulante e carvão ativado testados são também usados em contexto real. O tratamento convencional coagulação/floculação/sedimentação (C/F/S) demonstrou ter capacidade para remover NPs, tanto em águas sintéticas como naturais, utilizando um coagulante polimérico de alumínio. Este processo apresentou eficiências elevadas (*ca.* 95%) tanto na remoção das NPs individualmente, como na sua remoção simultânea (variando entre 93% e 99% dependendo da NP e das características da água. Contudo, foi observado que para alcançar remoções semelhante de NPs de TiO_2, as águas hidrofóbicas necessitam de uma dose de coagulante mais elevada do que as hidrofílicas. Ao contrário das características das águas, a presença de diferentes NPs em conjunto não afetou a dose de coagulante necessária. Determinou-se que o mecanismo de remoção de NPs mais provável foi a neutralização de cargas. No final do processo, as concentrações residuais de NPs nas águas tratadas foram, 6.5±2.1 e 2.5±0.7 µg Ti/L, 15.0±1.4 e 6.0±1.4 µg Ag/L, e 18.8±8.8 e 0.5±0.1 µg Cu/L, para a água natural com menor turvação e matéria orgânica natural (NOM) e para a água natural com maior turvação e NOM, respetivamente. De modo a diminuir as concentrações residuais de NPs na água tratada, o processo convencional C/F/S foi combinado com a adsorção por carvão ativado em pó (C/F/S+PAC) e integrado com o tratamento avançado ultrafiltração (UF) num processo de tratamento híbrido (C/F/S→UF). O processo C/F/S+PAC foi mais eficiente na remoção das NPs de TiO_2 (>99.9%), com o Ti a apresentar concentrações inferiores ao limite de deteção na água tratada. Para o mesmo tratamento as remoções de Ag e Cu foram superiores a 99.2%. Com a aplicação do tratamento híbrido (C/F/S→UF), não foram detetadas concentrações residuais nem de Ti nem de Cu na água filtrada. Contudo, foram detetadas concentrações entre 5.0 e 7.0 µg/L para a Ag. Este resultado foi associado à dissolução das AgNPs, uma vez que, tendo em conta o menor tamanho do poro da membrana comparado com o tamanho individual das NPs e dos agregados formados, a parte nanoparticulada foi removida.

Com o intuito de remover tanto AgNPs, como os iões provenientes da dissolução foi utilizado o tratamento avançado de nanofiltração (NF). Com este tratamento os agregados e as nanopartículas individuais foram completamente removidas por exclusão de tamanho, tendo a remoção de Ag dissolvida chegado aos 99.9%, dependendo do conteúdo de sais e matéria orgânica natural das águas testadas.

Os resultados obtidos permitem concluir que é possível remover de forma eficaz NPs durante o tratamento de água para consumo humano, utilizando uma combinação/sequência de tratamentos convencionais e avançados, sem prejudicar a qualidade da água final. Tal foi demonstrado pela comparação dos valores residuais de turvação, carbono orgânico dissolvido, SUVA (absorvência específica) e alumínio com os valores paramétricos nacionais e internacionais para a água para consumo humano. Uma linha de tratamento integrando C/F/S+PAC, seguido de UF ou até mesmo NF, apresenta-se como uma solução segura para eliminar a ameaça de ingestão de NPs através de água potável.

Palavras-Chave: Nanopartículas, água para consumo humano, águas superficiais, tratamento de água convencional, tratamento de água avançado.

.

.

Table of Contents

List of Figures

List of Tables

Abbreviations

AAS	Atomic absorption spectrometry
AHA	Aldrich humic acids
AOP	Advanced oxidation process
BET	Brunauer Emmett Teller method
C/F	Coagulation/ Flocculation
C/F/S	Coagulation/ Flocculation/ Sedimentation
CNT	Carbon nanotubes
COST	European Cooperation in Science and Technology
CPI	Consumer product inventory
DI	Deionised water
DLS	Dynamic light scattering
DLVO	Derjaguin, Landau, Verwey and Overbeek
DMSA	Dimercaptosuccinic acid
DNA	Deoxyribonucleic acid
DOC	Dissolved organic carbon
DW	Deionised water
DWT	Drinking water treatment
DWTP	Drinking water treatment plant
ECR	Effective coagulation zone
EFM	Environmental fate models
ELS	Electrophoretic light scattering
ENMs	Engineered nanomaterials
ENPs	Engineered nanoparticles
EU	European Union
FTIR	Fourier-transform infrared spectroscopy
HD	Hydrodynamic diameter
ICP-MS	Inductively coupled plasma mass spectrometry
ICP-OES	Inductively coupled plasma optical emission spectrometry
IEP	Isoelectric point
IS	Ionic strength
MF	Microfiltration

MFA	Material flow analysis
MWCO	Molecular weight cut-off
NF	Nanofiltration
NF270	Nanofiltration membrane 270
NF90	Nanofiltration membrane 90
NOM	Natural organic matter
NPs	Nanoparticles
NSW	Natural surface water
NTA	Nanoparticle tracking analysis
NW	Natural water
PAC	Powdered activated carbon
PACl	Polyaluminium chloride
PdI	Polydispersity index
PEC	Predicted environmental concentrations
PFS	Polyferric sulfate
PVA	Polyvinyl alcohol
PVDF	Polyvinyldine fluoride
PZC	Point of zero charge
ROS	Reactive oxygen species
SA	Salicylic acid
SEM	Scanning electron microscopy
sp-ICP-MS	Single-particle inductively coupled plasma mass spectrometry
SRHA	Suwannee River humic acid
SSW	Synthetic surface water
SUVA	Specific UV absorbance
TA	Tannic acid
TEM	Transmission electron microscopy
TMP	Transmembrane pressure
TOC	Total organic carbon
UF	Ultrafiltration
UK	United Kingdom
USA	United States of America
UV	Ultraviolet

UV_{254}	UV absorbance at 254 nm
UV-Vis	Ultraviolet-visible
WHO	World Health Organization
WIP	Waste incineration plant
WRR	Water recovery rate
WWTP	Wastewater treatment plant
XRD	X-ray diffraction
ZP	Zeta potential

Chapter 1
General Introduction

1.1 Nanoparticles, a threat to the quality of drinking water?

The increasing production and application in consumer goods of engineered nanoparticles (ENPs) over the past decade will inevitably lead to their release into the aquatic environment and thereby cause the exposure of living organisms to these contaminants, resulting in growing environmental and human health concerns (Dwivedi et al., 2015; Giese et al., 2018; Lead et al., 2018; Nowack et al., 2016). It has been shown that ENPs-containing products release nanoparticles (NPs) into the environment during their production, useful life or upon final disposal (Caballero-Guzman and Nowack, 2016; Giese et al., 2018; Gottschalk and Nowack, 2011; Sun et al., 2017; Williams et al., 2019). This leads to direct exposure to ENPs for humans via inhalation, skin contact and ingestion of contaminated drinking water or indirect exposure from ingestion of seafood (Liu et al., 2014; Tiede et al., 2015). Therefore, ENPs should be considered an emerging water contaminant, and their removal during drinking water treatment should be ensured and monitored (Abbott Chalew et al., 2013). Estimated NPs concentrations in surface waters range from ng/L to µg/L (Donovan et al., 2016; Peters et al., 2018; Yang and Westerhoff, 2014), but these concentrations are anticipated to increase over time with higher use and disposal of ENPs-containing products (Adam et al., 2018; Nowack et al., 2016). Although the effects of ingested ENPs are still being investigated, several recent *in vitro* and *in vivo* experiments have already shown that there are adverse health effects from nanoparticles exposure. At the cellular level, nanoparticles exposure led to cell death, DNA damage and increased reactive oxygen species (Kumbıçak et al., 2014; Missaoui et al., 2018; Yu et al., 2013).

Due to their small size, NPs can accumulate inside cells, and, once inside, may release ions that can directly impact cell functioning (Carlson et al., 2008; Missaoui et al., 2018). *In vivo* studies demonstrated that TiO_2 NPs are genotoxic (Chen et al., 2014) and after five days of ingesting TiO_2 NPs from drinking water, rats had detectable DNA damage (Trouiller et al., 2009). Other studies reported histological evidence of inflammation, as well as increased liver enzymes related to necrosis, in rats and mice in response to Ag and ZnO NPs in drinking water (Cha et al., 2008; Park et al., 2010). Human exposure to Ag NPs has been shown to cause liver and kidney damage, eye and skin irritations, and changes to blood cells (Ahamed et al., 2010). Furthermore, the ability of these particles to penetrate the body and cells provides potential routes for the delivery of nanoparticle-associated toxic pollutants to sites that they would not usually reach (Missaoui et al., 2018; Moore, 2006). Despite the evidence of ENPs released into surface waters and consequently drinking waters sources, only a few studies investigated the

removal of ENPs by water treatment processes. These studies have found that conventional treatment is not completely effective in ENPs removal from drinking water and removal efficiencies are highly dependent on water characteristics (Abbott Chalew et al., 2013; Honda et al., 2014; Kinsinger et al., 2015; Sun et al., 2013; Zhang et al., 2008). In addition, these studies did not test ENPs removal in natural waters with complex chemistries. Water characteristics such as pH, natural organic matter content and salt composition can affect the size, aggregation, dissolution and stability of NPs in water (Serrão Sousa and Ribau Teixeira, 2013). Abbott Chalew et al., 2013 have found that ultrafiltration was more effective in the removal of Ag, ZnO_2 and TiO_2 than conventional treatment, however, finished water contained considerable metal concentrations that may pose hazards to human health. Once again, ENPs removal was affected by stability, aggregation and dissolution. Most of these studies were conducted using nanoparticles spiked into ultrapure, tap water, or synthetic freshwaters at high nanoparticle concentrations. To date, no studies have investigated removal through the combination of conventional and advanced drinking water treatment processes using natural surface waters and environmentally relevant ENPs mixtures taking into account the release of metal ions from NPs. If ENPs are not removed from the drinking water, they represent a threat to human health. Thus, their removal is essential to minimize their potential hazards. Due to ENPs potential adverse effects, the discussion about their safety in terms of human health and the environment has become a priority for several governments and regulatory agencies all over the world (Geissen et al., 2015a; Giese et al., 2018; Houtman, 2010).

1.2. Nanoparticles properties

Nanotechnology is often defined as the design, development, production and application of structures by controlling and manipulating shape and size at the nanometric scale, allowing the creation of novel materials or the improvement of existing ones (Jeevanandam et al., 2018; The Royal Society and Royal Academy of Engineering, 2004). Amongst engineered nanomaterials (ENMs), ENPs (structures with 100 nm or less in a least one dimension) play a central role, with massive production in the last decade, and application to a wide range of different areas such as electronics, biomedical, pharmaceutical, cosmetic, environmental remediation, food and several other daily products (Chekli et al., 2015; Dwivedi et al., 2015).

Nanoparticles show a different behaviour comparing to bulk counterparts, with surface and quantum effects conducting these differences. Due to size reduction, ENPs have a higher

surface area to volume ratio, showing a higher number of atoms present at the surface instead of on the interior of the particle and increasing their reactivity. At the nanoscale, quantum effects, such as electron localisation, binding energy shift, surface collective charge excitation, are also significant, influencing mechanical, optical, electrical and magnetic properties of ENPs (Khan et al., 2019; Klaine et al., 2008; Nel et al., 2009).

ENPs are usually classified by their chemical composition. However, the wide variety of ENPs (size, specific area and shape) will result in different chemical reactivity, bioavailability and toxicity. Metal-based ENPs comprise the most significant number of nanoparticles, which includes oxides, such as titanium dioxide (TiO_2) and copper oxide (CuO), two of the most commonly used metal oxides, and bare metals, such as silver (Ag) (Bhatt and Tripathi, 2011; Klaine et al., 2008). TiO_2 is amongst the first ENMs made readily commercially available. Nano-TiO_2 is widely used in sunscreen due to its effectiveness in UV reflection and absorption (Botta et al., 2011), it is also used as a thickener and whitening additive (Piccinno et al., 2012; Savage et al., 2007). Due to these specific and unique characteristics, it is also applied in cosmetics, toothpaste, plastics, paints, coatings, sporting goods and water treatment (Menard et al., 2011; Piccinno et al., 2012). CuO ENPs present an elevated thermal and electrical conductivity, being intensively used as heat transfer fluid in machinery, polymers and plastics, gas sensors, wood preservation, inks, integrated circuits and batteries coatings (Maisano et al., 2015; Pang et al., 2012). Also, due to antimicrobial properties, CuO ENPs are applied in skin products and textiles (Maisano et al., 2015). Ag ENPs are one of the most commercialised nanoparticles due to their antibacterial properties, making them widely used in textiles, food storage, kitchenware, cosmetics, personal hygiene products and household appliances (Cascio et al., 2015; Tolaymat et al., 2010). Moreover, these ENPs are used in several medical equipments and medical textiles (Li et al., 2008).

1.3. Aims and outline

Although water treatment is one of the main strategies to avoid the ingestion of harmful contaminants from drinking water, a few studies have already demonstrated that conventional water treatment is not able to remove nanoscale particles. As environmental ENPs concentrations increase, it is necessary to adapt drinking water treatment processes to entirely remove nanoparticles, reducing their potential harmful health effects.

This thesis aims to fill the gap of knowledge about the effectiveness of conventional and advanced drinking water treatments in the removal of single and multiple ENPs from surface waters. Hence, the primary objective of this work is to explore and evaluate effective water treatment processes to avoid the nanoparticles breakthrough into treated drinking water, determining the effects of ENPs and water characteristics on the removal processes. Commonly present in consumer products and also likely to be present in water, TiO_2, Ag and CuO ENPs were chosen to conduct the experiments in this program. Although these ENPs toxicity was already shown by several studies they are highly produced. Additionally, Ag and TiO_2 ENPs are increasingly used to improve water quality in drinking water treatment, being important to ensure that these NPs do not breakthrough into finished drinking water.

To achieve this goal, this thesis intends to study advanced water treatment processes as also explore new approaches to optimise conventional water treatment to remove nanoparticles and released ions from water and thereby answering the main questions:

a) Can conventional drinking water treatment be optimised to be able to remove nanoparticles?
b) Can advanced water treatments effectively remove nanoparticles and released ions from water?
c) Can advanced/optimised conventional water treatments explored in this thesis be incorporated in a drinking water treatment plant (DWTP) to remove nanoparticles and released ions without compromising the quality of the treated drinking water?

To answer these questions and achieve the purpose, this thesis is divided into eight chapters, including five main chapters (Chapters 2 to 6), a general introductory chapter (Chapter 1), a final concluding chapter (Chapter 7), and the references (Chapter 8). Supplemental materials associated with the main chapters are compiled at the end of the document (Appendices A, B and C). Thesis chapters are outlined below.

Chapter 1: General introduction

Brief description of the subject approached by this thesis, the objectives and the outline.

Chapter 2: Metal-based engineered nanoparticles in drinking water systems.

This Chapter critically reviewed and evaluated the effectiveness of drinking water treatment processes to control human health risks associated with ENPs presence. The most

extensively studied water treatment processes to remove metal-based ENPs, specifically conventional and advanced processes, were discussed and highlighted in detail, identifying the research gaps regarding ENPs removal in DWTPs and discussing future aspects of ENPs in water treatment. The Chapter also reviewed the available information on production, presence, potential hazards to human health and environment, and release and behaviour of metal-based ENPs in surface waters and drinking water.

Chapter 3: The effect of TiO_2 nanoparticles removal on drinking water quality produced by conventional treatment C/F/S.

The aim of this Chapter was to address the removal efficiency of TiO_2 ENPs from surface water, using conventional coagulation/ flocculation/ sedimentation (C/F/S), exploring their removal mechanisms and evaluating if the nanoparticles removal affected the ability of C/F/S to remove natural organic matter (NOM) and turbidity, and consequently affected the quality of the treated water. The effect of the water characteristics on the TiO_2 NPs removal was evaluated using four synthetic waters with different NOM content, and one natural surface water.

Chapter 4: Simultaneous removal of different metal-based engineered nanoparticles from surface waters by conventional treatment: a shift from single to multiple nanoparticles control.

Given the high-efficiency removals of TiO_2 ENPs from waters observed in Chapter 3, the same process was used to simultaneous remove ENPs from a mixture (TiO_2, Ag and CuO) in natural drinking water sources. The removal of single ENPs was firstly evaluated to optimise and select the most adequate coagulant for their removal, then a mixture of the same compounds was tested, shifting from single to multiple nanoparticle removal. The impact of ENPs removal was evaluated for drinking water parameters such as turbidity and NOM.

Chapter 5: Multiple nanoparticles in surface water: removal through enhanced conventional treatment versus hybrid membrane processes.

Since residual ENPs concentrations were found in the treated water by C/F/S, in this Chapter the performance of enhanced conventional coagulation with addition of powdered activated carbon (C/F/S+PAC) and of hybrid membrane treatment integrating conventional C/F/S and advanced ultrafiltration (C/F/S$\rightarrow$UF) were studied to maximise the simultaneous

removal of TiO_2, Ag and CuO ENPs from drinking water sources. PAC doses were optimised for ENPs removal and UF membrane was selected according to the ENPs nominal size and the size of the aggregates formed. Turbidity, dissolved organic carbon (DOC), specific UV absorbance (SUVA) and aluminium residual concentrations were compared to the Portuguese and WHO guidelines for DWT, and to those found in DWTPs.

Chapter 6: Silver nanoparticles separation from the water using nanofiltration membranes: the role of mono-divalent salts and NOM.

With the intent to remove the residual metal concentrations present in treated water after C/F/S+PAC and C/F/S→UF due to ENPs dissolution, a more refined treatment, nanofiltration (NF) was studied. To fully understand the removal mechanisms of both nanoparticulate and ionic form and solution-NPs interaction, Ag ENPs removal was assessed under several salts and NOM conditions, worst scenarios hypotheses were tested.

Chapter 7: Concluding remarks.

This Chapter presents general conclusions that gather all the results obtained in the previous Chapters. Recommendations for future research are also considered.

Chapter 8: References.

Finally, this last Chapter comprises all the studies referred to in the thesis.

Chapter 2

Metal-based Engineered Nanoparticles in Drinking Water Systems

This Chapter was published in:

Serrão Sousa, V., Ribau Teixeira, M. (2020). Metal-based ENPs in drinking water systems: A Critical Review. Science of the Total Environment, 707, 136077.

https://doi.org/10.1016/j.scitotenv.2019.136077

ABSTRACT

The emergence of nanotechnologically-enabled materials, compounds or products inevitably leads to engineered nanoparticles (ENPs) released into surface waters. ENPs have already been detected in wastewater streams, drinking water sources and even in tap water at concentrations in the ng/L and μg/L range, making the latter a potential route for humans. The presence of ENPs in raw waters raises concerns over the possibility that ENPs might pose a hazard to the quality and security of drinking water and whether drinking water treatment plants (DWTPs) are prepared to handle this problem. Therefore, it is essential to critically evaluate if ENPs can be effectively removed through water treatment processes to control environmental and human health risks associated with their release. This review includes a summary of the available information on production, presence, potential hazards to human health and environment, and release and behaviour of metal-based ENPs in surface waters and drinking water. In addition, the most extensively studied water treatment processes to remove metal-based ENPs, specifically conventional and advanced processes, are discussed and highlighted in detail. Furthermore, this work identifies the research gaps regarding ENPs removal in DWTPs and discusses future aspects of ENPs in water treatment.

2.1. Introduction

Over the last years the presence of emerging contaminants in the environment, including engineered nanomaterials (ENMs), has raised concerns about environmental protection, industrial and municipal wastewater treatment and drinking water production (Geissen et al., 2015b; Giese et al., 2018; Houtman, 2010).

The emergence of nanotechnologically-enabled materials, compounds or products, widely applied in distinct areas such as medicine, pharmaceutics, cosmetics, textiles, agriculture, energy, electronics or environment (Chekli et al., 2015; Dwivedi et al., 2015), due to their tailoring potential for specific applications (Prajitha et al., 2019), is currently a globally recognised issue. In day-to-day life, humans are getting exposed to thousands of engineered nanoparticles (ENPs), via contact, inhalation or ingestion. For example, titanium dioxide (TiO_2) ENPs are used in sunscreens, toothpaste and other cosmetics or as a whitening additive in food and drinks. Silver (Ag) ENPs are being applied in a broad range of consumer products due to their antimicrobial properties (socks, washing machines, cosmetics, and medicines) (Jahan et al., 2017; Troester et al., 2016).

The estimated value for produced/imported ENPs or ENPs-containing products was around 1,615,000 ton in 2016 only in the European Union (Ricardo Energy & Environment et al., 2016). With the predicted growth of nanomaterials production, the volume and diversity of ENPs released (intentionally or unintentionally, directly or indirectly) into the aquatic environment during production, use and disposal will increase accordingly, producing a detrimental effect on the quality of surface waters, potentially used to public water supply (Adam et al., 2018; Jahan et al., 2017; Nowack et al., 2016). The uncontrolled release of heterogeneous (various forms, shapes, sizes, surface functionalities) and unknown ENMs to surface water pose concerns towards their ecological and human health toxicity (Jahan et al., 2017). This growing trend demands a wide-ranging analysis of present and future releases, toxicity exposure and environmental concentrations and distribution to prepare preventive and regulatory measures (Giese et al., 2018).

In the past, the technologies available could not detect ENPs in wastewater streams, so the potential release of ENPs into the environment was modelled (Giese et al., 2018; Gottschalk et al., 2009, 2013; Gottschalk and Nowack, 2011; Keller et al., 2013; Sun et al., 2014). Now, ENPs have already been detected in wastewater streams, drinking water sources and even in tap water at concentrations in the ng/L and µg/L range making the latter a potential route for humans (Donovan et al., 2016; Peters et al., 2018; Yang and Westerhoff, 2014). Despite this, data on

measured environmental concentrations of ENPs in surface waters is still lacking, however, several researchers have estimated values between 21 and 10,000 ng/L for TiO_2 NPs only (Gottschalk et al., 2013; Gottschalk and Nowack, 2011).

Although more research is needed to establish the impact of these emerging contaminants on human health and environment, there has been a considerable increase in the studies on ENPs toxicology. ENPs exposure experiments have already been associated with toxic effects, including phototoxicity under UV radiation from the topic application of sunscreens. Properties like the high surface area-to-volume ratio and binding affinity to cells associated with ENPs small size (properties that provide specific functionality) can affect their behaviour in the environment and organisms, which may result in different exposures. The presence of ENPs will affect the entire organ system, affecting even the reproduction and fetal developmental stages (Oomen et al., 2018; Prajitha et al., 2019). In parallel, ENPs can transport other harmful chemicals used during the manufacturing process or adsorb to them due to the strong adsorption properties, thereby enabling the entry of these substances into organisms (Bakaraki Turan et al., 2019; Prajitha et al., 2019). This toxicological data combined with models of exposure can contribute to a prospective risk assessment, regardless, from a regulatory point a view, data on ENPs actual release and exposure is required to estimate the associated risk. Yet, the results of exposure and toxicology models have to be validated based on reliable model input data, which is mostly missing in nanomaterials context (Oomen et al., 2018; Williams et al., 2019).

Therefore, if nanoparticles occur in surface water reservoirs and pass rough water treatment processes, they may potentially be consumed by populations via tap water, leaving individuals exposed to their adverse effects. The presence of ENPs in raw waters raises the question of whether drinking water treatment plants (DWTPs) are prepared to handle this problem and produce safe drinking water. Therefore, it is essential to critically evaluate if ENPs can be effectively removed through water treatment processes to control the environmental and health risks associated with ENPs exposure. Despite the particle removal is one of the main objectives of drinking water treatment, with operations like coagulation, flocculation and sedimentation (C/F/S), granular media filtration or membrane filtration, very little is known about the ability of these treatment processes to remove particles smaller than 1 μm and the behaviour of these particles within the treatment systems (Troester et al., 2016).

Earlier reviews summarised the production, release, fate and behaviour of ENPs in the aquatic environment. However, the potential hazard of nanoparticles to drinking water safety has not been sufficiently addressed. With restricted data available for ENPs occurrence in

surface water and tap water, it is still unclear whether the current processes for drinking water treatment (DWT) have the ability to remove ENPs. So, a systematic description of the fate and breakthrough of ENPs in DWTP is still missing.

This review integrates previous information and discusses the peer-reviewed articles published on metal-based ENPs in surface waters. Thus, the objective of this work is to critically review and summarise published studies on the occurrence, behaviour and detection of ENPs in surface waters, as well as to assess the ability of DWTPs processes to remove ENPs. Since previous reviews focused primarily on bench-scale studies, in this article an effort was made to keep up with the growth of studies on ENPs pilot and full-scale water treatment plants. Rather than focusing on a particular nanoparticle, a broader approach of metal-based ENPs was followed to cover a wider variety of water treatments and conditions relevant to drinking water supplies. Both conventional and promising, though less commonly employed, treatment options are discussed. Despite the lack of literature, the present review also attempts to link the unique characteristics and properties of ENPs with their removal in water treatment. To provide further context this review also includes a brief summary of the behaviour and toxicological significance of ENPs in drinking water.

2.2. Methodology

This review integrates previous information and discusses the peer-reviewed articles and book chapters published in the last decade addressing the issues and raising questions on the release, occurrence and detection of metal-based ENPs in surface waters and their potential removal in drinking water treatment.

SCOPUS database search (June 2019) using the keyword “nanoparticles” resulted in a total of 1,209,826 articles and book chapters. Only original English research published between 2009 and 2019 was considered.

Within these results, it was observed that the majority of these papers (86.8%) was on the production, application or characterization of nanoparticles (including for environmental remediation purposes), while a small percentage was dedicated to toxicological studies (12.7%) and only 0.5% addressed the themes release, occurrence, detection or removal (Figure 2.1).

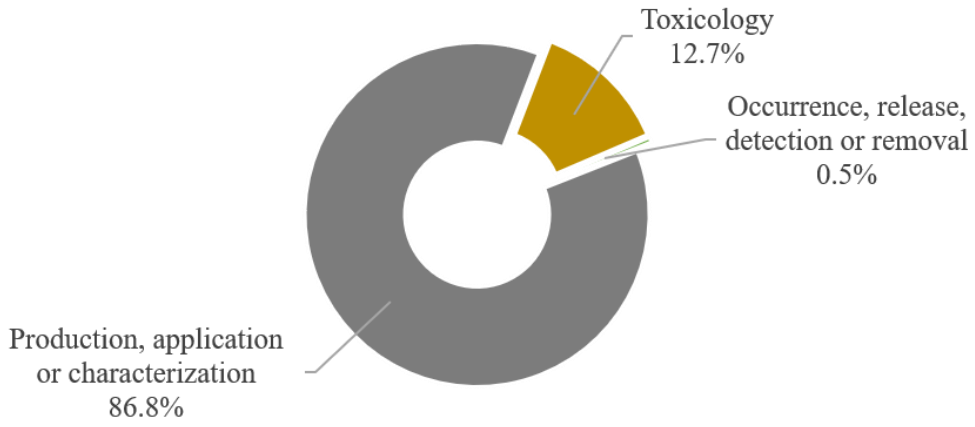

Figure 2.1. Literature on "Nanoparticles" (source SCOPUS) from 2009 to 2019 represented by three main areas: Production, application or characterisation, Toxicology and Occurrence, release, detection, or removal.

A more refined search using the keywords "nanoparticles in freshwater", "nanoparticles in drinking water", and "nanoparticles removal" AND "water treatment" resulted in 138, 90 and 129 articles, respectively. Figure 2.2 shows the number of papers per year, indicating that the topics about the presence of nanoparticles in freshwater and their removal by water treatments have experienced exponential growth in the number of papers published since 2014. In comparison, the topic on the nanoparticles in drinking water raised a greater interest in the scientific community only from 2015. Most of the literature was on nanoparticles toxicological studies (34%) and the application of these substances to environmental remediation (32%), mainly for water purification. As expected, research on the occurrence (and detection) of nanoparticles in natural waters, as also on their removal by water treatment processes was scarce, 12% and 18% respectively (Figure 2.2), with publication increasing in more recent years, in particular from 2017 onwards. Papers on risk assessment of nanoparticles in freshwater or drinking water, or both, represent only 2% of the results.

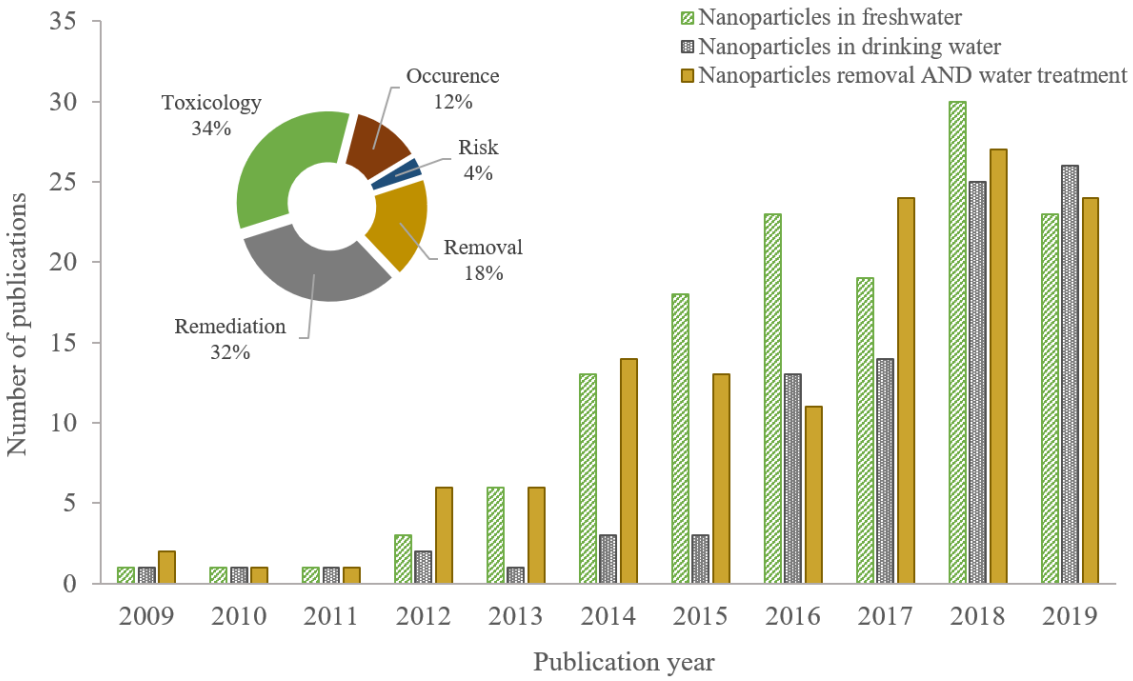

Figure 2.2. Literature on topics "nanoparticles in freshwater", "nanoparticles in drinking water" and "nanoparticles removal" AND "water treatment" (source SCOPUS) between 2009 and 2019, analysed by year (bars chart). Analysis of the total number of publications by theme (circular chart).

In this review, it was also assessed which subjects have more publications within each combination of the keyword searched on SCOPUS database (Figure 2.3). For the "nanoparticles in freshwater", the toxicity studies represented most of the publications (80%) and the works on the NPs removal represented the minority (1%). Under this topic, information is still very scarce on the occurrence of nanoparticles (9%) and even more about detection and actual concentrations determined in freshwaters (<<1%). Furthermore, some papers have already tackled some steps of the risk assessment in freshwaters (6%), using the data published about ENPs toxicity.

Under the topic "nanoparticles in drinking water", half the papers (50%) were on the application of ENPs to remediation, specifically for water purification, and a similar result was found under the topics "nanoparticles removal" AND "water treatment". Likewise, works on the ENPs occurrence were also similar for both topics, 18% and 13%, respectively. Toxicity and risk are only represented under the "nanoparticles in drinking water" topic (approximately 16% of the works), not having any representativeness in the topic "nanoparticles removal" AND "water treatment".

Even within this last-mentioned topic combination, focused on nanoparticles removal, most published papers were on the use of ENPs for remediation purposes (50%), and only 37% about their removal.

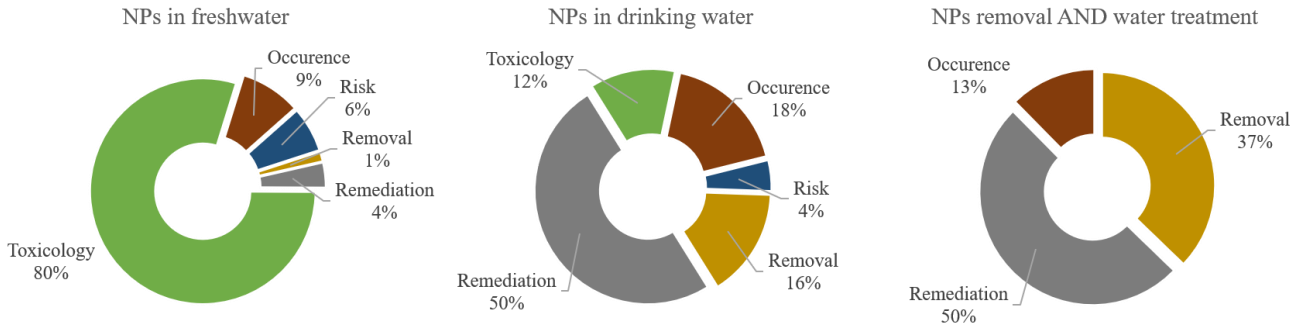

Figure 2.3. Literature by topics "nanoparticles in freshwater", "nanoparticles in drinking water" and "nanoparticles removal" AND "water treatment" (source SCOPUS) between 2009 and 2019, analysed by theme within each topic.

2.3. Why can ENPs pose a risk to the environment and human health?

According to the European Union (EU), nanomaterials are defined by their physical characteristics rather than their chemical composition (Williams et al., 2019). Based on EU recommendation, the definition of nanomaterial is *"a natural, incidental or manufactured material containing particles, in a boundless state or as an aggregate (or agglomerate) and where, for 50% or more of the particles in the number size distribution, one or more external dimensions are in the size range 1 – 100 nm*" (EC - European Commission, 2011). The main technological interest in ENMs is due to their modifiable and enhanced physicochemical properties which provide them high chemical reactivity at the nanoscale level (Clavier et al., 2019; Jeevanandam et al., 2018).

ENPs are synthesised to achieve unique physicochemical properties including size, structure, composition and surface area different from their bulk material, which can be tailored due to the number of atoms lying on the surface (Amde et al., 2017; Jiang et al., 2009; Khan et al., 2019; Lead et al., 2018). With size reduction, properties such as electrical conductivity, magnetic characteristics, active surface area, chemical reactivity and biological activity undergo significant changes differing from those presented by their bulk counterparts (Karlsson

et al., 2009). At the nanoscale the ratio between the surface area and volume is higher than in the bulk material (Cupaioli et al., 2014).

These appellative characteristics to technological development can also represent a significant, and still largely unknown, hazard to human health, scarcely faced by researchers (Tosco and Sethi, 2018). The exceptionally small size range and distinct surface properties determine their behaviour, biological effects and consequently their toxicity, enhancing ENPs entry, absorption and further distribution inside the living systems (Peralta-Videa et al., 2011; Prajitha et al., 2019). ENPs may enable harmful effects in biological organisms, reaching targets not reachable for their bulk counterparts (Pietroiusti et al., 2018).

The widespread of ENPs has increased the human exposure to these substances by inhalation, dermal penetration or ingestion. The potential release into the environment, especially to surface waters, raises serious concerns about the ENPs ingestion through drinking water or the food chain (Tiede et al., 2015). The ingestion by drinking water intake may pose a direct human health hazard or an indirect risk due to the release of trace metal ions from ENPs (Abbott Chalew et al., 2013). Exposure to ingested metal-based ENPs or metal ions released can result in adverse effects, such as kidney damage, increased blood pressure, gastrointestinal inflammation, neurological damage and cancerous implications (Kavcar et al., 2009; Missaoui et al., 2018; Vahter et al., 2002). Once ingested, ENPs are absorbed through the digestive system and later transported to the lymphatic tissues and may cause local toxic effects. They also can either be excreted if unstable or accumulated in the digestive system, which can ultimately result in obstruction of the gastrointestinal tract. The interaction with the intestinal microbiota may cause relevant local and systemic biological effects (Fröhlich and Roblegg, 2016; Pietroiusti et al., 2018; Shvedova et al., 2012). Primary toxicity effects from the ingestion of ENPs are organ inflammation, oxidative stress and DNA damage (Missaoui et al., 2018). If the ENPs reach the bloodstream, they can accumulate in several organs like liver, spleen, kidneys and lungs due to their leaky blood vessels (Desai, 2012; Weir et al., 2012).

Despite the lack of information, some ENPs are already known by their toxicity, such as cationic NPs (e.g. metal-based NPs). These nanoparticles can biodegrade swiftly and penetrate deeply into tissues and cells, due to small size, which will result in the destabilisation of the plasma membrane, tissue damage and organ dysfunction (Missaoui et al., 2018). Metallic oxide ENPs, like TiO_2 and ZnO, are among the types with the highest likelihood of human exposure and are also within the most produced ones (Tiede et al., 2015).

Human exposure to ENPs by ingestion is expected to become more common as the production and application of nanomaterials are increasing. While for contained in consumer products dermal or inhalation exposure during use is the most significant route, for ENPs in clothing and some paint products, exposure by ingestion of contaminated drinking water appears to be higher than by other routes (Tiede et al., 2015). Since ENPs toxicity to humans widely depends on exposure duration, amount and entry portals (Prajitha et al., 2019), understanding the ability of drinking water treatment to effectively remove these substances is required.

2.4. ENPs annual production and application to consumer products

Due to the scarcity of available data related to the company's secrecy in the nanomaterials market and inconsistency in viable data sources, uncertainness in annual ENPs volumes produced is still very high, but clearly is situated in the tonnes-per-year range (Giese et al., 2018; Hendren et al., 2011; Piccinno et al., 2012; Ricardo Energy & Environment et al., 2016; Sun et al., 2014).

The annual production estimates for ENPs published in the literature are extremely uncertain with a considerable variance between studies and even within the same work as shown in Figure 2.4. These differences are observed for the European production (2009-2010) (Figure 2.4a) for TiO_2, ZnO and SiO_2 ENPs that varies between 55 and 42,000, 5.5 and 28,000, and 55 and 55,000 t/year, respectively. Despite the data variance, it is commonly agreed that nano-SiO_2 is the most produced for the three scenarios analysed, followed by TiO_2 (Figure 2.4). This was already expected since both materials have long been used in nano-particulate form, even before nanotechnology widespread (Piccinno et al., 2012). In general, the ENMs with the highest production also present the values with higher variability, compared to the less produced ones (Figure 2.4). The high production (and its variance) of SiO_2 and TiO_2 ENPs could be associated to the difficulty to clearly define when a specific material is considered an ENM or a conventional material (Nowack et al., 2015). Overcome the constrains associated with the variability of production data will be challenging, since it is mostly collected through responses given by manufactures.

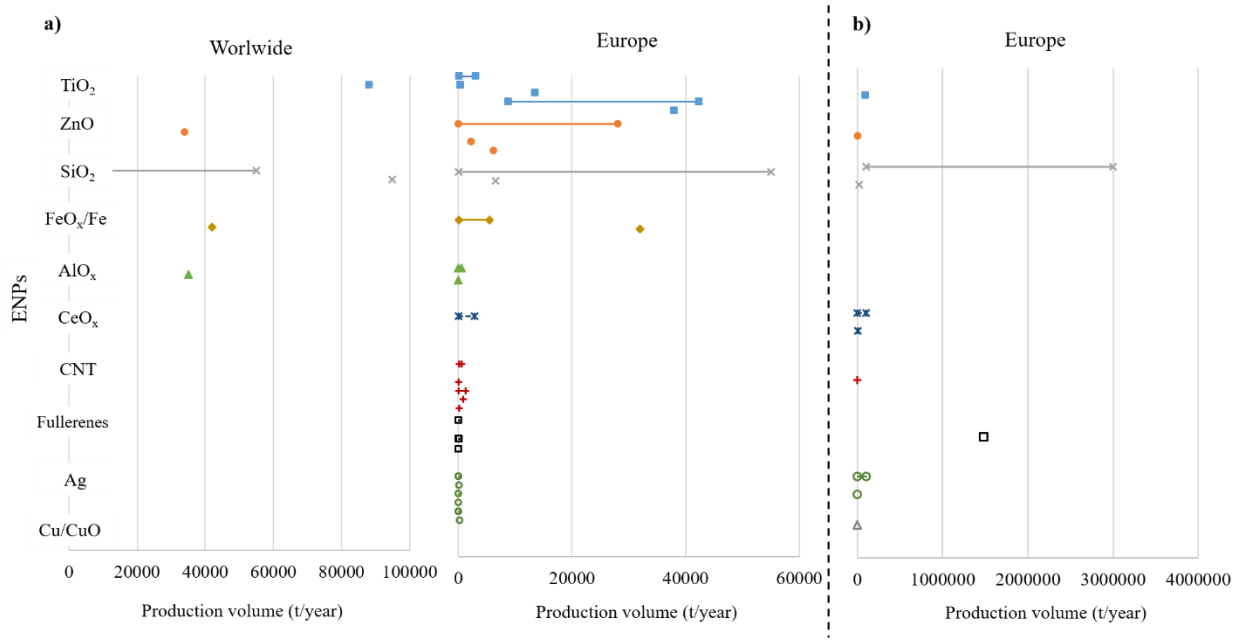

Figure 2.4. ENPs production volumes from literature: a) Worldwide and Europe between 2009 and 2010 and b) Europe in 2013 (Caballero-Guzman and Nowack, 2018; Future Markets, 2012; Giese et al., 2018; Hendren et al., 2011; Keller et al., 2013; Piccinno et al., 2012; Ricardo Energy & Environment et al., 2016; Sun et al., 2014; Windler et al., 2013).

A recent European Commission report (Ricardo Energy & Environment et al., 2016) estimated that the global volume of produced/imported substances or ENPs-containing products was around 1,615,000 t in 2016 for the EU. This report was mainly extrapolated from French production and importation registry. Due to the number of assumptions used to reach the indicative inventory, numerical production and release, estimates were considered highly uncertain. Based on this report, Giese et al. (2018) derived a median annual growth of 5% to the produced amount of ENMs. Inshakova and Inshakov (2017) foresee a compound annual growth rate of 20.0% during 2016-2022 for the European market. These estimations confirm that the annual production of ENMs will continue to grow fast to keep abreast of developments in nanotechnology field.

Other sources to understand the magnitude of ENPs production and their incorporation in consumer goods are the inventory lists of ENPs-containing products. In 2005 the Nanotechnology Consumer Product Inventory (CPI) was created (Woodrow Wilson International Center, 2005), the first-of-its-kind inventory on ENPs-containing products, listing 54 products. Despite the critics to its lack of science-based data to support the manufactures information's (Berube et al., 2010; Matthews, 2014), this inventory is significantly cited in scientific literature and government reports worldwide. In 2010, the CPI listed 1012 products

from 24 different countries and at the time of this writing, the inventory showed 1829 products with USA, Europe and Korea leading the list with 44%, 35% and 8% ENPs-containing products, respectively.

A more recent database, "The Nanodatabase" (Danish Consumer Council, 2012), an ENPs-containing products inventory available in the European consumer market, presented considerably higher values (Figure 2.5). The difference in the listed products between the databases could be related to the lack of substantial updates of the CPI in the last years. Currently, "The Nanodatabase" (Danish Consumer Council, 2012) lists a total of 3109 ENPs-containing products for 2019, two and half times higher than for 2012 (first report), as shown in Figure 2.5. More than 60% of these products are listed under the "Health and Fitness" category that also includes personal care products, like cosmetics, sunscreens or toothpaste. According to this database, the leading nanoparticle producers are Europe (53%), USA (37%) and Asia (7%) (Figure 2.5, circular graph). Of the 3109 products listed in "The Nanodatabase" for 2019, only 1161 (approximately 37%) advertise the composition of at least one ENP and the remaining does not present the composition, or a detailed description of the nanomaterial used. Despite TiO_2 and SiO_2 are the most produced ENMs (Figure 2.4), and the annual production of AgNPs only represented a small amount of the global production, AgNPs are the most prevalent advertised nanoparticle, present in 379 products (12%), followed by TiO_2 (123 products) (Danish Consumer Council, 2012).

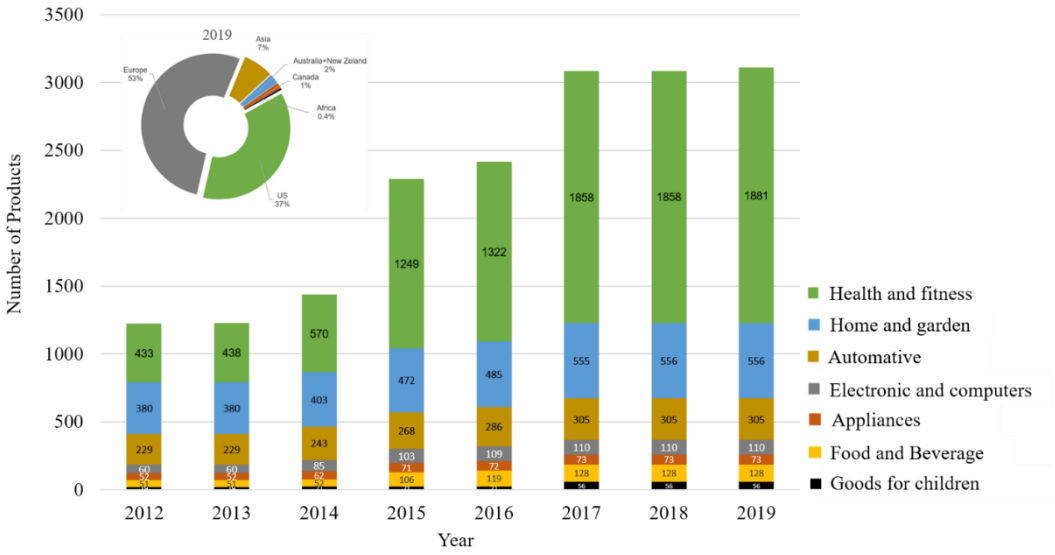

Figure 2.5. Inventory of ENPs-containing products available in the European consumer market, listed from 2012 to 2019 and grouped under seven categories (bars chart). Analysis of the total ENPs-containing products listed for 2019 by production region (circular chart). Source: "The Nanodatabase" (Danish Consumer Council, 2012).

2.5. ENPs in surface waters

Freshwater is the key source for potable water production for human consumption, industry, agriculture and energy production (Teodosiu et al., 2018), which includes surface waters, like rivers or lakes (or reservoirs), and groundwaters. This review focuses on surface waters often affected by organic and inorganic emerging contaminants, that are of serious concern for human health and environment (Geissen et al., 2015b; Houtman, 2010; Sauvé and Desrosiers, 2014; Snow et al., 2017).

Surface waters are vulnerable to anthropogenic contamination due to the wide exposure to human and industrial activities and consequent impacts. Waste streams, discharges of inadequately treated wastewaters, agricultural and urban runoff, and releases from contaminated sludge placed in landfills, applied as fertiliser or dumped in aquatic environments are important causes of surface water contamination by ENPs (Baalousha et al., 2016; Park et al., 2017). ENPs released concentrations are strongly dependent on the volume of industrial production and application to consumer products thus will continue to increase as the widespread of nanomaterials continues to grow (Caballero-Guzman and Nowack, 2016; Sajid et al., 2015).

ENPs released into surface waters are a threat not only for the well-being of the aquatic ecosystem but also to the security of resources used for drinking water production. Thus, understanding ENPs occurrence and behaviour, as also detect and quantify their real concentrations in surface waters, is mandatory to assess the potential impacts to human health and to determine the required treatment processes to produce safe drinking water without ENPs.

The current accepted approach to assess the multiple sources and pathways trough which ENPs can be introduced into the different environmental compartments and consequently in surface waters, follows a lifecycle principle tracking ENPs flow and release from the production through their final settling place in environment or waste streams (Caballero-Guzman and Nowack, 2016; Giese et al., 2018; Gottschalk et al., 2009; Gottschalk and Nowack, 2011; Liu and Cohen, 2014; Sun et al., 2017; Williams et al., 2019) (Figure 2.6). It is expected that the most substantial unintentional and unrestrained, direct or indirect release to surface waters occurs during the use phase (Caballero-Guzman and Nowack, 2016; Froggett et al., 2014).

ENPs can be released to technical compartments (or technosphere) like WWTPs, waste incineration plants (WIPs), landfills and recycle process during production, use and disposal (Figure 2.6). These compartments are considered transitional since ENPs will be transferred later to an environmental compartment such as atmosphere, soil, and surface and ground waters

(Duester et al., 2014; Nowack, 2017). As shown in Figure 2.6, they can also be released directly to the environmental compartments without going through the technical ones and move across the boundaries of environmental compartments (Duester et al., 2014; Williams et al., 2019).

Surface waters potentially receive ENPs directly from production, use and disposal, technical compartments and other environmental compartments due to transport phenomena like runoff, erosion or leaching (Figure 2.6). The main ENPs pathways into surface water systems are expected to be direct discharges of insufficiently treated wastewater, release from sludge applied to soils as a fertiliser, landfills trough leaching streams, urban runoff or directly dumped (Baalousha et al., 2016; Bolyard et al., 2013; Brar et al., 2010; Duester et al., 2014; Nowack et al., 2012). The application of nanopesticides in agriculture could potentially result in the most considerable intentional diffuse input of ENPs into surface waters, followed by TiO_2 applied in water treatment (Troester et al., 2016) or nano zero-valent iron in groundwater remediation (Grieger et al., 2010). Cosmetics and personal care products, foods, textiles, electronics, vehicle components, construction materials and products applied in agriculture or environmental remediation (e.g. soil and water purification) are within the main sources of ENPs released to surface waters (Giese et al., 2018; Gondikas et al., 2018; Gottschalk and Nowack, 2011; Kaegi et al., 2017; Keller et al., 2013; Morgeneyer et al., 2018; Shandilya et al., 2015; Som et al., 2011).

At the end of their lifecycle (disposal), instead of being stored in an environmental compartment as its final sink, ENPs may flow back to another application if a nanomaterial fraction is recovered and reused or recycled. However, currently ENPs that are recycled are more likely to be used in the production of other type of materials, such as plastics, than in nano-applications (Adam et al., 2018; Caballero-Guzman and Nowack, 2016; Nowack et al., 2016), which is illustrated in Figure 2.6 by the interruption of the path between recycling and production.

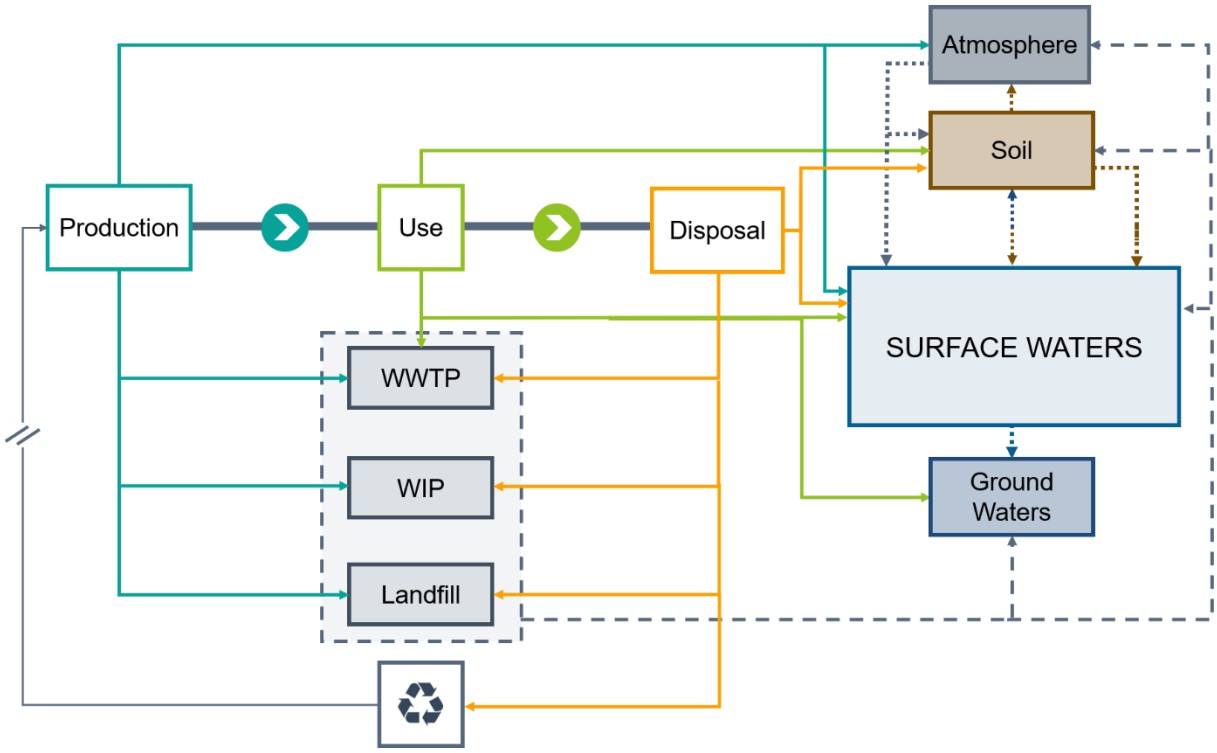

Figure 2.6. ENPs flows throughout the entire lifecycle: ENPs production, use and disposal; ENPs release during production, from products during use and disposal; transport and fate of ENPs between and within technical (WWTP, WIP and landfill) and environmental compartments (atmosphere, soil, surface and ground waters). Adapted from (Duester et al., 2014; Gottschalk et al., 2013; Sun et al., 2014).

The wastewater effluents are usually considered one of the most significant point sources of ENPs in surface waters due to the consumer goods, that are washed down the drains during household use (hygiene routine, laundry and food preparation) (Keller et al., 2013; Park et al., 2017; Weir et al., 2012). Since wastewater treatment processes are not entirely effective in the removal of ENPs, any remain ENPs in treated wastewater effluents are discharged into surface waters (Westerhoff et al., 2018). Water quality of DWTP intakes is highly affected by upstream possible WWTP discharges (Westerhoff et al., 2018). According to Duester et al. (2014), three potential pathways were considered research priorities by the european COST program due to their significance: (i) wastewater → WWTP → surface water, (ii) wastewater → stormwater → surface water and (iii) landfill leachate → treatment → surface.

2.5.1. The occurrence of ENPs in surface water

The continuous growth of nanomaterials production, the volume and diversity of ENPs released into the aquatic environment will lead to the rapid increase of ENPs in surface waters (Giese et al., 2018; Nowack et al., 2016).

According to recent studies (Giese et al., 2018; Ricardo Energy & Environment et al., 2016), ENPs release during production is expected to be between 0.7 and 1.6% of the total mass (this value can increase until 5% for formulations of suspensions). Considering an annual production of 1,624,285 t (Europe), the potential release can vary between 11,301 and 25,830 t of ENPs during production. Giese et al. (2018) estimated that, through use phase, the release of nano-Ag, CeO_2 and SiO_2 into environmental compartments (Figure 2.6) in 2017 was 17,080 t (2.5 to 3 times more than for technical compartments) and 7 t during disposal phase. Their forecast follows the already stated trend of an increase in ENPs released to the environment, 30,105 and 73,315 t/year during use phase and 7 and 17 t/year during disposal phase for 2030 and 2050, respectively. As earlier described, during the disposal phase the amount of ENPs released is expected to be higher to technical compartments, 37,010, 56,715 and 149,030 t/year for the years 2017, 2030 and 2050, respectively (Giese et al., 2018).

Detecting, characterising and quantifying ENPs in surface waters or WWTP effluents, by field monitoring would be an asset for assessing the environmental distribution of these substances (Liu and Cohen, 2014). However, these analyses are hampered by the limited resolution of the techniques applicable for ENPs detection in natural aquatic environments, the complexity of the sample's matrices and the levels of naturally occurring nanoparticulate matter (Laborda et al., 2016). Even with more advanced methods available, the development of a field monitoring campaign would be a daunting and costly endeavour, which could be unfeasible for such diversity of ENPs (Liu and Cohen, 2014). Therefore, ENMs-specific estimation models have been extensively used as a valuable tool to inform decision-makers about ENPs potential environmental releases.

Within the ENMs-specific models, a distinction must be made between environmental fate models (EFM) and material flow analysis (MFA). EFM describe nanomaterials fate and behaviour in one or more environmental compartments. An exhaustive and useful description of these models had already been made in previous model reviews (Dale et al., 2015; Gottschalk et al., 2013; Nowack, 2017). MFA models estimate nanomaterials release into the environment from products during their use, recycling and final disposal, following the lifecycle principle and tracking the materials mass-flows. MFA models are essential to know the predicted

environmental concentrations (PEC) of nanomaterials to understand their potential hazards to the environment and human health.

One of the earliest nano-MFA models was presented by Gottschalk et al. (2009), where five nanomaterials (TiO_2, ZnO, Ag, CNT and fullerenes) were modelled to calculate PEC for the US, Europe and Switzerland, using production volumes, product categories and releases as model inputs. Over the last decade, this kind of model has undergone several improvements, such as the addition of a temporal dimension, allowing the assessment of release variability over time (Sun et al., 2017, 2016). Table 2.1 summarises the predicted concentrations of ENMs in surface waters and in WWTP effluents published since 2009, using MFA models. It includes the most cited and the most up to date works. Due to the different dynamic and static modelling concepts applied in the studies, it is not possible to draw a direct comparison between the predicted released concentrations from the works. However, an overall analyse can be made to get a general knowledge of the expected range of ENPs released to WWTP effluents and surface waters.

The ENPs releases to surface waters and to WWTP effluents presented in Table 2.1, show the relation between release and production, since nano-SiO_2 generally presented the highest concentration for both WWTP effluents and surface waters, followed by TiO_2 and ZnO (Figure 2.4). The available modelled data suggests that ENPs may occur in some surface waters with amounts that can reach 25.5 µg/L (SiO_2 ENPs, Table 2.1).

Additional studies also predicted ENPs occurrence in European rivers. Dumont et al. (2015) predicted concentrations higher than 0.002 and 1.5 ng/L of Ag and ZnO ENPs, respectively, in 50% of river stretches studied, and 18 (Ag) and 150 ng/L (ZnO) in 10%. For the River Rhone (France), based in one WWTP as single emission source of TiO_2, Sani-Kast et al. (2015) predicted concentrations of 30, 10 and approximately 0 ng/L at 0, 151 and 303 km after the emission source, respectively. The authors considered that heteroaggregation and sedimentation were the major contributors to the nanoparticles decay. Quick et al. (2015) reported that 50% of the assumed ENPs emission concentration (10 ng/L) decreased due to heteroaggregation within 40 km from the WWTP source in Dommel River (Netherlands).

Table 2.1. Estimates of ENPs releases to WWTP and surface waters based on MFA models.

ENPs	Data	WWTP Effluent	Surface Water	Reference
TiO_2	Mode ($Q_{0.15}$-$Q_{0.85}$) µg/L	3.47 (2.50-10.8)	0.015 (0.012-0.057)	(Gottschalk et al., 2009)*
		1.75 (1.37-6.70)	0.002 (0.002-0.010)	(Gottschalk et al., 2009)**
		16 (13-110)	0.53 (0.40-1.4)	(Sun et al., 2014)*
	Mean µg/L	1640	-----	(Tiede et al., 2015)
ZnO	Mode ($Q_{0.15}$-$Q_{0.85}$) µg/L	0.43 (0.34-1.42)	0.01 (0.008-0.055)	(Gottschalk et al., 2009)*
		0.3 (0.22-0.74)	0.001 (0.001-0.003)	(Gottschalk et al., 2009)**
		2.3 (1.7-21)	2.3 (1.7-21)	(Sun et al., 2014)*
	Mean µg/L	636	----	(Tiede et al., 2015)
SiO_2	Mode (min-max) µg/L	44.4 (0.01-1557.6)	5.34 (0.0-25.5)	(Giese et al., 2018)*
	Mean µg/L	400	----	(Tiede et al., 2015)
CeO_2	Mode (min- max) ng/L	199.9 (0.03-1867.9)	7.01 (0.00-61.74)	(Giese et al., 2018)*
	Mean µg/L	0.000467	-----	(Tiede et al., 2015)
Ag	Mode ($Q_{0.15}$-$Q_{0.85}$) ng/L	42.5 (32.9-111)	0.76 (0.59-2.16)	(Gottschalk et al., 2009)*
		21.0 (16.4-74.7)	0.12 (0.09-0.43)	(Gottschalk et al., 2009)**
		0.17 (0.06-16)	0.66 (0.51-0.94)	(Sun et al., 2014)*
	Mode (min-max) ng/L	18.89 (0.06-151.2)	0.38 (0.00-4.17)	(Giese et al., 2018)*
	Mean µg/L	107	-----	(Tiede et al., 2015)
Al /AlO_x	Mean µg/L	1.29	-----	(Tiede et al., 2015)

The values presented are the most probable values (mode values - Mode) and their 15th and 85th percentiles ($Q_{0.15}$-$Q_{0.85}$) or minimum (min) and maximum (max).
*Europe data; **US data.

Although they are a valuable tool, the field-validation of models is currently hampered by the lack of reliable data on ENPs environmental concentrations. Nevertheless, a few nanoparticles have already been measured in some environmental compartments with concentrations in the ng/L and µg/L range (Table 2.2). The highest concentration for surface waters, 52-86 µg/L (Table 2.2), was found for nano-TiO_2 in a river stream in northern China (Shi et al., 2016). This value is significantly higher than the one found in WWTP effluents (27-43 µg/L, Table 2.2) in the same study, implying the presence of other important nano-TiO_2 sources (possible urban runoff or direct discharge). A concentration of 2.2 µg/L was found in

Missouri River (Donovan et al., 2016) also for nano-TiO_2. Neal et al. (2011) reported an average concentration of 1.81 µg/L (Table 2.2), for the same nanoparticles in some England rivers. These concentrations are higher than the modelled values reported for the same nanoparticles in surface waters (Table 2.1). The authors described that the highest concentrations were found in urban and industrialised areas, indicating anthropogenic origin. Gondikas et al. (2014) measured variations of Ti over one year in Lake Old Danube (Austria) and used the increase in Ti/Al ratio to discriminate between natural and engineered TiO_2 nanoparticles, since the abundance of local aluminium was much higher than titanium. Based on this ratio, they reported an average concentration of 1.38 µg/L for the TiO_2 ENPs (Table 2.2). The authors concluded that the TiO_2 ENPs found in in the lake water suspended mineral had similar composition to those usually used in sunscreens. Yang and Westerhoff (2014) published one of the first reports on ENPs particle mass concentrations measured in tap water, rivers and effluents from WWTPs using single-particle ICP-MS (sp-ICP-MS), which justifies the lower concentrations shown by these authors for TiO_2 in rivers (Table 2.2). In my best knowledge this is the only study that detected ENPs in tap water, 3.1 and 1.9 ng/L of Ti and Ag, respectively. More recently, De Klein et al. (2016) reported concentrations of Ce (0.04-0.27 µg/L) and Al (2.2-5.9 µg/L) in the Dommel River in the Netherlands (Table 2.2). Based on the well-established geochemistry of these elements, the authors assumed that Ce occurs as CeO_2 and $Al(OH)_3$, with sizes between 2 and 450 nm. They also detected Ti (0.63-1.15 µg/L) and Zr (0.074-0.23 µg/L) in <450 nm filtrates (Table 2.2). Since these metals are known to be insoluble, the authors assumed them to be in particulate form, as TiO_2 and ZrO_2. Markus et al. (2018) also analysed samples from the same river and a WWTP nearby. They concluded that there were nanoparticles in the treatment plant, as they found Ti and Au particles in both influent and effluent. They also observed, that in the river water samples, 80-90% of the mass concentration of the particles were attached to natural colloids or as clusters of smaller particles. Peters et al. (2018) reported nano-Ag concentrations from 0.3 to 2.5 ng/L (Table 2.2) with an average concentration of 0.8 ng/L and an average particle size of 15 nm, measured in multiple surface waters samples collected along rivers from Netherlands. In the same locations, nano-CeO_2 was detected with concentrations ranging from 0.4 to 5.2 ng/L (Table 2.2), with an average concentration of 2.7 ng/L and an average size of 19 nm. In the same study concentrations between 0.2 and 8.1 µg/L of TiO_2 particles in the range of 300 nm were also reported, probably due to aggregation. The particles were present in all the water samples, and sizes were comparable with the particle sizes that are used in nanomaterial applications and to consumer products (Peters et al., 2018). Despite the

predicted and measured values not exceeding the µg/L range, the above-mentioned expected increase of production and consequent use and release will raise the risk of contamination for surface water in the future. Point sources of ENPs contamination and long periods between ENPs input and the use of water contribute to an increase in the possibility of them to reach DWTP (Troester et al., 2016). However further research is needed to corroborate this hypothesis.

Table 2.2. Overview of ENPs concentrations measured in WWTP effluents, surface waters and tap water.

ENPs	Analytical method	WWTP	Surface freshwater	Tap water	Reference
TiO_2	sp-ICP-MS	95 ng/L 124 ng/l 169 ng/L (inf); 57 ng/L (eff)*	895 ng/L 67 ng/L	3.1 ng/L	(Yang and Westerhoff, 2014)[b]
		-----	2.2 µg/L	-----	(Donovan et al., 2016)
		30.5 µ/L (inf); 3.2 µg/L (eff)	-----	-----	(Johnson et al., 2011)
	ICP-MS**	-----	0.63 – 1.15 µg/L	-----	(De Klein et al., 2016)
		27 – 43 µg/L	52 – 86 µg/L	-----	(Shi et al., 2016)
	Sequential filtration / ICP-MS	-----	0.94 – 1.81 µg/L	-----	(Neal et al., 2011)[a]
	Electron microscopy	-----	1.38 µg/L	-----	(Gondikas et al., 2014)[a]
Ag	sp-ICP-MS	2.1 ng/L 0.4 ng/L 0.1 ng/L (inf); 0.1 ng/L (eff)*	0.2 ng/L 0.1 ng/L	1.9 ng/L	(Yang and Westerhoff, 2014)[b]
		-----	0.3 – 2.5 ng/L	-----	(Peters et al., 2018)
CeO_2	ICP-MS**	-----	0.04 – 0.27 µg/L	-----	(De Klein et al., 2016)
	sp-ICP-MS	-----	0.4 – 5.2 ng/L	-----	(Peters et al., 2018)
$Al(OH)_3$	ICP-MS**	-----	2.2 – 5.9 µg/L	-----	(De Klein et al., 2016)
ZrO_2	ICP-MS**	-----	0.074 – 0.23 µg/L		(De Klein et al., 2016)

Concentrations are presented as Ti or Ag, respectively.
* For this WWTP values were determined before microfiltration process (inf) and after (eff).
**0.45µm filtration prior to ICP-MS measurements
[a] Concentrations as total Ti or Ag.
[b] Particle mass concentrations as Ti or Ag.

2.5.2. ENPs behaviour in surface waters

When released into complex media as surface water, ENPs will suffer transformations that can be divided into physical, chemical and biological processes. These transformations depend on two complex and variable factors, the nature of the nanomaterial and the environmental conditions, which make the processes characterisation and prediction highly challenging (Lead et al., 2018).

Several works have already investigated the behaviour and fate of ENPs in aquatic environments (Chekli et al., 2015; Dale et al., 2015; Elzey and Grassian, 2010; Kaegi et al., 2013; Van Koetsem et al., 2015; Von Der Kammer et al., 2010; Weinberg et al., 2011), also, exhaustive and comprehensive description of these processes has been made in previous reviews (Klaine et al., 2008; Lead et al., 2018; Lowry et al., 2012; Nowack et al., 2012; Peijnenburg et al., 2015). In 2008, Klaine et al. were pioneers in summarising the escalating progress of nanomaterials in the environment, with a review about their behaviour, fate, bioavailability and effects, which become the most cited paper on nanoparticles in the environment and nanotoxicology. Recently, Klaine´s original co-authors with other colleagues updated this review (Lead et al., 2018). In the present review, the behaviour of ENPs in surface waters is approached from a perspective of water treatment, since knowing these transformations is extremely useful to better understand the behaviour of ENPs in drinking water treatment processes and select the most appropriate operations to remove them effectively remove.

Once in surface waters, ENPs might interact with each other or with naturally occurring water components, such as natural organic matter (NOM), colloidal matter and dissolved molecules. These interactions can result in the formation or breakdown of aggregates or agglomerates and sedimentation and deposition (physical processes). It can also occur chemical transformations including redox reactions, dissolution and subsequent speciation variations and photochemical reactions. Biological processes can comprise biodegradation and biomodification, most likely microbially mediated (Amde et al., 2017; Baalousha, 2009; Dale et al., 2015; Lead et al., 2018; Lowry et al., 2012; Merdzan et al., 2014).

Currently, it is generally accepted that Derjaguin, Landau, Verwey and Overbeek (DLVO) theory as the combination of repulsive and attractive forces works well to understand nanoparticles charge (de)stabilisation (Baalousha, 2009; Baalousha and Lead, 2013; Gottschalk and Nowack, 2011; Serrão Sousa and Ribau Teixeira, 2013). The key factors in the aggregation of charge-stabilised nanoparticles in surface waters are the surrounding solution chemistry,

expressed in terms of parameters such as pH, ionic strength, NOM concentration and type, hydrodynamic conditions and temperature, along with the concentration of ENPs. The structure and aggregation mechanisms of nanoparticles are both pH- and NOM-dependent, and the ionic strength, type and valence of the electrolytes also have a high effect on these mechanisms (Amde et al., 2017; Fabrega et al., 2011; Karlsson et al., 2009; Lead et al., 2018; Lowry et al., 2012). pH influences the aggregation and disaggregation of nanoparticles by altering surface charge (Baalousha, 2009) whereas ionic strength increase will lead to aggregation (Lead et al., 2018). Humic and fulvic acids can have a significant effect on the stability of nanoparticles against aggregation (Chekli et al., 2015; Yang et al., 2017; Yu et al., 2018; Zhang et al., 2009). NOM adsorbs to the surfaces of colloidal nanoparticles, which modifies surface characteristics, in turn, increasing the particles stability. Surface coating of nanoparticles by NOM influences the aggregation rate of particles by electrostatic stabilisation mechanisms and electrosteric repulsion (Chekli et al., 2015; Gallego-Urrea et al., 2011; Keller et al., 2010; Loosli et al., 2013; Lowry et al., 2012; Mohd Omar et al., 2014; Ottofuelling et al., 2011; Peng et al., 2017; Serrão Sousa and Ribau Teixeira, 2013; Yang et al., 2017).

Recent studies have shown that dissolution and solubility are affected by specific intrinsic nanoparticle properties like size, coating and doping (Adeleye et al., 2018; Toncelli et al., 2017; Tsiola et al., 2017). In addition, external factors like NOM may enhance dissolution along with particle ripening and precipitation (Merrifield et al., 2017; Xiao et al., 2018). Wasmuth et al. (2016) reported that the complex system of natural waters substantially affects the dissolution of nanomaterials. Other factors, such as sunlight can change the environmental fate and toxicity of some nanoparticles and affects their dispersion in the natural water environment (Li and Lenhart, 2012; Mittelman et al., 2015; Wodka et al., 2010). Silver released during particle dissolution can occur under particle irradiation by a variety of light such as sunlight. Odzak et al. (2017) concluded that Ag NP dissolution increased with visible light for natural waters studied in comparison to dark conditions, while UV-light decreased the dissolved Ag^{+} after longer exposure time. Ag NP particle dissolution is reduced by photoreduction catalysed by photoreactive species at the surface of the original nanoparticles and subsequently changing particle shape and morphology (Li and Lenhart, 2012; Mittelman et al., 2015). For ZnO NPs, Odzak et al. (2017) observed that pH was predominant for dissolution, with visible and UV-light promoting dissolution. UV light and visible light led to the formation of reactive oxygen species (ROS), which caused increased dissolution of silver by oxidation and of zinc oxide due to the loss of organic coating compounds (Odzak et al., 2017). UV radiation also promotes the

generation of ROS for TiO_2 NPs, which can degrade contaminants entirely in a short reaction time (Lu et al., 2016). However, under visible light the photocatalytic properties of the TiO_2 NPs are relatively imperceptible due to the large energy gap (Lu et al., 2016; Wodka et al., 2010).

Questions remain about the reversibility and time periods of ENPs transformations and their effects on persistence and bioaccumulation in surface waters, and more research is needed. In addition, the high variability of ENPs entering the market hamper the accurate prediction of fate and behaviour of these substances in surface waters.

2.6. Water treatment plants ability to cope with the ENPs in drinking water

The release of ENPs into surface waters raises the concern about contamination of drinking water sources. Therefore, DWTPs should be a barrier to these materials between source to tap to provide safe potable water (Westerhoff et al., 2018). However, the appealing innovative and unique configurations and properties of ENPs make them more likely to persist in water and hamper their effective removal, increasing the risk of human exposure via ingestion of drinking water. Thus, to be sure that ENPs do not pose hazards to human health, it is necessary to ensure their complete removal during DWT.

To authors best knowledge, only two studies have been published reporting ENPs predictions in treated drinking water. O'Brien and Cummins (2010) estimated concentrations between 0.0441 and 1.4482 µg/L for TiO_2 ENPs, 0.0009 and 0.0295 µg/L for Ag ENPs and 0.00074 and 0.0243 and 0.0243 µg/L for CeO_2 ENPs in Irish drinking waters. In turn, Tiede et al. (2015) presented estimations for UK treated drinking water between $4.91x10^{-4}$ and $1.55x10^{-1}$ µg/L for TiO_2, $3.21x10^{-5}$ and $1.02x10^{-2}$ µg/L for Ag and $1.40x10^{-10}$ and $4.43x10^{-8}$ µg/L for CeO_2. The estimates from the first study are somewhat higher than the latter one, which is most likely due to differences in the removal efficiencies during DWT assumed by authors in their studies (0% removal for Irish´s DWTP and 97-99% for the UK).

2.6.1. ENPs characterisation required for drinking water treatment

As well known, the effectiveness of the drinking water treatments is strongly dependent on the source water characteristics and contaminants. Thus, to target specifically the removal of

ENPs in DWTP, it is not only imperative to understand their behaviour in surface waters, but also an appropriate physicochemical characterisation is critical. The ENPs size, surface charge, aggregation state and dissolution, interactions with NOM and ionic strength will influence the efficiency of ENPs removal during DWT. Therefore, the knowledge of those characteristics is crucial to specifically design an operational treatment line able to remove ENPs as also other target contaminants and naturally occurring compounds present in the water sources, whose removal is required in DWT.

Dynamic Light Scattering (DLS) is one of the most used high-throughput techniques to measure NPs size in aqueous media. According to their size, the nanoparticles and aggregates acquire different mobility, namely Brownian motion. In DLS, this movement is measured trough time-dependent fluctuations in scattering intensity and related to an equivalent hydrodynamic diameter (Brar et al., 2010; Laborda et al., 2016). However, this technique presents inherent limitations. The presence of heterogeneous size distributions or interfering particles, like environmental samples, difficult the correct interpretation of the data acquired by DLS. Another drawback is associated to the powerlessness to detect small particles among bigger ones, because of the intensity of scattered light that is proportional to the sixth power of the diameter, and the analysis is heavily weighted towards larger particle size (Laborda et al., 2016; Maguire et al., 2018). This is particularly important in samples containing particles with heterogeneous size distributions like surface waters (Laborda et al., 2016; Stetefeld et al., 2016). Despite drawbacks, DLS is very valuable to determine aggregates size and to monitor aggregation behaviours (Laborda et al., 2016). In its turn, microscopic techniques provide an accurate assessment of the individual size and shape of nanoparticles dispersed in water.

Nanoparticle tracking analysis (NTA) is also a light scattering technique, where Brownian movement is measured by video microscopy, and the hydrodynamic diameter is calculated using a modified Stokes-Einstein equation. Firstly, single particles are detected, and the distance travelled by the particle in each time period is related to their hydrodynamic diameter. In the end, particle-number concentration and hydrodynamic-size distribution are obtained. Since NTA tracks individual particles, it is not subjected to the limitations of DLS in polydisperse samples. This technique also shows high sensitivity related to particle-number concentration and reliable size distribution in samples with large particles or aggregates and consumes less time than microscopy techniques to measure a large number of individual ENPs. However, due to detection limitations, reliable data cannot be obtained for particles under 20 nm (Gallego-Urrea et al., 2011; Laborda et al., 2016; Saveyn et al., 2010).

Electron microscopy (scanning and transmission electron microscopy, TEM and SEM) is considered one of the most powerful techniques to analyse nanoparticles, since it provides surface images of nanoparticles allowing the collection of information about size, shape and aggregation state (Calzolai et al., 2012; Hendrickson et al., 2011; Lapresta-Fernández et al., 2014). Despite the fact that TEM provides precise information about size dimension, it is not considered the ideal approach for quantification due to the high number of particles to be counted and sized to get statistically significant and representative results, therefore, it is a time-consuming and low-throughput technique (Howard, 2010).

To determine the surface charge of nanoparticles is commonly used electrophoretic light scattering (ELS), expressed as zeta potential. In this technique, an electric field is applied and the electrophoretic mobility of suspended nanoparticles in the medium is measured (Rocha et al., 2015; Varenne et al., 2015). Zeta potential is usually affected by ionic strength and pH of water (Serrão Sousa and Ribau Teixeira, 2013).

The sedimentation rate of nanoparticles is another parameter of great interest in water treatment, mainly if conventional operations will be considered for ENPs removal. This parameter can be measured by any quantification method. However, the change in turbidity with time is a simple, immediate and less expensive way to determinate the sedimentation rate as showed by Serrão Sousa and Ribau Teixeira (2013). Moreover, turbidity is an essential parameter to evaluate the performance of water treatments, especially if conventional treatments are used. Sedimentation rate can be related to the normalised nanoparticle turbidity C/C_0, where C is the turbidity at time t and C_0 the initial turbidity at time 0. The sedimentation rate is $\delta(C/C_0)/\delta t$, which is estimated from the initial 5% decrease in normalized particle turbidity, which occurs within the first hour for the fast sedimentation conditions and within 12 hours for slow sedimentation conditions (Keller et al., 2010; Li and Sun, 2011).

At last, to evaluate the efficiency of the water treatments in the removal of ENPs, detection and quantification techniques must be applied to the raw surface water and the treated drinking water. Atomic spectrometry techniques, like atomic absorption spectrometry (AAS), inductively coupled plasma mass spectrometry (ICP-MS) or optical emission spectrometry (ICP-OES) are valuable tools for sensitive detection, as well as for quantification of the ENPs presents in the water samples (Krystek et al., 2011). ICP-MS is one of the most used to quantified inorganic ENPs, due to the low detection limits achievable (down to ng/L). In its turn, ICP-OES provides detection limits in the µg/L range, and AAS offers a half-way performance between both (Krystek et al., 2011; Laborda et al., 2016). The main goal of these

techniques is to determine the total element concentration in the sample since they are not capable of providing any data about physicochemical form (dissolved or particulate) nor about size, charge or aggregation state (Krystek, 2012). In the case of ICP-MS, these limitations can be overcome by coupling it to a continuous separation technique where ICP-MS acts as on-line element-specific detector. On the other hand, single particle ICP-MS (sp-ICP-MS) is gaining significant interest due to the ability to provide information about the nanoparticles number concentration and the elemental mass content (Dimkpa et al., 2012; Laborda et al., 2016). With additional data about shape, composition and density, the number size distributions can be obtained. Aggregation processes and polydisperse systems can also be analysed, due to the sp-ICP-MS range extended up to micrometres. Although the presence of dissolved species is determined, they may hamper the detection of the nanoparticles (Montaño et al., 2014). sp-ICP-MS detection limits are within the range of 1000 particles/mL for number concentration and 10-20 nm for size of mono-element NPs or more than 100 nm for oxides (Laborda et al., 2013; Lee et al., 2014). This technique has already been used to detect the presence of NPs, dissolved forms or both in wastewaters and to track the NPs dissolution and agglomeration in natural waters (António et al., 2015; Mitrano et al., 2014, 2012; Tuoriniemi et al., 2012).

2.6.2. ENPs removal in drinking water treatment

Conventional DWT processes, such as pre-oxidation, coagulation, flocculation, sedimentation (C/F/S) and granular media filtration, are focused on the removal of small particles, suspended solids, NOM, and other soluble inorganic compounds from water (Zouboulis et al., 2009), microorganisms and pathogens (Teodosiu et al., 2018). Coagulation (destabilisation of dissolved particles by the action of coagulants), flocculation (destabilised particles aggregate into larger flocs) and sedimentation (removal of flocs by gravity) (Abbott Chalew et al., 2013; EPA, 1999) are critical processes in conventional treatment, due to cost-efficiency rate (Jiang, 2015). Thus, C/F/S is a key step for the removal of ENPs in the DWTP. However, to effectively remove ENPs, the adoption of advanced treatment technologies may be necessary due to nanoparticles specific characteristics. Within advanced DWT, there are membrane processes, advanced oxidation processes (AOPs), and adsorption on activated carbon and other materials. Considering the wide range of ENPs that belong to metal-based category, individual treatment operations may be needed to maximise the overall removal efficiencies of ENPs.

Since 2009, few studies (summarised in Table 2.3) have been undertaken on the removal of metal-based ENPs in drinking water concluding that, although most water treatment processes have not been designed to remove such substances, some removal occurs.

2.6.2.1. ENPs removal by the conventional water treatment C/F/S

Sun et al. (2013), Abbott Chalew et al. (2013), Honda et al. (2014), Kinsinger et al. (2015) and Serrão Sousa et al. (2017) investigated the removal of ZnO, Ag and TiO_2 ENPs by conventional treatment C/F/S applying aluminium and iron-based coagulants to different types of water (Table 2.3). These studies were performed using scaled-down jar-test experiments (100 to 150 mL) (Abbott Chalew et al., 2013; Honda et al., 2014; Kinsinger et al., 2015) or bench-scale jar-test unit (500 and 800 mL) (Serrão Sousa et al., 2017; Sun et al., 2013). Similar C/F/S operating parameters (mixing speed and time) were applied to all the jar-test experiments since they were set based on these processes typical conditions. The adopted methodology comprised a rapid mixture, followed by slow mixture and finishing with settling. The parameter with the highest variability between the referred studies was sedimentation time, 1 h to the scaled-down experiments (Abbott Chalew et al., 2013; Honda et al., 2014; Kinsinger et al., 2015) and 20-30 min to bench-scale (Serrão Sousa et al., 2017; Sun et al., 2013).

Sun et al. (2013) tested four different coagulants in natural surface water (NSW) spiked with 1 mg/L of synthesised Ag ENPs. They used Al-based coagulants, namely alum (495 mg/L) and polyaluminium chloride (PACl) (30 mg/L) and iron-based, ferric chloride (400 mg/L) and polyferric sulfate (47 mg/L). The dosages were predetermined based on the minimum quantity of coagulants to produce flocs. Results are shown in Table 2.3. The authors used stock suspensions of Ag nanoparticles diluted with borate buffer, which is known to have a reduction effect on the release of silver ions (Liu and Hurt, 2010) and therefore may mask the removal results, since particulate form of nanoparticles is more favourable to be removed by C/F/S than dissolved ions.

Abbott Chalew et al. (2013) investigated the breakthrough of three commercial ENPs, Ag, TiO_2 and ZnO, into finished drinking water using NSW and synthetic surface water (SSW) with and without NOM (Table 2.3). The coagulant tested was potassium alum, and the optimal dose to each water was achieved as the minimum dose required to effectively remove both turbidity and total organic carbon (TOC). When the optimal dose was not the same for both parameters,

the highest dose was selected. Potassium alum optimal doses varied between 1.42 and 3.84 mg Al/L with the highest dose applied to the SSW with NOM.

Honda et al. (2014) and Kinsinger et al. (2015) used the same SSW and commercial TiO_2 ENPs (Table 2.3), while Honda et al. (2014) used only bare ENPs, Kinsinger et al. (2015) used both bare and synthetic organic coating model (DMSA) nanoparticles. This was the only study where the influence of synthetic organic coating on the nanoparticle's removal was evaluated. Honda et al. (2014) tested three different coagulants (iron chloride, iron sulphate and alum) to investigate their role in the removal of 10, 25, 50 and 100 mg/L TiO_2 NPs. Kinsinger et al. (2015) tested only alum at fixed TiO_2 NPs concentration of 100 mg/L using SSW and SSW with Suwannee River Humic Acid (SRHA) to simulate NOM (SSW_NOM).

Serrão Sousa et al. (2017) used four SSW with different organic matter concentration (moderate, *ca.* 2-3 mg C/L, or moderate-high, *ca.* 6 mg C/L) and nature (hydrophilic, SUVA < 3, or hydrophobic, SUVA > 4) to simulate diverse natural waters and NSW from a dam used for public supply. C/F/S experiments were conducted with a commercial polyaluminium coagulant/flocculant used in real context water industry at concentrations between 0 and 10 mg Al_2O_3/L to achieve the optimal dose to maximise the nanoparticles removal in each water. These authors not only investigate the efficiency of C/F/S to remove commercially available TiO_2 NPs but also explored if the nanoparticles removal affected the ability of this treatment to remove NOM and turbidity and consequently the quality of treated water.

As presented in Table 2.3, the efficiency rates showed high variability, demonstrating that ENPs removal by C/F/S depends largely on the type of ENP, dosage, type of coagulant/flocculant and water matrix (Abbott Chalew et al., 2013; Honda et al., 2014; Kinsinger et al., 2015; Serrão Sousa et al., 2017; Sun et al., 2013). As previously described, ionic strength and NOM affects the ENPs properties influencing the efficiency of ENPs removal during DWT. Abbott Chalew et al. (2013) reported that TiO_2 ENPs, with a nominal size of 33.7 nm, formed aggregates with 1147±234 nm in NSW and 3338±984 nm in SSW due to the high ionic strength of these waters. As expected, when the same ENPs were dispersed in SSW with 5 mg C/L (SSW_NOM), the aggregates were reduced to 248.1±8.03 nm, since NOM imparts a negative charge to NPs surfaces and raises their absolute surface potential (Zhang et al., 2009), having a general stabilizing effect upon nanoparticles. The difference in TiO_2 aggregates size between NSW and SSW was also due to the NSW higher content of NOM. Additionally, Serrão Sousa et al. (2017) observed the formation of TiO_2 ENPs (nominal size < 100 nm) aggregates with similar sizes ranging from 300±18 to 440±56 nm when dispersed in SSW (for the same

ionic strength) with the lowest sizes corresponding to higher NOM content and vice versa. Ag ENPs with individual size of 83.6 nm (Table 2.3) formed aggregates with approximately 223 and 248 nm in NSW and SSW, respectively (Abbott Chalew et al., 2013). ZnO ENPs with 35.6 nm (Table 2.3) presented aggregates with 353 and 7021 nm in NSW and SSW, respectively (Abbott Chalew et al., 2013). As observed for TiO_2, Ag and ZnO, aggregation was also reduced in the presence of NOM (SSW_NOM), being approximately 199 and 321 nm, respectively (Table 2.3) (Abbott Chalew et al., 2013). In all these studies, aggregates sizes were determined by DLS technique, described previously in this review.

As discussed earlier, the presence of NOM in raw water increases the stability of ENPs, imparting a negative charge to their surface, consequently increasing the absolute surface potential. Serrão Sousa and Ribau Teixeira (2013) showed that NOM enhanced CuO NPs stability, reducing their aggregation and limiting the size of aggregates, which decreased the removal of ENPs in waters with a high NOM content. As shown by Kinsinger et al. (2015), the presence of NOM decreased the removal of TiO_2 NPs by alum (50 mg/L) from 98.7%±1.5% (SSW) to 80.4%±2.6% (SSW_NOM) (Table 2.3), due the interaction ENPs-NOM (coating formation) and NOM-coagulant (Honda et al., 2014; Kinsinger et al., 2015; Serrão Sousa and Ribau Teixeira, 2013). Additionally, metal species, like aluminium, preferentially react more readily with free NOM than ENPs in aqueous media (Park et al., 2017). Serrão Sousa et al. (2017) showed that, besides concentration, NOM nature also plays an important role in the removal of TiO_2 NPs. As shown in Table 2.3, for hydrophobic synthetic waters (SSW2 and SSW4), a higher coagulant dose was needed to achieve similar Ti removals to those observed in hydrophilic waters. Among hydrophilic/hydrophobic waters, for the same NOM concentration, waters with higher SUVA values needed a higher coagulant dose to achieve similar Ti removals. These authors also demonstrated that after "effective coagulation zone" the excess of coagulant promoted the re-stabilisation of the TiO_2 NPs decreasing the removal efficiencies. These results demonstrated that during the coagulation process, the behaviour of ENPs is governed by the same mechanisms that control colloidal stability.

The effectiveness of Al or Fe-based coagulants can also be compared through the results presented in Table 2.3. Overall, the Al-based coagulants showed higher removals when compared directly with Fe-based (Honda et al., 2014; Sun et al., 2013). Among the Fe-based coagulants tested in these studies, polyferric sulfate was more effective than $FeCl_3$ in the removal of Ag ENPs (Sun et al., 2013) and $FeSO_4$ more effective than $FeCl_3$ in the removal of TiO_2 ENPs (Honda et al., 2014). Among the Al-based coagulants, polyaluminium chloride was

the most effective in the removal of Ag ENPs (Sun et al., 2013), as also in the removal of TiO_2 ENPs (Honda et al., 2014; Kinsinger et al., 2015; Serrão Sousa et al., 2017), at doses well below those applied to alum and for different concentrations and nature of NOM (Serrão Sousa et al., 2017) (Table 2.3). In those studies, removals were as high as 96-100% (Table 2.3). The effectiveness of PACl is related to its high positive charge. The negatively charged ENPs surface can be destabilised (neutralised) through the addition of positively charged coagulant, resulting in higher ENPs aggregation due to reduced electrostatic repulsion, improving their sedimentation and consecutive removal. As demonstrated by Serrão Sousa et al. (2017), high contents of NOM in the water matrix needed a higher coagulant dose to achieve the same removal of ENPs, which showed that the main driver in determining optimal coagulant dose was NOM rather than the ENP concentration in water. The same authors confirmed TiO_2 initial concentrations, ranging between 0.2 and 10 mg/L, had not a significant impact on NPs removal and the removal efficiency was always higher than 90%.

Apart from the aggregation state, nanoparticles removal is also associated with other properties such as dissolution and ENPs coating. Abbott Chalew et al. (2013) related the low removal of Zn and Ag to the high dissolution rate of these ENPs. ZnO had the highest breakthrough, with removals of 35% and 5% for NSW and SSW_NOM, respectively. For SSW, the breakthrough was complete without any removal observed for ZnO. This was not observed in the results of Sun et al. (2013) since the authors used borate buffer in the Ag NPs suspension to reduce the release of silver ions. Kinsinger et al. (2015) reported high removal for bare TiO_2NPs with alum, 98.7%±1.5%. However, when TiO_2NPs coated with DMSA (synthetic organic coating model) were used, the removal decreased to 74.9%±1.6%. Similar drop trend happened when 1 mg/L of SRHA was used to simulate NOM. In the presence of NOM, the removal of coated NPs decreased to 68.7±3.4% (Table 2.3). This suggests that due to the dependence of ENPs removal on their physicochemical properties, the optimal dose of coagulant might be different even for ENPs of the same elemental composition. However further research on this issue is required.

To my best knowledge, Serrão Sousa et al. (2017) were the only authors that showed that the high removals of Ti from NSW, using coagulant doses optimised to ENPs removal, did not compromise the quality of final treated water, since all the quality parameters studied were below guidelines (turbidity, Al concentration, pH, conductivity and Ti).

2.6.2.2. ENPs removal by advanced membrane filtration treatment processes

Membrane filtration has become an attractive advanced technology for physical removal of contaminants in drinking water. Currently, there are few drinking water contaminants that cannot be removed by membrane filtration (Edzwald, 2011). Low-pressure membranes filtration such as microfiltration (MF) and ultrafiltration (UF) with pore sizes typically larger than 0.1 µm and between 0.001 and 0.1 µm, respectively, are processes specially designed to remove particles.

Despite several studies have been performed to evaluate the extent to which membrane filtration removes ENPs (Abbott Chalew et al., 2013; Ladner et al., 2012; Serrão Sousa and Ribau Teixeira, 2015; Springer et al., 2013), only few were applied to surface waters and DWT (Abbott Chalew et al., 2013; Serrão Sousa and Ribau Teixeira, 2013) (Table 2.3).

Abbott Chalew et al. (2013) simulated advanced treatments MF and UF in DWTP to evaluate the removal of Ag, TiO_2 and ZnO ENPs from NSW, SSW and SSW_NOM. Flat-sheet membranes with a nominal pore size of 0.45 µm (MF) and 0.02 µm (UF) were used (Table 2.3). In the MF experiments, the highest removal was obtained for TiO_2 NPs in SSW (99.6%±0.21%, Table 2.3) which corresponds to the highest aggregates formed and smaller aggregates or stabilised ENPs breakthrough MF membrane. The lowest removal was achieved for the ZnO ENPs in SSW (17.3%±5.62%, Table 2.3) due to dissolution, similarly to what occurred in C/F/S experiments. Dissolution of ZnO ENPs was confirmed by the authors through the similar removals observed for MF and UF since UF pore size was smaller than primary particles. Therefore, only dissolved ions could breakthrough the membrane. UF removals were higher than 95% for Ag and TiO_2 ENPs in all the water types tested (Table 2.3). These results showed a clear removal efficiency dependence on membrane pore size, ENPs size and ENPs stability (either aggregation or dissolution). Abbott Chalew et al. (2013) results also demonstrated that constant ENPs removal occurred when pore sizes were smaller than nanoparticles size. However, dissolved ions released by ENPs and some stabilised nanoparticles breakthrough UF membranes, showing that tighter membranes would be required for their effective removal. Bearing in mind this concern, Serrão Sousa and Ribau Teixeira (2015) studied the removal of silver nanoparticles from synthetic waters by nanofiltration (NF). The authors simulated the NF treatment using a lab scaled-up unit with 1.44 m^2 of membrane area at an operational pressure of 10 bar. Two sets of negatively charged membranes were used, NF90 and NF270, and SSW with different NOM nature and concentration were tested (Table 2.3). The authors reported Ag-total removals between 92.6% and 97.5% under the first 0.25 h of operation with NF90

membrane and 82.2% and 93.7% with NF270, but some ions were able to breakthrough into treated water (Table 2.3). However, with operation time all the removals increased, and after 3 h of operation, removals were between 97.4% and 99.0% for NF90 and 98.7% and 99.7% for NF270 (Table 2.3). The results showed that size exclusion was the main mechanism of Ag ENPs removal. The removal of Ag ions was suggested to be trough the complexation with salts and adsorption on NOM or NOM-Ag complexes in solution.

Table 2.3. Summary of experimental studies on metallic nanoparticle removal in drinking water treatment processes.

Drinking Water Treatment	ENPs	[ENPs] mg/L	Water Type	Removal (%)				References
C/F/S Potassium alum 1.42 - 3.84 mg Al/L	Ag (83.6 nm) TiO_2 (33.7 nm) ZnO (35.6 nm)	10	NSW SSW SSW_NOM		NSW	SSW	SSW_NOM	(Abbott Chalew et al., 2013)
				Ag	79.6±12.8	97.9±1.19	87.5±17.7	
				TiO_2	91.5±3.86	94.1±3.20	96.6±0.96	
				ZnO	51.7±7.12	4.49±2.42	0.46±2.42	
C/F/S $Al_2(SO_4)_3$ – 495 mg/L $FeCl_3$ – 400 mg/L PACl[a] – 30 mg/L PFS[b] – 47 mg/L	Ag (12.1 nm)	1	NSW	99±1 ($Al_2(SO_4)_3$) 91±9 ($FeCl_3$) 100 (PACl) 92±7 (PFS)				(Sun et al., 2013)
C/F/S $FeCl_3$ $FeSO_4$ Alum ($Al_2(SO_4)_3$) 50 mg/L	TiO_2 (≈ 20 nm)	10, 25, 50, 100	SSW	32-68 ($FeCl_3$) 80-90 ($FeSO_4$) 90-99 (Alum)				(Honda et al., 2014)
C/F/S Alum ($Al_2(SO_4)_3$ 50 mg/L	TiO_2 bare and DMSA coated (≈ 20 nm)	100	SSW SSW_NOM (1 mg/L SRHA)			SSW	SSW_NOM	(Kinsinger et al., 2015)
				Bare		98.7±1.5	80.4±2.6	
				DMSA coated		74.9±1.6	68.7±3.4	
C/F/S Commercial polyaluminium chloride WAC® (0 – 10 mg/L Al_2O_3)	TiO_2 (< 100 nm)	10	NSW SSW (4 with different concentration and nature of organic matter)	SSW1: ≈96.5 (0.5 mg/L Al_2O_3)[c] SSW2: ≈96.0 (3.0 mg/L Al_2O_3) SSW3: ≈98.0 (3.0 mg/L Al_2O_3) SSW4: ≈98.0 (5.5 mg/L Al_2O_3) NSW: ≈99.8 (2.0 mg/L Al_2O_3)				(Serrão Sousa et al., 2017)

Table 2.3. (cont.). Summary of experimental studies on metallic nanoparticle removal in drinking water treatment processes.

Microfiltration[d] 0.45 µm (pore size)	Ag (83.6 nm) TiO_2 (33.7 nm) ZnO (35.6 nm)	10	NSW SSW SSW_NOM		NSW	SSW	SSW_NOM	(Abbott Chalew et al., 2013)
				Ag	85.5±10.4	95.6±6.48	92.1±4.23	
				TiO_2	83.1±0.81	99.6±0.21	56.2±25.8	
				ZnO	31.4±24.1	17.3±5.62	44.4±26.1	
Ultrafiltration 0.02 µm (pore size)	Ag (83.6 nm) TiO_2 (33.7 nm) ZnO (35.6 nm)	10	NSW SSW SSW_NOM		NSW	SSW	SSW_NOM	(Abbott Chalew et al., 2013)
				Ag	98.2±2.44	98.6±4.68	99.7±0.37	
				TiO_2	99.8±0.24	95.6±0.99	98.7±1.58	
				ZnO	3.93±33.0	15.0±7.20	64.0±16.2	
Nanofiltration[e] NF90 (0.34 nm pore radius) NF270 (0.42 nm pore radius)	Ag (<100 nm)	100	SSW_NOM (4 and 16 mg/L AHA[f]) (4 and 16 mg/L TA[g])		4 mg/L AHA	16 mg/L AHA	4 mg/L TA	16 mg/L TA	(Serrão Sousa and Ribau Teixeira, 2015)
				NF90	97.5[h] 99.0[i] 99.1[j]	92.9[h] 99.8[i] 99.8[j]	92.9[h] 97.7[i] 98.3[j]	92.6[h] 97.4[i] 98.4[j]	
				NF270	82.2[h] 99.5[i] 99.7[j]	93.7[h] 99.7[i] 99.9[j]	89.1[h] 98.7[i] 99.3[j]	89.1[h] 98.7[i] 99.2[j]	

NSW – Natural Surface Water
SSW – Synthetic Surface Water
SSW_NOM – Synthetic Surface Water with NOM
SRHA – Suwannee River Humic acid
[a] Polyaluminium chloride
[b] Polyferric sulfate
[c] Optimal coagulant dose for each water tested
[d] Polyvinyldine fluoride (PVDF) membrane
[e] Polyamide/polysulfone membrane
[f] Aldrich Humic Acids
[g] Tannic Acid
[h] After 0.25h of operation
[i] After 3h of operation
[j] After 7h of operation

2.6.2.3. ENPs removal by other water treatments

Other treatments have also been studied, to a minor extent, in lab-scale experiments, but more research is needed to be able to understand their effectiveness on ENPs removal from drinking water. Li et al. (2013) undertake a first study in evaluating the potential removal of metal and metal oxides ENPs by granular media filtration with a sand bed, which is a conventional treatment commonly used in DWT. They reported that sand filters were able of retaining some portion of ENPs with bare surfaces, but for coated ENPs (ZnO-PVA, Ag-citrate and Ag-PVA) low or no measurable retention was achieved. These experimental and modelled results demonstrated the limited ability of this process to remove metal ENPs, however in DWTP C/F is usually performed prior to sand filtration which could improve its efficiency. Gicheva and Yordanov (2013) applied powder activated carbon (PAC), with particle sizes from 20 to 80 μm, to model solutions spiked with Ag ENPs (40-100 nm) to evaluate their removal by adsorption. The authors reported fast and complete removal of Ag ENPs (105 μg/mL), using 0.5 mg/mL of PAC. However, this high removal could only be achieved due to the addition of 40 mM NaCl. The high adsorption of Ag ENPs at increased salt concentrations indicated that adsorption is favoured when the electrostatic stabilisation of particles decreases. In addition, there is no data showing that these removals would also be achieved in waters with lower ionic strength. Thus, more in-depth studies will be worth it to understand in detail the adsorption extension and mechanism of ENPs in surface waters.

Despite the high ENPs removals found in the literature for water treatments such as C/F/S, MF, UF and NF, this review demonstrates that some metal breakthrough into finished waters can occur in all the studied processes. Although experimental concentrations of ENPs were higher than those predictable to surface waters, it is not expected a significant change in removal efficiencies, as previously referred. As illustrated in this review, ENPs aggregates size is an important parameter for ENPs removal in both conventional and advanced treatments. Higher aggregates are removed by floc settling during C/F/S, while smaller aggregates, individual ENPs and released ions can possibly be removed by physical separation during membrane filtration. Therefore, an integrated solution with a sequence of conventional and advanced processes may be necessary for an optimal removal of ENPs.

2.7. Conclusions and Perspectives

This review highlighted the presence, potential hazard to human health and environment, release and behaviour of metal-based ENPs in surface source waters and the susceptibility of drinking waters systems to these contaminants. Moreover, their removal from drinking water was discussed in detail. Considering that nanoparticles have already been detected in wastewater, surface water, raw and treated drinking water and tap water, ranging from ng/L to μg/L, DWTPs have to face their presence and occurrence in potable water so as not to endanger human health.

However, further research is still needed to address the challenge of DWTP to cope with these contaminants. Up to now, both conventional and advanced drinking water treatment have shown the potential to remove ENPs from drinking water. The reviewed studies show that if C/F/S, optimised to ENPs removal, and membrane filtration are applied in DWT, ENPs retention can be expected and the hazard can be mitigated. Yet, if only conventional treatment is applied, there is a high risk of ENPs presence in drinking water. Since less is known about ENPs toxicity by tap water ingestion compared with traditional contaminants, further research should be performed to develop strategies to entirely eliminate nanoparticles from drinking water. Nevertheless, comprehensive evaluation of ENPs toxicity is urgently needed, as also stringent requirements in the frameworks of the government environmental regulation.

More research is needed in the field of ENPs in DWT: i) develop suitable analytical techniques for the quantification of ENPs in complex matrices, like surface water sources, ii) investigate the efficiency of ENPs removal by conventional and advanced combined treatments operating at typical plant conditions, since the vast majority of studies have focused only in individual processes, iii) assess the effect of multiple types of ENPs (mixtures) in their removal in DWT, and iv) investigate ENPs removal at pilot-scale.

The water industry regulators tend to be cautious when regulating, however DWTPs are not yet required to monitor ENPs. It will be prudent for the drinking water community to conduct periodical analysis to measure the most common metal-based ENPs, because of the potential health impact on populations. Also, a focus on monitoring hotspots of ENPs releases could be an asset, particularly for DWTP intakes located downstream of large urban communities.

Chapter 3

The Effect of TiO_2 Nanoparticles Removal on Drinking Water Quality Produced by Conventional Treatment C/F/S

This Chapter was published in:

Serrão Sousa, V., Corniciuc, C. Ribau Teixeira, M. (2017). The effect of TiO_2 nanoparticles removal on drinking water quality produced by conventional treatment C/F/S. Water Research, 109, 1-12.

http://dx.doi.org/10.1016/j.watres.2016.11.030

ABSTRACT

Engineered nanoparticles (ENPs), namely titanium dioxide (TiO_2), are emerging contaminants widely used to commercial and industrial applications, are a potential hazard and can cause damage to the environment and human health due to their toxicity. Therefore, their removal from the water is urgent to minimise or eliminate the adverse environmental and human health effects. This work investigates the efficiency of conventional coagulation/ flocculation/ sedimentation (C/F/S) from drinking water treatment to remove TiO_2 ENPs from surface waters and pretends to understand if the removal of TiO_2 NPs affects the ability of C/F/S to remove natural organic matter (NOM) and turbidity, and consequently affects the quality of the treated water.

Results show that TiO_2 NPs removal is high (>95%) for all the waters studied (hydrophobic and hydrophilic waters) and the treated water quality is not compromised (turbidity, Ti and Al concentrations, pH and conductivity are below the national and international guidelines). In addition, TiO_2 initial concentrations, ranging between 0.2 and 10 mg/L, have not a significant impact on NPs removal by C/F/S. Therefore, the widely used polyaluminium based coagulants are effective in the removal of TiO_2 NPs by conventional C/F/S treatment, but removal is strongly influenced by the water characteristics. Hydrophobic waters need a higher coagulant dose than hydrophilic waters to achieve the same TiO_2 NPs removals, as well as water with higher UV_{254nm} values. The principal mechanism involved in TiO_2 NPs removal is charge neutralisation.

3.1. Introduction

Engineered nanoparticles (ENPs) have applications in several commercial products and industrial processes or materials, including cosmetics, drug delivery, electronics, energy technology, agricultural and environmental sciences (Handy et al., 2008; Popowich et al., 2015; Wiesner et al., 2009). There is evidence that during their usage and disposal, these nanoparticles will be released into aquatic systems (Gottschalk et al., 2013; Zheng et al., 2015). If the wastewater treatments processes are unable to remove nanoparticles from water, ENPs will enter in drinking water sources and natural aquatic environments, increasing the risk of exposure for plants, animals and humans (Farré et al., 2010). ENPs properties, like the large surface area to volume ratio and small size, provide unique materials with new applications compared to the corresponding bulk materials. However, these same properties may also result in the enhancement of the bioavailability, increasing their toxicity.

Titanium dioxide (TiO_2) is the most widely used nanomaterial due to its application as a pigment in cosmetics and paints, coatings and materials for environmental and energy technology (Piccinno et al., 2012; Savage et al., 2007). The annual production of this nanomaterial is around 40000 t in the USA (Savage et al., 2007) and 10000 t in Europe (Piccinno et al., 2012). According to Keller et al. (2013), 54% of the globally produced amount is expected to enter wastewater treatment plants (WWTP). TiO_2 nanoparticles have already been detected in biosolids and wastewater treatment effluents, which suggests that it may ultimately end up in surface water bodies (Keller et al., 2013; Westerhoff et al., 2011). Emissions to aquatic environmental via WWTP effluents are estimated to be around 1100 to 29000 t/year globally (Savage et al., 2007). Several researchers have estimated values between 21 and 10000 ng/L (Gottschalk et al., 2013; Gottschalk and Nowack, 2011; Mueller and Nowack, 2008).

Some researchers reported that nanoscale TiO_2 is a potential hazard and can cause damage to aquatic environmental and human health due to their toxicity. Nano-TiO_2 is photoinducible, redox-active and thus a generator of potential reactive oxygen species (ROS) (Menard et al., 2011). Canesi et al. (2010) have recently demonstrated that suspensions of selected nano-titanium dioxide induce oxyradical production and lysosomal enzyme release in the hemocytes of the marine mussel Mytilus in vitro, and Long et al. (2006) showed adverse effects of these NPs such oxidative stress in human cells.

Therefore, it is essential to evaluate how NPs can be effectively removed through water treatment processes to control the environmental and health risks associated with NPs exposure.

Conventional water treatment comprises coagulation, flocculation, sedimentation (C/F/S), filtration and disinfection. Coagulation is a key step for efficient and cost-effective water treatment process (Jiang, 2015). The objective of C/F is the removal of small particles, suspended solids, natural organic matter (NOM), and other soluble inorganic compounds from aqueous suspensions (Zouboulis et al., 2009). Therefore, coagulation is a critical process for the effective removal of NPs in drinking water treatment plants (DWTP) (Feng and Johnson, 2014). Few authors had already studied the removal of NPs by coagulation process. Chalew et al. (2013) simulated conventional wastewater processes to access the removal efficiency of NPs under conventional conditions. They observed that 2-20%, 3-8% and 48-99% of the spiked Ag, TiO_2 and ZnO NPs, respectively, remain in the treated water after the treatment process. Other studies have investigated the efficiency of nanoparticles removal using alum or iron coagulants for CuO NPs (Y. Wang et al., 2015), Ag NPs (Sun et al., 2013) as well as the most commercialised ENPs, nano-TiO_2 (Honda et al., 2014; Kinsinger et al., 2015; Wang et al., 2013). Despite the high removals obtained by these authors for TiO_2 ENPs using aluminium-based coagulants, high coagulant doses were applied (up to 50 mg/L of alum) (Honda et al., 2014; Kinsinger et al., 2015) and NOM reduced the TiO_2 NPs removal by coagulation (Kinsinger et al., 2015; Wang et al., 2013). Moreover, in these studies, the removal mechanisms involved in the ENPs removal (including TiO_2 NPs) is not well known, although all the authors agreed that one of the main influences in NPs removal by C/F/S is the water characteristics. Yet in any of those studies, natural waters were used.

These findings indicate that coagulation seems to be a good option for the removal of TiO_2 NPs from water. However, more attention should be paid to the effects of water quality when using coagulation to remove TiO_2 NPs. Therefore, it is imperative to conduct a study that assesses the current ability of conventional water treatment processes to remove nanoparticles from water, providing a possible solution to reduce the potential hazard caused by TiO_2 NPs.

The aim of this study is to investigate the removal of TiO_2 NPs by conventional drinking water treatment, C/F/S, and understand its overall effect in the processes. First, it is pretended to evaluate and improve the capacity of conventional C/F/S to remove TiO_2 NPs from surface waters and to study the influence of the water characteristics, namely NOM, on their removal. Second, this work pretends to determine if the removal of TiO_2 NPs affects the ability of C/F/S to remove NOM and turbidity, and consequently affects the quality of the treated water. These two objectives until now were not addressed together, which is the novelty of this work.

3.2. Material and methods

3.2.1. Model and natural waters

Four synthetic waters (W1, W2, W3 and W4) of different concentration (moderate/ moderate-high) and nature (hydrophilic/ hydrophobic) of organic matter were used to simulate different water characteristics. Inorganic matrix background was maintained in all the four waters (Table 3.1) as described in previous work (Ribau Teixeira et al., 2010). Dissolved organic carbon (DOC) was controlled by the addition of two natural organic matter (NOM) surrogates, Salicylic Acid (SA) and Aldrich Humic Acids (AHA) representing the hydrophilic, low molar mass NOM and the hydrophobic, high molar mass NOM, respectively. Both model substances were obtained from commercial sources and have been used to provide consistent experimental conditions (Campinas and Rosa, 2006; Hong and Elimelech, 1997; Tercero Espinoza and Frimmel, 2008). SA certified analytical grade reagent (>99.0% purity), with 138.12 g/mol (Merck, VWR International) was used with no further purification. AHA (Sigma-Aldrich) was prepared by dissolving it in deionised water and raising the pH to 8 through the addition of NaOH. Hydrophobic and hydrophilic DOC (based on SUVA values above 4 L/(m mgC) and below 3 L/(m mgC) respectively, Edzwald and Van Benschoten, 1990), and moderate and moderate-high DOC concentrations (2-3 mgC/L and ca. 6 mgC/L respectively, EPA, 1999) were studied. The water background ionic strength (IS) was provided by certified analytical grade (Merck, VWR International) mono (KCl) and divalent ($CaCl_2$) salts establish at 4.0 mM, which corresponds to moderately-hard water (AWWA, 2000). Hydrophilic waters presented lower pH values (Table 3.1) due to the addition of higher salicylic acid concentrations.

A natural water (NW) was also used in this work, collected from *Odelouca* dam (Algarve, South of Portugal), during the Spring season, courtesy of Algarve water company *Águas do Algarve, S.A.*. This dam supplies water to the *Alcantarilha* WTPs, which have a maximum capacity of 3 m^3/s (620,000 inhabitants). The characteristics of this water are also present in Table 3.1.

Table 3.1. Model and natural waters used in the experiments.

DOC concentration[a]	DOC nature[b]	Water	DOC (mgC/L)	$UV_{254\ nm}$ (1/cm)	SUVA (L/(m.mg))	Turbidity (NTU)	Conductivity (µS/cm)	pH (25ºC)
Moderate (*ca.*2-3 mgC/L)	Hydrophilic SUVA < 3	**W1**	2.67±0.29	0.03±0.00	1.25±0.06	1.13±0.01	375±1.0	4.7±0.0
	Hydrophobic SUVA > 4	**W2**	2.56±0.14	0.19±0.04	7.64±1.41	4.87±0.13	379±1.0	6.3±0.0
Moderate-high (*ca.* 6 mgC/L)	Hydrophilic SUVA < 3	**W3**	6.21±0.20	0.04±0.01	0.66±0.09	1.18±0.27	384±1.7	4.2±0.0
	Hydrophobic SUVA > 4	**W4**	5.83±1.66	0.50±0.02	8.55±0.65	9.49±0.72	387±1.0	6.8±0.1
Low-Moderate (*ca.*<*2* mgC/L)	Hydrophilic SUVA < 3	**NW**	1.66±0.03	0.03±0.00	2.02±0.0	2.12±0.01	163±0.1	7.6±0.0

[a] Edzwald and Van Benschoten (1990).
[b] EPA (1999) classification, *i.e.* moderate DOC concentration between 2.0 and 4.0 mgC/L, moderate-high between 4.0 and 8.0 mgC/L, and high DOC concentration above 8.0 mgC/L.
W1 – W4: model waters.
NW: natural water.

3.2.2. Characterisation of TiO_2 nanoparticles

Commercially available titanium (IV) dioxide (mixture of rutile and anatase forms) nanopowder (Sigma-Aldrich, LOT#02527PH) was used. According to the supplier, the particle size is <100 nm in diameter (by Brunauer Emmett Teller (BET) method), purity of 99.5 % trace metals basis, the specific surface area is 46.3 m^2/g, and the molecular weight is 79.87 g/mol.

The size of NPs suspensions was independently confirmed using dynamic laser scattering (DLS) as described below. The TiO_2 NPs were dispersed in deionised water (DW), without further purification, and suspensions were sonicated using a bath sonicator (USC500TH, VWR International) for 20 minutes. The sonication time was set after several optimisation experiments. The concentration of TiO_2 NPs was set at 50 mg/L to ensure the quality of the DLS analysis, as suggested by the equipment supplier. At least three measurements with 50-100 runs were made for each replicate (3 per sample) to ensure the quality of the analyses.

The TiO_2 NPs optical absorption measurements in the UV-Vis range were made in a Spectronic Unicam (UV300) spectrophotometer at room temperature. The wavelength used in experiments ranged from 200 to 800 nm.

The hydrodynamic diameter (HD) and zeta potential (ZP) of TiO_2 NPs were determined at 25°C by DLS and electrophoretic light scattering (ELS), respectively using a Zetasizer Nano ZS analyser (Malvern Instruments Inc., UK), as previously described (Serrão Sousa and Ribau Teixeira, 2013). The variation of HD and ZP with the pH was also evaluated. These parameters were determined in all the synthetic, and natural waters studied.

The sedimentation rate of the nanoparticles was measured by the turbidity variation with time as described in previous work (Serrão Sousa and Ribau Teixeira, 2013). Since turbidity increases with nanoparticle concentration, the sedimentation rate can be related to the normalised nanoparticle turbidity C/C_0, where C is the turbidity at time t and C_0 the initial turbidity at time 0 (Li and Sun, 2011). The sedimentation rate is $\delta(C/C_0)/\delta t$, which is estimated from the initial 5% decrease in normalised particle turbidity, which occurs within the first 1 h for the fast sedimentation conditions and within 12 h for slow sedimentation conditions (Keller et al., 2010). The sedimentation experiments were made using 1.0 and 10.0 mg/L of TiO_2 NPs.

3.2.3. Experimental setup and procedure

Coagulation/flocculation/sedimentation (C/F/S) experiments were carried out in a jar-test lab-scale unit (Flocumatic, Selecta, Spain) with four paddles at room temperature (21 ± 1ºC) using 800 mL/sample. The operating parameters (mixing speed and time) were set based on the typical operating conditions for C/F/S in drinking water treatment. Standard experimental procedure included: (a) coagulation at a velocity gradient (G) of 743 s^{-1}, corresponding to 200 rpm, for 2 minutes; (b) flocculation at G of 24 s^{-1} (20 rpm) for 20 minutes; (c) sedimentation at G of 0 s^{-1} for 30 minutes. Prior to the start of the experiment (i.e. before the coagulation stage), the TiO_2 suspensions were sonicated as described above. After sonication TiO_2, suspensions were placed into jars and stirred prior to coagulant addition for approximately 1 minute. Then the coagulant was added to the jars immediately after the start of the rapid mixture and when coagulation finished, TiO_2 zeta potential was measured. After sedimentation, an aliquot of 100 mL of the supernatant was sampled using a volumetric glass pipette from the mid-depth of the water column. Triplicate jar tests experiments were performed.

The coagulant/flocculant tested in this work was a commercial polyaluminium chloride WAC® from Elf Atochem (France) with 60 to 70% relative basicity (stock solution with 850 mg/L Al_2O_3). This coagulant/flocculant is commonly used in the real context water industry and applied in *Alcantarilha* WTP. The influence of coagulant dose was investigated for all the tested waters at doses between 0 to 10 mg/L Al_2O_3. The same C/F/S experiments were carried out with no coagulant added as a control trial.

C/F/S experiments were conducted with 10 mg/L of TiO_2 NPs for all the studied waters. This value is higher than the value estimated in the environment by several authors (Gottschalk et al., 2013; Gottschalk and Nowack, 2011; Mueller and Nowack, 2008) but it was chosen to provide good accuracy in DLS and spectrophotometer measures. In addition, these values are lower than the value used in TiO_2 NPs coagulation studies, namely 30 mg/L (Wang et al., 2013), 100 mg/L (Kinsinger et al., 2015) and 10 to 100 mg/L (Honda et al., 2014). Additional C/F/S experiments were made with W1, W4 and natural waters, using 0.2, 0.5, 1.0 and 5.0 mg/L of TiO_2 NPs. The optimal coagulant dosage was determined based on TiO_2 NPs removal efficiencies. For all the waters, a control trial was made where no coagulant was added (0.0 mg/L Al_2O_3).

3.2.4. Analytical methods

Samples were analysed for pH (at 25ºC, Whatman WTW pH340 meter), conductivity (Crison GLP32 conductimeter), turbidity (HACH 2100N turbidity meter of high resolution, 0.001 NTU), and UV_{254nm} absorbance (Beckman DU 640B, UV/VIS spectrophotometer) and dissolved organic carbon (DOC) (Shimadzu TOC 5000A analyser, 50 ppb–4000 ppm), using standard methods of analysis (Eaton et al., 2005b).

Titanium concentrations in bulk and treated waters and aluminium in treated water were determined by atomic absorption spectrometry (AAS AAnalyst 800, Perkin–Elmer, detection limit: 0.350 µg/L), after acid digestion with 2% nitric acid (HNO_3). Ti and Al were analysed by graphite furnace using standard methods (Eaton et al., 2005a). The accuracy of the analytical procedure was assessed by the injection of titanium standards at the beginning of sample quantification and at every ten samples. TiO_2 removal efficiencies were based on Ti concentrations measured in bulk and treated waters.

3.3. Results and Discussion

3.3.1. Characterisation of TiO_2 nanoparticles

The optical absorption spectrum of TiO_2 NPs dispersed in deionised water shows a distinct peak at 337 nm (Figure 3.1) similarly to the results obtained by Dalai et al. (2012). As shown in Figure 3.1, the absorbed light by the nanoparticles is proportional to the mass concentration present in the suspension.

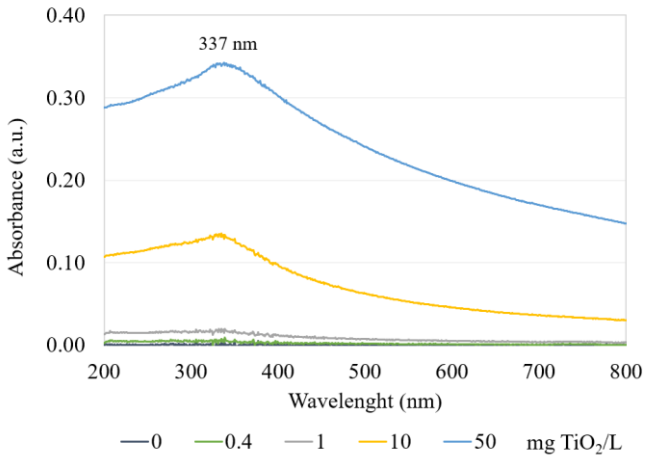

Figure 3.1. Optical absorption spectra for 0, 0.4, 1, 10 and 50 mg/L TiO_2 NPs.

Figure 3.2a presents the effect of the pH in the hydrodynamic diameter and the zeta potential values in deionised water. According to supplier information, the NPs individual diameter is lower than 100 nm. Allouni et al. (2012) characterised the same TiO_2 NPs used in this work by BET method and determined the individual diameter around 74 nm. However, when dispersed in deionised water, the NPs show a hydrodynamic diameter higher than individual particles for all the pH tested (Figure 3.2a), which indicates that when suspended in water TiO_2 NPs form aggregates. According to Jiang et al. (2009), when nanoparticles are dispersed in liquids, their hydrodynamic size is often larger than the primary dry particle size, due to interaction between nanoparticles and the surrounding solution, that promotes the formation of NPs aggregates with higher sizes. Surface charge (zeta potential) and consequently the hydrodynamic diameter size can be altered by changing solution pH or ionic strength. Both zeta potential and consequently hydrodynamic diameter are highly affected by solution pH (Figure 3.2a). The zeta potential is positive between pH 2.9 and <5.4, and negative from this point until the highest pH value tested, 8.6 (varied between 38.1±2.6 and -54.3±0.9 mV). The point of zero charge (PZC) is near pH 5.4, where zeta potential is zero. These results are in good agreement with those find in the literature (Ottofuelling et al., 2011; Sahu et al., 2011; Suttiponparnit et al., 2010). These authors determined that the isoelectric point (IEP) of TiO_2 NPs was between pH 5 and 6, and at pH values lower than 5-6 the zeta potential was positive and negative at higher pH values than IEP. In addition, Von Der Kammer et al. (2010) assumed that, under pure electrostatic interaction, TiO_2 NPs with a zeta potential within ±15 mV would be unstable and tend to aggregate, from ±15 mV to ±30 mV they would be in a transitional state, from ±30 mV they would be predominantly stable and above ±40 mV they would be well stabilised. As shown in Figure 3.2a, the highest aggregates (778.2±91.8 nm, approximately) are at pH 5.4, where the zeta potential is -2.7±2.8 mV and the lowest (168.9±15.6 nm, approximately) at pH 8.6 where the zeta potential is -54.3±0.9 mV. At the point of zero charge (pH ≈ 5.4) particles have little or no charge, leading to a substantial weakening in the repulsive forces between nanoparticles, which implies that each collision between primary nanoparticles and aggregates causes particle adherence (Baalousha, 2009). Therefore, at this pH TiO_2 nanoparticles present the highest hydrodynamic diameter (778±91.8 nm, Figure 3.2a), which results in larger aggregates that settle rapidly owing to gravitational forces. For pH values between 6.7 and 8.6 (-40.0±1.0 and -54.3±0.9 mV) TiO_2 NPs are highly charged and stable, so aggregation is minimised and HD less than 190 nm, because of the high repulsion forces. As pH increases, the concentration of OH^- and the electrostatic repulsion

between particles increases which provide NPs stabilisation. Consequently, the hydrodynamic diameter decreases. At these pH values, electrostatic repulsive forces dominate the van der Waals forces (Baalousha, 2009). For the pH values prior to isoelectric point, the nanoparticles are in a transitional state. Therefore, the hydrodynamic values ranged between 488.3±118.8 nm and 556.5±4.8 nm (Figure 3.2a).

For model and natural waters, the polydispersity index (PdI) was 0.31±0.02 for W1, 0.34±0.04 for W2, 0.35±0.02 for W3, 0.28±0.04 for W4 and 0.29±0.02 for NW, which for this DLS equipment indicates a good accuracy in the samples (Malvern, 2009). As shown in Figure 3.2b, the presence of NOM shifts both zeta potential and hydrodynamic diameter of TiO_2 NPs. TiO_2 NPs become negatively charged, and the HD values are very similar (ranging between 300±18 and 440±56 nm) in all the waters studied. Therefore, NOM imparts a negative charge to NPs surfaces and raises their absolute surface potential (Zhang et al., 2009), having a general stabilising effect upon TiO_2 NPs, which coincides to previously reported results (Romanello and Fidalgo de Cortalezzi, 2013; Zhang et al., 2009). According to Ottofuelling et al. (2011), NOM adsorbs to metal oxides surfaces and may reduce or neutralise the positive surface charge, or at sufficient concentrations induce a reversal of charge from positive to negative.

For W1 with a pH near the IEP (≈5.4), the TiO_2 NPs absolute ZP value increases (become more negative) and consequently HD decreases. For W3, which $pH < pH_{PZC}$, the surface charge of TiO_2 NPs is positive, so adsorption to negatively charged NOM through electrostatic attraction occurs, as also demonstrated by (H. Wang et al., 2015).

However, the TiO_2 NPs in hydrophobic waters, W2 and W4, present ZP higher negative values than the hydrophilic waters, W1 and W3. Thus, the hydrophobic NOM (humic acids) contributes more for the negativity of NPs surface charge than the hydrophilic NOM. This is also observable in the natural water (NW) tested, since this water is a hydrophilic based on the SUVA values (Table 3.1). Baalousha (2009) also showed an increase in the nanoparticles coverage, as well as the thickness of the surface coating, with the increase of AHA concentration. This surface coating increases the effect of steric stabilisation in addition to the effect on the surface charge that governs particle interactions in aqueous media. In addition, Loosli et al. (2015) study indicated that the main driving force in the adsorption of NOM onto TiO_2 NPs is a complex combination of electrostatic attractive and repulsive interactions. Moreover, when complex and heterogenous compounds like humics acids were present, Van der Walls interactions and steric effects also played a role in the NPs stability.

a) b)

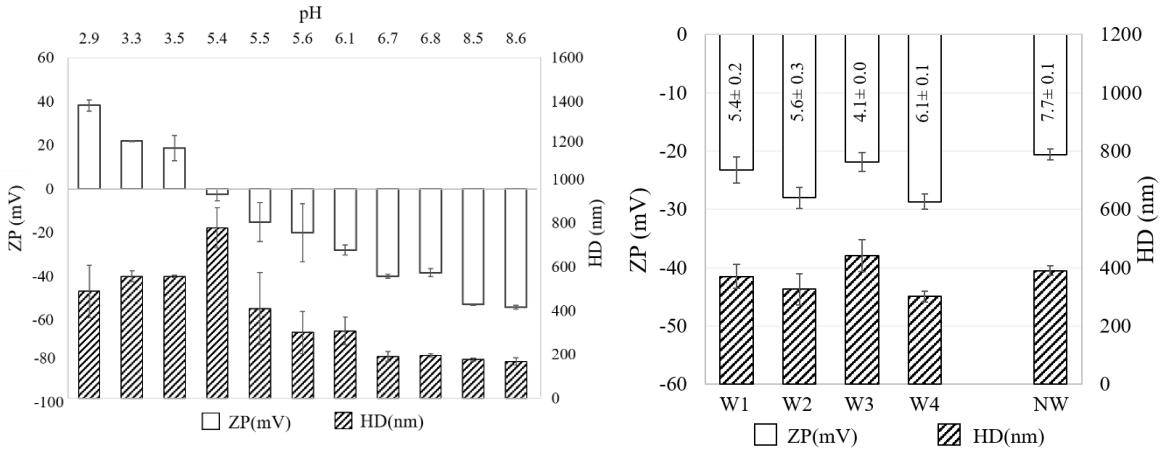

Figure 3.2. (a) Zeta potential (ZP) and hydrodynamic diameter (HD) of TiO_2 NPs at different pH values in deionised water, (b) zeta potential (ZP) and hydrodynamic diameter (HD) of TiO_2 NPs in the studied waters (values presented as mean, standard deviations (n=6) are shown by the error bars).

3.3.2. Sedimentation of TiO_2 nanoparticles

Figure 3.3a shows that TiO_2 NPs dispersed in deionised water (DW) sediment faster than in the other waters, which is proven by the highest sedimentation rate presented in Figure 3.3b. This happened because, at this pH (≈ 5.4), TiO_2 NPs in deionised water are at the IEP, where the NPs are unstable and form larger aggregates (Figure 3.2a), so sedimentation is higher. According to Narong and James (2006) calculations based on DLVO theory, close to the isoelectric point, there is no energy barrier to flocculation meaning that the turbidity of suspensions at this pH should be lower. Therefore, when particles are aggregated (i.e. have greater size), they have a higher tendency for sedimentation.

For the hydrophobic waters W2 and W4, nanoparticles form the smallest aggregates (Figure 3.2b), the sedimentation is less pronounced and consequently, the sedimentation rate is the lowest (0.04 h^{-1}, Figure 3.3b). Hydrophilic waters, W1 and W3, present sedimentation and sedimentation rate (~0.07 h^{-1}) similar between them, due to the similarity of the size of the aggregates (Figure 3.2b). Therefore, the sedimentation of TiO_2 NPs is higher in the waters with hydrophilic NOM.

For lower TiO_2 NPs concentrations (1 mg/L), NPs settle slower than for higher concentrations (10 mg/L) in studied waters (W1, W4 and NW) (Figure 3.4a). Therefore, the reduction in NPs concentrations from 10 mg/L to 1 mg/L caused a decrease in the sedimentation

rate for the tested waters (compare Figure 3.3b and Figure 3.4b). However, despite the observed decrease, the sedimentation behaviour between waters was similar. Sedimentation of TiO_2 NPs is faster in waters with hydrophilic NOM, like W1 and NW, and consequently sedimentation rate is higher than in hydrophobic waters like W4.

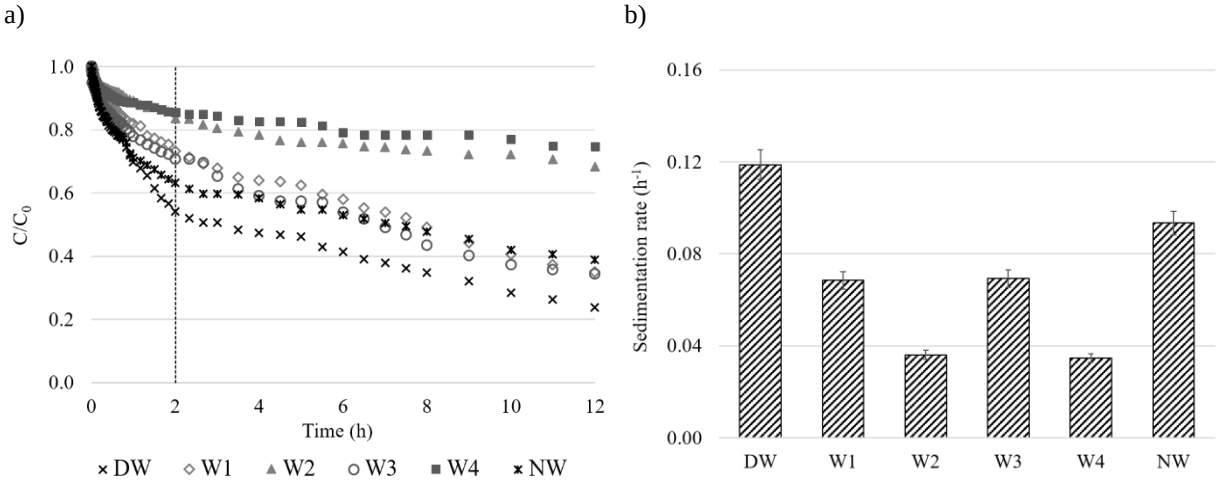

Figure 3.3. (a) TiO_2 sedimentation and (b) sedimentation rates (h^{-1}) in the studied waters (sedimentation rate at the first 2 hours, instead of 1 hour as described by Keller et al. (2010) (values presented as mean, standard deviations (n=6) are shown by the error bars).

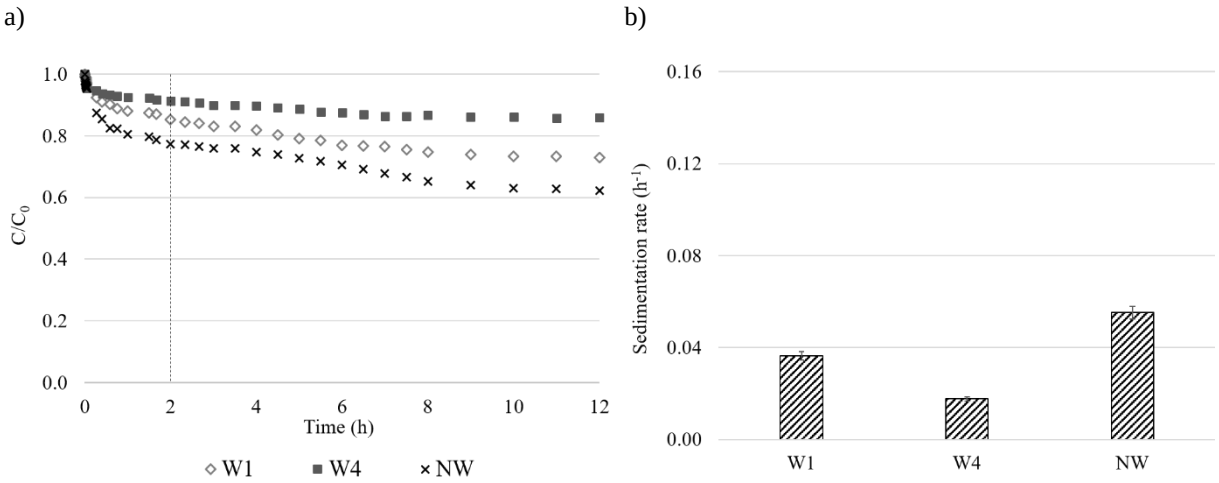

Figure 3.4. a) TiO_2 NPs (1 mg/L) sedimentation and b) sedimentation rates (h^{-1}) for W1, W4 and NW (1 mg/L TiO_2 NPs; sedimentation rate at first 2 h, instead of 1 h as described by (Keller et al., 2010) (values presented as mean, standard deviations (n=6) are shown by the error bars).

3.3.3. Removal of TiO_2 nanoparticles

Figure 3.5 shows the removal efficiency of TiO_2 NPs by C/F/S process and the TiO_2 NPs zeta potential values after the coagulation step, for the model waters (W1 to W4) and the natural water (NW) using different coagulant doses.

For all the waters studied, high removal of Ti is achieved without adding the coagulant. Hydrophilic waters (W1, W3 and NW) present Ti removal efficiencies of approximately 80%, whereas for hydrophobic waters are around 75%. At these conditions, the TiO_2 NPs are aggregated, and the hydrodynamic diameter is between 302±18 and 441±56 nm, with the highest values for the hydrophilic waters (Figure 3.2b). The high aggregates size results in auto-sedimentation of TiO_2 NPs, as shows the sedimentation experiments presented in Figure 3.3, where the hydrophilic waters (W1, W3 and NW) show a higher sedimentation rate than the hydrophobic ones. Similar results were reported by Zhang et al. (2015), where TiO_2 NPs with humic acid and size of ~500 nm auto-precipitated in the absence of coagulant ($AlCl_3$). In addition, the high removals observed for TiO_2 at these conditions (without coagulant added) could also be related to the presence of inorganic compounds such as divalent ions like Ca^{2+}. Kinsinger et al. (2015) reported that bare TiO_2 NPs were more easily remove in complex waters containing divalent cations. At a wider range of pH, divalent cations may cause NPs aggregation due to specific adsorption (Romanello and Fidalgo de Cortalezzi, 2013).

Although the removal rate curves do not present a distinct reverse "U", Ti removal efficiencies increase for all the waters when coagulant was added (Figure 3.5). In addition, removal efficiencies also increase with the increase of coagulant concentration until the removal reaches a plateau, at ~90% of removal. Zhang et al. (2015) called this plateau "effective coagulation zone (ECR)". For the hydrophilic synthetic waters, the ECR varies between 0.2 and 2.0 mg Al_2O_3/L for W1 (optimal dose 0.5 mg Al_2O_3/L, Figure 3.5a), between 3.0 and 4.0 mg Al_2O_3/L for W3 (optimal dose 3.0 mg Al_2O_3/L, Figure 3.5c), and between 0.5 and 3.0 mg Al_2O_3/L for NW (optimal dose 2.0 mg Al_2O_3/L, Figure 3.5e). For hydrophobic waters, W2 presents the ECR between 2.5 and 3.5 mg Al_2O_3/L with the best removal at 3.0 mg Al_2O_3/L, and W4 between 5.0 and 6.0 mg Al_2O_3/L being the best removal at 5.5 mg Al_2O_3/L. For the most efficient Al_2O_3 concentrations, Ti removals are higher than 96% (Figure 3.5). These results show a clear dependency of the NPs removal on source water characteristics and dosage of coagulant as reported by Popowich et al. (2015). Figure 3.5 results show the important role of the water background NOM on the coagulant demand and the overall performance of the C/F/S process. For hydrophobic waters (W2 and W4), a higher coagulant dose is needed to

achieve similar Ti removals of those observed in hydrophilic waters. For the same DOC concentration, among hydrophilic/hydrophobic waters, higher UV_{254nm} values need a higher coagulant dose to achieve similar Ti removals. After the ECR zone, the excess of coagulant promotes the re-stabilization of the TiO_2 NPs and the removal efficiencies decrease. Pinotti and Zaritzky (2001) had reported the re-stabilization of coagulated colloids due to polyelectrolytes oversaturation.

TiO_2 nanoparticles in synthetic and natural waters are negatively charged (between -20.6±0.9 and -29±1.3 mV), at the experiments pH, as presented in Figure 3.2 and in the zeta potential of the control samples (Figure 3.5). The addition of polyaluminium chloride coagulant induces the destabilisation of TiO_2 NPs, due to the neutralisation of the TiO_2 negative charges by hydrolysed Al^{3+} when added to the waters. Consequently, the Al hydrolysis product adsorbs onto the NPs surface, zeta potential increases and approaches zero. At the optimal coagulant dose, nanoparticles are completely destabilised, the surface charge is practically neutral and nanoparticles precipitate due to the decrease of the electrostatic repulsion between them (Figure 3.5). Zhang et al. (2015) showed that in the range of zeta potential between -20 and 20 mV, nanoparticles could be destabilised and effectively removed, as observed in this study. As coagulant dose increases, the zeta potential also increases and become positive to values higher than +20 mV. The overdose of the coagulant induces the re-stabilization of the TiO_2 nanoparticles, becoming nanoparticles surface charge highly positive, as shown for all the synthetic waters at the highest coagulant dose tested (Figure 3.5a to Figure 3.5d). The re-stabilization of the nanoparticles decreases the Ti removal rate due to the excess of the positive charges in solution, resulting in lower removal efficiency of TiO_2 NPs (Figure 3.5). For the natural water (Figure 3.5e), a higher dose of coagulant may be needed to observe this effect of coagulant overdosing. Based on the results obtained, the dominant mechanism proposed for TiO_2 NPs in water with NOM is charge neutralisation, which is in accordance with the mechanism proposed by Liu et al. (2012) for the removal of nanoparticles by aluminium based coagulants.

As expected, no significant variation is observed in the pH values with the addition of polyaluminium chloride coagulant (Figure A 1, in Appendix A). However, in the hydrophobic waters a slight decrease of pH values is observed. As previously investigated (Ribau Teixeira et al., 2010; Teixeira and Rosa, 2006) this type of coagulants, due to pre-polymerisation, have the ability to minimize the water pH reduction during coagulation process compared to non pre-polymerised ones. The pre-polymerisation process enhances the charge interaction mechanism

of colloid destabilisation as a consequence of the slowing down the hydrolysis of the metal salts (Eckenfelder, 2000). As well known the initial water pH has a great effect on the coagulation process by Al-based coagulants. Zhang et al. (2015) had shown that with the pH increasing the ECR became broader and the nanoparticle removal curves moved to the right. So more coagulant dose was consumed to achieve the same removal rate. According to the same authors, this resulted from the NPs tendency of aggregate in more acidic conditions, since smaller NPs will consume more Al-based coagulant to neutralise their charges. A similar effect was observed in the present work (Figure 3.5).

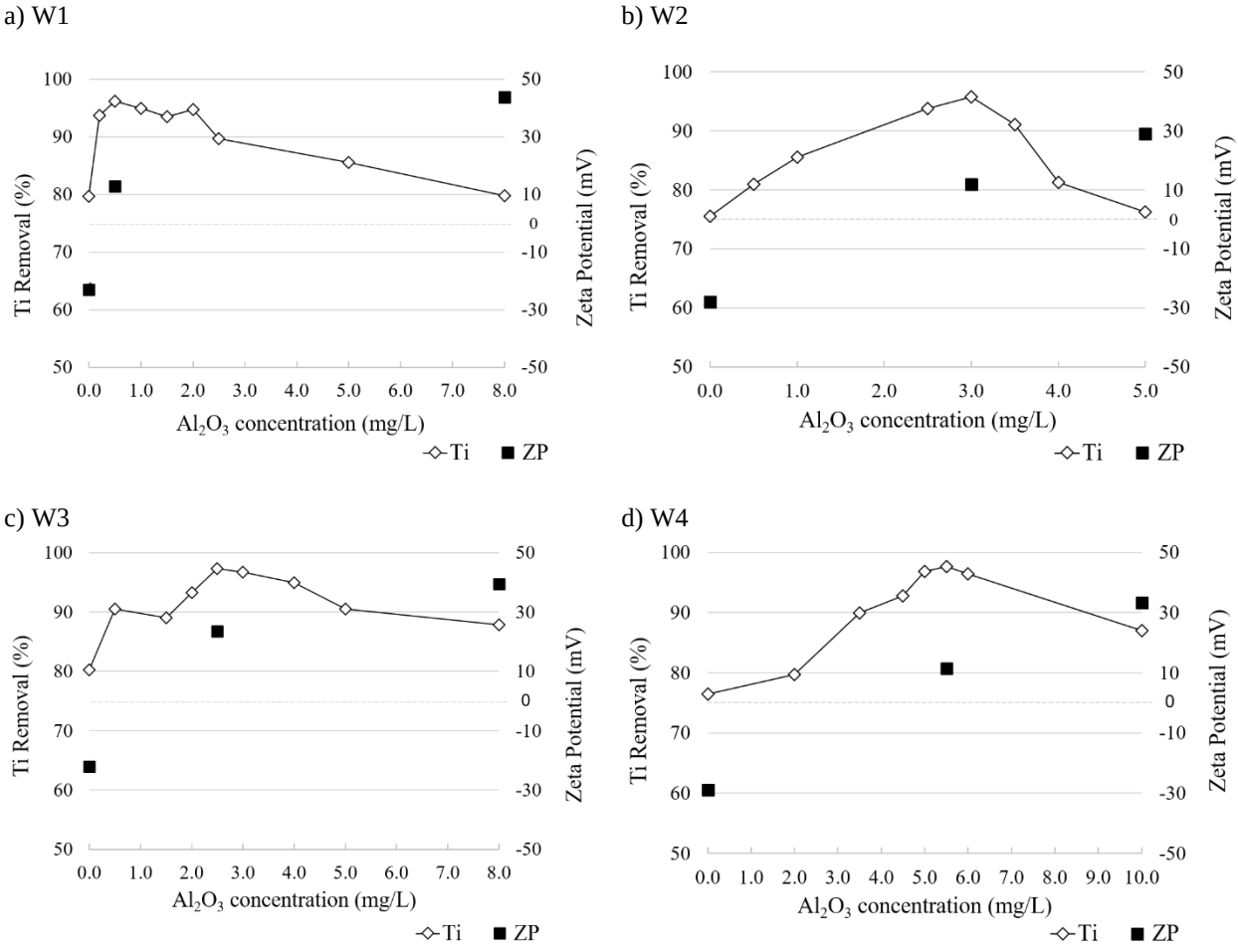

Figure 3.5. Variation of Ti removal and zeta potential with coagulant dose for: (a) W1 (pH 4.7±0.1), (b) W2 (pH 5.9±0.5), (c) W3 (pH 4.3±0.1), (d) W4 (pH 6.3±0.5) and (e) NW (pH 7.6±0.1).

e) NW

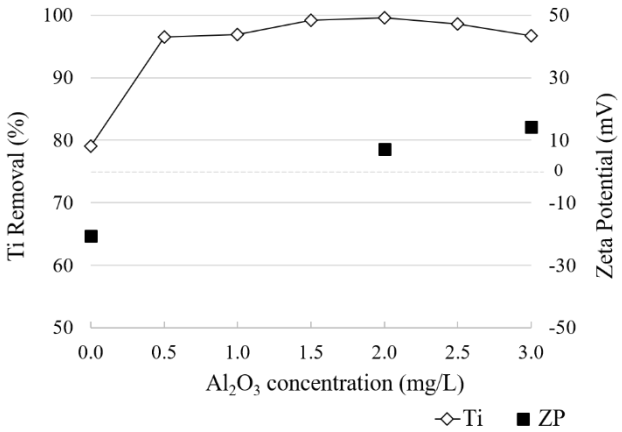

Figure 3.5 (cont.). Variation of Ti removal and zeta potential with coagulant dose for: (a) W1 (pH 4.7±0.1), (b) W2 (pH 5.9±0.5), (c) W3 (pH 4.3±0.1), (d) W4 (pH 6.3±0.5) and (e) NW (pH 7.6±0.1).

In order to understand the influence of NPs concentration in their removal, additional experiments were made using 0.2, 0.5, 1.0 and 5.0 mg/L of TiO_2 dispersed in W1 (hydrophilic), W4 (hydrophobic) and NW (Figure 3.6). Figure 3.6 shows the removal efficiency of TiO_2 NPs by C/F/S process for the model waters (W1 and W4) and the natural water (NW) using the optimal Al_2O_3 dose for each water, namely 0.5, 5.5 and 2.0 mg/L Al_2O_3 for W1, W4 and NW, respectively (see Figure 3.5). Results show high removals of Ti (>90%) for all the TiO_2 NPs concentrations and waters tested, using the optimal coagulant dose. However, a slight decrease in the Ti removal can be observed when compared with the results from the experiments made with 10 mg/L of TiO_2 NPs (Figure 3.5). These could be related to the dose of coagulant used, that has been optimised for 10 mg/L of TiO_2 NPs. These results indicate that C/F/S process is effective for TiO_2 NPs removals and that the TiO_2 NPs initial concentrations (ranging between 0.2 and 10 mg/L) do not influence the Ti removal significantly. Once again, these results show a clear dependency of the NPs removal on source water characteristics and coagulant dosage, since for W4 (hydrophobic water) a higher dose of Al_2O_3 was applied.

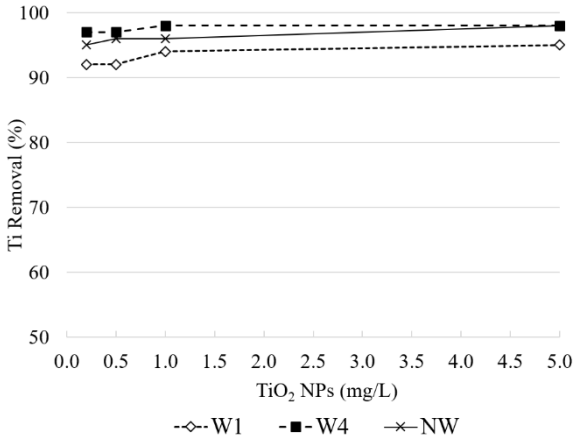

Figure 3.6. Ti removals using 0.2, 0.5, 1.0 and 5.0 mg/L of TiO_2 NPs for W1, W4 and NW (W1: pH 4.5±0.1, W4: pH 6.3±0.5, NW: pH 7.5±0.1).

3.3.4. Removal of NOM and turbidity

Although conventional treatment showed to be efficient in the TiO_2 removal, it is important to determine if their presence affect the overall water treatment, namely the removal of NOM and turbidity. Figure 3.7 shows removal efficiencies of TiO_2 NPs compared with the removal of NOM related parameters, DOC and UV_{254nm}, and turbidity for the synthetic and natural waters.

For all the waters studied, the DOC and UV_{254nm} removal are higher in the hydrophobic waters (>95% in ECR, Figure 3.7b for W2 and Figure 3.7d for W4) than in the hydrophilic ones (<25%, Figure 3.7a, Figure 3.7c and Figure 3.7e for W1, W3 and NW, respectively), showing that the hydrophobic fraction of NOM is removed more efficiently than the hydrophilic fraction. These results are in accordance with Edzwald and Tobiason (1999) statements: i) in waters with SUVA > 4, NOM controls the coagulation process and good DOC removals are achieved, usually higher than 50%, since are mostly composed by aquatic humic with high hydrophobicity and high molecular mass compounds; ii) in waters with SUVA < 2, NOM has little influence in the coagulation process and with poor DOC removals, typically lower than 25%, since are mostly non-humics, with low hydrophobicity and low molecular mass compounds. Globally, UV_{254nm} is more reduced than DOC in all waters, which suggests that aromatic organic matter is removed more efficiently than other NOM fractions. Hydrophobic NOM fraction has a low IEP, due to the presence of carboxylic and phenolic groups, which induced high negative charges as observed in Figure 3.2b and showed by Sharp et al. (2006a). Actually, due to its increased number of anionic binding sites, the hydrophobic NOM is more easily removed by

charge neutralisation with cationic aluminium hydrolysis products than the hydrophilic NOM. Therefore, the hydrophobic fraction dominates the specific colloidal charge character (Bond et al., 2010; Sharp et al., 2006b). Sharp et al. (2006c) identified an operational zeta potential window (-10 and +3 mV) where the residual DOC was optimised and stable. These authors also concluded that the removal of hydrophobic fractions is most strongly related to the magnitude of the coagulation zeta potentials. The DOC and UV_{254nm} results of hydrophobic waters (W2 and W4) show high removals (>90%) for zeta potential around +10 mV, i.e. for the TiO_2 removal optimised coagulant dose. For negative (~ -30 mV) and positive (~ +30 mV) zeta potentials, removals decrease to values lower than 50%. In fact, the DOC and UV_{254nm}, as well as turbidity, removal curves accompany the Ti removals for these waters. These findings confirm the efficacy of conventional coagulation for the removal of hydrophobic organic fractions from the water as already shown by other authors (Jiang, 2015; Joseph et al., 2012; Matilainen et al., 2010), but in this case when TiO_2 NPs are present in water. The DOC and UV_{254nm} removals in hydrophilic waters (W1, W3, NW) are much lower than the ones observed in hydrophobic waters. DOC removals vary between 1% and 25%, and UV_{254nm} removals between 10% and 60% (Figure 3.7a, Figure 3.7c, Figure 3.7e). Hydrophilic waters present weaker acidic groups and low molecular weight compounds and competitive interactions between coagulants and NOM are not favoured.

Turbidity removals are similar to Ti removals (compare Figure 3.5 and Figure 3.7). The optimal coagulant dosage for turbidity removal matches with the optimal one for the Ti removal for the same waters. However, hydrophobic waters show a higher turbidity removal than hydrophilic. This is related to the higher initial turbidity of the hydrophobic waters, due to the major concentration of humic acids, which improved removal.

The presence of TiO_2 NPs could contribute to high removals of NOM and turbidity. This improvement could be related directly with the presence of Ti-based nanoparticles, since titanium compounds have been recently studied as coagulant for water treatment due to their effectiveness in particle, nutrients and organic matter removal (Zhao et al., 2014). Shon et al. (2007) showed that titanium salts successfully achieved high organic matter removal to the same extent as Al and Fe salts and the formed flocs had better settleability. More recently, Zhao et al. (2014) demonstrated that $TiCl_4$ was more effective in the removal of DOC, UV_{254nm} and turbidity. Therefore, the coagulation capacities of TiO_2 NPs associated with the polyaluminium coagulant may have a positive effect on the removal of NOM and turbidity.

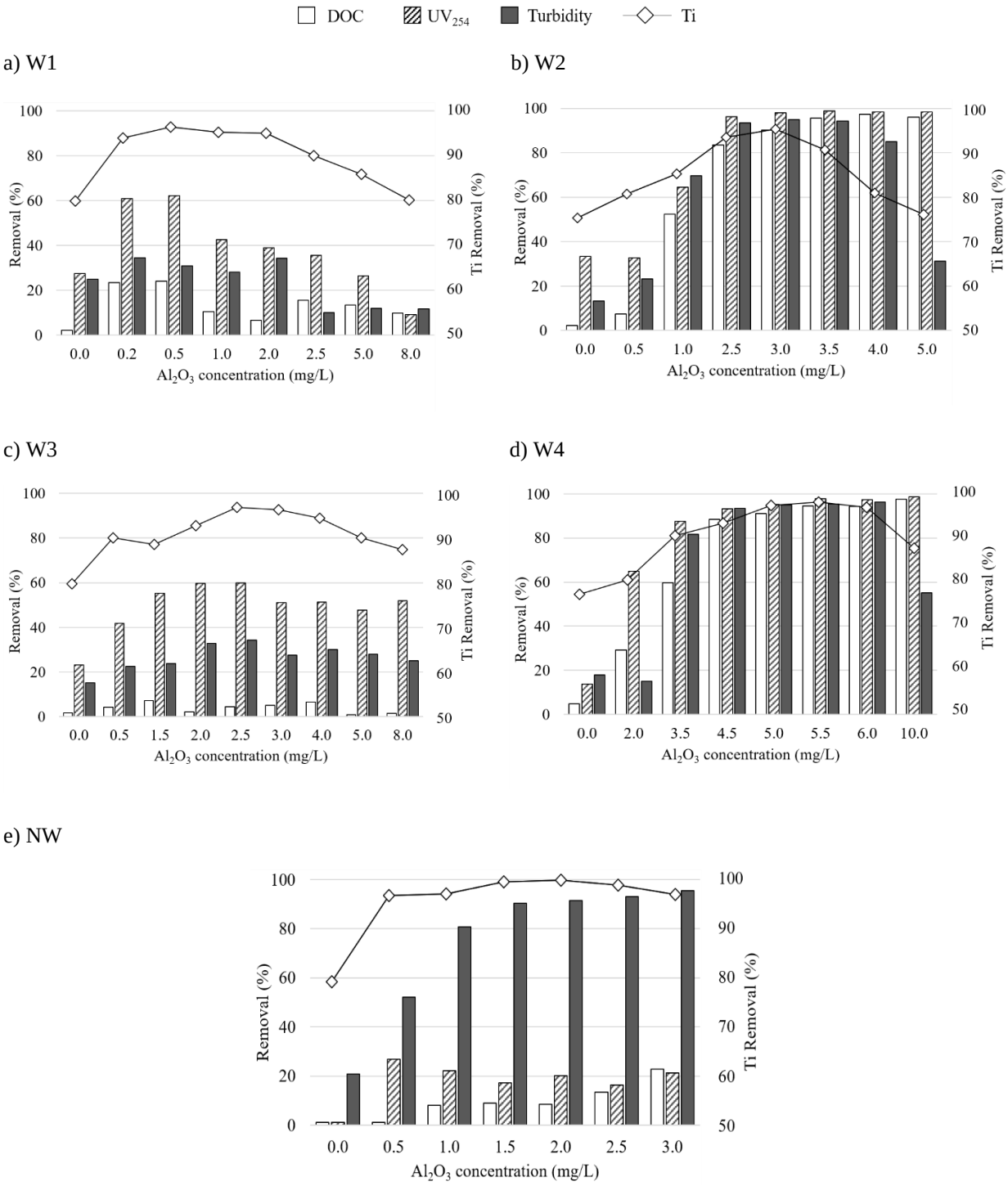

Figure 3.7. DOC, UV_{254nm} and turbidity removal for studied waters with coagulant dose (Ti removal is presented for comparison proposes).

3.3.5. Water quality – case study

Despite the results of the TiO_2 NPs removals by conventional drinking water treatment, C/F/S, it is crucial to ensure that the quality of the final treated water is not affected. Therefore, the natural water (NW) was used as a case study. The quality of the NW treated by C/F/S is compared with Portuguese national guidelines for drinking water (turbidity, pH, conductivity and aluminium) (Portuguese Government, 2007) and with the *Alcantarilha* WTP treated water for the same season (Figure 3.8a to Figure 3.8e). Since there is not a parametric value for DOC in drinking water, the WTP treated water value is used for comparison purpose (Figure 3.8d). For the titanium, the values in the NW treated by C/F/S are compared with the Chinese national guideline for drinking water (Sharma, 2015), since no other guidelines were found (Figure 3.8f).

As can be seen in Figure 3.8a, turbidity in treated water (4.85 NTU) for the optimal dose for Ti removal (2.0 mg Al_2O_3/L) is higher than the value measured in treated water by WTP (0.20 NTU). However, the WTP value is measured at the end of the treatment line, after filtration, and not after C/F/S process. Even so, this value is just slightly higher than the guideline for turbidity (4.0 NTU), also applied to final treated water, so it can be concluded that the removal of TiO_2 NPs did not affect negatively the overall removal of turbidity in drinking water treatment process.

For pH and conductivity (Figure 3.8b and Figure 3.8c), no significant variations are observed even at higher coagulant doses. At optimal coagulant dose, pH value (7.6) is similar to WTP treated water (pH = 7.8) and within the guidelines range. Conductivity (184 μS/cm) in treated water is much lower than the guideline (2500 μS/cm) and lower than WTP treated water (280 μS/cm), for this time of the year, which could be related with the low coagulant concentration used in the C/F/S experiments.

DOC values in treated water show that the optimal coagulant dose for Ti removal, DOC is lower than the values of the *Alcantarilha* WTP treated water, whereby the removal of TiO_2 NPs does not affect negatively the removal of NOM during the C/F/S process (Figure 3.8d).

This work used an aluminium-based coagulant, so it is essential to access the Al residual concentration in the water after C/F/S process, due to the harmful impacts associated to aluminium ingestion (Bondy, 2010; Flaten, 2001). The Portuguese national parametric value is 200 μg Al/L in the treated water, corresponding to the maximum level of Al in drinking water recommended by the World Health Organization (WHO). Figure 3.8e shows the concentration of Al in the water after C/F/S is always below the guideline, for the coagulant doses tested. For the optimal Ti removal coagulant dose (Ti removal ~99%), the Al residual (120 μg/L) was 40%

below the limit, which indicates the Al residual concentration is already acceptable after the C/F/S. The mean value of residual Al in the WTP was about 90 μg/L, however and once again this value is measured in the final treated water after all the treatment processes.

Finally, Figure 3.8f shows the Ti concentration in treated water after C/F/S. As expected, the optimal coagulant dose (2.0 mg Al_2O_3/L) corresponds to the lowest concentration of Ti in water (26.7 μg/L). This value is below the guideline value found for titanium in drinking water, which indicates that C/F/S could be a good option for eliminating TiO_2 NPs from the water.

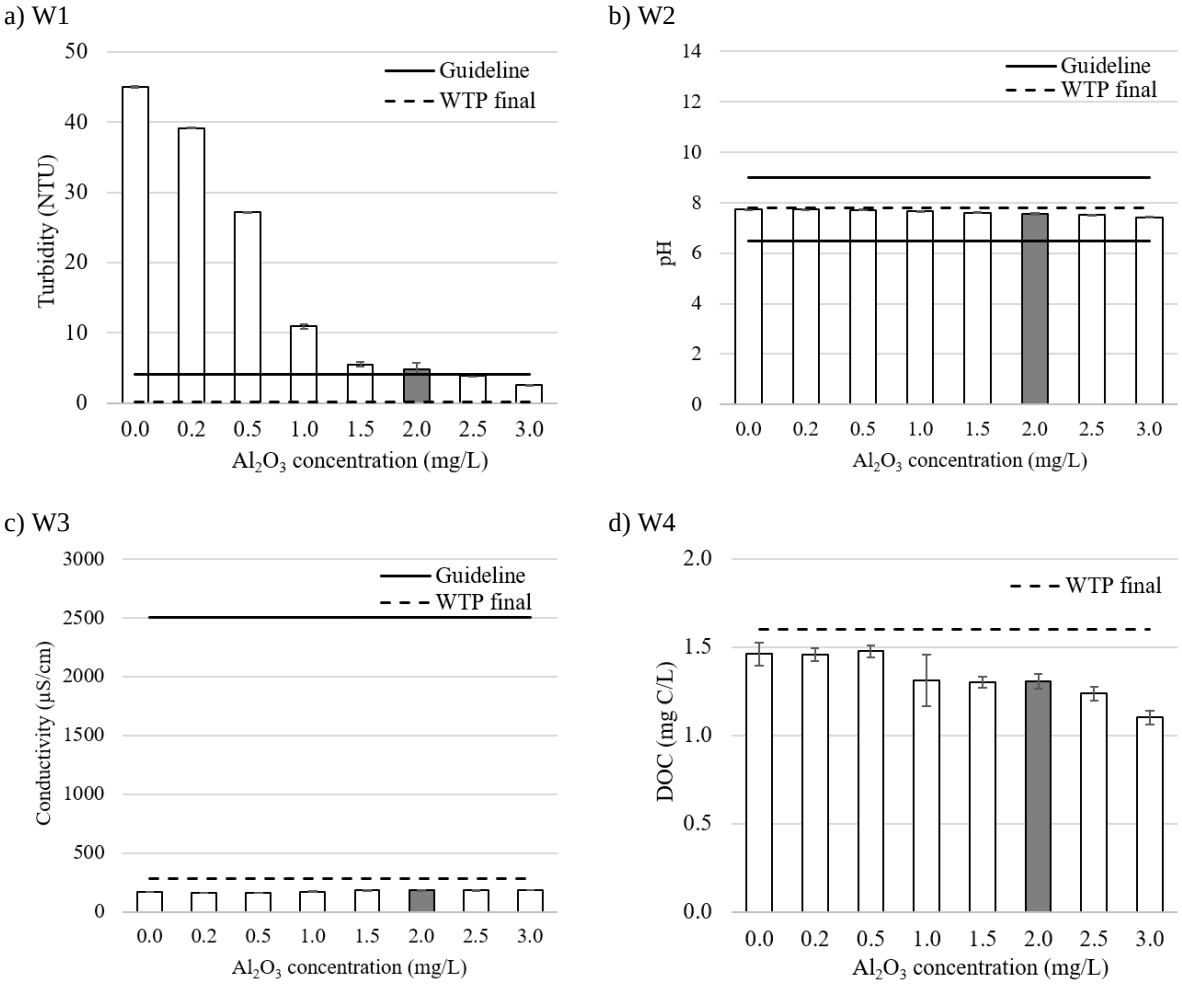

Figure 3.8. Water quality parameters: (a) turbidity, (b) pH, (c) conductivity, (d) DOC, (e) aluminium concentration and (f) titanium concentration for the natural water (NW) after the C/F/S experiments. The grey columns represent the optimal Al_2O_3 dose for the removal of Ti (values presented as mean, standard deviations (n=6) are shown by the error bars). The solid line represents the Portuguese national guidelines (except for titanium that represents the Chinese national guideline) for drinking water. The dashed line represents the WTP final treated water values.

e) NW

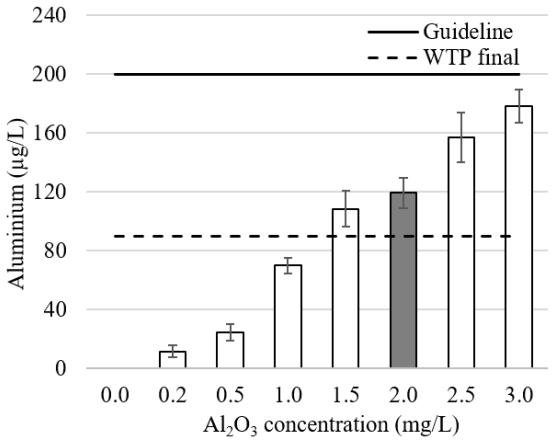

f)

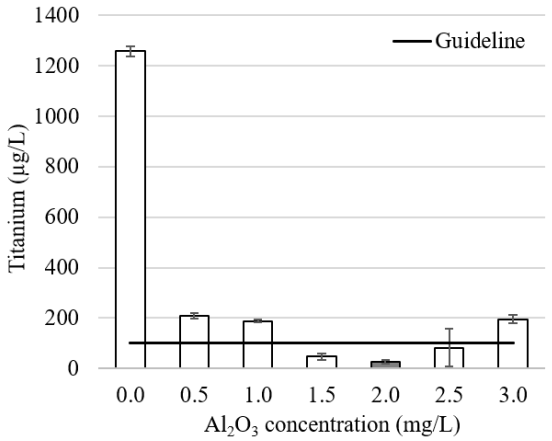

Figure 3.8 (cont.). Water quality parameters: (a) turbidity, (b) pH, (c) conductivity, (d) DOC, (e) aluminium concentration and (f) titanium concentration for the natural water (NW) after the C/F/S experiments. The grey columns represent the optimal Al2O3 dose for the removal of Ti (values presented as mean, standard deviations (n=6) are shown by the error bars). The solid line represents the Portuguese national guidelines (except for titanium that represents the Chinese national guideline) for drinking water. The dashed line represents the WTP final treated water values**.**

3.4. Conclusions

This work demonstrates that it is possible to remove TiO_2 NPs from surface water, using conventional treatment C/F/S. Widely used polyaluminium based coagulants are effective in the removal of TiO_2 NPs to values higher than 95%, without affecting the removal of NOM. High removals of TiO_2 NPs are obtained independently the NOM type and concentration but is strongly influenced by the water characteristics. Hydrophobic waters need more coagulant to achieve similar Ti removals, whereas hydrophilic waters achieved high removal with lower coagulant doses. For the same DOC concentration, among hydrophilic/hydrophobic waters, higher UV_{254nm} values need more coagulant dose to achieve similar Ti removals. Results also demonstrate that the principal mechanism involved in TiO_2 NPs removal is charge neutralisation for surface waters with different type/concentration of NOM.

Finally, the removal of TiO_2 NPs by C/F/S from natural water does not compromise the quality of the final treated water, with all the quality parameters below the national and international guidelines, namely turbidity, Ti and Al concentrations, pH and conductivity.

Chapter 4

Simultaneous Removal of Different Metal-based Engineered Nanoparticles from Surface Waters by Conventional Treatment: A Shift from Single to Multiple Nanoparticles Control

This Chapter was submitted to:

Serrão Sousa, V., Ribau Teixeira, M. Simultaneous removal of different metal-based engineered nanoparticles from surface waters by conventional treatment: a shift from single to multiple nanoparticles control. Submitted to Journal of Cleaner Production in December 2019.

ABSTRACT

Some engineered nanoparticles (ENPs), such as TiO_2, Ag and CuO NPs, are widely used in industrial products and consumer goods due to their physicochemical and antimicrobial properties. As a result of their wide application, these ENPs may be present in natural surface water systems or wastewater treatment plants and, therefore, be a hazard to human health specially if they occur in surface waters used for human consumption. In this work, the efficiency of conventional coagulation/ flocculation/ sedimentation (C/F/S) processes to remove a mixture of ENPs from drinking water sources was assessed. Thus, the novelty of the present study is the evaluation of the simultaneous removal of different co-existing ENPs from natural surface waters. Results showed that C/F/S is effective to remove co-existing ENPs from the studied hydrophilic natural waters (low and medium turbidities and moderate and moderate-high NOM content) with efficiencies above 93% for TiO_2, Ag and CuO NPs. The negative charge of the metal-ENPs in natural waters with NOM was destabilised through neutralisation by hydrolysed Al^{3+} coagulant, promoting ENPs precipitation. Higher ENPs removals were found for the natural water with the highest turbidity, due to the increase in the collision frequency of particles. In addition, the coagulant dose optimised for single ENPs is still effective in the simultaneous removal of ENPs in the mixture. Results also demonstrated that ENPs did not hamper the quality of the water treated by C/F/S for turbidity and NOM. For the lowest turbidity and NOM content studied water, ENPs appear to contribute to higher removal of these parameters.

4.1. Introduction

Over the past decades, widespread nanotechnologically-enabled materials have raised concerns about environmental protection, industrial and municipal wastewater treatment, and drinking water production (Nowack and Bucheli, 2007). These compounds or products are widely applied in distinct areas such as medicine, pharmaceutics, cosmetics, textiles, agriculture, energy, electronics or environment (Chekli et al., 2015; Dwivedi et al., 2015), due to their tailoring potential for specific applications (Prajitha et al., 2019). However, waste streams, discharges of inadequately treated wastewaters, runoff, and releases from contaminated sludge placed in landfills, applied as fertiliser or dumped in aquatic environments, are important causes of surface water contamination by engineered nanoparticles (ENPs) (Baalousha et al., 2016; Park et al., 2017). With an estimated value for produced/imported ENPs (or ENPs-containing products) around 1,615,000 t only in European Union (Ricardo Energy & Environment et al., 2016) and with forecasts predicting a continuous growth of engineered nanomaterials (ENMs) production, the volume and diversity of nanoparticles released into surface waters will increase (Giese et al., 2018; Nowack et al., 2016). ENPs have already been detected in drinking water sources and even in tap water at concentrations in the ng/L to µg/L range making it a potential route for humans (Donovan et al., 2016; Peters et al., 2018; Yang and Westerhoff, 2014). ENPs appellative properties, such as the large surface area to volume ratio and small size, provide unique materials with new applications compared to the corresponding bulk materials. However, these same properties may also result in the enhancement of the bioavailability, increasing their toxicity and becoming a threat not only for the well-being of the aquatic organisms but also to the security of sources used for drinking water production (Casals et al., 2008; Cupaioli et al., 2014; Klaine et al., 2008; Tosco and Sethi, 2018). The ingestion of ENPs trough drinking water may pose a direct hazard to human health or an indirect risk due to the release of trace metal ions (Abbott Chalew et al., 2013). Exposure to ingested metal ENPs or metal ions released can result in adverse effects, such as kidney damage, increased blood pressure, gastrointestinal inflammation, neurological damage and cancerous implications (Kavcar et al., 2009; Missaoui et al., 2018; Vahter et al., 2002).

Therefore, the presence of ENPs in raw waters raises the question of whether current drinking water treatment plants (DWTPs) are prepared to handle this problem, being imperative to evaluate their removal effectiveness. Conventional coagulation/flocculation/sedimentation (C/F/S) is an important water treatment process dedicated to removing small particles, suspended solids, natural organic matter (NOM), microorganisms/pathogens and some

inorganic compounds. Thus, it may also be a valuable process to remove nanoparticles. Some studies already investigated the removal of ZnO, Ag and TiO_2 ENPs by conventional C/F/S treatment applying aluminium and iron-based coagulants to different types of contaminated waters Sun et al. (2013), Abbott Chalew et al. (2013), Honda et al. (2014), Kinsinger et al. (2015) and Serrão Sousa et al. (2017)). Although some ENPs removals had been observed in the referred studies, efficiency rates showed high variability. Removals for TiO_2 ENPs ranged approximately between 32 and 99% (Abbott Chalew et al., 2013; Honda et al., 2014; Kinsinger et al., 2015; Serrão Sousa et al., 2017), Ag ENPs from approximately 79 to 99% (Abbott Chalew et al., 2013; Sun et al., 2013) and ZnO ENPs between 0.46 and 51.7% (Abbott Chalew et al., 2013). The results also demonstrated that ENPs removals by C/F/S depend largely on the type of ENP, the dosage and type of coagulant/flocculant, and the water matrix, but little is known about the removal mechanisms. Moreover, those studies were conducted mainly with synthetic waters and the experiments were only performed with each ENPs individually.

In a previous study, Serrão Sousa et al. (2017) already showed that it is possible to remove TiO_2 ENPs from synthetic and natural surface water (removals higher than 90%) using C/F/S treatment. It was also demonstrated that high removals of Ti were obtained, independently of the initial TiO2 NPs concentration (ranging from 0.2 to 10 mg/L). The present study pretends to evaluate if C/F/S treatment is also efficient in the simultaneous removal of multiple ENPs dispersed in natural surface waters since in natural aquatic systems different ENPs co-exist. To my best knowledge, this has never been assessed. Thus, the aims of this study are: (1) evaluate the efficiency of simultaneous removal of co-existing ENPs in natural waters by C/F/S, (2) understand the ENPs removal behaviours and mechanisms by multiple ENPs control (3) assess the water quality parameters that may affect or be affected by the ENPs removal during C/F/S, mainly turbidity and NOM, and (4) explore the C/F/S overall performance in the presence of ENPs. Three different commercial metal-based ENPs were tested (Ag, TiO_2 and CuO NPs) and two natural waters from Portuguese dams (Alentejo and Algarve regions) currently used to public supply were chosen based on the difference between their turbidity and NOM.

4.2. Materials and methods

4.2.1. Natural water samples

Surface waters were collected from two different dams in Alentejo and Algarve regions (Portugal), currently used to the public water supply. The characteristics of the two waters used are presented in Table 4.1.

Table 4.1. Characteristics of the natural waters used in the experiments (values presented as mean ± standard deviation, n=6).

Water	Sampling local	DOC (mgC/L)	UV_{254} (1/cm)	$SUVA_{254}$ (L/(m.mg))	Turbidity (NTU)	Conductivity (µS/cm)	pH (25ºC)
NW1	Algarve	2.16±0.29	0.046±0.002	2.10±0.09	1.91±0.36	206±3	7.3±0.1
NW2	Alentejo	4.01±0.03	0.088±0.001	2.19±0.04	63.33± 5.37	357±0	7.8±0.1

4.2.2. Characterisation of the metal-based ENPs

Commercially available titanium dioxide (LOT#02527PH), silver (LOT#MKBH2895V) and copper oxide (LOT#02005PH) nanopowders from Sigma-Aldrich were used (Table 4.2).

Table 4.2. Metal-based nanoparticles characteristics used in the experiments.

Nanoparticle	Average diameter (nm)	Particle size[d,f] (nm)	Molecular weight[f] (g/mol)	Surface area[f] (m^2/g)	Purity[f,g] (%)
TiO_2	74.0±0.0[a,d]	< 100	79.87	46.3	99.5
Ag	41.7±1.1[b,e]	< 100	107.87	5.0	99.5
CuO	33.0±2.6[c,e]	< 50	79.55	29.0	99.5

[a] Allouni et al. (2012).
[b] Serrão Sousa and Ribau Teixeira (2015).
[c] Serrão Sousa and Ribau Teixeira (2013).
[d] Determined by Brunauer Emmett Teller (BET) method.
[e] Determined by transmission electron microscopy (TEM).
[f] According to supplier information.
[g] Trace metals basis.

Nanoparticles were characterised individually without any purification for hydrodynamic diameter (HD) and zeta potential (ZP) in natural waters. They were dispersed in the waters and sonicated using a bath sonicator (USC500TH, VWR International) for 20 min. The sonication time was set after several optimisation experiments. This procedure was applied to all characterisation measurements. The HD and ZP of ENPs were determined by dynamic light scattering (DLS) and electrophoretic light scattering (ELS), respectively, using a Zetasizer Nano ZS analyser (Malvern Instruments Inc., UK), as previously described (Serrão Sousa and Ribau Teixeira, 2013). NPs concentration was set at 10 mg/L to ensure the quality of measurements, especially in DLS and as suggested by the equipment supplier. At least, three measurements with 50-100 runs were made for each replicate (3 per sample) to guarantee the quality of the analyses. More detailed information about characterisation of the same ENPs, namely the HD and ZP variation with pH, ionic strength, and nature and concentration of NOM, as well as the sedimentation rate were published in previous works (Serrão Sousa et al., 2017; Serrão Sousa and Ribau Teixeira, 2013; Serrão Sousa and Teixeira, 2015).

4.2.3. Experimental setup and procedure

C/F/S lab-scale experiments were performed in a jar-test unit to simulate the conventional process typically used in DWTPs. The jar-test experiments were carried out in a four paddles unit (Flocumatic, Selecta, Spain) using 800 mL/sample and at controlled room temperature (21±1 °C). Experimental procedure comprised: (a) coagulation at a velocity gradient (G) of 743 s^{-1} (200 rpm) for 2 min; (b) flocculation at G of 24 s^{-1} (20 rpm) for 20 min; (c) sedimentation for 30 min without any mixing. Mixing speed and time were set based on the typical operating conditions for C/F/S in DWT. Prior to coagulant addition, NPs suspensions were sonicated as described above, placed into 1000 mL jars and stirred for approximately 1 min. Then, the coagulant was added to the jars immediately after the start of the rapid mixture. After sedimentation, aliquots of 200 mL of the supernatant were sampled using a volumetric glass pipette from the mid-depth of water column for further analysis.

A commercial polyaluminium chloride coagulant/flocculant (WAC® from Elf Atochem, France), commonly applied to the real context water industry, with 60-70% relative basicity (stock solution with 850 mg/L Al_2O_3) was used in the experiments. Optimal coagulant dosage was determined by carrying out a series of C/F/S tests with incremental increases in the coagulant dose (between 0 and 5 mg/L Al_2O_3 for NW1 and 0 and 30 mg/L Al_2O_3 for NW2),

with 1 mg/L of ENP (TiO_2, Ag and CuO) individually. The optimal dose was established as the lowest dose corresponding to over 90% removal of individual Ti, Ag and Cu, which was then used for the experiments with the ENPs mixture with a total concentration of 1 mg/L of nanoparticles (ratio 1:1:1). A higher coagulant dose was also tested in the latter experiments. For the same conditions, a C/F/S controlled trial was carried out where no coagulant was added (0.0 mg/L Al_2O_3). Replicates of all the experiments were also performed.

4.2.4. Analytical methods

Samples were analysed for NOM by measuring dissolved organic carbon (DOC) (Shimadzu TOC 5000A analyser, 50 ppb-4000 ppm) and UV absorbance at 254nm (UV_{254}) (Beckman DU 640B, UV/VIS spectrophotometer), for turbidity (HACH 2100N turbidity meter of high resolution, 0.001 NTU), pH (at 25 °C, Whatman WTW pH340 m) and conductivity (Crison GLP32 conductimeter), using standard methods of analysis (Eaton et al., 2005b). Titanium, silver and copper concentrations in bulk and treated waters and aluminium in treated water were determined by atomic absorption spectrometry (AAS AAnalyst 800, PerkineElmer, detection limit: 0.350 µg/L), after acid digestion with 2% nitric acid (HNO_3). Ti, Ag, Cu and Al were analysed by graphite furnace using standard methods (Eaton et al., 2005a). The accuracy of the analytical procedure was assessed by the injection of Ti, Ag, Cu and Al standards at the beginning of sample quantification and every ten samples.

4.2.5. Statistical analysis

Linear regression analysis was performed using XLSTAT add-in for Microsoft Excel to determine the Pearson's correlations between ENPs removal and turbidity, UV_{254} and DOC removals. The linear coefficient (R), p-value, and equation were obtained.

4.3. Results and discussion

4.3.1. Natural waters and nanoparticle characterisation

The characteristics of the natural waters used in the C/F/S experiments are presented in Table 4.1. These waters were chosen first because they come from dams currently used to produce water for human consumption and secondly because they have different turbidities (low and medium turbidity, respectively 1.91±0.36 NTU (NW1) and 63.33±5.37 NTU (NW2)) and NOM. According to EPA (1999) classification, water is moderate in DOC concentration if its concentration varies between 2.0 and 4.0 mg C/L and moderate-high if its concentration varies between 4.0 and 8.0 mg C/L. Based on this classification, NW1 is a moderate DOC concentration water (2.16±0.29 mg C/L), while NW2 is a moderate-high DOC concentration water (4.01±0.03 mg C/L). For $SUVA_{254}$ values (specific ultraviolet absorbance, determined by normalising the absorbance at 254 nm with DOC, and presented in L/(m.mg)) both waters are classified as hydrophilic since $SUVA_{254}$ is below 3 (Edzwald and Van Benschoten, 1990) ($SUVA_{254}$ values are 2.10±0.09 and 2.19±0.04 L/(m.mg) for NW1 and NW2, respectively). According to Matilainen et al. (2010) and Edzwald and Van Benschoten (1990) classification, waters with SUVA values between 2 and 4 present a mixture of aquatic humics, a mixture of hydrophobic and hydrophilic NOM and a mixture of molecular weights. Since in this study, the natural waters used present SUVA values close to 2, hydrophilic and non-humic NOM with low molecular weight and low aromaticity prevails in the mixture.

According to supplier information, ENPs individual diameter is <100 nm for TiO_2 and Ag, and <50 nm for CuO (Table 4.2). Based on previous studies that characterised the same NPs, TiO_2 NPs individual diameter is around 74 nm (Allouni et al., 2012), Ag NPs is 41.7±1.1 nm (Serrão Sousa and Ribau Teixeira, 2015) and CuO NPs is 33.0±2.6 nm (Serrão Sousa and Ribau Teixeira, 2013) (Table 4.2). Figure 4.1 shows the variation of ZP and HD for TiO_2, Ag and CuO ENPs in the studied waters. Comparing the HD values of the three nanoparticles in Figure 4.1 with the values presented in Table 4.2, it is observed that when dispersed in water, ENPs showed a HD larger than the individual size, which indicates the formation of aggregates due to interaction between nanoparticles and with the surrounding solution that promotes nanoparticles aggregation (Jiang, 2015). Aggregation can be distinguished between homo-aggregation and hetero-aggregation. Homo-aggregation occurs due to the interaction between the same NPs, and hetero-aggregation is due interactions between NPs and the mixture of components present in the natural waters, such as NOM (Hotze et al., 2010; Lowry et al., 2012;

Quik et al., 2012). Following DLVO (Derjaguin-Landau-Verwey-Overbeek) theory, aggregation in aqueous dispersions mainly results from the combination of van der Waals attraction and electrostatic repulsion due to the electric double layer of the counterions (Loosli et al., 2015; Peijnenburg et al., 2015). However, interactions such as hydration forces, magnetic and hydrophobic interactions (not DLVO theory interactions), also contribute significantly to the aggregation process (Dwivedi et al., 2015; Sendra et al., 2017).

As already referred, NOM has an essential role in the aggregation and stability of ENPs in water. However, the understanding of the exact effect of NOM is a challenge, which is ubiquitous in natural waters (Amde et al., 2017). Even though, it is certain that NOM adsorbs to the surfaces of the nanoparticles, imparting negative charge and providing charge and steric stabilisation (Amde et al., 2017; Loosli et al., 2019; Sendra et al., 2017) (Figure 4.1). According to Ottofuelling et al. (2011), NOM may reduce or neutralise the positive charge of metal oxides surfaces, or even induce a reversal of charge from positive to negative at sufficient NOM concentration. The latter effect was observed for the CuO ENPs since these nanoparticles have a pH point of zero charge (pH_{PZC}) around pH 10 (Serrão Sousa and Ribau Teixeira, 2013). At pH_{PZC}, higher aggregates are expected since particles are unstable with little or no charge, so repulsive forces between nanoparticles are weaker, which implies that each collision between primary nanoparticles and aggregates causes particles adherence (Baalousha, 2009). At pH below pH_{PZC}, as the pH of NW1 and NW2 (Table 4.1), CuO ENPs are positively charged and stable. However, when dispersed in the natural waters the ZP shifted and became negative, -18.8±3.4 mV for NW1 and -34.9±3.4 mV for NW2 (Figure 4.1). The negatively charged NOM neutralises the positive charge of CuO nanoparticles, favouring the adsorption of organic matter onto the nanoparticle surfaces. Although the increasing of NOM content (from NW1 to NW2) imparts more negativity to surface charge of CuO ENPs, HD remains practically unchanged (400.1±16.2 nm for NW1 and 381.0±17.5 nm for NW2, Figure 4.1), possibly because the of the already installed surface coating layer of NOM on the CuO particles (Amde et al., 2017; Yang et al., 2017). This surface coating increases the effect of steric stabilisation in addition to the effect on surface charge that governs particle interactions in aqueous media causing the particle-particle repulsion (Amde et al., 2017; Phenrat et al., 2007). Unlike the ENPs of CuO and TiO_2, Ag were negatively charged at the pH of the natural water (around pH 7) (Serrão Sousa et al., 2017; Serrão Sousa and Ribau Teixeira, 2015). TiO_2 ENPs pH_{PZC} is around 5.4 and above this pH these nanoparticles are negatively charged (Serrão Sousa et al., 2017). When dispersed in natural waters, in the presence of the negatively charged NOM, the surface charge

remains negative, resulting in ZPs between approximately -22 mV (NW1) and -28 mV (NW2), and HDs of around 390 nm (NW1) and 348 nm (NW2) (Figure 4.1). Similar results were reported by Ottofuelling et al. (2011) and Zhang et al. (2009). At DOC concentrations above 0.4 mg C/L and pH above pH_{PZC}, the organic matter stabilised the TiO_2 nanoparticles in suspension, the NPs were covered with organic matter, resulting in zeta potentials around -20 mV. Despite the increase of NOM from NW1 to NW2, ZP and HD remained practically unchanged, possibly due to the already installed surface coating layer of NOM onto TiO_2 nanoparticles, which promotes the effect of steric stabilisation. The Ag ENPs pH_{PZC} is most likely at pH values under 2.6, as demonstrated in previous work (Serrão Sousa and Teixeira, 2015) and also reported by Elzey and Grassian, (2010). Therefore, when dispersed in the studied natural waters, these ENPs were more negatively charged than the TiO_2, with ZP about -40 mV (NW1) and -43 mV (NW2) and HD around 202 nm (NW1) and 195 nm (NW2) (Figure 4.1). The same stabilisation trend observed for TiO_2 ENPs was also observed for Ag ENPs (Figure 4.1).

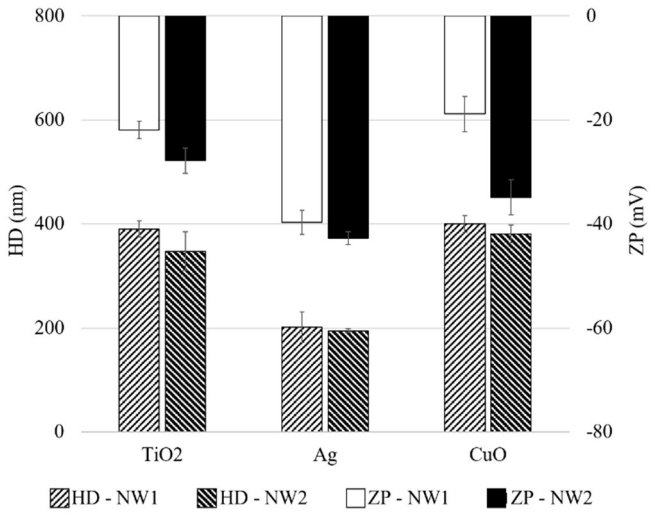

Figure 4.1. Hydrodynamic diameter (HD) and zeta potential (ZP) of TiO_2, Ag and CuO NPs in the studied natural waters (pH 7.3 ± 0.1 for NW1 and 7.8 ± 0.1 for NW2; HD and ZP values presented as mean standard deviations (n=6) are shown by the error bars).

4.3.2. Engineered nanoparticles removal

Figure 4.2 shows the ENPs efficiency removals by C/F/S in natural waters (NW1 and NW2) using different coagulant doses for the experiments with single and multiple ENPs.

Ti, Ag and Cu show an increase in removal efficiencies with the increase of coagulant dose for both waters. Ti, Ag and Cu present some removals without the addition of coagulant (around 25% and 37% for NW1 and 48% and 53% for NW2, Figure 4.2), due to the high aggregate's size formed when ENPs are dispersed in the natural waters (Figure 4.1). These results demonstrate that these aggregates have good settleability which favours the removal of nanoparticles by C/F/S process. The differences between ENPs removals are due to their specific properties, since nanoparticle type affects the deposition behaviour, and deposition process is likely determined by a combination between ENPs properties and physicochemical characteristics of the medium (Amde et al., 2017). The removal efficiencies increase with the coagulant concentration until a plateau is reached, and no significant variations are observed in the ENPs removal rates (Figure 4.2). This plateau is achieved at 3.0 mg/L Al_2O_3 (NW1), and 15.0 mg/L Al_2O_3 (NW2), corresponding to the optimal coagulant doses. For NW1, the plateau remains for the coagulant doses tested. For NW2, the plateau remains until 20.0 mg/L A_2O_3, afterwards the removal starts to decrease (Figure 4.2). As observed in ENPs ZP values (Figure 4.1), the three nanoparticles are negatively charged (between -19 and -40 mV in NW1 and -28 and -43 mV in NW2) at the beginning of the experiment. The addition of the positively charged commercial coagulant (polyaluminium chloride WAC®) to the natural waters induces the ENPs destabilisation through neutralisation of negative charges by hydrolysed Al^{3+}. Consequently, ZP increases and approaches zero as shown in Table 4.3. At the optimal coagulant dose, ENPs are destabilised with surface charge close to zero promoting their precipitation due to the decrease of the electrostatic repulsion between them (Zhang et al., 2015). Zhang et al. (2015) showed that, in the range of ZP between -20 and 20 mV, nanoparticles could be destabilised and effectively removed, as observed in this study. These results indicate that the major mechanism acting in the removal of these ENPs is charge neutralisation, as already demonstrated in a previous study (Serrão Sousa et al., 2017) and in accordance to Abbott Chalew et al. (2013) and Liu et al. (2012). With the increase in the coagulant dose, the ZP become more positive (Table 4.3), which can induce the re-stabilization of ENPs and the consequent decrease in the removal rate, due to the excess of positive charges as observed for 25.0-30.0 mg/L Al_2O_3 in NW2. The higher ENPs removals found in NW2 could also be related

to higher particulate content (higher turbidity) that increases the collision frequency of particles, enhancing coagulation (Sun et al., 2019).

Results also show there is no need to increase coagulant dose in the ENPs mixture within the same water, since the optimal coagulant doses of 3.0 mg Al_2O_3/L for NW1 and 15.0 mg Al_2O_3/L for NW2, based on the individual ENPs experiments, are highly effective to remove the ENPs mixture (Figure 4.2, Figure 4.3.a1 and Figure 4.3.b1). Regarding the ENPs residual concentrations in NW1 at 3.0 mgAl_2O_3/L, 6.5±2.1 µg/L, 15.0±1.4 µg/L and 18.8±8.8 µg/L of Ti, Ag and Cu, respectively (Figure 4.3.a1 and Figure 4.3.a2), Ti presents the lowest value, which can be related to the titanium properties that have been shown to be effective in particle, nutrients and organic matter removals (Zhao et al., 2014). In NW2 at 15.0 mgAl_2O_3/L, the residual Cu concentration is the lowest (2.5±0.7 µg/L, 6.0±1.4 µg/L and 0.5±0.1 µ/L of Ti, Ag and Cu, respectively, Figure 4.3.b1 and Figure 4.3.b2), and the Ti effect is not observed possibly due to the water characteristics, namely moderate-high DOC water with medium turbidity (Table 4.1). Although both waters are hydrophilic, the differences between their characteristics play an important role on the coagulant demand, on the overall performance of C/F/S process and consequently on the ENPs removal (Abbott Chalew et al., 2013; Honda et al., 2014; Kinsinger et al., 2015; Serrão Sousa et al., 2017; Sun et al., 2013). For the 4.0 mg/L (NW1) and 20 mg/L Al_2O_3 (NW2), the ENPs residual concentrations are also low, with similar values to those obtained for the optimal coagulant dose (Figure 4.3.a1 and Figure 4.3.b1), which indicates that the coagulant dose can be increased if necessary to improve the removal of other contaminants or naturally occurring substances in surface waters. Therefore, the high removals obtained for Ti, Ag and Cu in the mixture (above 93%) and the single (above 90%) ENPs experiments for both studied waters (Figure 4.2) demonstrate that C/F/S is efficient in the simultaneous removal of TiO_2, Ag and CuO ENPs from hydrophilic surface waters.

a) NW1 b) NW2

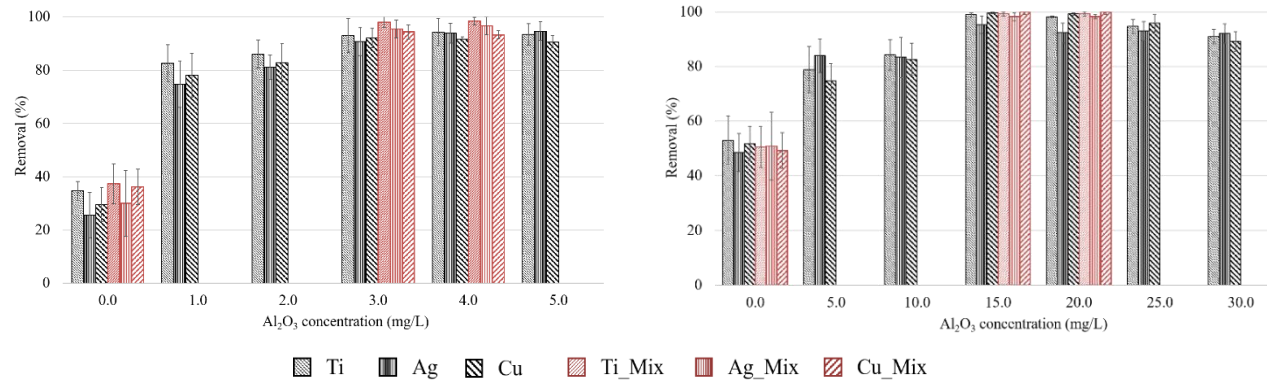

Figure 4.2. Variation of Ti, Ag and Cu removals with coagulant dose for: (a) NW1 and (b) NW2. Experiments performed with the mixture (Mix) and each nanoparticle individually (Ti, Ag and Cu removals presented as mean, standard deviations (n=6) are shown by the error bars).

Table 4.3. Variation of ENPs zeta potential with selected coagulant doses for NW1 and NW2, in single ENPs experiments (ZP values presented as mean ± standard deviation, n=6).

	Al_2O_3 (mg/L)	**Zeta Potential (mV)**		
		Ti	**Ag**	**Cu**
NW1	3.0	11.2±1.5	9.1±1.4	15.0±2.2
	4.0	12.9±1.8	10.7±0.7	17.3±2.6
NW2	15.0	12.5±1.7	13.8±1.5	9.9±2.2
	20.0	18.8±1.2	15.9±2.1	12.4±3.3

a) NW1

a1. a2.

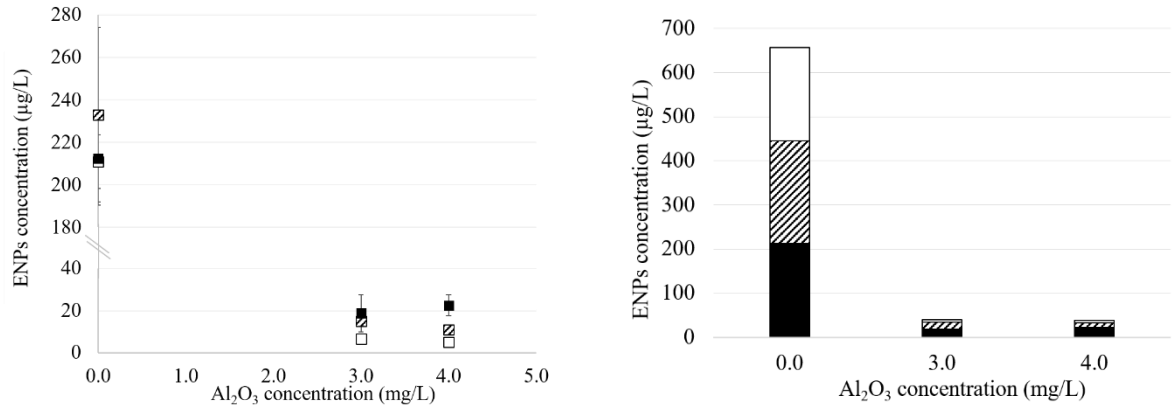

Figure 4.3. Variation of (1) ENPs residual concentration and (2) ENPs ratio with coagulant dose for: (a) NW1 and (b) NW2. Experiments performed with ENPs mixture (Ti, Ag and Cu concentrations presented as mean, standard deviations (n=6) are shown by the error bars).

b) NW2

b1. b2.

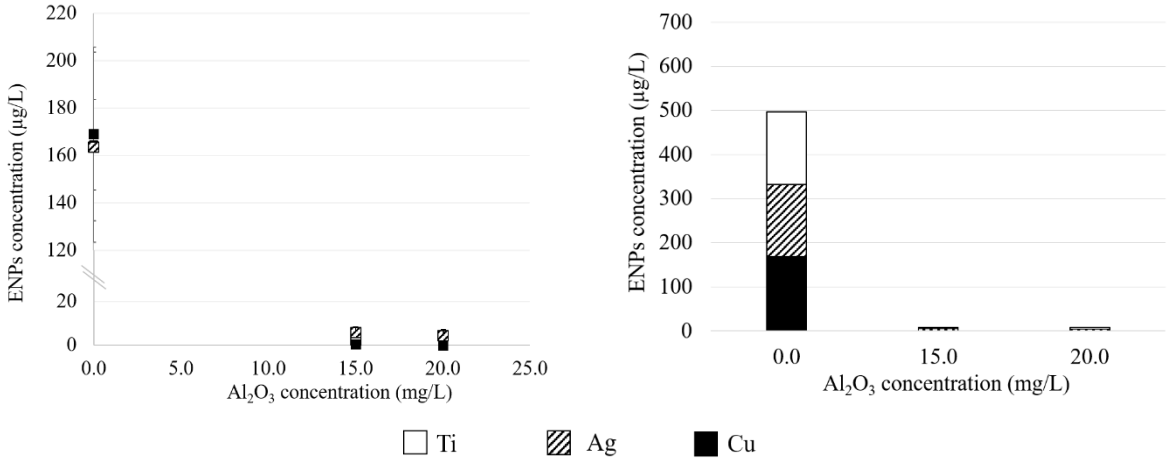

Figure 4.3 (cont.). Variation of (1) ENPs residual concentration and (2) ENPs ratio with coagulant dose for: (a) NW1 and (b) NW2. Experiments performed with ENPs mixture (Ti, Ag and Cu concentrations presented as mean, standard deviations (n=6) are shown by the error bars).

4.3.3. Turbidity and NOM removal

ENPs results show that C/F/S is a good option for the simultaneous ENPs removal from natural waters. However, from the drinking water treatment point of view, it is imperative to evaluate if the presence of ENPs affects the overall performance of the processes and the treated water quality. It is also essential to explore the relation between the ENPs and turbidity and NOM removal, to verify if the coagulant dose can be optimised for the ENPs removal without hampering the removal of other target compounds. Therefore, Figure 4.4 shows the removal efficiencies of turbidity, DOC and UV_{254} absorbance and Figure 4.5 the correlation between the ENPs removal efficiencies and the turbidity, DOC and UV_{254} removal efficiencies. Table 4.4 presents the treated water quality for turbidity, DOC, UV_{254} absorbance, pH, conductivity and aluminium concentration for the studied natural waters after the C/F/S treatment.

The turbidity removal efficiency was very high despite the presence of single or multiple ENPs in both studied waters (Figure 4.4). Moreover, turbidity removal trend is similar to the ENPs removal (Figure 4.2) for single and mixture experiments independently of the water. The presence of ENPs does not appear to negatively affect turbidity removal. Indeed, in NW1 the presence of ENPs, especially TiO_2, seems to have a positive impact on turbidity removal, despite the highest turbidity removal observed without ENPs (90.1±5.4%) at the Al_2O_3 concentration of 2.0 mg/L (Figure 4.4.a1). As already mentioned, the presence of Ti-based nanoparticles can contribute to high removals of turbidity, nutrients and organic matter due to

the titanium coagulation capacities (Shon et al., 2007; Zhao et al., 2014). When ENPs are present, higher coagulant doses are needed due to the turbidity increase related to the addition of the ENPs to the natural waters (Figure 4.4.a1). In the NW2 neither the Ti effect on the turbidity removal nor the higher coagulant demand are observed in the presence of ENPs (Figure 4.4.a2), most likely due to the water characteristics, namely the high turbidity overlaps those effects. At higher particulate matter content (higher turbidity), greater coagulant doses can promote the enmeshment of the particles by "sweep flocculation" in a mass of amorphous Al-based coagulant, improving turbidity removal (Sun et al., 2019), which could also be observed in NW2. In addition, Sun et al. (2019) concluded that in a nanoparticle system, charge neutralisation was the main mechanism for turbidity removal for low alum concentrations and sweep flocculation for high alum doses. Similarly, the removal of ENPs from NW2 could also involve the "sweep flocculation" mechanism. However, further experiments are necessary to fully understand the presence of this mechanism. Nevertheless, at the selected coagulant doses of 3.0 mg/L Al_2O_3 (NW1) and 15.0 mg/L Al_2O_3 (NW2) for ENPs removal, the turbidity removal efficiencies are very high, around 89.0-93.1% (NW1, Figure 4.4.a1) and 98.6-99.9% (NW2, Figure 4.4.a2). Similarly, to the ENPs removal, higher doses of coagulant are not necessary to the turbidity removal in the multiple ENPs experiments (Figure 4.4a).

The mixture of ENPs does not show a significant impact on the DOC removals for both waters (Figure 4.4b). Indeed, no significant variations are observed for DOC removals in experiments without ENPs, single ENPs and mixture ENPs. However, the DOC removals increase with the increase of the coagulant dose, as shown in Figure 4.4.b1 and Figure 4.4.b2. A similar trend is observed for the UV_{254} absorbance removal efficiencies (Figure 4.4c). For the optimal coagulant dose, the NOM removals efficiencies range between 21-23% for DOC (Figure 4.4.b1) and 36-42% for UV_{254} (Figure 4.4.c1) in NW1. In NW2, removals vary between 33-38% for DOC (Figure 4.4.b2) and 50-54% for UV_{254} (Figure 4.4.c2.). The DOC and UV_{254} removal efficiencies are higher in NW2 than in NW1, since more coagulant was applied in the former. This is related to the negatively NOM charges in natural waters that induce the need for higher coagulant doses to charge neutralisation. In fact, the increase in coagulant dose in NW1 and NW2 is always followed by an increase in the DOC and UV_{254} absorbance removals, as also demonstrated by Clavier et al. (2019). Therefore, despite the presence of ENPs, DOC efficiencies removals are within an acceptable range of values for coagulation. According to Matilainen et al. (2010), in waters with SUVA between 2 and 4 L/(m.mg), DOC removals by Al-based coagulation ranged between 25 and 50%. This indicates that the optimal coagulant

doses achieved based on ENPs removal are suitable for the removal of NOM. Globally, UV_{254} presents higher removals than DOC in both waters, suggesting that aromatic organic matter is more efficiently removed.

The studied linear relationship between turbidity, UV_{254} and DOC and ENPs removal shows strong significant correlations between them with $0.8 < R \leq 1.0$ (p-values <0.05, Figure 4.5). These high correlations corroborate that ENPs form aggregates with NOM and particulate matter during coagulation and are removed together as a complex. For NW1 (Figure 4.5a), a slightly higher correlation between ENPs and turbidity is observed. However, in NW2, the strongest correlation is observed for ENPs and UV_{254} removals, which can be related to the content of aromatic compounds present in this water. The high correlations between the ENPs removal and these target compounds also demonstrate that the coagulant optimisation based on the ENPs removal does not have a negative impact on the overall performance of C/F/S.

a) Turbidity

a1. NW1

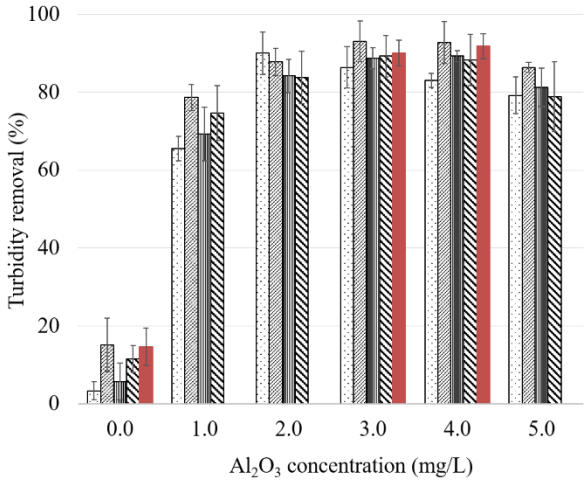

a2. NW2

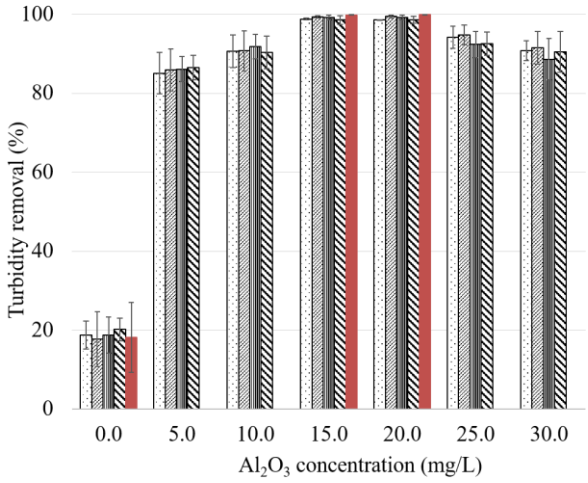

Figure 4.4. Turbidity (a), DOC (b) and UV_{254} absorbance (c) removal efficiencies with coagulant dose in NW1 (1) and NW2 (2) using no ENPs, single ENPs and the ENPs mixture (turbidity, DOC and UV_{254} removal presented as mean, standard deviations (n=6) are shown by the error bars).

b) DOC

b1. NW1

b2. NW2

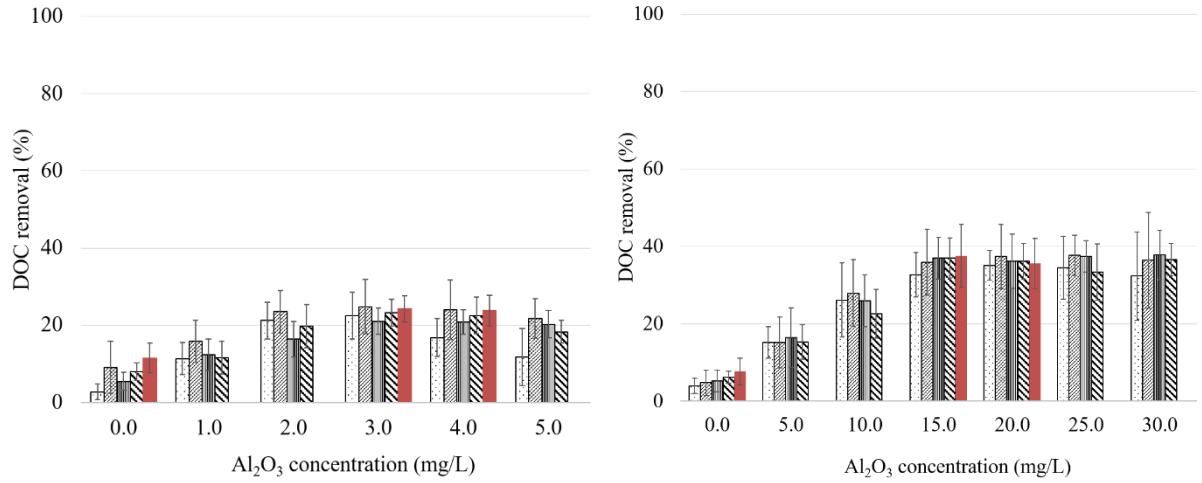

c) UV_{254}

c1. NW1

c2. NW2

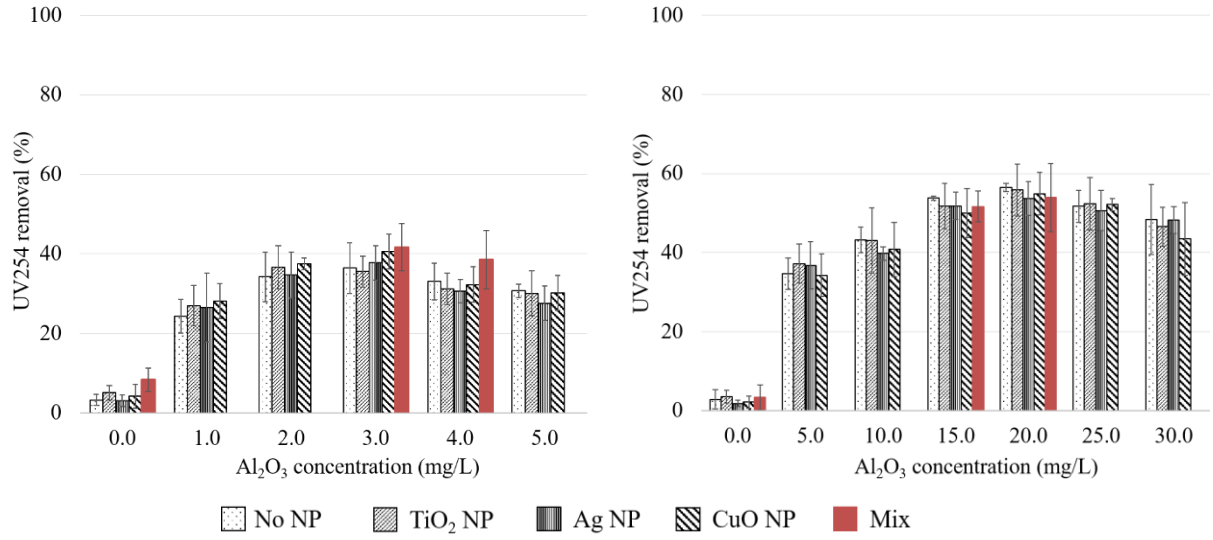

Figure 4.4 (cont.). Turbidity (a), DOC (b) and UV_{254} absorbance (c) removal efficiencies with coagulant dose in NW1 (1) and NW2 (2) using no ENPs, single ENPs and the ENPs mixture (turbidity, DOC and UV_{254} removal presented as mean, standard deviations (n=6) are shown by the error bars).

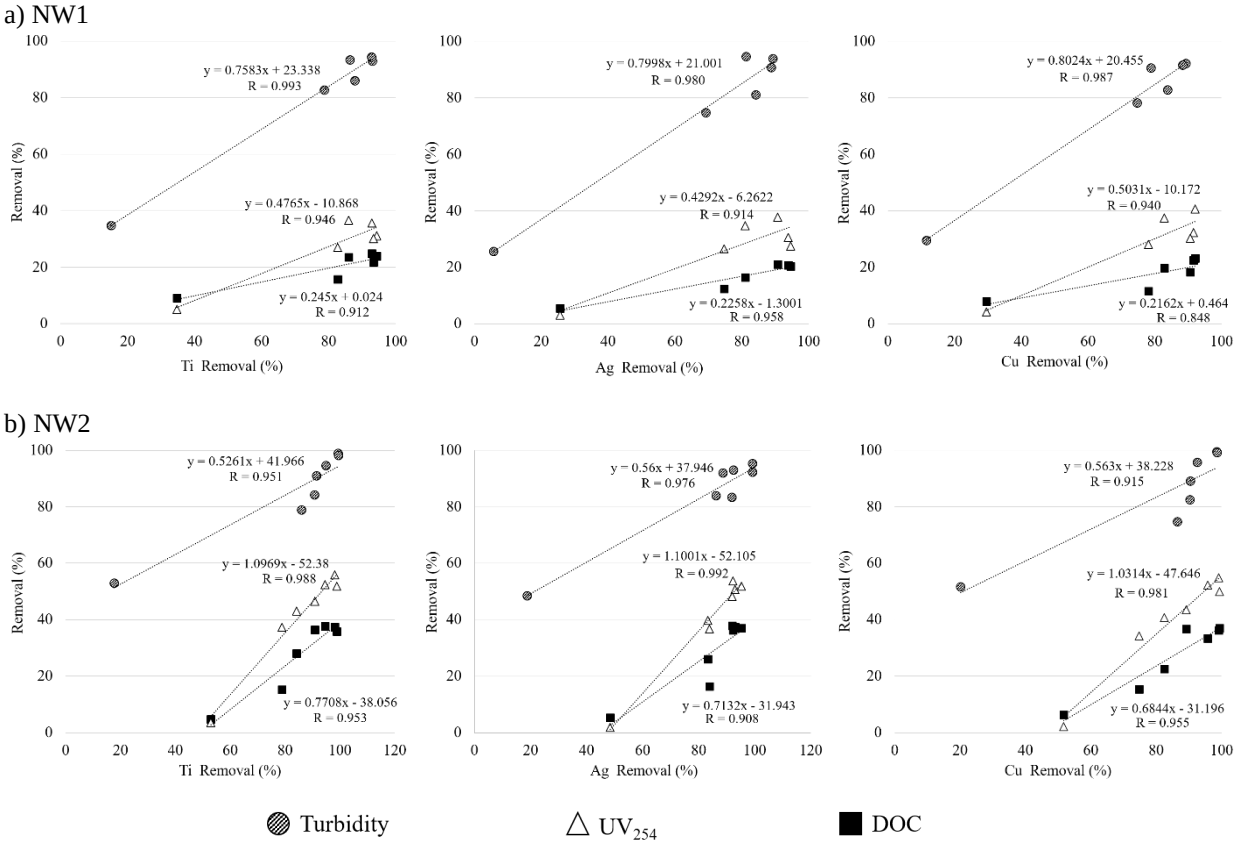

Figure 4.5. Correlation between ENPs removal and turbidity, UV_{254nm} and DOC removal efficiencies NW1 (a) and NW2 (b). Experiments performed with single ENPs (values presented as mean, n=6). *p-values* <0.05.

4.3.4. Treated water quality

The good C/F/S performance is also demonstrated by the results presented in Table 4.4. At the end of the C/F/S treatment, for the selected coagulant doses, the turbidity of both NW1 and NW2 is very low, 0.41±0.17 NTU and 0.07±0.02 NTU, respectively (Table 4.4). These values are under the national guideline for turbidity (4.0 NTU), which is applied to the final treated water and not at the end of C/F/S treatment. DOC final concentration is 1.50±0.07 mg C/L for NW1 and 2.62±0.33 mg C/L for NW2 (Table 4.4). The former value is below the average value of 1.6 mg C/L obtained in Portuguese WTPs (personal communication, there is no guideline for DOC). The latter DOC value is above the WTP value. However, this value is measured in WTP final treated water after filtration and disinfection. Therefore, most likely, the final DOC concentration in NW2 would be more similar to that measured at WTP if filtration and disinfection processes were applied to NW2 water. Conductivity and pH do not significantly

vary with coagulant doses during the experiments. At the optimal doses, pH is 7.2 (NW1) and 7.5 (NW2), which is similar to WTP treated water (pH 7.8) and within the guidelines range (pH 6.5-9) (Table 4.4). Conductivity, 212±1 µS/cm for NW1 and 364±1 µS/cm for NW2, is below the guideline of 2500 µS/cm. Aluminium in the treated water is also below the national guideline of 200 µg/L for both waters and within the range obtained in WTP final water (Table 4.4). WTP Al residual concentrations presented a high variability, ranged between 13 and 200 µg/L, with an average value of approximately 66.1 µg/L (AdA, 2019).

Table 4.4. Water quality parameters: DOC, UV_{254} absorbance, turbidity, pH, conductivity and aluminium concentration for the natural waters (NW1 and NW2) after the C/F/S in ENPs mixture experiments (all parameters concentrations presented as mean ± standard deviation, n=6).

	Coagulant dose (mg Al_2O_3/L)	**Turbidity (NTU)**	**DOC (mg C/L)**	**UV_{254} (1/cm)**	**pH**	**Conductivity (µS/cm)**	**Al (µg/L)**
NW1	3.0	0.41±0.17	1.50±0.07	0.028±0.003	7.2±0.5	212±5	78.1±1.2
	4.0	0.33±0.16	1.51±0.06	0.030±0.004	7.2±0.5	216±5	78.9±1.1
NW2	15.0	0.07±0.02	2.57±0.28	0.044±0.004	7.5±0.5	364±5	86.2±1.9
	20.0	0.07±0.03	2.65±0.21	0.042±0.008	7.5±0.5	368±5	87.9±2.3

4.4. Conclusions

This work shows for the first time that conventional treatment C/F/S can remove mixtures of ENPs from natural waters during drinking water treatment by optimising coagulant dose based in single ENPs removals. Commercial polyaluminium based coagulant was able to remove approximately 98%, 95% and 94% of Ti, Ag and Cu, respectively, from a low turbidity natural water (1.91±0.36 NTU), and approximately 99% of Ti, Ag and Cu from a medium turbidity natural water (63.33±5.37 NTU). For the selected coagulant doses, residuals concentrations of the co-existing ENPs were 6.5±2.1 and 2.5±0.7 µg Ti/L, 15.0±1.4 and 6.0±1.4 µg Ag/L, and 18.8±8.8 and 0.5±0.1 µg Cu/L, respectively, for the lowest turbidity and NOM content water (NW1) and for the highest turbidity and NOM content water (NW2) studied. Therefore, the differences between water characteristics play an important role on the coagulant demand, on the overall performance of C/F/S process and consequently on the ENPs removal, although both waters are hydrophilic.

The presence of single and multiple ENPs did not comprise the removal of C/F/S target parameters, namely turbidity and NOM. The presence of ENPs, mainly TiO_2, even seems to contribute to greater removal of these parameters in the low turbidity and lower NOM content water. Turbidity removals efficiencies were above 90% and NOM efficiencies ranged between 21-38% for DOC and 36-54% for UV_{254}, which are within the acceptable range for the efficiency's removals of these parameters by C/F/S. Similarly, neither the high turbidity or the high NOM content affected the multiple ENPs removal. Results also indicated that the major mechanism involved in ENPs removal by C/F/S was charge neutralisation. However, in NW2 sweep flocculation may also be involved, but more studies are needed to confirm this.

The water quality parameters after C/F/S were all within the values obtained in the water treatment plant, which demonstrated that ENPs removal did not hamper the overall performance of C/F/S. However, despite the high ENPs removal efficiencies observed, residual concentrations of Ti, Cu and Ag (between approximately 0.5 and 18.8 µg/L) were still found in the treated water by C/F/S. The presence of these concentrations, that could be associated with ENPs dissolution, may require a subsequent process to achieve the entire removal of these metals during drinking water treatment.

Chapter 5

Multiple Nanoparticles in Surface Water: Removal Through Enhanced Conventional Treatment versus Hybrid Membrane Process

This Chapter is in preparation to be submitted for publication:

Serrão Sousa, V., Ribau Teixeira, M.. Multiple nanoparticles in surface water: removal through enhanced conventional treatment versus hybrid membrane process.

ABSTRACT

In this study, the performance of enhanced conventional coagulation with addition of powdered activated carbon (C/F/S+PAC) and hybrid membrane treatment integrating conventional C/F/S with advanced ultrafiltration (C/F/S→UF) were evaluated to maximise the removal of multiple engineered nanoparticles (ENPs) from drinking water sources. Previous results demonstrated that C/F/S alone was not effective (>90%) for the complete removal of multiple metal-based ENPs present in surface waters. Therefore, to minimise the impact of plant requalification to remove these emerging contaminants from surface water sources, it is proposed to recover the most used process in drinking water production (C/F/S) combined or integrated with other conventional and advanced treatments.

Results demonstrated that both C/F/S+PAC and C/F/S→UF improved the removal of multiple ENPs compared to conventional C/F/S alone in hydrophilic natural waters with low and medium turbidity. In C/F/S+PAC treatment, Ti, Ag and Cu removal efficiencies were higher than 99.2%, with Ti concentration being below the detection limit. In the C/F/S→UF, at 90% of water recovery rate, Ti and Cu removal efficiencies were higher than 99.9% in studied waters and undetected in permeate flux. Ag residual concentrations (approximately 5.0-7.0 µg/L) were found in the permeate water indicating that some part of the Ag nanoparticles was in the dissolved form. Overall, the processes optimisation to the ENPs removal did not affect the ability of both processes to remove other target compounds, with residual turbidity, DOC, SUVA and aluminium below the Portuguese and WHO guidelines for drinking water, and similar to those found in drinking water treatment plants (DWTPs).

5.1. Introduction

Over the last years, the growing environmental presence of emerging contaminants, including engineered nanoparticles (ENPs), has received increasing attention from researchers and regulatory authorities. Despite the significant contribution of nanotechnology for technological innovation, its widespread usage and application, in a long list of daily consumer products, associated to their uncontrolled release have effectively produced a detrimental effect on aquatic ecosystems (Jahan et al., 2017). This uncontrolled release of ENPs-containing products eventually will end in the environment, via the municipal wastewater streams, run-off (Choi et al., 2017; Keller et al., 2013; Nowack et al., 2012), and surface waters. Therefore, ENPs may affect human health if not efficiently removed from surface waters used for human consumption, making the removal of nanoparticles from these surface waters relevant technological and societal issues to the supply of healthy and safe potable water.

Conventional coagulation/ flocculation/ sedimentation (C/F/S) treatment has already demonstrated the ability to remove ENPs from surface waters. However, the variability in the process efficiency was very high between studies, from 20 to 99% depending on nanoparticles type and water characteristics (Abbott Chalew et al., 2013; Honda et al., 2014; Kinsinger et al., 2015; Serrão Sousa et al., 2017; Sun et al., 2013).

As demonstrated in the previous chapter, C/F/S is a good option to remove ENPs using Al-based coagulants. However, this process is not effective in the complete removal of multiple metal-based ENPs from natural waters. To further improve the ENPs removal, conventional C/F/S was enhanced with the addition of powdered activated carbon (PAC). PAC characteristics, such as large surface area, pore structure, low toxicity and high surface activity and stability, allow for high removals of NOM and other organic contaminants from surface waters (Huang et al., 2020; Joseph et al., 2012). The addition of PAC as coagulant aid is a commonly used strategy to improve the quality of drinking water in full-scale drinking water treatment plants (DWTP) (Huang et al., 2020). It has been demonstrated that the combination of activated carbon adsorption and coagulation/flocculation (C/F) can achieve large floc sizes, improving the removal of low molecular weight dissolved organic matter and micropollutants that cannot be efficiently removed by C/F alone (Chang et al., 2019; Huang et al., 2020; Shen et al., 2020). This could be an asset to ENPs removal, however the impacts of PAC dosing strategy on the coagulation-flocculation process for water with multiple ENPs have not been assessed so far.

Other authors investigated the removal of ENPs by advanced treatments, namely membranes filtration processes, like micro, ultra and nanofiltration (Abbott Chalew et al., 2013; Serrão Sousa and Teixeira, 2015) once again with removals varying between 17 up to 99% depending on membrane type, nanoparticle and water characteristics. In addition, in most studies, a large amount of ENPs was observed in the treated water. Currently, ultrafiltration (UF) is one of the most promising and reliable membrane technologies applied to surface water treatment due to its high effectiveness in removing bacteria, viruses, dissolved organic matter and suspended particles (Liu et al., 2019; Rasouli et al., 2017). The UF membranes pore size generally range between 1 and 100 nm with molecular weight cut-off (MWCO) varying from 2 to 200 kDa, which makes UF a potential process towards the total retention of ENPs (Le Hir et al., 2018). However, the wide application of UF is still hampered by membrane fouling due to the reduction of membrane flux and the costs increase for the backwashing and membrane materials (Shao et al., 2014). To minimise fouling effect and exploit the C/F/S ability to remove ENPs, C/F/S was coupled with UF, in a hybrid process that integrates conventional and advanced treatments.

Therefore, the current research aims to study two treatment processes to maximise the removal of a mixture of ENPs from surface waters, enhanced conventional coagulation treatment and advanced hybrid membrane process. The enhanced coagulation included the simultaneous addition of PAC and aluminium-based coagulant on C/F/S (C/F/S+PAC). The advanced process integrates the C/F/S with UF (C/F/S→UF). The concept proposed was to minimise the impact of drinking water treatment plant (DWTP) requalification by recovering the most used processes in drinking water production, C/F/S, combined/integrated with other treatment processes. A mixture of metal-based commercial ENPs (TiO_2, Ag and CuO) dispersed in two surface waters was used in the experiments to simulate co-existing nanoparticles real conditions. The impact of ENPs removal on the target compounds of the drinking water treatment, such as turbidity and natural organic matter, was also studied.

5.2. Materials and methods

5.2.1. Surface waters characteristics

The surface waters used in this study were collected from Portuguese freshwater reservoirs currently used to public supply, namely Odelouca in Algarve region (NW1) and Roxo in Alentejo region (NW2). These two sampling locations were selected based on previous monitoring data due to the differences between natural organic matter (NOM) and turbidity (Table 5.1). The water samples were collected and transported in cool (4ºC) to the laboratory for experiments and analysis.

Dissolved organic carbon (DOC) and absorbance at 254 nm (UV_{254}) were used to assess NOM quantity and quality. The specific absorbance (SUVA), determined by normalising the absorbance at 254 nm with DOC, in L/(m.mg), has been used to indicate the degree of aromaticity of NOM (Edzwald and Van Benschoten, 1990; Weishaar et al., 2003). According to Matilainen et al. (2010) and Edzwald and Van Benschoten (1990) classification, waters with SUVA values between 2 and 4 L/(m.mg) present a mixture of aquatic humics, a mixture of hydrophobic and hydrophilic NOM and a mixture of molecular weights. Since, in this study, the natural waters used present SUVA values close to 2 (Table 5.1), hydrophilic and non-humic NOM with low molecular weight and low aromaticity prevails in the mixture. NW1 presents a moderate DOC concentration while NW2 a moderate-high DOC concentration as described in EPA (1999). Regarding turbidity, the waters present low and medium turbidity, namely 1.91 ± 0.36 NTU (NW1) and 63.30 ± 5.51 NTU (NW2).

Table 5.1. Characteristics of natural waters used in the experiments (values presented as mean ± standard deviation, n=6).

	NW1	**NW2**
DOC (mg C/L)	2.23 ± 0.32	4.07 ± 0.29
UV_{254} (1/cm)	0.052 ± 0.002	0.098 ± 0.004
SUVA (L/(m.mg))	2.35 ± 0.08	2.40 ± 0.06
Turbidity (NTU)	1.95 ± 0.30	63.86 ± 1.92
Conductivity (µS/cm)	208 ± 5	359 ± 4
pH (25ºC)	7.3 ± 0.4	7.8 ± 0.6

5.2.2. Metal-based ENPs used in the study

Three metallic commercially available nanoparticles, titanium dioxide (LOT#02527PH), silver (LOT#MKBH2895V) and copper oxide (LOT#02005PH), from Sigma-Aldrich, were used. According to supplier information, the molecular weights of the ENPs are 79.87, 107.87 and 79.55 g/mol for TiO_2, Ag and CuO, respectively, and the surfaces areas are 46.3, 5.0 and 29.0 m^2/g in the same order. Earlier works already determined, by transmission electron microscopy (TEM), that ENPs are spherical, with individual sizes of 74.0±0.0 nm for TiO_2 (Allouni et al., 2012), 41.7±1.1 nm for Ag (Serrão Sousa and Teixeira, 2015) and 33.0±2.6 nm for CuO (Serrão Sousa and Ribau Teixeira, 2013).

As shown in Figure 4.1 (Chapter 4), all the ENPs studied are negatively charged at the NW1 and NW2 conditions. Ag is the most negative charged in both waters, with a zeta potential (ZP) around -40 mV (NW1) and -43 mV (NW2) that corresponds to the lowest hydrodynamic diameter (HD) observed (202.0±29.3 and 195.0±3.7 nm, for NW1 and NW2, respectively). TiO_2 and CuO present similar HD and ZP in the same waters. These results show that NOM imparts a negative charge to NPs surfaces and raises their absolute surface potential, having a global stabilising effect, as described in detail in Section 4.3.1. (Chapter 4). More detailed information about the characterisation of the same ENPs was published in previous works (Serrão Sousa et al., 2017; Serrão Sousa and Ribau Teixeira, 2013; Serrão Sousa and Teixeira, 2015).

5.2.3. Enhanced coagulation and hybrid membrane treatment process

Two different water treatment processes were studied: conventional C/F/S with the addition of powdered activated carbon (C/F/S+PAC) and hybrid membrane process integrating conventional C/F/S with ultrafiltration (C/F/S→UF).

C/F/S experiments were conducted as described in Section 4.2.3. (Chapter 4) using the same operating conditions and commercial polyaluminium chloride coagulant/flocculant (WAC® from Elf Atochem, France) commonly used in the drinking water industry and kindly provided by *Águas do Algarve, S.A.* company. Coagulant doses were fixed at 3.0 and 15.0 mg/L Al_2O_3 for NW1 and NW2, respectively, optimised by series of C/F/S experiments for ENPs removal performed in Chapter 4.

5.2.3.1. C/F/S+PAC experiments

In C/F/S+PAC experiments, PAC was added simultaneously with the coagulant to the water at the beginning of the fast stirring phase (coagulation), followed by slow mixing (20 min) and sedimentation (30 min). PAC was separated from the water by sedimentation, corresponding to the last phase of the C/F/S process. Preliminary experiments with higher sedimentation times (60, 90 and 120 min) were done with no improvement in PAC removal compared to 30 min. After the C/F/S+PAC process, water samples (200 mL) were collected approximately 2 cm below the water surface for further analysis. These experiments were conducted in two steps. The first experimental step was made to optimise the PAC dose, aiming the removal of 99% of single ENPs. Thus, 0.0 to 20.0 mg/L (NW1) and 0.0 and 40.0 mg/L (NW2) of activated carbon were tested using 1.0 mg/L of single ENP (TiO_2, Ag and CuO). Then, the second experimental step was performed to remove the ENPs mixture with PAC doses selected from the first step. In these experiments, an ENPs mixture of TiO_2, Ag and CuO with a total concentration of 1 mg/L of nanoparticles (ratio 1:1:1) was used. In both experiments, a control trial was carried out where no PAC was added (0.0 mg/L PAC). Experiments were made in triplicate.

Commercial coal-based PAC commonly used in real drinking water treatment context, Sorbopor MV 118, was used in this study (kindly provided by *Águas do Algarve, S.A.* company). This PAC is produced by physical activation with a minimum iodine value of 1000 mg/g and particle size (>80%) <74 μm (200 US mesh). The specific area is 1050 m^2/g, determined according to the Brunauer-Emmett-Teller (BET) model, the apparent density is 500±50 kg/m^3, and ash content is 15% (according to supplier information). The FTIR results (Figure C 1, Appendix C) confirmed the participation of the functional groups of OH^-, COO^-, and CO present on the surface of PAC in the adsorption of the ENPs onto activated carbon.

5.2.3.2. C/F/S→UF experiments

In C/F/S→UF experiments, the water was first treated using C/F/S followed by ultrafiltration. Thus, after C/F/S process, the water passed to the membrane's unit feed tank. These experiments were conducted with 1.0 mg/L of single TiO_2, Ag and CuO and with the ENPs mixture in a total concentration of 1 mg/L of nanoparticles (ratio 1:1:1).

The UF experiments were conducted in a plate and frame unit (Lab-unit M20 from Alfa-Laval) using a polyethersulfone, negatively charged, ultrafiltration membrane (Nadir P150F;

Microdyn-Nadir GmbH). The total membrane area was 0.0720 m^2 and the molecular weight cut-off 150 kDa, corresponding to approximately 26 nm of pore diameter (Tian et al., 2013; Zheng et al., 2009). Before use, the membranes were first soaked in ultrapure water overnight, and then rinsed by filtering at least 2 L of deionised water (DI) to remove any organic residual on the membranes. Prior to the experiments, the membranes were compacted using DI at 5 bar until no variation in the flux was observed, after which the initial permeate flux was established. Normalised specific flux J/J0 was used for membrane performance, being J the flux at a stipulated condition and J0 the initial membrane flux. Concentration runs at a constant transmembrane pressure of 1 bar and room temperature (21±1 ºC) were performed to simulate the real scale UF operation. These runs consisted of testing different water recovery rates (WRR), defined as the ratio between the permeate volume collected so far and the initial feed volume, without recirculating the permeate to the feed tank. In these experiments, water samples from feed and permeate were collected at predefined WRR values (0, 40, 50, 60, 70, 80 and 90%) and flux was measured.

5.2.4. Analytical methods

Water samples were characterised for turbidity, pH, conductivity, dissolved organic carbon (DOC), UV absorbance at 254nm (UV_{254}) and metal concentration (Ti, Ag, Cu) in bulk and treated waters, and Al only in treated water, using standard methods of analysis (Eaton et al., 2005a, 2005b). Replicates of all experiments were performed to ensure accuracy. Turbidity was measured with a HACH 2100N turbidity meter of high resolution (0.001 NTU), pH at 25 °C was measured using a Whatman WTW pH340 and conductivity a Crison GLP32 conductimeter. DOC and UV_{254} water samples were pre-filtered through a 0.45 µm glass filter before analysis. DOC was measured in a Shimadzu TOC 5000A analyser, 50 ppb-4000 ppm, and UV_{254} in a Beckman DU 640B, UV/VIS spectrophotometer.

Titanium, silver, copper and aluminium concentrations were determined using atomic absorption spectrometry (AAS AAnalyst 800, PerkineElmer, detection limit: 0.350 µg/L), after acid digestion with 2% nitric acid (HNO_3). Ti, Ag, Cu and Al were analysed by graphite furnace. The accuracy of the analytical procedure was assessed by the injection of Ti, Ag, Cu and Al standards at the beginning of sample quantification and at every ten samples.

FTIR (Bruker, model Tensor 27) was employed to determine the presence of surface functional groups in the PAC, at room temperature over a spectral wavenumber ranging from

4000-500 1/cm. It was used the pellet (pressed-disk) technique, with a sample thoroughly mixed using a mortar and pestle to get a homogeneous mixture and further mixed with powdered KBr to form pellets using a pellet maker.

5.3. Results and Discussion

5.3.1. C/F/S+PAC performance

5.3.1.1. ENPs and turbidity removal

Figure 5.1 and Figure 5.2 show the ENPs and turbidity removal efficiencies by C/F/S+PAC treatment using natural waters (NW1 and NW2) for the experiments with single and multiple ENPs.

Results show an increase in Ti, Ag and Cu removal efficiencies with the addition of PAC, observed for both waters NW1 and NW2 (Figure 5.1), and consequently a decrease in the ENPs residual concentrations. Without PAC (only with 3 mg/L of Al_2O_3 in NW1 and 15 mg/L of Al_2O_3 in NW2), high removal efficiencies of Ti, Ag and Cu are observed (>90%). However, up to approximately 80 µg/L of residual metal concentration is still found in the treated water. When the PAC is added, in NW1, the single ENPs removal efficiencies increase to >99.2% and at PAC doses of 10 mg/L or higher remain almost constant (Figure 5.1a). In the NW2, the same trend is observed, with removals become consistent (>99.2%) at PAC doses of 20 mg/L or higher (Figure 5.1b) due to water characteristics. In the experiments with ENPs mixture, results show no need to increase PAC dose to remove the multiple ENPs in the waters, since the PAC doses of 10 mg/L (NW1) and 20 mg/L (NW2) are also highly effective (>99.2%, Figure 5.1a and Figure 5.1b). Generally, the addition of PAC selected doses enhances the removal of ENPs in approximately 10% compared with the C/F/S without PAC.

As already explained (Chapter 4), ENPs dispersed in natural waters showed a HD higher than the individual size, which indicates the formation of aggregates due to interactions between nanoparticles and with the surrounding solution that promotes aggregation (Jiang, 2015). Therefore, in the surface waters, ENPs would be coated with NOM, imparting a negative charge to nanoparticles (Chapter 4, Figure 4.1). The addition of the highly positively charged coagulant induced the ENPs destabilisation (decreasing repulsive forces), through neutralisation of negative charges by hydrolysed Al^{3+}, promoting the aggregation of the ENPs-NOM composite,

as also shown by Zhang et al. (2015). Under such conditions (ENPs-NOM destabilised with surface charge closer to zero), aggregation and adsorption on the PAC surface are favoured mediated by van der Walls attractive forces, leading to their almost complete removal (Gicheva and Yordanov, 2013). In another study, Syafiuddin et al. (2018) confirmed by XRD that the interaction mechanism between AgNPs and activated carbon surface was mainly electrostatic forces interaction via binding of Ag^{+} with O^{-} present on the activated carbon surface to form AgO. PAC acts not only as an adsorbent but also enhances the settleability of the aggregates (ENPs-NOM composite) formed during coagulation/flocculation, favouring ENPs removal by sedimentation, as described by Tomaszewska et al. (2004). On the other hand, the application of coagulant helps the removal of PAC, together with adsorbed ENPs-NOM composites from solutions (Tomaszewska et al., 2004). Piplai et al. (2017) stated that removal of NPs using activated carbon (without coagulant) became a promising method. However, these authors reported lower removal, around 78% and 69% for CuO and ZnO ENPs respectively, which confirmed that the combination of Al-based coagulant with PAC promotes a higher ENPs removal than PAC alone.

For the same water and between waters, slight differences in ENPs removals are observed. This is related to their specific properties which affect the aggregation and adsorption behaviour determined by a combination of ENPs properties and physicochemical characteristics of the medium (Amde et al., 2017). Ti, for example, has the highest removal efficiencies in both waters, for individual and mixture experiments (approximately 100%), which can be related to the adsorptive titanium properties, that have been shown to be effective in particle, nutrients and organic matter removal (Zhao et al., 2014).

The removal of turbidity from water usually follows the same trend observed for ENPs removal (as shown in previous chapters and Serrão Sousa and Ribau Teixeira, 2013). However, in C/F/S+PAC experiments, the turbidity removal decreases with the increase of PAC dose (Figure 5.2) showing a different trend from the ENPs removal presented in Figure 5.1. This is due to the relatively low PAC density (0.55 g/mL) whose addition resulted in residual PAC that did not adsorb to the composite ENPs-NOM and did not settle. Similar results for turbidity increase with the increase of PAC dose in combined coagulation/flocculation with adsorption were achieved by Huang et al. (2020). The turbidity removal efficiencies decrease from 87-93% to approximately 65% as the PAC dose increases from 0.0 to 20 mg/L in NW1. In water NW2, the decrease in turbidity removal is almost imperceptible from 99% to approximately 97%, as the PAC dose increases from 0.0 to 40 mg/L (Figure 5.1). These results are related with

higher particulate matter content (higher turbidity) of NW2 and the application of higher coagulant and PAC doses which can promote the enmeshment of the particles in a mass of amorphous Al-based coagulant, PAC and particulate matter improving the removal of residual PAC by some "sweeping" phenomenon (Huang et al., 2020; Sun et al., 2019).

The presence of single or multiple ENPs does not significantly impair the turbidity removal. Similarly to the ENPs removal, higher doses of PAC in mixtures experiments is not required to achieve the same turbidity removal as single experiments.

a) NW1 b) NW2

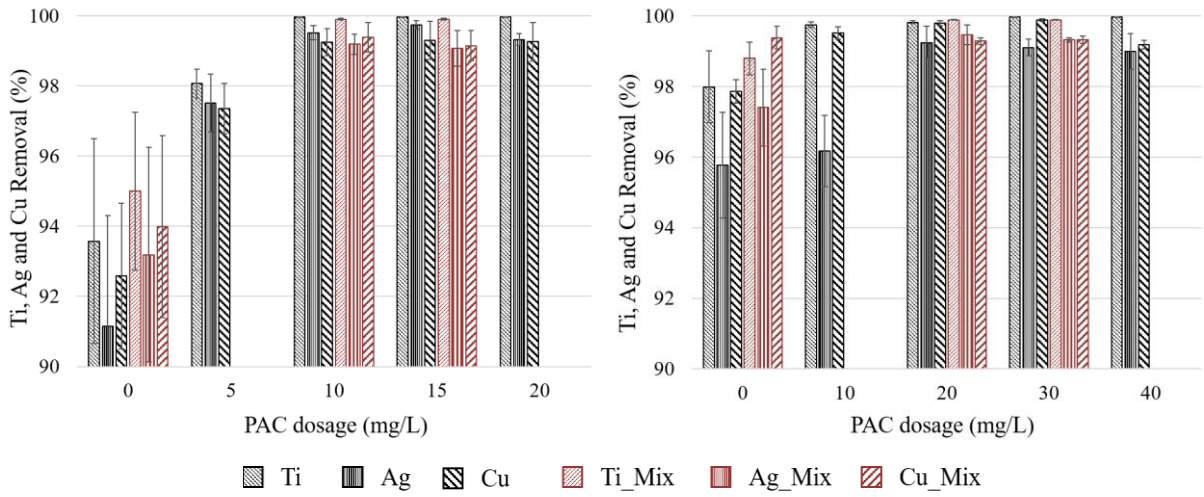

Figure 5.1. Variation of Ti, Ag and Cu removal efficiencies with PAC dose: (a) NW1 (3.0 mg Al_2O_3/L coagulant added) and (b) NW2 (15.0 mg Al_2O_3/L coagulant added) (21±1 °C). Experiments performed with the mixture (Mix) and each nanoparticle individually (removal values presented as mean, standard deviations (n=6) are shown by the error bars).

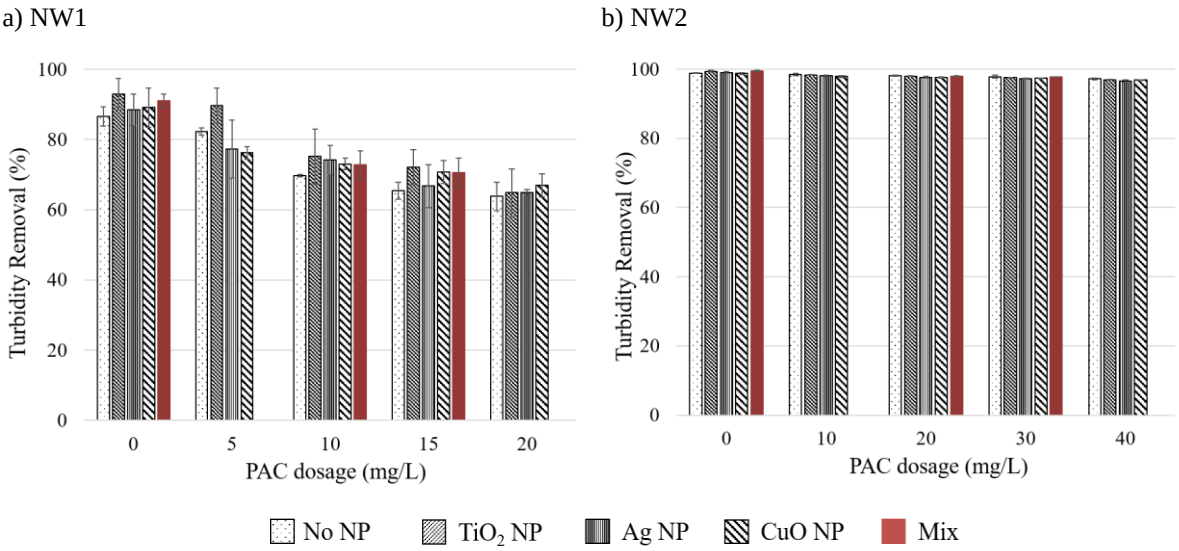

Figure 5.2. Variation of turbidity removal efficiencies with PAC dose: (a) NW1 (3.0 mg Al_2O_3/L coagulant added) and (b) NW2 (15.0 mg Al_2O_3/L coagulant added) (21±1 °C). Experiments performed with the mixture (Mix) and each nanoparticle individually (removal values presented as mean, standard deviations (n=6) are shown by the error bars).

5.3.1.2. NOM removal

Figure 5.3 shows the NOM removal efficiencies by C/F/S+PAC, trough the removal of DOC and UV_{254} in NW1 and NW2 for the experiments with single and multiple ENPs.

DOC and UV_{254} removal efficiencies show that the addition of PAC in combination with Al-based coagulant increases the NOM removal for both waters (Figure 5.3). In experiments without PAC (PAC dose of 0.0 mg/L, Figure 5.3), DOC removal ranges from 20 to 26% and 34 to 39% for NW1 and NW2, respectively, and UV_{254} varies between 38 and 43% (NW1) and 50 and 57% (NW2). For the selected PAC dose (10 mg/L for NW1 and 20 mg/L for NW2), DOC removals increase to 72-77% in NW1 and to 78-82% in NW2, while UV_{254} removals rise to 88-94% and 94-97% in NW1 and NW2, respectively. The increase observed in DOC and UV_{254} removal efficiencies demonstrates that the combination of these two processes also enhances the effectiveness of NOM removal. This improvement can be related to higher efficiency of coagulation to remove the hydrophobic fraction of NOM rather than hydrophilic. Since PAC is efficient in the removal of the prevalent low molecular hydrophilic NOM (even in waters with low SUVA), its addition improves the NOM removal by removing these compounds insufficiently removed by coagulation in NW1 and NW2 (Joseph et al., 2012; Matilainen et al., 2010). These results were somehow expected since several authors have

studied the combined use of coagulation and PAC adsorption to maximise the overall removal of NOM with removals up to 80% (Huang et al., 2020; Joseph et al., 2012; Jung et al., 2015; Sillanpää et al., 2018; Tomaszewska et al., 2004). As demonstrated by Huang et al. (2020), the addition of single PAC is also less efficient than the combination of the two processes (C/F/S and PAC). These authors showed that, for the same PAC dose, the addition of 8 mg/L of $Al_2(SO_4)_3$ doubled the NOM removal. Similarly, Tomaszewska et al. (2004) also observed an increase in humic acid reduction by the addition of Al-based coagulant to PAC.

The presence of ENPs does not affect the DOC and UV_{254} removals, which indicates that the optimisation of PAC dose based on the ENPs removal does not hamper the NOM removal by C/F/S+PAC process.

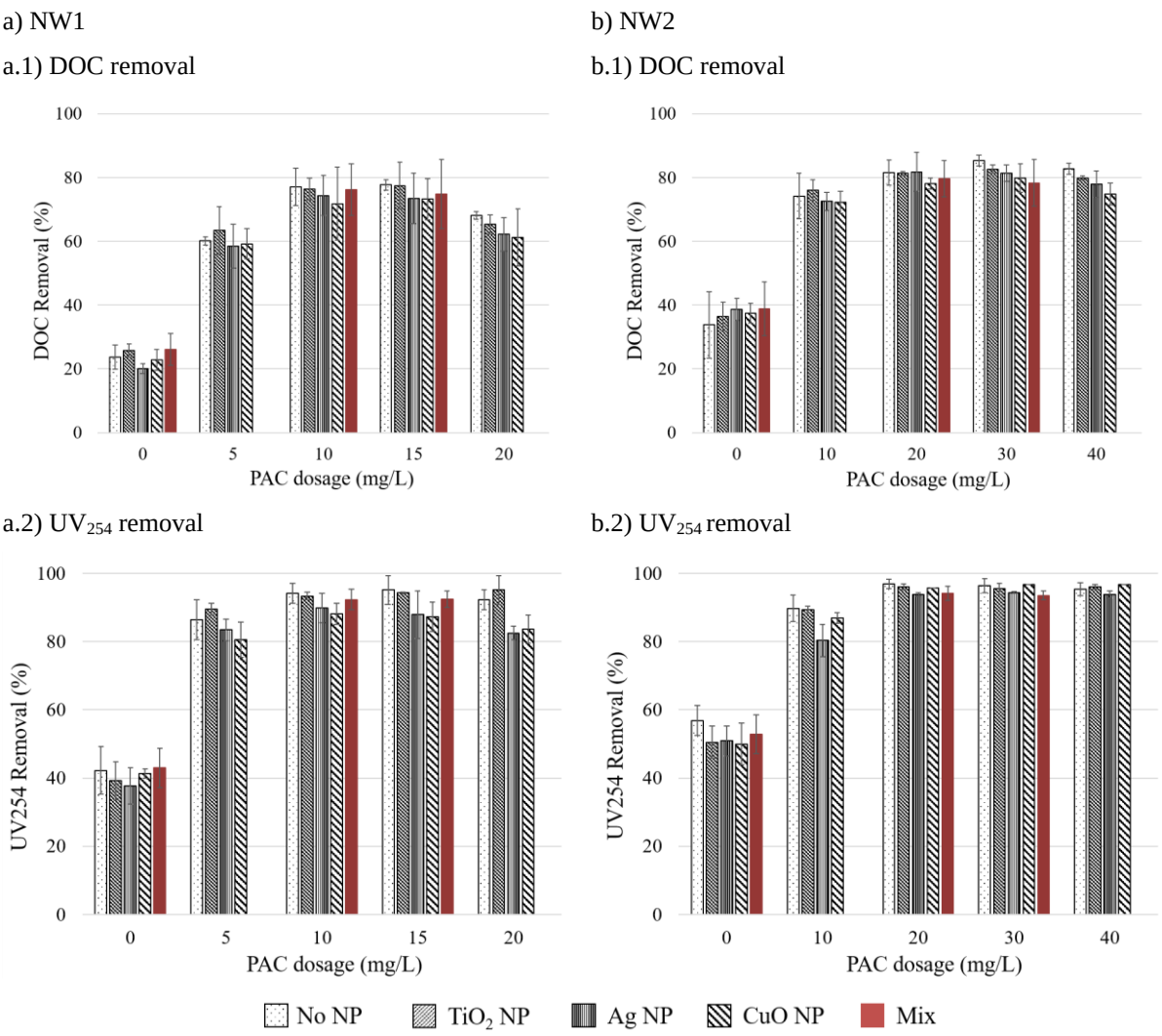

Figure 5.3. Variation of DOC (1) and UV_{254} absorbance (2) removal efficiencies with PAC dose: (a) NW1 (3.0 mg Al_2O_3/L coagulant added) and (b) NW2 (15.0 mg Al_2O_3/L coagulant added) (21±1 °C). Experiments performed with the mixture (Mix) and each nanoparticle individually (removal values presented as mean, standard deviationsμ (n=6) are shown by the error bars).

5.3.2. C/F/S→UF performance

5.3.2.1. ENPs and turbidity removal

Figure 5.4 and Figure 5.5 show the ENPs and turbidity removal efficiencies by the hybrid process C/F/S→UF in natural waters (NW1 and NW2) for the experiments with single and multiple ENPs. The ENPs removal efficiencies are higher than 98% for all the WRR tested, in both NW1 (Figure 5.4a) and NW2 (Figure 5.4b). Ti and Cu removal efficiencies are higher than 99.9% in both waters and undetected in permeate flux (concentration was below the detection limit of 0.350 µg/L) from the WRR of 60% for Ti and 70% for Cu until the WRR of 90%. However, this trend is not observed for the AgNPs. The maximum Ag removal efficiency in the single experiments is 99.1±0.17% in NW1 (Figure 5.4a) and 99.3±0.08% in NW2 (Figure 5.4b), whereas, for ENPs mixture, Ag removal is ≤ 98.1±0.25% (NW1, Figure 5.4a) and ≤ 98.5±0.49% (NW2, Figure 5.4b), indicating that some part of the AgNPs is not removed by the UF membrane. AgNPs aggregates (Figure 4.1, Chapter 4) and average individual size (41.7±1.1 nm, Table 4.2, Chapter 4) are higher than the membrane pore size of approximately 26 nm (150 kDa MWCO) (Tian et al., 2013; Zheng et al., 2009), so the Ag detected in the permeate can result from the release of silver ions from the nanoparticles. It is well-known that the high surface area of metal ENPs increases the potential of ions to be released from these nanoparticles (Bian et al., 2011; Mudunkotuwa and Grassian, 2011). Zhang et al. (2016) concluded that dissolution is higher for low AgNPs concentrations compared with high AgNPs concentrations, describing a dissolution higher than 20% for 1 mg/L of these nanoparticles, which is in accordance with the Ag residual concentrations found in the present study. In previous work (Serrão Sousa and Ribau Teixeira, 2015), the dissolution of the same AgNPs was determined at 3.0±0.4% of the total AgNPs concentration present in solutions (100 mg/L). However, Gomes et al. (2014) reported a higher dissolution for the same AgNPs, approximately 24.5% for a lower initial concentration of AgNPs (10 µg/L), which supports Zhang et al. (2016) findings. For CuO ENPs the dissolution was less than 1% of the initial concentration (Gomes et al., 2012, 2011) and TiO_2 ENPs are commonly considered insoluble metal oxide (De Klein et al., 2016).

Similarly to ENPs removal, turbidity removal efficiencies are also higher than 98% in NW1 (Figure 5.5a) and higher than 99% in NW2 (Figure 5.5b) for WRR ≥40%, becoming higher than 99% in NW1 and higher than 99.9% in NW2 for 90% of WRR. These results corroborate the assumption that nanoparticulate Ag is entirely removed by C/F/S→UF and the Ag present in permeate corresponds to silver ions since turbidity is related with NPs concentration, as discussed above. The highest turbidity removals in NW2 are due to the highest water turbidity (Table 5.1).

Based on the aggregates and individual nanoparticles sizes, size exclusion is proposed as the main mechanism for the removal of the ENPs used. In the studied waters, ENPs aggregates are formed with an HD minimum of 202±29 nm (NW1), and 195±3.7 nm (NW2) (Figure 4.1, Chapter 4) and the individual average sizes of nanoparticles are 74.0±0.0 nm, 41.7±1.1 nm and 33.0±2.6 nm for TiO_2, Ag and CuO, respectively (Table 4.2, Chapter 4). Thus, these sizes are larger than the pore size of the UF membranes used in the experiments (approximately 26 nm). Moreover, smaller aggregates of the ENPs-NOM that remain in waters after C/F/S are also bigger than membrane pore sizes. Several other authors have also proposed the same mechanism for the nanoparticles removal by UF. Guo et al. (2010) showed that Fe_3O_4 NPs with an average size of about 35 nm was fully retained by UF membranes with a nominal pore size of about 25 nm (MWCO of 150 kDa), during tangential filtration even under low transmembrane pressure (TMP) (0.25 bar). In another study, Wu et al. (2014) demonstrated that NPs with individual sizes between 1.5 nm and 4.5 nm were completely retained by flat membranes with cut-offs between 1 kDa and 10 kDa, presenting estimated pore size of 1.8 and 5.37 nm under a TMP of 2 bar. The importance of the operating conditions and water chemistry of filtered suspensions have been highlighted in all these studies.

One of the most important concerns in membrane filtration is fouling, however, since C/F/S was performed first, this problem is minimised.

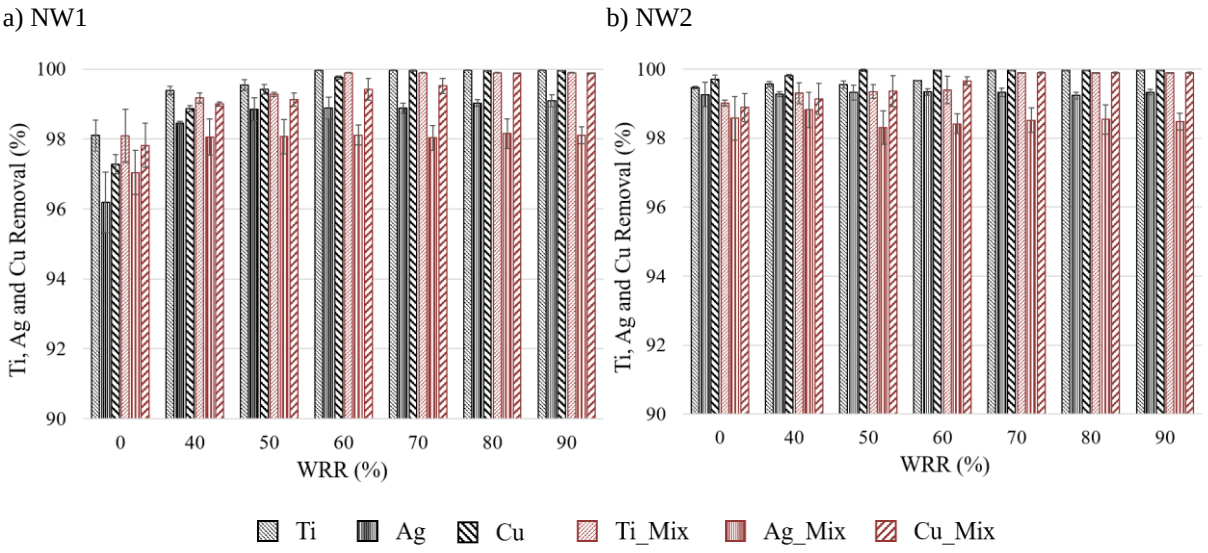

Figure 5.4. Variation of Ti, Ag and Cu removal efficiencies with WRR in C/F/S→UF process: (a) NW1 and (b) NW2 (21±1 °C). Experiments performed with the mixture (Mix) and each nanoparticle individually (removal values presented as mean, standard deviations (n=6) are shown by the error bars).

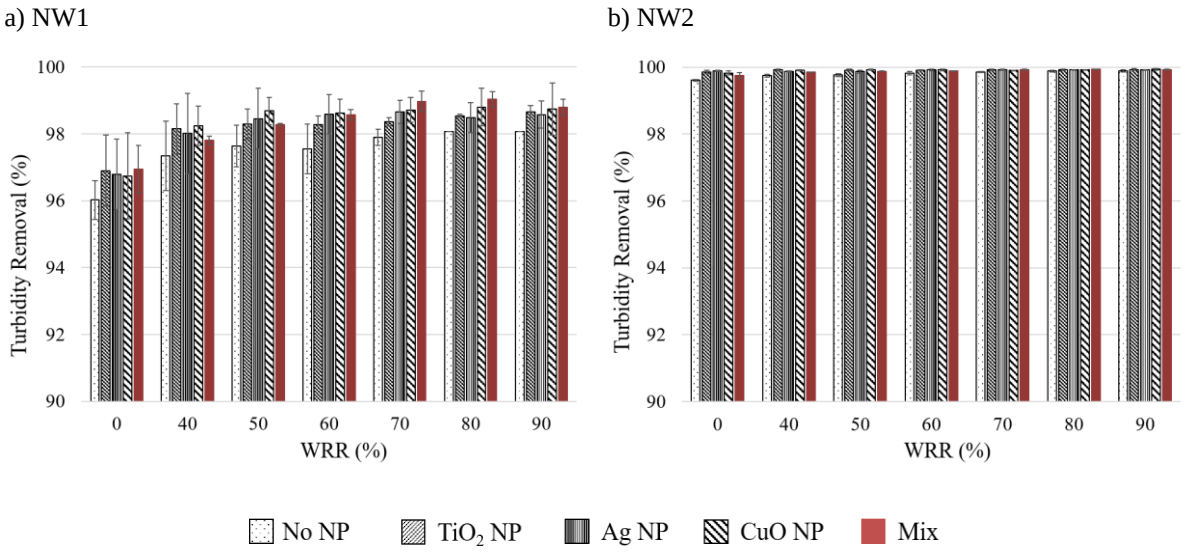

Figure 5.5. Variation of turbidity removal efficiency with WRR in C/F/S→UF process: (a) NW1 and (b) NW2 (21±1 °C). Experiments performed with the mixture (Mix) and each nanoparticle individually (removal values presented as mean, standard deviations (n=6) are shown by the error bars).

5.3.2.2. NOM removal

Figure 5.6 shows the NOM removal efficiencies by the hybrid membrane process C/F/S→UF, trough the removal of DOC and UV_{254} in NW1 and NW2 for the experiments with single and multiple ENPs. NOM removal is similar in both waters, with DOC and UV_{254} removal efficiencies showing the same trend in NW1 and NW2. DOC removal efficiencies increase with the WRR increase, achieving the maximum removal at the highest WRR tested (90%), for both NW1 (59-65%, Figure 5.6a.1) and NW2 (70-75%, Figure 5.6b.1). An increase in the UV_{254} removal efficiencies is also observed (NW1, Figure 5.6a.2 and NW2, Figure 5.6b.2) but less pronounced when compared to DOC. At 90% of WRR, the UV_{254} removal efficiencies range from approximately 81 to 84% for NW1 and 80 to 87% for NW2. Higher removal efficiencies of UV_{254} compared to DOC in both waters can be related to the highest affinity of aromatic NOM (high molecular weight).

The presence of single and multiple ENPs does not affect the removal of NOM by CFS→UF, since removals of DOC and UV_{254} are similar in experiments with and without ENPs in both waters.

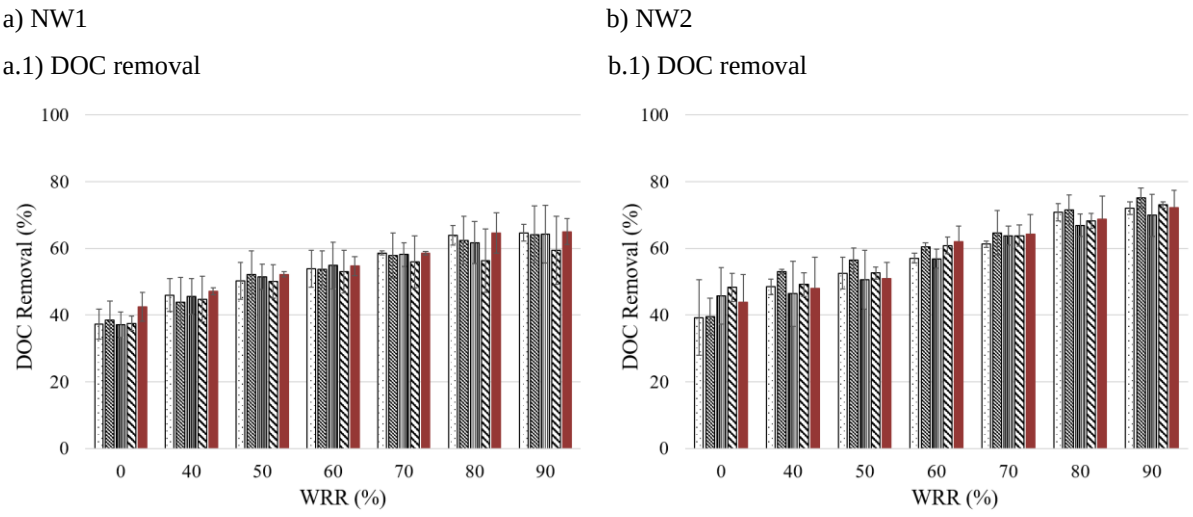

Figure 5.6. Variation of DOC (1) and UV_{254} absorbance (2) removal efficiencies with WRR in C/F/S→UF process: (a) NW1 and (b) NW2 (21±1 °C). Experiments performed with the mixture (Mix) and each nanoparticle individually (removal values presented as mean, standard deviations (n=6) are shown by the error bars).

a.2) UV_{254} removal

b.2) UV_{254} removal

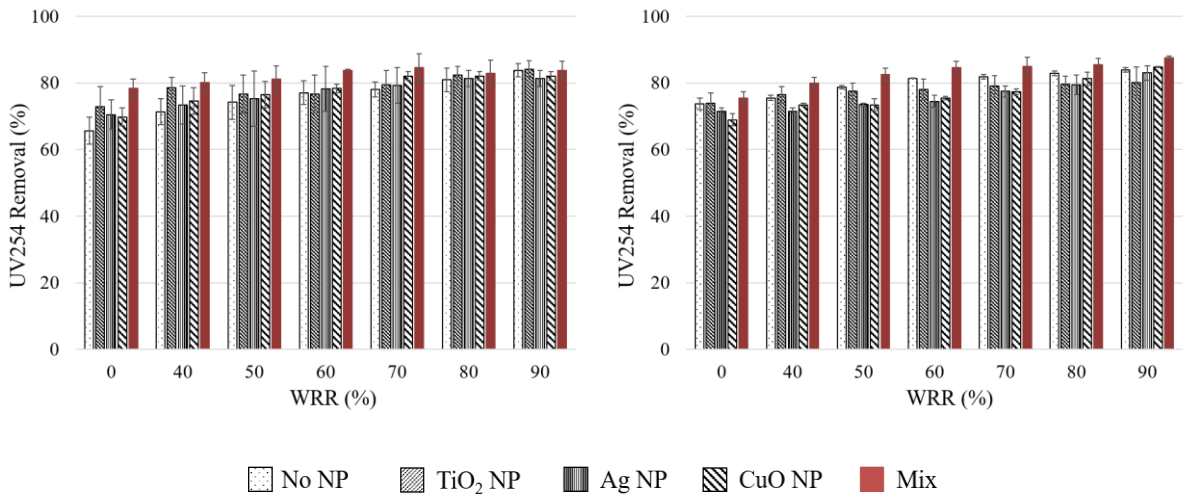

Figure 5.6 (cont.). Variation of DOC (1) and UV_{254} absorbance (2) removal efficiencies with WRR in C/F/S→UF process: (a) NW1 and (b) NW2 (21±1 °C). Experiments performed with the mixture (Mix) and each nanoparticle individually (removal values presented as mean, standard deviations (n=6) are shown by the error bars).

5.3.2.3. Ultrafiltration permeate flux

The variation of the normalised UF permeate flux (J/J_0) with the increase of WRR, using single and multiple ENPs, is shown in Figure 5.7 for the hybrid C/F/S→UF experiments.

For NW1 (Figure 5.7a), the trend of normalised flux is similar for all the conditions tested. An initial decline in flux is observed, and then a relatively steady plateau is achieved. Without the presence of ENPs, after this initial decline, the normalised flux stabilises (approximately at 0.82) until the highest WRR tested (90%) (Figure 5.7a). The addition of ENPs increases the initial flux decline, ranging from 0.77 and 0.72, with CuO ENPs having a higher impact in the UF membrane flux. At the highest WRR tested (90%), the normalised flux is 0.77 and 0.76 for TiO_2 and Ag nanoparticles, respectively, and 0.72 for both CuO NPs and ENPs mixture (Figure 5.7a). The highest flux decline in the presence of CuO may be due to slightly larger aggregates formed when dispersed in the natural waters compared to other nanoparticles studied (Figure 4.1, Chapter 4).

The normalised permeate flux for NW2 has a higher initial decline when compared with NW1 (Figure 5.7a and Figure 5.7b), dropping by nearly 35% and continuing the decrease until 90% of WRR. At this point, the normalised flux is about half of the initial flux (Figure 5.7b), varying between the maximum of 0.57 without ENPs and a minimum of 0.51 for Ag. In contrast with the NW1, the presence of ENPs does not have a negative impact on the flux of NW2

(compare Figure 5.7a and Figure 5.7b). Therefore, the observed decline in permeate flux is due to water characteristics such as NOM. In fact, NOM is one of the highest contributors to membrane fouling and has a great tendency to adhere to polysulfone membranes (Yu et al., 2019). After C/F/S process and prior to UF, NW2 presents a higher NOM content than NW1. DOC ranges from 1.50±0.07 to 1.68±0.27 mg C/L and UV_{254} between 0.028±0.003 and 0.031±0.002 1/cm in NW1, and in NW2 DOC varies from 2.49±0.23 to 2.70±0.21 mg C/L and UV_{254} from 0.040±0.003 to 0.046±0.006 1/cm. This difference in DOC and UV_{254} values between the two waters indicates that NOM content is responsible for the high flux decline observed in NW2. According to Yu et al. (2019), NOM accumulates on the UF membrane surface, promoting the formation of a cake layer and blocking the membrane pores which decreases the permeate flux.

The results described above show that despite the declines observed in the permeate flux, the effectiveness of ENPs (Figure 5.4), turbidity (Figure 5.5) and NOM (Figure 5.6) removal is not affected, and the overall performance of hybrid membrane process, C/F/S→UF, is not hampered.

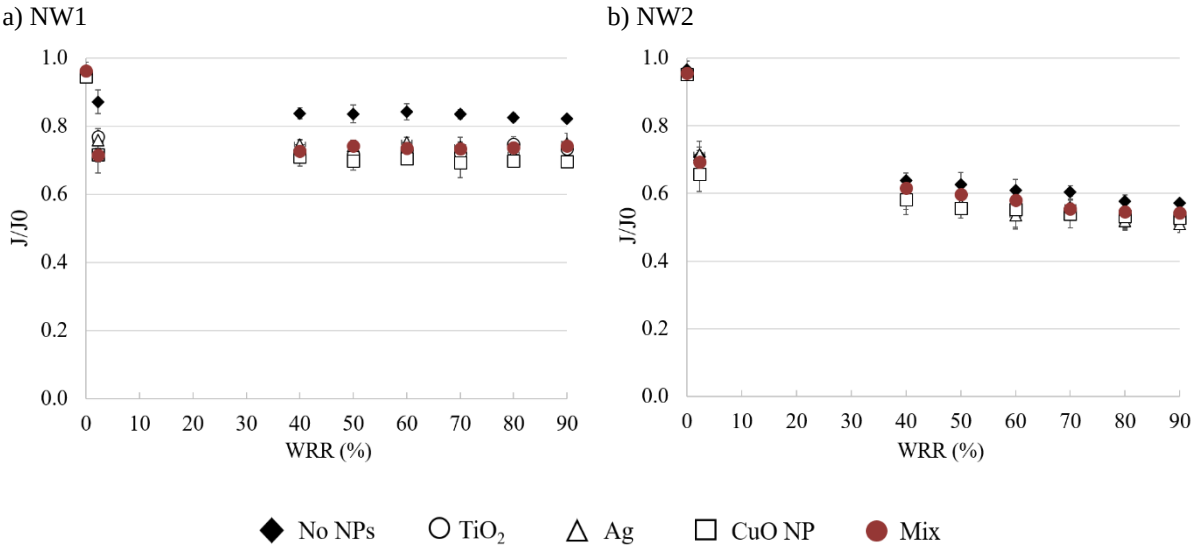

Figure 5.7. Normalised UF permeate flux during C/F/S→UF process: a) NW1 and b) NW2 (21±1 °C). Experiments performed with the mixture (Mix) and each nanoparticle individually (removal values presented as mean, standard deviations (n=3) are shown by the error bars).

5.3.3. C/F/S+PAC vs C/F/S→UF

5.3.3.1. Ti, Ag and Cu residual concentrations

Figure 5.8 shows the residual Ti, Ag and Cu concentrations measured in treated waters after C/F/S+PAC, for the selected dose of PAC (10 mg/L for NW1 and 20 mg/L for NW2) and after C/F/S→UF at the highest WRR tested (90%) for the ENPs mixture experiments.

Ti concentration is under the detection limit for both treatments and waters (Figure 5.8). This indicates that TiO_2 can be entirely removed by C/F/S+PAC and C/F/S→UF, optimised for the ENPs removal and using a membrane with an appropriate pore size for the target ENPs. The hybrid process (C/F/S→UF) outperforms the enhanced conventional process (C/F/S+PAC) in the removal of Cu from NW1 and NW2. However, this is not observed for Ag, since its residual concentration is higher after C/F/S→UF process than after C/F/S+PAC (Figure 5.8). As discussed earlier, this can be related to the dissolution of AgNPs, the nanoparticulate part is retained by the ultrafiltration membrane (with pore size lower to the individual size of AgNPs), while the ionic part passes through the membrane pores. However, the Ag residual concentration is far below the allowable limit for this metal (not specific for nanoparticles) established for drinking water by US EPA (2017) (100 µg/L). The best performance of C/F/S+PAC in the removal of Ag is related to the adsorption of Ag^+ by activated carbon, as described above.

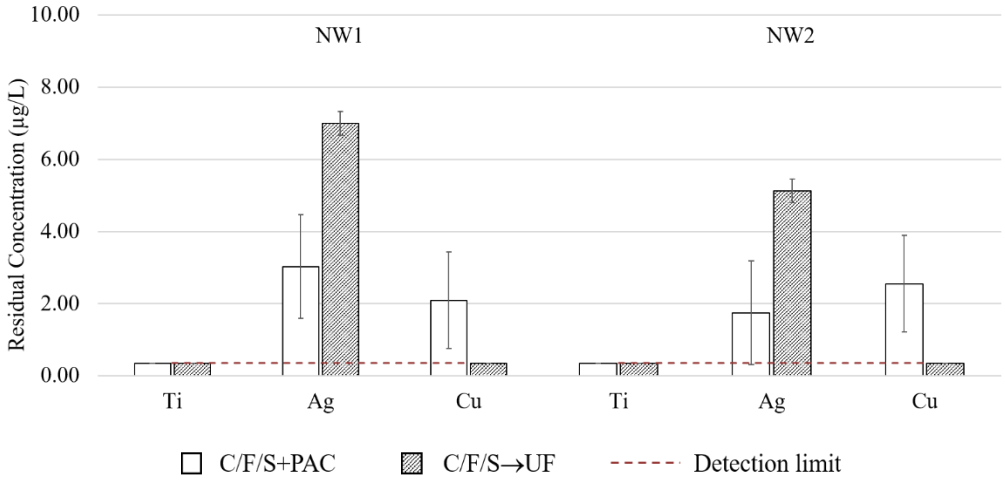

Figure 5.8. Residual concentrations of Ti, Ag and Cu for the selected PAC dose in C/F/S+PAC (10 mg/L for NW1 and 20 mg/L for NW2) and the highest WRR tested (90%) in C/F/S→UF for NW1 and NW2. Experiments performed with the ENPs mixture (residual values presented as mean, standard deviations (n=6) are shown by the error bars).

For comparison purposes, Figure 5.9 shows the residual metal concentrations after C/F/S with coagulant dose optimised for ENPs removal (Chapter 4), after C/F/S+PAC with PAC dose also optimised for ENPs removal, and after C/F/S→UF at the highest WRR tested (90%) for the ENPs mixture experiments. Overall, the combined use of coagulation and adsorption using PAC and the integration of C/F/S with UF exceed the Ti, Ag and Cu removal efficiencies of using only C/F/S (Figure 5.9). According to the previous and the present results (Chapters 4 and 5), the stand-alone coagulation process is not a suitable treatment process for the complete removal of ENPs in comparison to C/F/S+PAC and C/F/S→UF. The C/F/S+PAC process either matched or exceed the removals of the hybrid process, shown by the lowest metal residual concentrations presented in Figure 5.9. The poorest efficiency of C/F/S→UF is related to the dissolution of AgNPs. In this case, technology like nanofiltration could be more appropriate.

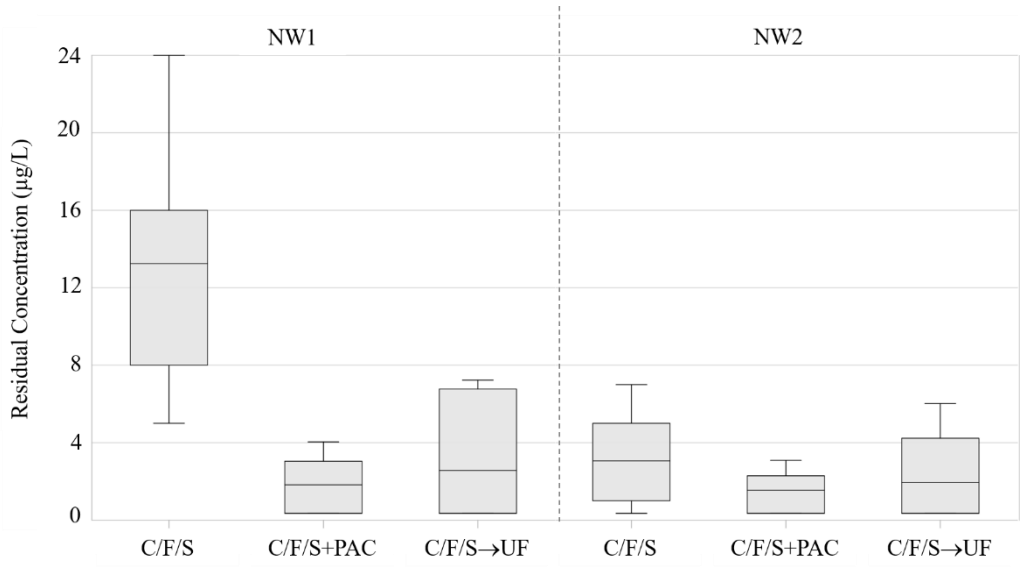

Figure 5.9. Residual concentrations of metals in treated water after C/F/S, C/F/S+PAC (with 10 mg/L of PAC (NW1) and 20 mg/L of PAC (NW2)), C/F/S→UF (at 90% WRR) for NW1 and NW2. Experiments performed with the ENPs mixture (box limits represent 25 and 75 percentiles, the line inside the boxes is the mean value of residual values, whiskers showed the minimum and maximum residual values) and using 3 mg/L of Al_2O_3 (NW1) and 15 mg/L of Al_2O_3 (NW2) in C/F/S.

5.3.3.2. Water quality

Although high-efficiency removals and low residual concentrations have been achieved for the three ENPs used with both studied treatments, it is imperative to evaluate the quality of the final treated waters. Therefore, in this section the residual turbidity (Figure 5.10a), DOC (Figure 5.10b) and $SUVA_{254}$ (Figure 5.10c) in the treated waters, after C/F/S+PAC and C/F/S→UF, are presented for the ENPs mixture experiments. These residuals values and also residual aluminium are compared with Portuguese guidelines for drinking water (Portuguese Government, 2007) and with real WTP parameters (personal communication).

According to WTP information, the average coagulant (WAC AB®) dose applied in C/F/S treatment is 34.7±9.1 mg/L of Al_2O_3 (with a minimum dose applied of 22.0 mg/L of Al_2O_3 and maximum of 52.1 mg/L of Al_2O_3), indicating that the doses applied in this study (3 and 15 mg/L of Al_2O_3) are far below the ones used in the WTP. For the PAC doses, the WTP average is 1.75±0.56 mg/L, ranging between 0.93 and 2.51 mg/L. In this case, the PAC doses used in this study are above the ones used in WTP. However, according to US EPA (2017b), PAC dosages can range between 1 to 100 mg/L depending on the type and concentrations of organic compounds present in water. Dosages of 1 to 20 mg/L are typical for DWTP (US EPA, 2017b). Therefore, the optimal PAC concentrations for NW1 and NW2 to remove ENPs used in this study are within the typical dosage applied in real water treatment context, not worsening the quality of treated water. Moreover, the decrease in the quantity of Al-based coagulant is an asset for human health and reduces the problem of metal sludge treatment and disposal.

Residual turbidities varied between 1.07±0.10 NTU (NW1) and 1.34±0.01 NTU (NW2) after the C/F/S+PAC treatment and from 0.05±0.01 NTU (NW1) and 0.05±0.02 (NW2) after the C/F/S→UF (Figure 5.10a). For the C/F/S→UF, turbidity residuals are below the values observed for the decanted water in the WTP, which ranged between 0.1 and 1.0 NTU, with an average value of approximately 0.2 NTU (Figure 5.10a). Moreover, residual turbidities after the C/F/S→UF is also below the WTP values obtained for the final treated water (ranged from 0.1 and 0.4 NTU, with an average value of approximately 0.1 NTU), as also below the WHO recommend maximum value for drinking water (1 NTU) (World Health Organization, 2017). For the C/F/S+PAC, turbidity residuals are above the WTP values obtained for the decantated water, with NW2 showing a higher value than NW1. However, all the residual turbidity values for both treatments are below the Portuguese guideline for this parameter (4.0 NTU) which matches the guideline established by WHO (World Health Organization, 2017).

DOC residual concentrations are under the average value measured in WTP final water (1.2 mg C/L), for both waters and in both treatments, although for this parameter the C/F/S+PAC treatment achieved lower residual values than C/F/S→UF (Figure 5.10b).

$SUVA_{254}$ values in the treated waters are presented in Figure 5.10c. This parameter was chosen because WTP uses $SUVA_{254}$ to control the water quality instead of UV_{254}. $SUVA_{254}$ is within the WTP range values for final water (between 0.86 and 1.46 L/(m.mg)) with C/F/S+PAC, showing a better performance than C/F/S→UF (Figure 5.10c).

Aluminium (Al) residual concentration in the NW1 after C/F/S+PAC were 19.3±2.6 mg/L and 24.0±3.9 mg/L for NW2. After C/F/S→UF, the Al concentration was 61.5±3.1 and 77.7±2.8 µg/L for NW1 and NW2, respectively. The lesser Al concentration found in the treated water after C/F/S+PAC indicates that PAC is able to remove some of the Al ions from the water. In the WTP final water, Al residual concentrations presented a high variability, ranged between 13 and 200 mg/L, with an average value of approximately 66.05 µg/L. Therefore, Al residuals after C/F/S+PAC for both waters are close to the minimal values obtain in the WTP whereas after C/F/S→UF both waters Al concentrations closer to the average value. Nevertheless, after both studied treatments the Al residuals were far below the Portuguese guideline for drinking water (200 µg Al/L). Furthermore, the benefits of the reduction in Al-based coagulant doses in these experiments is demonstrated in the final Al concentrations of the treated waters by both proposed treatment when compared with the WTP treated water.

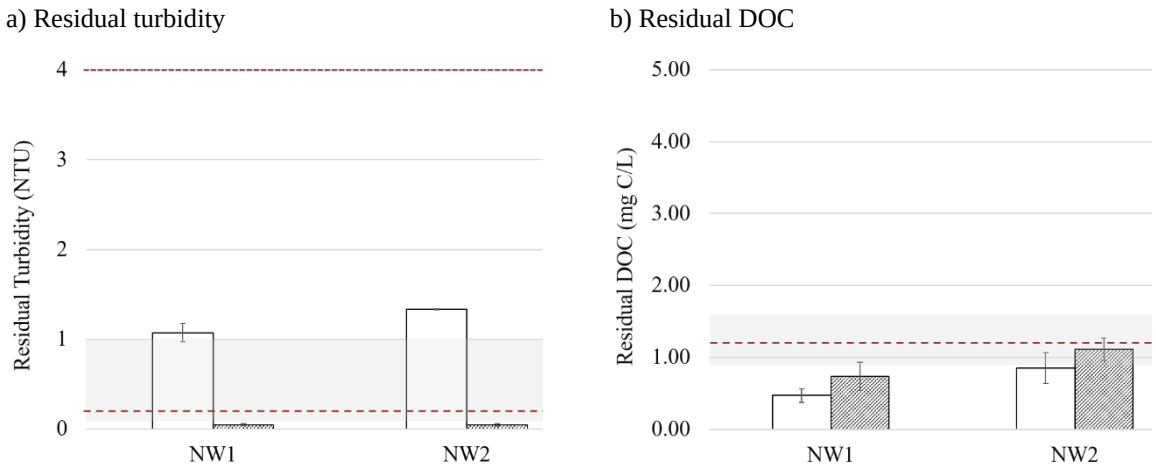

Figure 5.10. Residual concentrations for the selected PAC dose in C/F/S+PAC (10 mg/L for NW1 and 20 mg/L for NW2) and 90% WRR in C/F/S→UF, for NW1 and NW2: a) turbidity, b) DOC, c) $SUVA_{254}$ Experiments performed with the ENPs mixture (residual values presented as mean, standard deviations (n=6) are shown by the error bars).

c) Residual $SUVA_{254}$

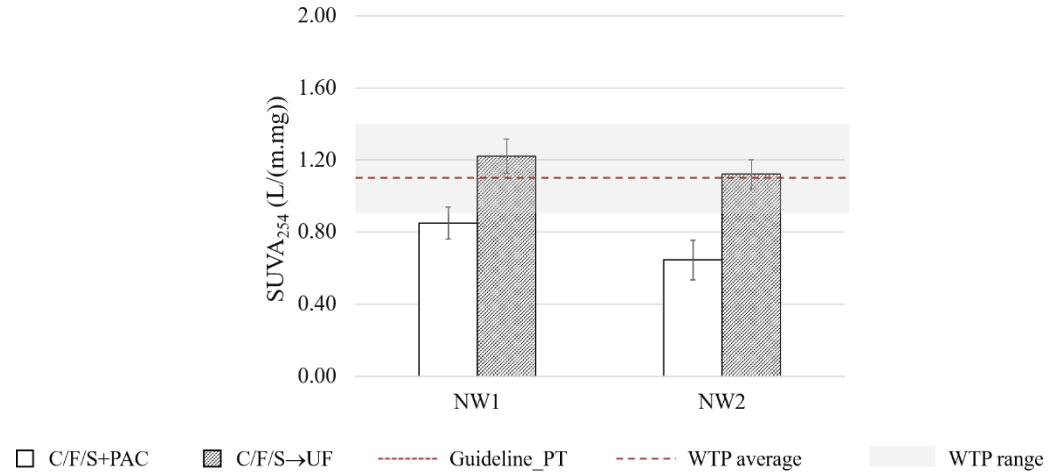

Figure 5.10 (cont.). Residual concentrations for the selected PAC dose in C/F/S+PAC (10 mg/L for NW1 and 20 mg/L for NW2) and 90% WRR in C/F/S→UF, for NW1 and NW2: a) turbidity, b) DOC, c) $SUVA_{254}$ Experiments performed with the ENPs mixture (residual values presented as mean, standard deviations (n=6) are shown by the error bars).

5.4. Conclusions

This work demonstrates that both enhanced conventional coagulation (C/F/S+PAC) and advanced hybrid membrane process (C/F/S→UF) improve the multiple ENPs removal compared to conventional C/F/S alone in hydrophilic natural waters with low and medium turbidity. In the C/F/S+PAC treatment, Ti, Ag and Cu removal efficiencies higher than 99.2% were obtained for both NW1 and NW2, in the single and mixture experiments. After C/F/S+PAC treatment, Ti presented the highest removal with residual concentration below the detection limit (0.350 µg/L) for both waters. The highest removal of Ti was associated with titanium specific adsorptive properties. In the C/F/S→UF treatment the ENPs removal efficiencies were higher than 98% for all the WRR tested, in both NW1 and NW2. At the 90% of WRR Ti and Cu removal efficiencies were higher than 99.9% in both waters and undetected in permeate flux (concentration was below the detection limit of 0.350 µg/L). The maximum Ag removal efficiency was 99.3±0.08% (NW2), indicating that some part of the Ag nanoparticles is not removed by the UF membrane, which could be related to dissolution. Due to the membrane pore size, and the size and charge of aggregates and individual ENPs, the main mechanisms proposed to C/F/S→UF are charge neutralisation and size exclusion.

The processes optimisation to the ENPs removal did not affect the ability of both processes to remove other target compounds of the drinking water treatment, namely turbidity and NOM.

Yet, C/F/S+PAC presented higher efficiencies for the NOM removal than C/F/S→UF, and for the turbidity removal, the reverse was observed. In the case of turbidity, the low density of the PAC used contributed to the presence of more particulate matter in the final water, anticipating the need to use a filtration step after the C/F/S+PAC. At the end of both processes, water quality parameters were analysed, showing that residual turbidity, DOC, SUVA and aluminium were below the Portuguese and WHO guidelines for DWT, and similar to those found in WTPs.

This study demonstrates that the most used processes used in drinking water production, C/F/S, combined or integrated with PAC and UF, are good options to protect human health against potential ENPs hazards. However, due to the dissolution of same ENPs and evoking the precautionary principle, a more refined treatment, such as nanofiltration (NF) could be necessary to the complete removal of the metal ions from ENPs.

Chapter 6

Silver Nanoparticles Separation from the Water Using Nanofiltration Membranes: The Role of Mono-divalent Salts and NOM

This Chapter was published in:

Serrão Sousa, V., Ribau Teixeira, M. (2015). Silver nanoparticles separation from the water using nanofiltration membranes: The role of mono- divalent salts and NOM. Separation and Purification Technology, 149, 165-173.

http://dx.doi.org/10.1016/j.seppur.2015.05.036

ABSTRACT

This study investigates the use of membrane processes to remove engineered silver nanoparticles (AgNPs) from waters and, at the same time, the dissolved silver (Ag) released from AgNPs. The effect of ionic strength and natural organic matter (NOM) on membrane performance is evaluated. Ionic strength has a significant effect on the permeate flux, stronger in the presence of AgNPs, decreasing it. The total dissolved silver in the permeate increases with ionic strength because the surface charge potential decreases, which promotes a reduction of the double layer thickness resulting in lower rejections. In addition, dissolved Ag is complexed with chlorine. Therefore, both AgNPs and dissolved Ag released from NPs were practically removed from water (removals higher than 92%). These results are due to the AgNPs charge and zeta potential since NPs are negative at the studied pH and approaches zero with ionic strength, increasing aggregation. In water with NOM and AgNPs, the variation in NOM concentration does not affect the permeate fluxes. The main mechanism involved in the AgNPs removal is size exclusion, while dissolved Ag (resulted for NPs dissolution) is removed by size exclusion and electrostatic interactions due to complexation with salts and NOM.

6.1. Introduction

Engineered silver nanoparticles (AgNPs) are currently used in a wide range of biomedical applications and consumer products, such as toothpaste and cosmetics, due to the well-known antimicrobial activity of the ionic Ag (Blaser et al., 2008; Chinnapongse et al., 2011). AgNPs have also been used in clothing, air purification systems and water filters, making silver the most prevalent commercial nanoparticle (Danish Consumer Council, 2012). The widespread use of AgNPs will inevitably lead to their release to the aquatic environment somewhere during their life-cycle, increasing the exposure of humans and other organisms to Ag (Jiang et al., 2009; Klaine et al., 2008). Accordingly, previous toxicology studies demonstrated that AgNPs are known to induce toxicity in many different species (Bilberg et al., 2011; Navarro et al., 2008).

Although it is not clear the degree of AgNPs toxicity that results from released silver ions and how much is related with AgNPs themselves (Beer et al., 2012), it is well known that the high surface area of metal-based NPs increases the potential of ions to be released from these NPs (Bian et al., 2011; Mudunkotuwa and Grassian, 2011). Some authors reported that measured silver ion concentration from the AgNPs suspension could not fully explain the observed toxicity of the AgNPs, so both silver ions and NPs contribute to toxicity (Kawata et al., 2009; Navarro et al., 2008). However, Kim et al. (2009) suggested that the toxicity of AgNPs was mainly due to oxidative stress and was independent of silver ions. Despite these results, all evidence indicates that silver ions partly contribute to the AgNPs toxicity and, although the well-known high toxicity of silver, the amount of silver ions within the investigated AgNPs suspensions has been rarely measured (Beer et al., 2012). Angel et al. (2013) concluded that AgNPs were less toxic than ionic silver, but much more toxic than micron-sized Ag. In addition, these same authors relate toxicity to the release of dissolved Ag, since this is more slowly released from micron-sized Ag due to the low surface area.

Some model and experimental data suggested that nanoparticles concentrations around ng/L may be present in surface waters, and predicted an exponential increase related with the increased usage and associated discharge (Gottschalk et al., 2009; Mitrano et al., 2012; Mueller and Nowack, 2008). One of the likely routes for introducing AgNPs in the environment is via waste streams (Benn et al., 2010), with a high probability for these nanoparticles to enter in waterways (Blaser et al., 2008).

Sun et al. (2013) have investigated the removal of AgNPs by conventional treatment, namely coagulation, flocculation and sedimentation, using high doses of four different

coagulants (495, 400, 30 and 47 mg/L for aluminium sulphate, ferric chloride, PACl and PFS). It was found that AgNPs can be removed from water by these treatments, but removals were largely affected by the water characteristics such as ionic strength (IS), natural organic matter (NOM) and suspended solids. Dissolved silver removal was not studied since the authors used borate buffer in the AgNPs suspension to reduce the releasing of silver ions. Springer et al. (2013) also investigated the removal of ENPs from water using ultrafiltration and showed that this process efficiently removed SiO_2 NPs from water. However, since they used turbidity and granulometry to detect NPs in the permeate water, they did not study the removal of the ionic form dissolved in the water.

Recent advances suggest that many of the issues involving water quality could be resolved or greatly ameliorated by nanotechnology (Tang and Lo, 2013). Nanofiltration (NF) has become an attractive alternative technology to conventional water treatment since the separation process primarily occurs due to steric hindrance and membrane solute interactions, so it could be a solution to remove from water both the metal-based NPs and the ions released from these NPs.

In this work, the performance of nanofiltration to remove both AgNPs and dissolved Ag (released from the AgNPs) from water are studied. NPs dissolve in water so the removal of both particulate and dissolved forms is essential to reduce the impact of releasing ENPs on the environment. The removal of both particulate and dissolved Ag forms by nanofiltration represents an integrated treatment solution to these emerging contaminants. Nanofiltration experiments were performed in the presence of mono- and divalent salts and NOM, given its relevance to understand the mechanisms and solution interactions that could influence the NPs removal in water purification processes. To the author knowledge, this is the first time of such approach is used to reduce ENPs in waters.

6.2. Materials and Methods

6.2.1. Preparation and characterisation of AgNPs suspensions

Commercially available silver nanopowder (Sigma-Aldrich, LOT#MKBH2895V) was used. According to the supplier, the particle size is <100 nm in diameter, the standardised surface area is 5.0 m^2/g and the molecular weight is 107.87 g/mol. In this study, the pristine compound was used to ensure control of the process variables. The NPs were dispersed in

deionised (DI) water, without further purification, and suspensions were sonicated using a bath sonicator (USC500TH, VWR International). The concentration of AgNPs was set at 100 mg/L to ensure the quality of the dynamic light scattering (DLS) analysis, as suggested by the equipment supplier. At least three measurements were made to ensure the quality of the analyses.

Transmission electron microscopy (TEM) was used to observe the size and shape of the AgNPs. A drop of NP suspension was deposited onto a 300 mesh copper grid coated with a carbon layer, and the excess solution was removed by tissue paper and allowed to dry at room temperature. The observation was made on a JEOL JEM-1011 microscope.

The X-ray diffraction (XRD) technique was used for identification of the crystal structure of AgNPs in a Panalytical X'Pert Pro diffractometer using CuKα radiation filtered by Ni and X'Celerator detector. The measurements were made using a step-scanning program with 0.167° per step and acquisition time of 100 s per step. The HighScore Plus Software, with ICDD PDF-2 database, was used for peak analysis and crystalline phase identification.

The AgNPs optical absorption measurements in the UV-Vis range were made in a Spectronic Unicam (UV300) spectrophotometer at room temperature. The wavelength used in experiments ranged from 320 to 600 nm.

The hydrodynamic diameter and zeta potential of AgNPs were determined at 25°C by a DLS and electrophoretic light scattering (ELS), respectively using a Zetasizer Nano ZS analyser (Malvern Instruments Inc., UK), as previously described (Serrão Sousa and Ribau Teixeira, 2013).

AgNPs characterisation was made in the feed waters used in NF experiments, so at different pHs, IS, and type and concentration of NOM, and prepared as presented in the next section.

Additional experiments were made to determine the dissolution of AgNPs using the same method presented by Mitrano et al. (2012). Briefly, disposable filter membranes (Anotop alumina 25 mm) from Whatman International (0.02 μm pore size) were used, pre-sonicated samples were hand-filtered by filling polypropylene 30-ml syringes with the sample and pushing it into 50-ml glass container and non-filtered and filtered samples were analysed by atomic absorption spectrometry (AAS) and dissolved Ag concentration was determined.

6.2.2. Experimental setup and procedure

NF270 and NF90 membranes were used in a laboratory commercial bench scale plate and frame unit, using two pairs of each membrane type with an area of 720 cm^2 each pair (M20 unit; maximum pressure 80 bar; maximum flow 18 L/min; and a constant temperature maintained by a heat exchanger). Table 6.1 summarises the characteristics of these membranes. Experiments were performed at a constant pressure of 10 bar and a temperature of 21±1°C. Prior to the experiments, the membranes were compacted using DI after which the initial permeate flux was established. Synthetic aqueous solutions of AgNPs of desired ionic strength or NOM concentration were fed to the feed tank. The experiments were performed using synthetic aqueous solutions of metal NPs and varying the ionic strength (100 200, 300 mM), the salt type (NaCl, NaCl+$CaCl_2$, $CaCl_2$), the NOM concentration (4, 16, 35 mg C/L) and the NOM type (hydrophilic - tannic acid (TA), hydrophobic - Aldrich humic acids (AHA)). Samples of permeate and retentate were collected at a given time interval, to measure the observed solute rejection (*R*) and permeate volume flux (*J*). Both the streams of permeate and retentate were recycled to the feed tank except for the samples drawn for analysis purpose. Certified analytical grade stock solutions of the reagents were used (>99.0% purity).

Table 6.1. Characteristics of NF90 and NF270 membranes.

	Membranes	
	NF90 (*)	**NF270 (*)**
Pure water permeability (L/(h.m^2.bar), 21ºC)	7.6	10.6
MWCO (Da)	110	170
Pore radius (nm)**	0.34	0.42
Charge (pH above 3)**	Negative	Negative

* Thin-film composite membranes are consisting of a semi-aromatic piperazine-based, polyamide layer on top of microporous polysulfone support, from Alfa Laval.
** Supplier information.

6.2.3. Analytical Methods

Samples were analysed for pH (at 25ºC, Whatman WTW pH340 meter), conductivity (Crison GLP32 conductimeter), turbidity (HACH 2100N turbidity meter of high resolution, 0.001 NTU) and dissolved organic carbon (DOC) (Shimadzu TOC 5000A analyser, 50 ppb–

4000 ppm), using standard methods of analysis (Eaton et al., 2005b). The permeate flux was determined by weight (Shimadzu, model BX 620S). All samples were analysed in triplicate. Turbidity was used to analyse AgNPs.

Silver concentrations in feed and permeate waters were determined by atomic absorption spectrometry (AAS AAnalyst 800, Perkin-Elmer, detection limit: 0.350 µg/L), after acid digestion with 2% nitric acid (HNO_3). Ag was analysed by graphite furnace using standard methods (Eaton et al., 2005a). The accuracy of the analytical procedure was assessed by the injection of the silver standard at the beginning of sample quantification and between every ten samples.

6.3. Results and Discussion

6.3.1. Characterisation of AgNPs

The XRD pattern of AgNPs is shown in Figure 6.1a, from which the phase and the crystal structure of the sample were analysed. It gives a cubic structure, and the intensities and positions of the diffraction peaks of nanoparticles are in good agreement with the reported values (JCPDS#01-087-0718). No peaks of impurities are found in the XRD pattern. The lattice parameters, *a*, *b* and *c* are all 4.0773 Å. Scherrer equation was not used to estimate the average size of the nanoparticles since it is unreliable at estimating particle size (Calvin et al., 2005; Hall et al., 2000) and TEM is the most accurate method to estimate the relative average sizes (Calvin et al., 2005).

The optical absorption spectrum of AgNPs suspension (Figure 6.1b) shows two absorption peaks at visible wavelength, approximately at 460 nm and at 530 nm.

Figure 6.1c presents the image obtained by TEM. The individual nanoparticles appear to be spherical in shape and aggregated, with an average diameter of about 41.7±11.1 nm. The particles hydrodynamic diameter is 164.2±2.7 nm in DI, measured by DLS. This larger size compared with Ag individual particle size obtained by TEM demonstrates that aggregates are formed in suspensions at the onset of DLS measurements. According to Jiang et al. (2009), when nanoparticles are dispersed in liquids, their hydrodynamic size is often larger than the primary dry particle size, due to interaction between nanoparticles and the surrounding solution.

Results from dissolution experiments revealed that about 3.0±0.4% of the total Ag concentration present in solutions was in dissolved form, indicating that most of the Ag was in nanoparticulated form.

Figure 6.2 presents the variation of zeta potential and hydrodynamic diameter of AgNPs in the studied waters. In Figure 6.2b and Figure 6.2c, pH was not adjusted. Zeta potential and consequently, the hydrodynamic diameter are highly affected by solution pH (Figure 6.2a). Results show that for the entire pH range tested (~2.6 to 12), zeta potential is negative. From pH ~5 to 2.6, AgNPs zeta potential approaches zero (thus, is less negative), and after pH 5 and until 12 zeta potential remained practically unchanged. These results show that the isoelectric point of the AgNPs is, most likely, at pH values under 2.6 as reported by (Elzey and Grassian, 2010). At the isoelectric point, particles have little or no charge; repulsive forces between nanoparticles are weaker, so each collision between primary nanoparticles and aggregates causes particles adherence (Baalousha et al., 2008). For hydrodynamic diameter, results show a decrease with pH increase, ranging between 226±22.5 nm (at pH 2.6) and 133±1.2 nm (at pH 12). The aggregation trend at acidic pH is due to the reduction of the electrostatic repulsion that could lead to particle precipitation and sedimentation. As pH increases, the concentration of OH^- and the electrostatic repulsion between particles increases which provides NPs stabilisation. Consequently, the hydrodynamic diameter decreases.

In the presence of NaCl, the zeta potential of AgNPs remained negative compared with DI water at same pH (respectively, -41 mV, Figure 6.2b, and -43 mV, Fig. Figure 6.2a). When $CaCl_2$ and NaCl are added together, zeta potential approached zero (approximately -10.1 mV, Figure 6.2b) and for $CaCl_2$ without NaCl addition, zeta potential is very close to zero (approximately -1.99 mV, Figure 6.2b). Therefore, as ionic strength increases, IS(NaCl)< IS(NaCl+$CaCl_2$)< IS($CaCl_2$), interparticle repulsions decrease, the electrical double layer is reduced, and zeta potential approaches zero. In this situation, there is a decline in the energy barrier between particles, which allows the attractive van der Walls interactions to dominate, favouring the formation of aggregates of higher dimensions (Chen and Elimelech, 2006; Jiang et al., 2009). Therefore, the hydrodynamic diameter is also affected by ionic strength: an increase in HD is observed as ionic strength increases (Figure 6.2b). Comparing the results presented in Figure 6.2b (salts added) with those in Figure 6.2a (no salts added), for the same pH, hydrodynamic diameter increases from 160 nm (with no salt added) to 556 nm when NaCl is added, from 140 nm (no salts added) to 860 nm for NaCl+$CaCl_2$, and from 140 nm to 1250 nm with the addition of $CaCl_2$. The increase in aggregation trend with the addition of salts could

be explained by the reduction in the electrical double layer thickness that allows higher particle-particle interactions, increasing aggregation. Some authors (Domingos et al., 2009; French et al., 2009), also observed that an increase in ionic strength led to the formation of micron-sized aggregates of titanium NPs. For fullerene NPs, Chen and Elimelech (2009) concluded that electrophoretic mobility of the fullerene nanoparticles became less negative as the electrolyte concentrations (NaCl, $CaCl_2$) increased, with divalent cations being more effective than monovalent cations, which may indicate specific adsorption of Ca^{2+} ions onto NPs surface.

When NOM (AHA or TA) is present, zeta potential is always negative, slightly more negative than without NOM at same pH, i.e. pH~5 (-50.8 mV and -48.0 mV with 4 mg/L of AHA and TA, respectively *vs* -42.0 mV without NOM; Figure 6.2a and Figure 6.2c). Thus, NOM imparts a negative charge to NPs surfaces and raises their absolute surface potential. In addition, the presence of NOM induced a slight increase in AgNPs hydrodynamic diameter (204 nm and 195 nm with 4 mg/L of AHA and TA, respectively *vs* 141 nm without NOM at same pH; Figure 6.2a and Figure 6.2c). Baalousha et al. (2008) showed an increase in the nanoparticles coverage, as well as the thickness of the surface coating, with the increase of AHA concentration. This surface coating increases the effect of steric stabilisation in addition to the effect on the surface charge that governs particle interactions in aqueous media.

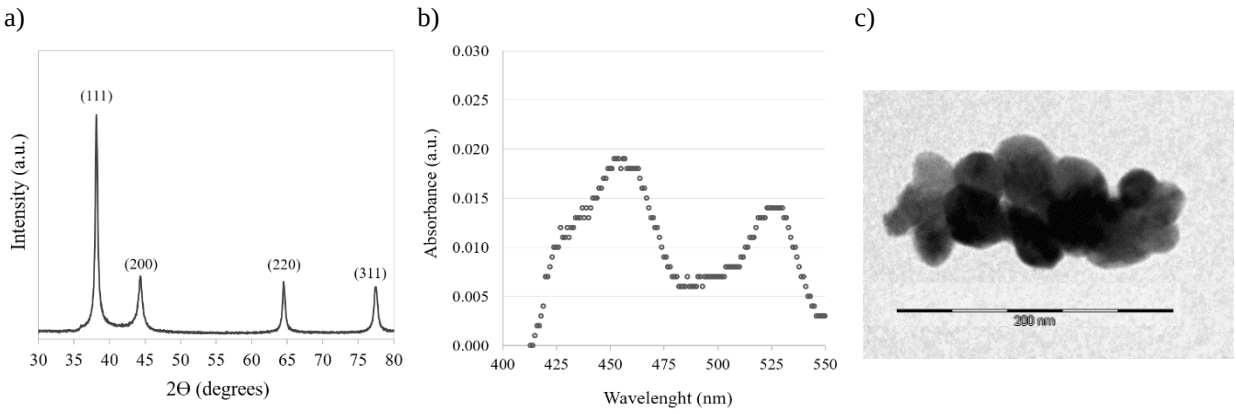

Figure 6.1. (a) XRD pattern of AgNPs, (b) UV-Visible absorbance and (c) TEM image of AgNPs suspension.

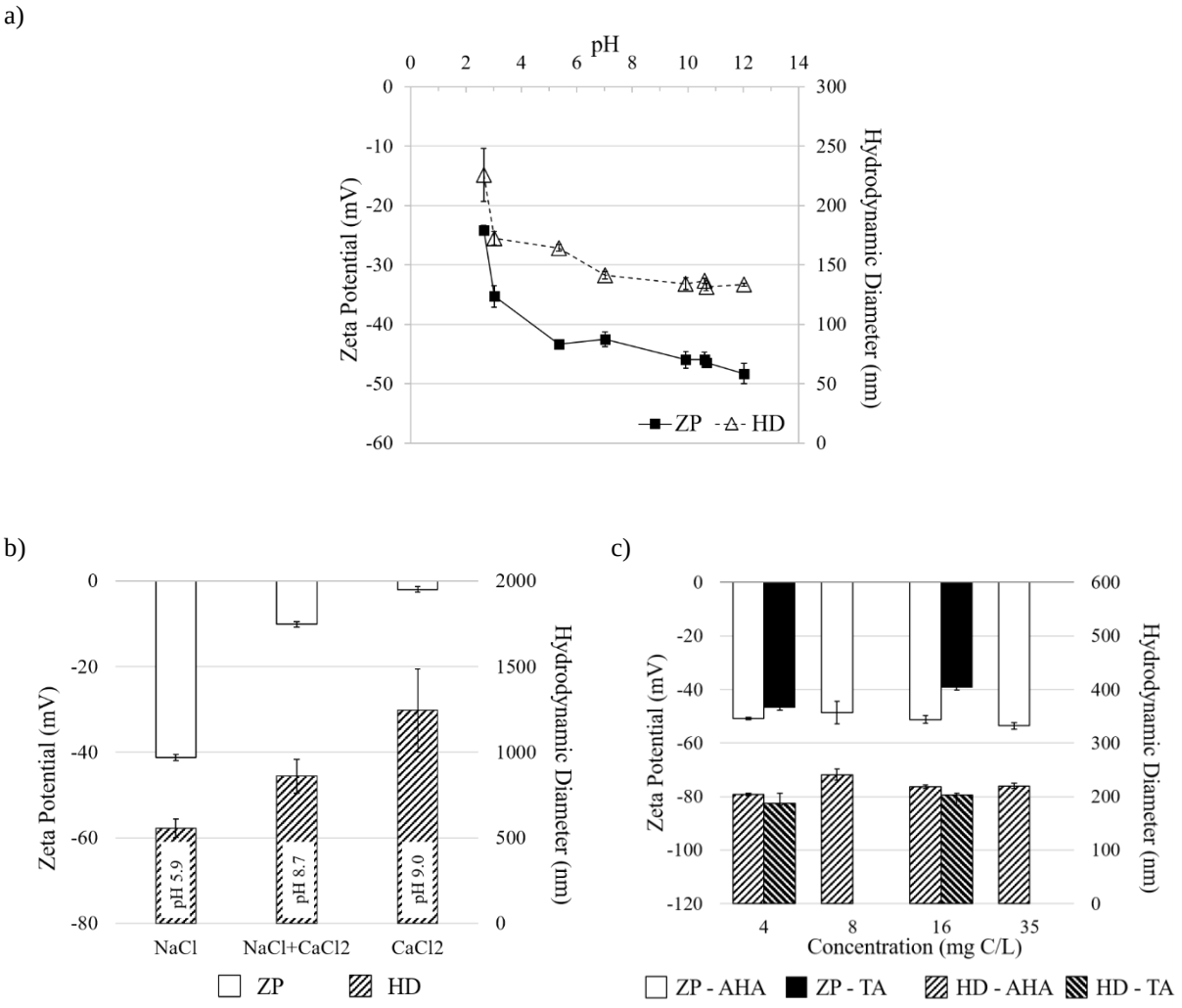

Figure 6.2. Variation of AgNPs zeta potential (ZP) and hydrodynamic diameter (HD) with: (a) pH, (b) mono and divalent salts, and (c) NOM (values presented as mean, standard deviations (n=6) are shown by the error bars).

6.3.2. Influence of salts and ionic strength

The influence of salts and ionic strength on the removal of AgNPs and dissolved Ag was evaluated. As can be seen in Figure 6.3, the ionic strength has a significant effect on the permeate flux, more pronounced in the presence of AgNPs. Permeate flux decreases with ionic strength, thus the highest flux is for water with NaCl and the lowest for water with $CaCl_2$ for both membranes (IS(NaCl)< IS(NaCl+$CaCl_2$)< IS($CaCl_2$)). For DI water, with or without AgNPs, the particle-membrane and the particle-particle repulsive forces at pH 5.4 prevent membrane fouling and flux remains practically unchanged. Therefore, NF270 permeate flux

decreases approximately 1% for DI water with AgNPs compared with DI water without NPs (Figure 6.3a), and NF90 flux decreases about 5% (Figure 6.3b). In the presence of salts, the increase in the ionic strength promotes: i) the neutralisation of counter-ions in the diffusion layer, resulting in contraction of the electrical double layer and increasing the attractive particle-particle interactions allowing NPs to come sufficiently close to produce aggregation according to the classical Derjaguin-Landau-Verwey-Overbeak (DLVO) theory (Figure C 1, Appendix C), and ii) the increase of the osmotic pressure difference between the filtrate and the feed solution adjacent to the membranes surface. Therefore, the flux through the membrane reduces.

Despite the presence of NPs in water, calcium has a larger effect on membrane fouling than sodium, through its complexation with the membrane functional groups contributing to membrane fouling (Hong and Elimelech, 1997). When both salts and AgNPs are present in the water, a more severe flux decline is observed (Figure 6.3). Permeate flux decreases because the characteristics (charge and hydrodynamic diameter) of the AgNPs change in the presence of salts (Figure 6.2b). Salts reduce AgNPs charge leading to the zeta potential approaching zero (ZP (DI< NaCl< NaCl+$CaCl_2$< $CaCl_2$), Figure 6.2a and Figure 6.2b) and promoting aggregation (HD (DI< NaCl< NaCl+$CaCl_2$< $CaCl_2$), Figure 6.2a and Figure 6.2b). Since AgNPs aggregates are much bigger than the membrane pore size (compare Figure 6.2 and Table 6.1), AgNPs accumulate next to the membrane surface, in the mass transfer boundary layer, reducing fluxes (Figure 6.3). A cake layer may be formed and hindered the back diffusion of the salts-AgNPs complexes to the bulk solution, which contributes to a build-up of a higher AgNPs concentration and removal of AgNPs aggregates remains almost constant during filtration time as previously reported for organic solutes (Ng and Elimelech, 2004), and turbidity presents values close to zero (Figure 6.4). Therefore, the main mechanism for NPs removal is size exclusion mechanism. With NaCl, AgNPs are smaller and more negative charged, and are bigger and practically with no charge in the presence of $CaCl_2$ (Figure 6.2b), which originates a lower flux for water with AgNPs and $CaCl_2$. The impact of the addition of AgNPs to the salt waters is more pronounced for NF90 membranes than for NF270. NF90 is a tight membrane so the effects of the NPs characteristics on the membrane fouling are more pronounced.

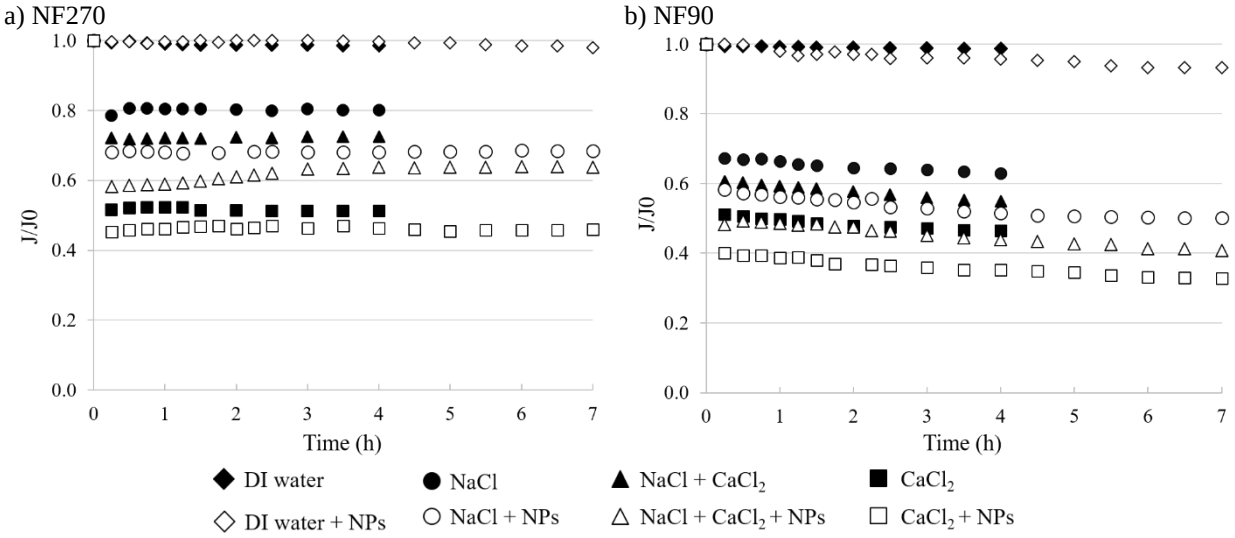

Figure 6.3. Variations of the relative permeate flux (J/J0, J is the flux at each time and J0 the initial pure water flux) with time for DI and salt waters with AgNPs using: (a) NF270 and (b) NF90 (water pH values: pH(DI) = 5.3±0.1; pH(NaCl) = 5.9±0.1; pH(NaCl+$CaCl_2$) = 8.7±0.1; pH($CaCl_2$) = 8.9±0.1).

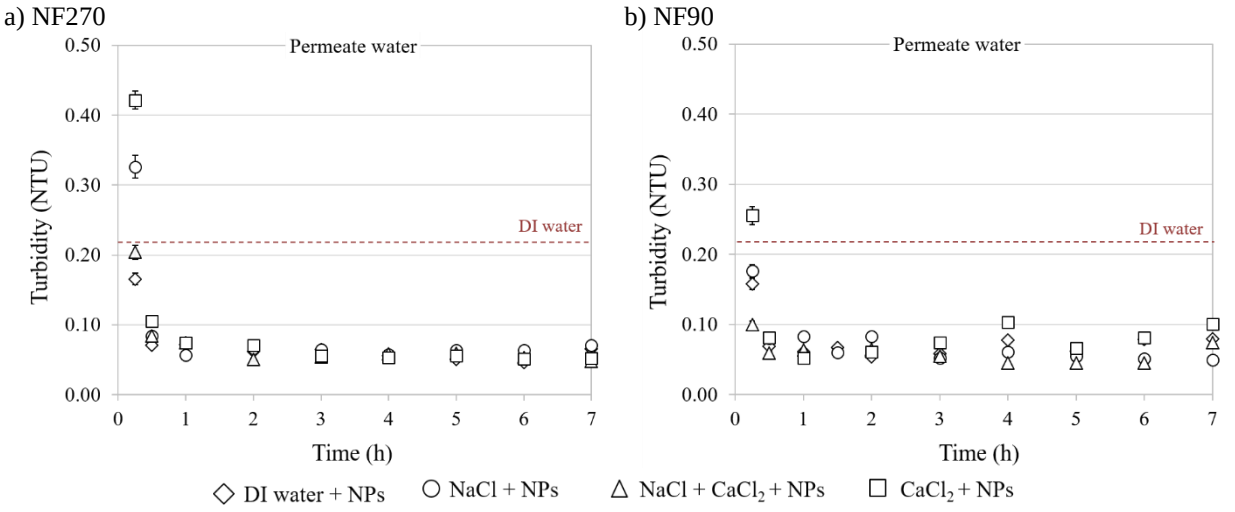

Figure 6.4. Variation of turbidity in the permeate water during experiments for DI and salt waters with AgNPs using: (a) NF270 and (b) NF90 (the dashed line represents the turbidity of DI water without NPs or salts).

The Ag concentration in permeate (Figure 6.5) corresponds to the Ag released from AgNPs dissolution and that was not removed by NF. In Figure 6.5 removals as high as 98% and Ag concentrations below 15 μg/L after 7 h of operation are shown. The total dissolved silver in the permeate increases with increasing ionic strength, more evident at 7 h of operation (Figure 6.5).

These results can be explained by the electrostatic repulsions between the membrane surface and the cations and anions present in the feed water. As ionic strength increases, the surface charge potential decreases, as well as the repulsions between particle-particle and particle-membrane. Thus, the increase in ionic strength promotes the reduction of the thickness of the double layer resulting in lower rejections. In addition, the shielding effect is stronger and a decrease of the repulsions forces of the anions is also observed. According to Kent and Vikesland, (2012), the dissolution of AgNPs is linear as a function of NaCl in the range of 10 to 550 mM. Based on the prediction by Visual MINTEQ (3.0), the equilibrium speciation of dissolved silver in the test conditions would be mainly $AgCl2^-$ and AgCl (about 80% and 14%, respectively) and only about 1% of free Ag^+ and 7% of $AgCl_3^{2-}$. These results are in accordance with other authors (Yang et al., 2014). The latter authors concluded that at higher ionic strength, a higher total silver concentration would be in the permeate, since a higher concentration of added Cl^- generated more soluble silver chloride species and the Cl^- had time to complex with AgNPs during filtration. Therefore, the removal of dissolved Ag is controlled by surface chemistry, since dissolved Ag complexed with the salts present in waters, influencing the charge and size of dissolved-Ag.

These membranes present some selectivity to the studied salts (Figure 6.6). Conductivity removal sequence is $R(CaCl_2) > R(NaCl_2) > R(NaCl+CaCl_2)$, more evident for membrane NF270 (Figure 6.6). Size and charge effects are the main factors affecting separation process of ionic species in high ionic conditions, as of brackish waters and studied waters NF membranes appeared to be positively charged in the presence of Ca^{2+} cations by adsorption at high salt concentration (Peeters et al., 1998), and thus salts rejection can be explained by Donnan exclusion theory: higher valence co-ion caused a higher ion rejection. For salts mixture, rejection decreases when compared with single solutions, due to the increase of electrolyte concentration, responsible for higher ionic strength.

Finally, these results also show that NF can be used to recover AgNPs present in the waters. Since AgNPs are widely used and are synthesised by chemical processes, the recovery of AgNPs by NF membranes will be a more sustainable process.

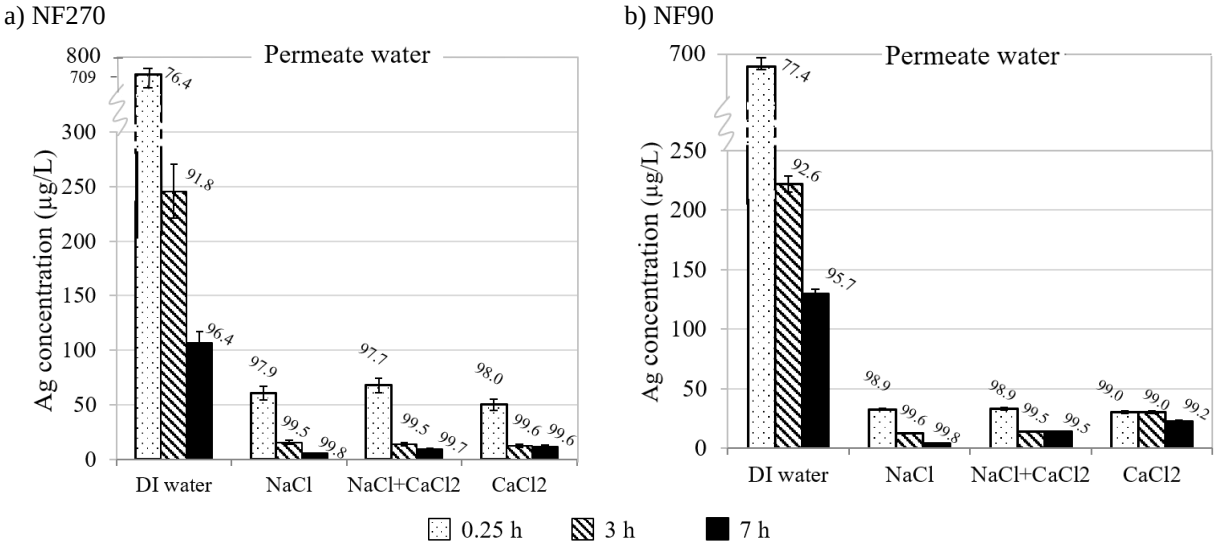

Figure 6.5. Variation of ionic Ag concentration and removals during experiments for DI and salt waters with AgNPs using: (a) NF270 and (b) NF90 (the values above the bars are the removals (%) of dissolved Ag).

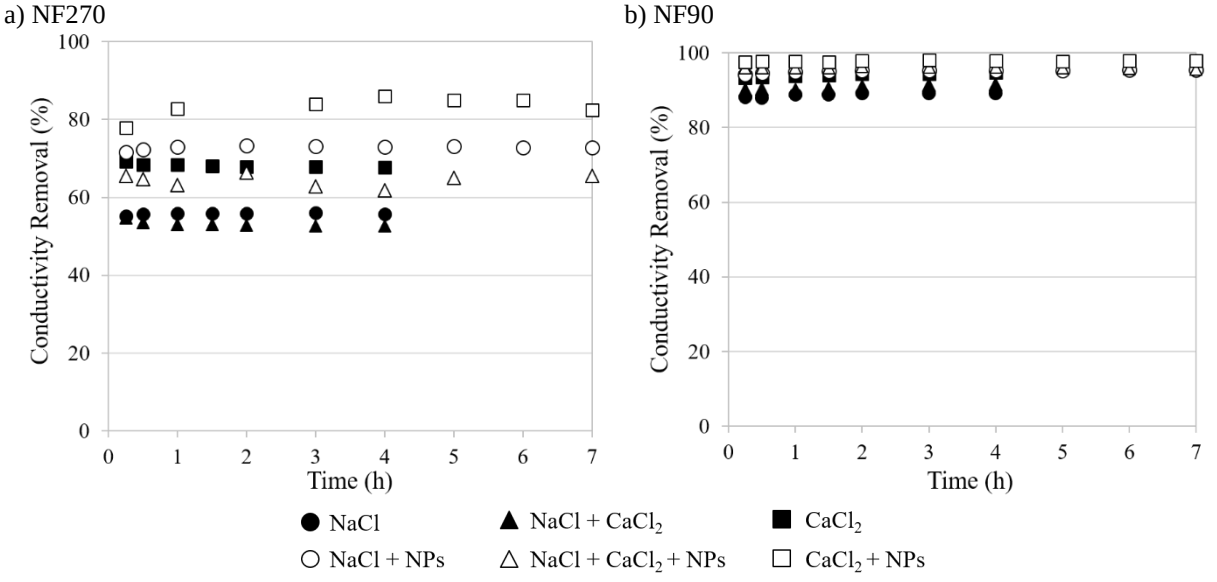

Figure 6.6. Conductivity removals for salt waters without and with AgNPs, using (a) NF270 and (b) NF90 membranes.

6.3.3. Influence of NOM type and concentration

The influence of NOM type and concentration on the removal of AgNPs and dissolved Ag was also evaluated. Figure 6.7 shows different behaviour in the permeate flux between membranes when permeating NOM waters. While for NF270 permeate flux is more affected by the type than the concentration of organic matter, for NF90 no significant difference is observed between the type and the concentration of NOM (Figure 6.7). For the same organic matter type (AHA or TA) and independently of the membrane used, no significant differences were obtained between NOM concentrations, despite the slightly lower flux observed for high NOM concentrations (Figure 6.7). However, NF270 membrane permeate flux is quite reduced in the presence of TA (flux decreases approximately 35% from DI to TA waters), in both experiments with and without AgNPs (Figure 6.7.a1 and Figure 6.7.b1). These results show that the permeation ability of the hydrophilic NF270 membrane is more affected by TA than the hydrophobic NF90 membrane, suggesting that TA contributes to the fouling of NF270 membrane during nanofiltration. Although hydrophobic surfaces are known to foul at higher rates, fouling of hydrophilic membranes also occurs (Brant and Childress, 2002).

There are two main reasons that could explain the results obtained for TA compared with AHA by NF270 membranes. On one hand, for TA with small molecular weight, at pH values lower than its ionization constant, the molecule is weakly negative-neutral and may form a compact coiled conformation, and subsequent cake formation, because of the ionogenic groups dissociation suppression (Brant and Childress, 2002; Lin et al., 2007). This suppression effect leads to a restriction of electrostatic repulsion and a reduction in the TA size, which could contribute to the fouling of the hydrophilic membrane. Lin et al. (2007) demonstrated a reduction of 30% of the permeate flux of NF hydrophilic membrane in the presence of TA, near pH 5 and using 5 mg/L of TA. Plakas and Karabelas (2009) showed that adsorption of TA to the NF270 membrane surface was seven times higher than the adsorption of humic acids, and for NF90 the adsorption of TA was similar to those present by humic acids. On the other hand, neutral and positively charged solutes engage in hydrophobic interactions with negatively charged membranes, whereas negatively charged solutes do not engage in hydrophobic interactions since they cannot approach the membrane surface as previously demonstrated (Verliefde et al., 2008). Negative charges of NF270 promote high electrostatic repulsion between the humic substances (high negatively charged) and the membrane. This repulsion prevents humic acids from being retained in the membrane surface, not contributing to membrane fouling and consecutively to the permeate flux reduction.

The DLVO calculations (Figure C 1, Appendix C) indicate that the energy barriers are slightly higher for AgNPs in the presence of AHA compared with TA, consistent with the measured zeta potential values (Figure 6.2c). The interaction energy between colloids is influenced by size, surface charge density and surface composition of the colloids (Boussu et al., 2007). The slight largest repulsion observed for AgNPs in the presence of AHA and their large size could also contribute to the flux results observed.

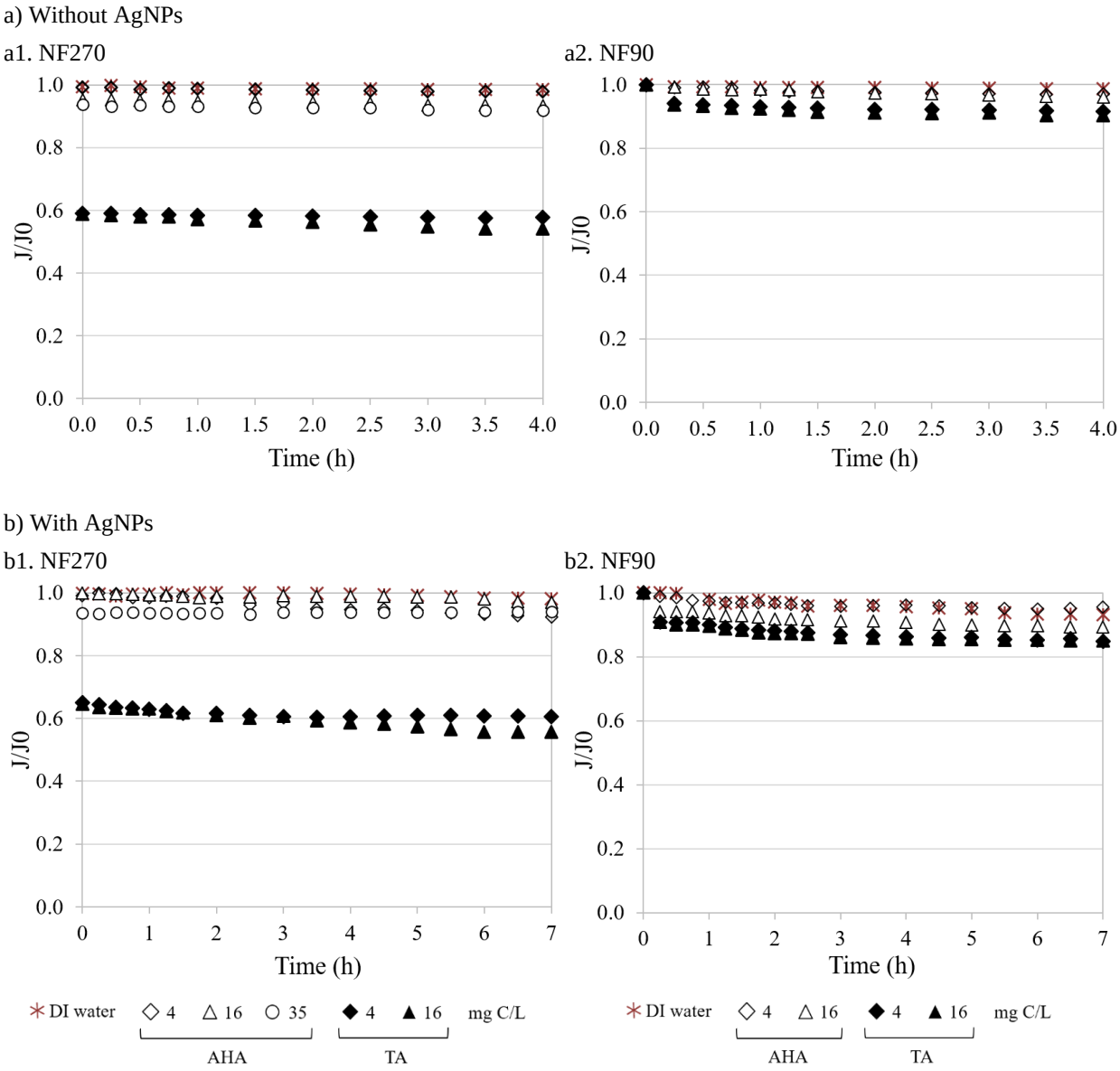

Figure 6.7. Variation of the relative permeate flux ((J/J0), J is the flux at each time and J0 the initial pure water flux) with time for DI and NOM waters (a) without and (b) with Ag NPs, using: (1) NF270 and (1) NF90 (water pH values: pH ($AHA_{4\ mgC/L}$) = 5.0±0.4; pH ($AHA_{16\ mgC/L}$) = 5.4±0.2; pH($TA_{16\ mgC/L}$) = 4.6±0.1; pH ($AHA_{35\ mgC/L}$) = 7.2±0.2).

Results demonstrate that turbidity decreases rapidly at the beginning of the experiments to values above the initial turbidity of DI water (Figure 6.8). Therefore, NF membranes remove all the turbidity from waters, AgNPs turbidity and suspended and colloidal particles from AHA and TA (Figure 6.8). Turbidity values in permeate water are as low as 0.1 NTU for both membranes and independently of the type and concentration of the NOM added (Figure 6.8). Since the hydrodynamic diameter of AgNPs aggregates is around 220 nm with NOM (no significant differences were observed between TA and AHA, Figure 6.2c), and AgNPs are negative at the studied conditions (Figure 6.2c), the AgNPs removal mechanism is size exclusion. The presence of NOM leads to a surface coating of the nanoparticles with NOM molecules as referred by Baalousha et al. (2008). As referred by Mashayekhi et al., (2012) for fullerene NPs, the NOM organic coating on the surface of NPs aggregates did not allow aggregates to get close enough to form bigger aggregates, and aggregation stability increased due to steric stabilisation. Thus, a fouling layer on the surface of the membrane is promoted, that results in a decrease in the feed turbidity over time. However, since NF membranes used in this work are both negatively charged (Table 6.1), electrostatic interaction between negatively charged AgNPs-NOM and negatively charged membranes make the fouling layer reversible (membrane cleaning was made with DI water).

For dissolved Ag, results demonstrate that removals are high (>77%) and increase during operation for both membranes (Figure 6.9). After 3 h of operation, removals become higher than 92% independently the type and concentration of NOM. In addition, results also show that removals are higher for NOM water than for DI water (Figure 6.9). This suggests that dissolved Ag is adsorbed to NOM or NOM-Ag complexes un-dissolved the silver in solution, which promotes their removal. Furthermore, dissolved Ag removals are slightly higher in AHA waters than in TA waters for both membranes which could be related with the hydrophilic character of TA and the enhanced negative charge of the AgNPs coated by AHA (-40 to -50 mV).

Finally, DOC removals are very high (>80%) for all the situations studied, and waters without AgNPs present removals slightly higher than water with AgNPs, especially using NF270. Therefore, AgNPs do not influence significantly the removal of DOC, which means that these membranes can be used to treat water and recover AgNPs.

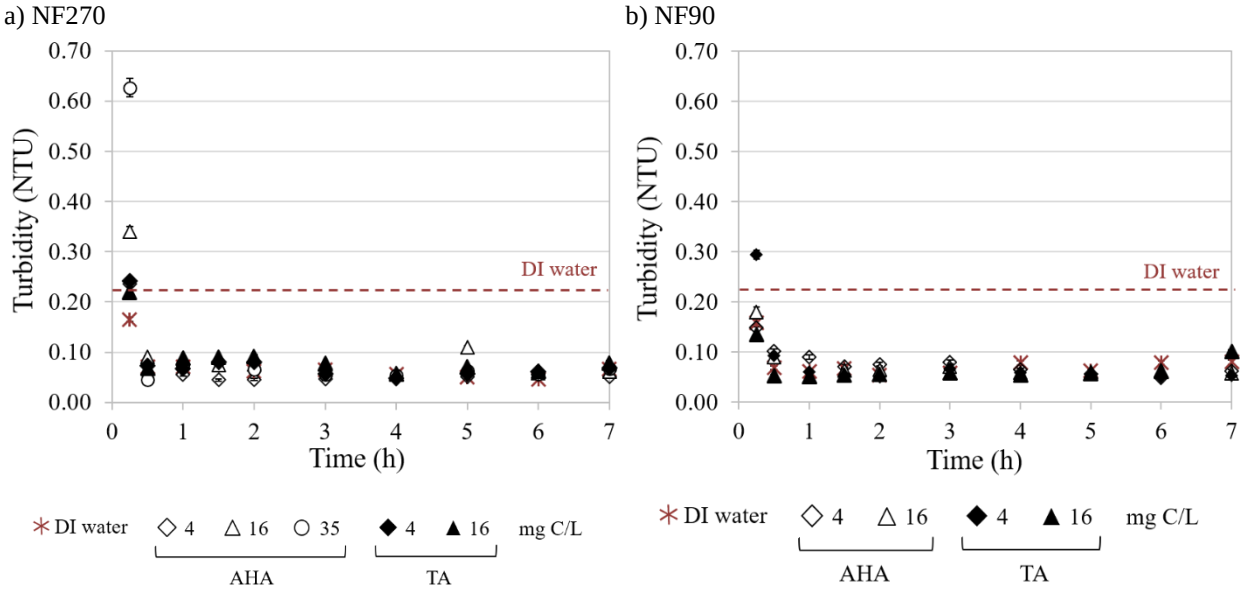

Figure 6.8. Variation of turbidity in the permeate with time, for DI and NOM waters using (a) NF270 and (b) NF90 (the dashed line represents the turbidity of DI water without NPs or salts).

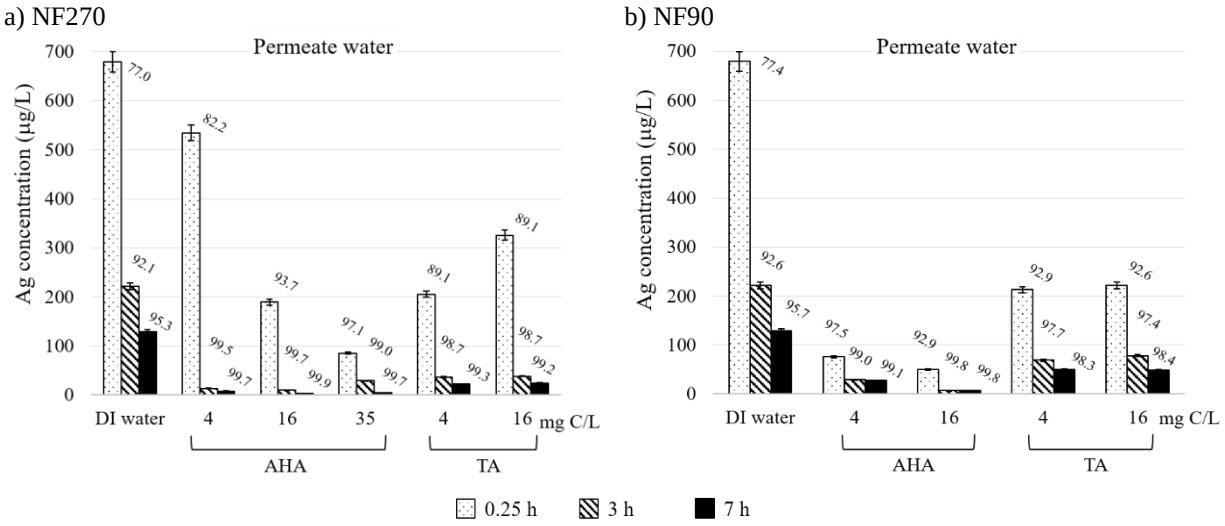

Figure 6.9. Variation of Ag concentration in the permeate and removals with time, for DI and NOM waters using (a) NF270 and (b) NF90 (the values above the bars in the permeate water are the removals (%) of Ag).

6.4. Conclusions

This work shows that nanofiltration is an efficient technology to remove AgNPs, and simultaneous dissolved Ag released by AgNPs, from waters. AgNPs were completely removed and dissolved Ag presented removals higher than 92% for the studied waters and the membranes tested.

Results also demonstrate the role of the ionic strength on the nanofiltration performance to treat waters with dissolved Ag released by AgNPs. The increase of the ionic strength reduces the electrostatic repulsions force and the thickness of the double layer, reducing rejection of dissolved Ag. In addition, ionic strength and, therefore, the concentration of added Cl^- influences the Ag-species in solution, which generates more soluble silver chloride species and increases the concentration of Ag in the permeate. Therefore, the removal of dissolved Ag is controlled by surface chemistry, since dissolved Ag complexes with the salts present in waters, influencing the charge and size of dissolved-Ag.

The impact of NOM is just observed for NF270 membrane and NOM type. Permeate flux reduces approximately 35% when permeating TA. This is due to the weakly negative-neutral charge and compact coiled conformation of TA, and a restriction of electrostatic repulsion, which contribute to the fouling of the hydrophilic membrane. Dissolved Ag in NOM waters presents removals higher than >77% increasing with operation type to values higher than 92%.

Finally, the main mechanism of AgNPs removal by these membranes is size exclusion, due to the size of AgNPs aggregates compared with the membrane size. The removal of dissolved Ag is suggested to be by complexation with salts and adsorption to NOM or NOM-Ag complexes un-dissolved the silver in solution. However, this needs further investigation.

In this work, it was proved that it is possible to remove both AgNPs that are the in aquatic environments and simultaneously remove the dissolved Ag (released from NPs) from the water. To the author's knowledge, this was the first time of such approach has been applied to the removal of NPs. In this work pristine nanoparticles and model waters were used to control the variables involved in the process. The next step and in future work, non-pristine nanoparticles should be tested since silver nanoparticles can be transformed during treatment.

Chapter 7
Concluding Remarks

7.1. General conclusions

At the beginning of this work (2015) less was known about the actual effectiveness of drinking water treatments (DWTs) to remove engineered nanoparticles (ENPs) from water. At that time, only a few works had addressed the ENPs removal efficiencies from surface water, with high variability in the reported data. Although an exponential growth in the research published on nanoparticles in freshwater and their removal by water treatments was observed since 2014, the interest of the scientific community in these emergent contaminants in drinking water only started to raise after 2015 (Chapter 2). Even so, research on the occurrence (and detection) of nanoparticles in natural waters, as also on their removal, was still scarce. In addition, at that time there was no systematic review compiling the information available on the fate and breakthrough of ENPs in DWT. Therefore, in the present thesis previous information was reviewed by discussing the peer-reviewed articles published on metal-based ENPs occurrence, behaviour and detection in surface waters, as well as on the ability of DWTPs processes to remove ENPs (Chapter 2). Based on this review and in the unique characteristics and properties of ENPs, water treatment processes were chosen, and treatment strategies defined and developed to avoid the ENPs breakthrough into treated drinking water, reducing or even eliminating their hazards to human health (Chapters 3-6). For the first time: (i) conventional treatment (C/F/S) was optimised focused on the ENPs removal, instead of turbidity or NOM, as reported by other authors; (ii) simultaneous removal of three co-existing ENPs from drinking waters sources was assessed; (iii) conventional and advanced treatments were used alone or combined to assess the ENPs simultaneous removal; (iv) the advanced treatment nanofiltration was applied to evaluate the complete removal of ENPs and released ions and (v) treated waters quality was evaluated under national and international guidelines and by comparison with DWTP actual values, to explore the effect of ENPs removal in other target parameters. Considering that nanoparticles have already been detected in surface water, raw and treated drinking water and tap water, ranging from ng/L to µg/L, this thesis came to fill a knowledge gap in nanoparticles and water treatment disciplines representing an important contribution not only to those subjects, as also to the public health field.

The strategies employed in this thesis comprised two levels of water treatments: conventional (Chapters 3-5) and advanced (Chapters 5 and 6) processes, which have been applied alone or together. The removal efficiency of the conventional treatment coagulation/ flocculation/ sedimentation (C/F/S) was primarily explored to remove TiO_2 NPs from synthetic

and natural surface waters, based on promising results reported by earlier studies (Chapter 3). It was demonstrated that TiO_2 NPs could be removed at concentrations up to 95% using C/F/S, by the main mechanism of charge neutralisation. The high ENPs removals were obtained using an Al-based coagulant applied in actual drinking water treatment (DWT) and with operating parameters (mixing speed and period) set based on the typical real conditions. Other important findings were demonstrated with these initial experiments, namely hydrophobic waters need more coagulant to achieve similar Ti removals than hydrophilic waters, showing a strong influence of the water characteristics. In addition, hydrophobic waters showed higher turbidity removal than hydrophilic waters because of the initial turbidity of the former water, which improved removal. The presence of TiO_2 NPs also contributed to high removals of NOM and turbidity, since titanium compounds have some coagulant properties. Likewise, C/F/S also presented high efficiency in the simultaneous removal of different co-existing metal-based ENPs (TiO_2, Ag and CuO) from hydrophilic natural surface waters used for public supply by optimisation of the coagulant dose based in single ENPs removals (Chapter 4). Removal efficiencies above 93% (depending on the ENP) were observed for a low turbidity natural water (1.91±0.36 NTU, NW1), and above 98% for a medium turbidity natural water (63.33±5.37 NTU, NW2). It was also concluded that the main mechanism involved in simultaneous ENPs removal by C/F/S was charge neutralisation. However, in NW2 sweep flocculation may also be involved, but more studies are needed to confirm the presence of this mechanism. Once again, the differences between water characteristics play an important role on the coagulant demand, on the overall performance of C/F/S process and consequently on the ENPs removal, despite both waters were hydrophilic. Although conventional C/F/S had shown to highly remove co-existing metal-based ENPs from surface waters, residual concentrations of Ti, Ag and Cu were still found in the treated water, namely 6.5±2.1 and 2.5±0.7 µg Ti/L, 15.0±1.4 and 6.0±1.4 µg Ag/L, and 18.8±8.8 and 0.5±0.1 µg Cu/L, respectively, for the lowest turbidity and NOM content water (NW1) and for the highest turbidity and NOM content water (NW2) studied. The enhancement of the conventional coagulation by the addition of powdered activated carbon (C/F/S+PAC) and the hybrid membrane treatment integrating conventional C/F/S and advanced ultrafiltration (C/F/S→UF) improved the multiple ENPs removal compared to conventional C/F/S (Chapter 5). After C/F/S+PAC treatment, Ti presented the highest removal with residual concentration below the detection limit (0.350 µg/L) for both natural waters. In C/F/S+PAC treatment, Ti, Ag and Cu removal efficiencies were higher than 99.2%, and in the C/F/S→UF Ti and Cu removal efficiencies were higher than 99.9% and undetected in permeate flux. On

the other hand, Ag residual concentrations were found in the UF permeate (approximately 5.0-7.0 µg/L). This indicated that some part of the Ag was not removed by the UF membrane, which could be related to AgNPs dissolution, since membrane pores were smaller than the individual ENPs and aggregates size. Yet, C/F/S+PAC presented higher efficiencies for the NOM removal than C/F/S→UF, and for the turbidity removal, the reverse was observed. In the case of the turbidity, the low density of the PAC used contributed to the presence of more particles in the final water, anticipating the need to use a filtration step after the C/F/S+PAC. Due to the membrane pore size, and the size and charge of aggregates and individual ENPs, the main mechanisms proposed to C/F/S→UF were charge neutralisation (C/F/S) and size exclusion (UF).

The application of the advanced treatment nanofiltration (NF) alone using synthetic waters (Chapter 6) had proven, for the first time, that AgNPs and dissolved Ag released from AgNPs can be completely removed with removals up to 99.9% depending on salts and NOM content, membrane type and operation time. In NF operation the main mechanism of AgNPs removal is size exclusion, as also shown for UF, due to the size of AgNPs aggregates and individual particles compared with the membrane size. The removal of dissolved Ag was suggested to be by complexation with salts and adsorption on NOM or NOM-Ag complexes un-dissolved the silver in solution. However, since NF was tested without any pre-treatment, NF 270 permeate fluxes reduces approximately 35% in the presence of waters with the NOM surrogate tannic acid (TA) due to the weakly negative-neutral charge and compact coiled conformation of TA, and a restriction of electrostatic repulsion, which contribute to the fouling of the hydrophilic membrane.

Overall, the processes optimisation (C/F/S, C/F/S+PAC and C/F/S→UF) to the ENPs removal did not affect the ability of all processes to remove other target compounds of the drinking water treatment, with residual turbidity, DOC, SUVA and aluminium below the Portuguese and WHO guidelines for DWT, and similar to those found in WTPs. The target parameters were within the acceptable range for removal efficiencies by C/F/S, with strong correlations ($R > 0.8$) between the ENPs removal and the turbidity, DOC and UV_{254} removal observed, indicating that coagulant doses achieved based in ENPs removal are suitable for the removal of other parameters. Unlike the water's characteristics, the presence of multiple ENPs did not influence the Al-based coagulant demand.

Therefore, based on the results presented in Chapters 3 and 4 it is possible to answer to the first hypothesis purposed in this thesis, yes, conventional DWT can be optimised to be able to remove nanoparticles, with high removal efficiencies. Chapter 5 clearly demonstrated that C/F/S, combined or integrated with PAC and UF, are highly effective in the metal-based ENPs removal being good options to protect human health against the exposure to nanoparticles through drinking water, without compromising the target parameters in DWT. The high ENPs removal efficiencies were obtained simulating typical operational conditions at water plants, using commercial Al-based coagulant and PAC, both largely applied in the actual DWT context and natural waters currently used for drinking water production, to enable a future scale-up of these treatments. Moreover, coagulant and PAC doses were within the range of DWT typical doses. Therefore, Chapter 5 (together with Chapters 3 and 4) answer to the third hypothesis purposed in this thesis. However, Ag ions were not completely removed, which leads to the second hypothesis purposed in this thesis. Advanced treatments can effectively remove metal-based ENPs, but the completely removal of ions released from nanoparticles is extremely dependent on the water characteristics.

The use and integration of the advanced treatments approach showed additional advantages. Nevertheless, conventional treatments, especially when combined, also proved to be a valuable alternative with the advantage of being more cost-effective. Membrane processes, such as UF and NF are usually considered more environmental-friendly, since they are physical processes, without the need for chemical addition. Yet, these processes presented a higher energetic demand, which is a drawback from the sustainability point of view. Within the conventional treatments, enhanced treatment C/F/S+PAC can be seen as a more ecological option, since the application of PAC (from natural compounds) could imply a reduction in the Al-based coagulant doses, often associated with neurological diseases such as Alzheimer's. Also enhancing or integrating the most used process in drinking water production (C/F/S) minimises the impact of WTP requalification.

At the end of this thesis, it can be assumed that optimised conventional treatment C/F/S is able to remove metal-based ENPs from surface waters with high effectiveness. To improve this removal other treatments (conventional or advanced) must be coupled to C/F/S and both C/F/S+PAC and C/F/S→UF could be applied to achieve ENPs removals close to 100%. However, due to the dissolution of some ENPs a more refined treatment may be needed. Therefore, due to the knowledge gap on the possible toxic effects of ENPs on human health, a

treatment line integrating C/F/S+PAC, followed by UF or even NF processes emerges as the best solution to eliminate ENPs threat to human health.

7.2. Future perspectives

The treatment strategies applied in this study were an efficient approach to remove ENPs during DWT and reduce the threat of these emergent contaminants, representing objective and reproducible methodologies, which can be adopted in DWTPs. Furthermore, from a broader perspective of research, the delineation of these water treatment strategies could be relevant to explore the simultaneous removal of multiple emergent contaminants, such as ENPs, pharmaceuticals and micro and nanoplastics. The results of this thesis and the knowledge acquired during its development identified a set of additional research that could further improve the effectiveness of ENPs removal by DWT and their application to full-scale context. Additional research includes:

- The development of more suitable analytical techniques for the quantification of ENPs in complex matrices, like surface water sources, as also in treated drinking water;

- The knowledge improvement on ENPs toxicity to human health and environment, to enable the settlement of stringent requirements and guidelines specific for nanoparticles in the frameworks of the government environmental regulation;

- The evaluation of ENPs and released ions removal by NF using hydrophilic and hydrophobic natural surface waters, integrating NF with C/F/S to reduce the fouling effect and decrease the influence of water characteristics in the removal;

- The full assessment of the mechanisms involved in the ENPs removal by C/F/S, namely the possibility of sweep flocculation acting in the natural water with a higher content of turbidity and NOM;

- The evaluation of ENPs removal by C/F/S+PAC and C/F/S→UF using hydrophobic waters;

- The scale-up (pilot and full-scale) of the purposed treatments and strategies.

From a preventive perspective, it would also be advantageous to investigate ENPs point sources, focusing on ENPs release hotspots monitoring, especially for DWTP monitoring intakes located downstream of large urban communities. It also would be an asset to conduct periodical analyses measuring the most common metal-based ENPs, due to the potential hazards on public health.

Chapter 8
References

Abbott Chalew, T.E., Ajmani, G.S., Huang, H., Schwab, K.J., 2013. Evaluating nanoparticle breakthrough during drinking water treatment. Environ. Health Perspect. 121, 1161–1166. https://doi.org/10.1289/ehp.1306574

AdA, 2019. Águas do Algarve, S.A. [WWW Document]. Qual. da Água. URL https://www.aguasdoalgarve.pt/content/qualidade-da-agua (accessed 9.20.10).

Adam, V., Caballero-Guzman, A., Nowack, B., 2018. Considering the forms of released engineered nanomaterials in probabilistic material flow analysis. Environ. Pollut. 243, 17–27. https://doi.org/10.1016/j.envpol.2018.07.108

Adeleye, A.S., Pokhrel, S., Mädler, L., Keller, A.A., 2018. Influence of nanoparticle doping on the colloidal stability and toxicity of copper oxide nanoparticles in synthetic and natural waters. Water Res. 132, 12–22. https://doi.org/10.1016/J.WATRES.2017.12.069

Ahamed, M., Alsalhi, M.S., Siddiqui, M.K.J., 2010. Silver nanoparticle applications and human health. Clin. Chim. Acta. 411, 1841–1848. https://doi.org/10.1016/j.cca.2010.08.016

Allouni, Z.E., Høl, P.J., Cauqui, M.A., Gjerdet, N.R., Cimpan, M.R., 2012. Role of physicochemical characteristics in the uptake of TiO2 nanoparticles by fibroblasts. Toxicol. In Vitro 26, 469–479. https://doi.org/10.1016/j.tiv.2012.01.019

Amde, M., Liu, J. fu, Tan, Z.Q., Bekana, D., 2017. Transformation and bioavailability of metal oxide nanoparticles in aquatic and terrestrial environments. A review. Environ. Pollut. 230, 250–267. https://doi.org/10.1016/j.envpol.2017.06.064

Angel, B.M., Batley, G.E., Jarolimek, C. V., Rogers, N.J., 2013. The impact of size on the fate and toxicity of nanoparticulate silver in aquatic systems. Chemosphere 93, 359–365. https://doi.org/10.1016/J.CHEMOSPHERE.2013.04.096

António, D.C., Cascio, C., Jakšić, Ž., Jurašin, D., Lyons, D.M., Nogueira, A.J.A., Rossi, F., Calzolai, L., 2015. Assessing silver nanoparticles behaviour in artificial seawater by mean of AF4 and spICP-MS. Mar. Environ. Res. 111, 162–169. https://doi.org/10.1016/J.MARENVRES.2015.05.006

AWWA, 2000. Water Quality and Treatment. A handbook of community water suplies., 5th ed. McGraw-Hill, USA.

Baalousha, M., 2009. Aggregation and disaggregation of iron oxide nanoparticles: Influence of particle concentration, pH and natural organic matter. Sci. Total Environ. 407, 2093–2101. https://doi.org/10.1016/j.scitotenv.2008.11.022

Baalousha, M., Lead, J.R., 2013. Characterization of natural and manufactured nanoparticles by atomic force microscopy: Effect of analysis mode, environment and sample

preparation. Colloids Surfaces A Physicochem. Eng. Asp. 419, 238–247. https://doi.org/10.1016/j.colsurfa.2012.12.004

Baalousha, M., Manciulea, A., Cumberland, S., Kendall, K., Lead, J.R., 2008. Aggregation and surface properties of iron oxide nanoparticles: influence of pH and natural organic matter. Environ. Toxicol. Chem. 27, 1875–1882. https://doi.org/10.1897/07-559.1

Baalousha, M., Yang, Y., Vance, M.E., Colman, B.P., McNeal, S., Xu, J., Blaszczak, J., Steele, M., Bernhardt, E., Hochella, M.F., 2016. Outdoor urban nanomaterials: The emergence of a new, integrated, and critical field of study. Sci. Total Environ. 557–558, 740–753. https://doi.org/10.1016/J.SCITOTENV.2016.03.132

Bakaraki Turan, N., Erkan, H.S., Onkal Engin, G., Bilgili, M.S., 2019. Nanoparticles in the aquatic environment: usage, properties, transformation and toxicity-A review. Process Saf. Environ. Prot. https://doi.org/10.1016/J.PSEP.2019.08.014

Beer, C., Foldbjerg, R., Hayashi, Y., Sutherland, D.S., Autrup, H., 2012. Toxicity of silver nanoparticles - nanoparticle or silver ion? Toxicol. Lett. 208, 286–292. https://doi.org/10.1016/j.toxlet.2011.11.002

Benn, T., Cavanagh, B., Hristovski, K., Posner, J.D., Westerhoff, P., 2010. The Release of Nanosilver from Consumer Products Used in the Home. J. Environ. Qual. 39, 1875. https://doi.org/10.2134/jeq2009.0363

Berube, D.M., Searson, E.M., Morton, T.S., Cummings, C.L., 2010. Project on emerging nanotechnologies - Consumer product inventory evaluated. Nanotechnol. Law Bus. 7, 152–163.

Bhatt, I., Tripathi, B.N., 2011. Interaction of engineered nanoparticles with various components of the environment and possible strategies for their risk assessment. Chemosphere 82, 308–317. https://doi.org/10.1016/J.CHEMOSPHERE.2010.10.011

Bian, S.-W., Mudunkotuwa, I. a, Rupasinghe, T., Grassian, V.H., 2011. Aggregation and dissolution of 4 nm ZnO nanoparticles in aqueous environments: influence of pH, ionic strength, size, and adsorption of humic acid. Langmuir 27, 6059–6068. https://doi.org/10.1021/la200570n

Bilberg, K., Døving, K.B., Beedholm, K., Baatrup, E., 2011. Silver nanoparticles disrupt olfaction in Crucian carp (Carassius carassius) and Eurasian perch (Perca fluviatilis). Aquat. Toxicol. 104, 145–152. https://doi.org/10.1016/J.AQUATOX.2011.04.010

Blaser, S.A., Scheringer, M., Macleod, M., Hungerbühler, K., 2008. Estimation of cumulative aquatic exposure and risk due to silver: contribution of nano-functionalized plastics and

textiles. Sci. Total Environ. 390, 396–409. https://doi.org/10.1016/j.scitotenv.2007.10.010

Bolyard, S.C., Reinhart, D.R., Santra, S., 2013. Behavior of engineered nanoparticles in landfill leachate. Environ. Sci. Technol. 47, 8114–8122. https://doi.org/10.1021/es305175e

Bond, T., Goslan, E.H., Parsons, S.A., Jefferson, B., 2010. Disinfection by-product formation of natural organic matter surrogates and treatment by coagulation, MIEX and nanofiltration. Water Res. 44, 1645–1653. https://doi.org/10.1016/j.watres.2009.11.018

Bondy, S.C., 2010. The neurotoxicity of environmental aluminum is still an issue. Neurotoxicology 31, 575–581. https://doi.org/10.1016/j.neuro.2010.05.009

Botta, C., Labille, J., Auffan, M., Borschneck, D., Miche, H., Cabié, M., Masion, A., Rose, J., Bottero, J.Y., 2011. TiO2-based nanoparticles released in water from commercialized sunscreens in a life-cycle perspective: Structures and quantities. Environ. Pollut. 159, 1543–1550. https://doi.org/10.1016/j.envpol.2011.03.003

Boussu, K., Belpaire, A., Volodin, A., Van Haesendonck, C., Van der Meeren, P., Vandecasteele, C., Van der Bruggen, B., 2007. Influence of membrane and colloid characteristics on fouling of nanofiltration membranes. J. Memb. Sci. 289, 220–230. https://doi.org/10.1016/J.MEMSCI.2006.12.001

Brant, J.A., Childress, A.E., 2002. Assessing short-range membrane–colloid interactions using surface energetics. J. Memb. Sci. 203, 257–273. https://doi.org/10.1016/S0376-7388(02)00014-5

Brar, S.K., Verma, M., Tyagi, R.D., Surampalli, R.Y., 2010. Engineered nanoparticles in wastewater and wastewater sludge--evidence and impacts. Waste Manag. 30, 504–520. https://doi.org/10.1016/j.wasman.2009.10.012

Caballero-Guzman, A., Nowack, B., 2018. Prospective nanomaterial mass flows to the environment by life cycle stage from five applications containing CuO, DPP, FeOx, CNT and SiO2. J. Clean. Prod. 203, 990–1002. https://doi.org/10.1016/j.jclepro.2018.08.265

Caballero-Guzman, A., Nowack, B., 2016. A critical review of engineered nanomaterial release data: Are current data useful for material flow modeling? Environ. Pollut. 213, 502–517. https://doi.org/10.1016/J.ENVPOL.2016.02.028

Calvin, S., Luo, S.X., Caragianis-Broadbridge, C., McGuinness, J.K., Anderson, E., Lehman, a., Wee, K.H., Morrison, S. a., Kurihara, L.K., 2005. Comparison of extended x-ray absorption fine structure and Scherrer analysis of x-ray diffraction as methods for determining mean sizes of polydisperse nanoparticles. Appl. Phys. Lett. 87, 1–3. https://doi.org/10.1063/1.2137872

Calzolai, L., Gilliland, D., Rossi, F., 2012. Measuring nanoparticles size distribution in food and consumer products: A review. Food Addit. Contam. - Part A Chem. Anal. Control. Expo. Risk Assess. 29, 1183–1193. https://doi.org/10.1080/19440049.2012.689777

Campinas, M., Rosa, M.J., 2006. The ionic strength effect on microcystin and natural organic matter surrogate adsorption onto PAC. J. Colloid Interface Sci. 299, 520–529. https://doi.org/10.1016/j.jcis.2006.02.042

Canesi, L., Ciacci, C., Vallotto, D., Gallo, G., Marcomini, A., Pojana, G., 2010. In vitro effects of suspensions of selected nanoparticles (C60 fullerene, TiO2, SiO2) on Mytilus hemocytes. Aquat. Toxicol. 96, 151–158. https://doi.org/10.1016/j.aquatox.2009.10.017

Carlson, C., Hussain, S.M., Schrand, a M., Braydich-Stolle, L.K., Hess, K.L., Jones, R.L., Schlager, J.J., 2008. Unique cellular interaction of silver nanoparticles: size-dependent generation of reactive oxygen species. J. Phys. Chem. B 112, 13608–13619. https://doi.org/10.1021/jp712087m

Casals, E., Vázquez-Campos, S., Bastús, N.G., Puntes, V., 2008. Distribution and potential toxicity of engineered inorganic nanoparticles and carbon nanostructures in biological systems. TrAC Trends Anal. Chem. 27, 672–683. https://doi.org/10.1016/j.trac.2008.06.004

Cascio, C., Geiss, O., Franchini, F., Ojea-Jimenez, I., Rossi, F., Gilliland, D., Calzolai, L., 2015. Detection, quantification and derivation of number size distribution of silver nanoparticles in antimicrobial consumer products. J. Anal. At. Spectrom. 30, 1255–1265. https://doi.org/10.1039/c4ja00410h

Cha, K., Hong, H.-W., Choi, Y.-G., Lee, M.J., Park, J.H., Chae, H.-K., Ryu, G., Myung, H., 2008. Comparison of acute responses of mice livers to short-term exposure to nano-sized or micro-sized silver particles. Biotechnol. Lett. 30, 1893–1899. https://doi.org/10.1007/s10529-008-9786-2

Chang, H., Liu, B., Yang, B., Yang, X., Guo, C., He, Q., Liang, S., Chen, S., Yang, P., 2019. An integrated coagulation-ultrafiltration-nanofiltration process for internal reuse of shale gas flowback and produced water. Sep. Purif. Technol. 211, 310–321. https://doi.org/10.1016/j.seppur.2018.09.081

Chekli, L., Zhao, Y.X., Tijing, L.D., Phuntsho, S., Donner, E., Lombi, E., Gao, B.Y., Shon, H.K., 2015. Aggregation behaviour of engineered nanoparticles in natural waters: characterising aggregate structure using on-line laser light scattering. J. Hazard. Mater. 284, 190–200. https://doi.org/10.1016/j.jhazmat.2014.11.003

Chen, K.I., Elimelech, M., 2006. Aggregation and deposition kinectics of fullerene (C-60) nanoparticles 22, 10994–11001.

Chen, K.L., Elimelech, M., 2009. Relating colloidal stability of fullerene (C60) nanoparticles to nanoparticle charge and electrokinetic properties. Environ. Sci. Technol. 43, 7270–7276. https://doi.org/10.1021/es900185p

Chen, Z., Wang, Y., Ba, T., Li, Y., Pu, J., Chen, T., Song, Y., Gu, Y., Qian, Q., Yang, J., Jia, G., 2014. Genotoxic evaluation of titanium dioxide nanoparticles in vivo and in vitro. Toxicol. Lett. 226, 314–319. https://doi.org/10.1016/j.toxlet.2014.02.020

Chinnapongse, S.L., MacCuspie, R.I., Hackley, V.A., 2011. Persistence of singly dispersed silver nanoparticles in natural freshwaters, synthetic seawater, and simulated estuarine waters. Sci. Total Environ. 409, 2443–2450. https://doi.org/10.1016/j.scitotenv.2011.03.020

Choi, S., Johnston, M. V., Wang, G.S., Huang, C.P., 2017. Looking for engineered nanoparticles (ENPs) in wastewater treatment systems: Qualification and quantification aspects. Sci. Total Environ. 590–591, 809–817. https://doi.org/10.1016/j.scitotenv.2017.03.061

Clavier, A., Praetorius, A., Stoll, S., 2019. Determination of nanoparticle heteroaggregation attachment efficiencies and rates in presence of natural organic matter monomers. Monte Carlo modelling. Sci. Total Environ. 650, 530–540. https://doi.org/10.1016/j.scitotenv.2018.09.017

Cupaioli, F.A., Zucca, F.A., Boraschi, D., Zecca, L., 2014. Engineered nanoparticles. How brain friendly is this new guest? Prog. Neurobiol. 119-120C, 20–38. https://doi.org/10.1016/j.pneurobio.2014.05.002

Dalai, S., Pakrashi, S., Kumar, R.S.S., Chandrasekaran, N., Mukherjee, A., 2012. A comparative cytotoxicity study of TiO2 nanoparticles under light and dark conditions at low exposure concentrations. Toxicol. Res. (Camb). 1, 116–130. https://doi.org/10.1039/c2tx00012a

Dale, A.L., Casman, E. a., Lowry, G. V., Lead, J.R., Viparelli, E., Baalousha, M., 2015. Modeling Nanomaterial Environmental Fate in Aquatic Systems. Environ. Sci. Technol. 150204132813009. https://doi.org/10.1021/es505076w

Danish Consumer Council, 2012. The Nanodatabase [WWW Document]. URL http://nanodb.dk/ (accessed 6.19.19).

De Klein, J.J.M., Quik, J.T.K., Bäuerlein, P.S., Koelmans, A.A., 2016. Towards validation of

the NanoDUFLOW nanoparticle fate model for the river Dommel, the Netherlands. Environ. Sci. Nano 3, 434–441. https://doi.org/10.1039/c5en00270b

Desai, N., 2012. Challenges in Development of Nanoparticle-Based Therapeutics. AAPS J. 14, 282–295. https://doi.org/10.1208/s12248-012-9339-4

Dimkpa, C.O., McLean, J.E., Latta, D.E., Manangón, E., Britt, D.W., Johnson, W.P., Boyanov, M.I., Anderson, A.J., 2012. CuO and ZnO nanoparticles: Phytotoxicity, metal speciation, and induction of oxidative stress in sand-grown wheat. J. Nanoparticle Res. 14, 1125–1140. https://doi.org/10.1007/s11051-012-1125-9

Domingos, R.F., Tufenkji, N., Wilkinson, K.J., 2009. Aggregation of titanium dioxide nanoparticles: Role of a fulvic acid. Environ. Sci. Technol. 43, 1282–1286. https://doi.org/10.1021/es8023594

Donovan, A.R., Adams, C.D., Ma, Y., Stephan, C., Eichholz, T., Shi, H., 2016. Single particle ICP-MS characterization of titanium dioxide, silver, and gold nanoparticles during drinking water treatment. Chemosphere 144, 148–153. https://doi.org/10.1016/j.chemosphere.2015.07.081

Duester, L., Burkhardt, M., Gutleb, A.C., Kaegi, R., Macken, A., Meermann, B., von der Kammer, F., 2014. Toward a comprehensive and realistic risk evaluation of engineered nanomaterials in the urban water system. Front. Chem. 2, 1–6. https://doi.org/10.3389/fchem.2014.00039

Dumont, E., Johnson, A.C., Keller, V.D.J., Williams, R.J., 2015. Nano silver and nano zinc-oxide in surface waters – Exposure estimation for Europe at high spatial and temporal resolution. Environ. Pollut. 196, 341–349. https://doi.org/10.1016/j.envpol.2014.10.022

Dwivedi, A.D., Dubey, S.P., Sillanpää, M., Kwon, Y.-N., Lee, C., Varma, R.S., 2015. Fate of engineered nanoparticles: Implications in the environment. Coord. Chem. Rev. 287, 64–78. https://doi.org/10.1016/j.ccr.2014.12.014

Eaton, A., Clesceri, L.S., Rice, E., Greenberg, A.E., 2005a. Standard Methods for Examination of Water and Wastewater - 3030E and 3110, 21st ed. American Public Health Association, the American Water Works Association and the Water Environment Federation, Washigton D.C.

Eaton, A., Rice, E., Baird, R.B., 2005b. Standard Methods for Examination of Water and Wastewater - 2130, 2510, 4500-H+, 5310, 21st ed. American Public Health Association, the American Water Works Association and the Water Environment Federation, Washigton D.C.

EC - European Commission, 2011. Commission Recommendation of 18 October 2011 on the definition of nanomaterial. Off. J. Eur. Union 275, 38.

Eckenfelder, W.W., 2000. Industrial Water Pollution Control, 3 rd. ed. Company, McGraw-Hill Book, New York.

Edzwald, J.K., 2011. Water Quality and Treatment: A handbook on drinking water, Sixth. ed. McGraw-Hill.

Edzwald, J.K., Tobiason, J., 1999. Enhanced coagulation: Us requirements and a broader view. Water Sci. Technol. 40, 63–70. https://doi.org/10.1016/S0273-1223(99)00641-1

Edzwald, J.K., Van Benschoten, J.., 1990. Aluminium coagulation of natural organic matter, in: Hahn, H.H., Klute, R. (Eds.), Chemical Water and Wastewater Treatment. Springer-Verlag, Berlin, pp. 341–359.

Elzey, S., Grassian, V.H., 2010. Agglomeration, isolation and dissolution of commercially manufactured silver nanoparticles in aqueous environments. J. Nanoparticle Res. 12, 1945–1958. https://doi.org/10.1007/s11051-009-9783-y

EPA, 1999. Enhanced Coagulation and Enhanced Precipitate Softening Guidance Manual. EPA 814-R-99-012, Office of Water (4607). United States Environmental Protection Agency.

Fabrega, J., Luoma, S.N., Tyler, C.R., Galloway, T.S., Lead, J.R., 2011. Silver nanoparticles: behaviour and effects in the aquatic environment. Environ. Int. 37, 517–531. https://doi.org/10.1016/j.envint.2010.10.012

Farré, M., Pérez, S., Gajda-Schrantz, K., Osorio, V., Kantiani, L., Ginebreda, A., Barceló, D., 2010. First determination of C60 and C70 fullerenes and N-methylfulleropyrrolidine C60 on the suspended material of wastewater effluents by liquid chromatography hybrid quadrupole linear ion trap tandem mass spectrometry. J. Hydrol. 383, 44–51. https://doi.org/10.1016/j.jhydrol.2009.08.016

Feng, X., Johnson, D.W., 2014. Aggregated Nanoparticle Morphology Effects on Membrane Filtration. Chem. Eng. Commun. 202, 1000–1010. https://doi.org/10.1080/00986445.2014.891508

Flaten, T.P., 2001. Aluminium as a risk factor in Alzheimer's disease, with emphasis on drinking water. Brain Res. Bull. 55, 187–196. https://doi.org/10.1016/S0361-9230(01)00459-2

French, R. a., Jacobson, A.R., Kim, B., Isley, S.L., Penn, R.L., Baveye, P.C., 2009. Influence of ionic strength, pH, andcation valence on aggregation kinetics of titanium dioxide nanoparticles. Environ. Sci. Technol. 43, 1354–1359. https://doi.org/10.1021/es802628n

Froggett, S.J., Clancy, S.F., Boverhof, D.R., Canady, R.A., 2014. A review and perspective of existing research on the release of nanomaterials from solid nanocomposites. Part. Fibre Toxicol. 11, 1–28. https://doi.org/10.1186/1743-8977-11-17

Fröhlich, E., Roblegg, E., 2016. Oral uptake of nanoparticles: human relevance and the role of in vitro systems. Arch. Toxicol. 90, 2297–2314. https://doi.org/10.1007/s00204-016-1765-0

Future Markets, 2012. The Global Market for Nanomaterials 2002-2016: Production Volumes, Revenues and End Use Markets 371.

Gallego-Urrea, J.A., Tuoriniemi, J., Hassellöv, M., 2011. Applications of particle-tracking analysis to the determination of size distributions and concentrations of nanoparticles in environmental, biological and food samples. TrAC Trends Anal. Chem. 30, 473–483. https://doi.org/10.1016/J.TRAC.2011.01.005

Geissen, V., Mol, H., Klumpp, E., Umlauf, G., Nadal, M., van der Ploeg, M., van de Zee, S.E.A.T.M., Ritsema, C.J., 2015a. Emerging pollutants in the environment: A challenge for water resource management. Int. Soil Water Conserv. Res. 3, 57–65. https://doi.org/10.1016/J.ISWCR.2015.03.002

Geissen, V., Mol, H., Klumpp, E., Umlauf, G., Nadal, M., van der Ploeg, M., van de Zee, S.E.A.T.M., Ritsema, C.J., 2015b. Emerging pollutants in the environment: A challenge for water resource management. Int. Soil Water Conserv. Res. 3, 57–65. https://doi.org/10.1016/J.ISWCR.2015.03.002

Gicheva, G., Yordanov, G., 2013. Removal of citrate-coated silver nanoparticles from aqueous dispersions by using activated carbon. Colloids Surfaces A Physicochem. Eng. Asp. 431, 51–59. https://doi.org/10.1016/j.colsurfa.2013.04.039

Giese, B., Klaessig, F., Park, B., Kaegi, R., Steinfeldt, M., Wigger, H., Von Gleich, A., Gottschalk, F., 2018. Risks, Release and Concentrations of Engineered Nanomaterial in the Environment. Sci. Rep. 8, 1–18. https://doi.org/10.1038/s41598-018-19275-4

Gomes, T., Pereira, C.G., Cardoso, C., Pinheiro, J.P., Cancio, I., Bebianno, M.J., 2012. Accumulation and toxicity of copper oxide nanoparticles in the digestive gland of Mytilus galloprovincialis. Aquat. Toxicol. 118–119, 72–79. https://doi.org/10.1016/j.aquatox.2012.03.017

Gomes, T., Pereira, C.G., Cardoso, C., Sousa, V.S., Teixeira, M.R., Pinheiro, J.P., Bebianno, M.J., 2014. Effects of silver nanoparticles exposure in the mussel Mytilus galloprovincialis. Mar. Environ. Res. 101, 208–214.

https://doi.org/10.1016/j.marenvres.2014.07.004

Gomes, T., Pinheiro, J.P., Cancio, I., Pereira, C.G., Cardoso, C., Bebianno, M.J., 2011. Effects of copper nanoparticles exposure in the mussel Mytilus galloprovincialis. Environ. Sci. Technol. 45, 9356–9362. https://doi.org/10.1021/es200955s

Gondikas, A., Von Der Kammer, F., Kaegi, R., Borovinskaya, O., Neubauer, E., Navratilova, J., Praetorius, A., Cornelis, G., Hofmann, T., 2018. Where is the nano? Analytical approaches for the detection and quantification of TiO2 engineered nanoparticles in surface waters. Environ. Sci. Nano 5, 313–326. https://doi.org/10.1039/c7en00952f

Gondikas, A., Von der Kammer, F., Reed, R.B., Wagner, S., Ranville, J.F., 2014. Release of TiO2 nanoparticles from sunscreens into surface waters: a one-year survey at the Old Danube Recreational Lake. Environ. Sci. Technol. 48, 5415–5422. https://doi.org/https://doi.org/10.1021/es405596y

Gottschalk, F., Nowack, B., 2011. The release of engineered nanomaterials to the environment. J. Environ. Monit. 13, 1145–1155. https://doi.org/10.1039/c0em00547a

Gottschalk, F., Sonderer, T., Scholz, R.W., Nowack, B., 2009. Modeled Environmental Concentrations of Engineered Nanomaterials (TiO2, ZnO, Ag, CNT, Fullerenes) for Different Regions. Environ. Sci. Technol. 43, 9216–9222. https://doi.org/10.1021/es9015553

Gottschalk, F., Sun, T., Nowack, B., 2013. Environmental concentrations of engineered nanomaterials: Review of modeling and analytical studies. Environ. Pollut. 181, 287–300. https://doi.org/10.1016/J.ENVPOL.2013.06.003

Gregory, J., 1981. Approximate expressions for retarded van der waals interaction. J. Colloid Interface Sci. 83, 138–145. https://doi.org/10.1016/0021-9797(81)90018-7

Grieger, K.D., Fjordbøge, A., Hartmann, N.B., Eriksson, E., Bjerg, P.L., Baun, A., 2010. Environmental benefits and risks of zero-valent iron nanoparticles (nZVI) for in situ remediation: Risk mitigation or trade-off? J. Contam. Hydrol. 118, 165–183. https://doi.org/10.1016/J.JCONHYD.2010.07.011

Guo, H., Wyart, Y., Perot, J., Nauleau, F., Moulin, P., 2010. Application of magnetic nanoparticles for UF membrane integrity monitoring at low-pressure operation. J. Memb. Sci. 350, 172–179. https://doi.org/10.1016/j.memsci.2009.12.025

Hall, B.D., Zanchet, D., Ugarte, D., 2000. research papers Estimating nanoparticle size from diffraction measurements research papers 1335–1341. https://doi.org/10.1107/S0021889800010888

Handy, R.D., Owen, R., Valsami-Jones, E., 2008. The ecotoxicology of nanoparticles and nanomaterials: current status, knowledge gaps, challenges, and future needs. Ecotoxicology 17, 315–325. https://doi.org/10.1007/s10646-008-0206-0

Hendren, C.O., Mesnard, X., Dröge, J., Wiesner, M.R., 2011. Estimating production data for five engineered nanomaterials as a basis for exposure assessment. Environ. Sci. Technol. 45, 2562–2569. https://doi.org/10.1021/es103300g

Hendrickson, O.D., Safenkova, I. V., Zherdev, A. V., Dzantiev, B.B., Popov, V.O., 2011. Methods of detection and identification of manufactured nanoparticles. Biophysics (Oxf). 56, 961–986. https://doi.org/10.1134/s0006350911060066

Honda, R.J., Keene, V., Daniels, L., Walker, S.L., 2014. Removal of TiO2 Nanoparticles During Primary Water Treatment: Role of Coagulant Type, Dose, and Nanoparticle Concentration. Environ. Eng. Sci. 31, 127–134. https://doi.org/10.1089/ees.2013.0269

Hong, S., Elimelech, M., 1997. Chemical and physical aspects of natural organic matter (NOM) fouling of nanofiltration membranes. J. Memb. Sci. 132, 159–181. https://doi.org/10.1016/S0376-7388(97)00060-4

Hotze, E.M., Phenrat, T., Lowry, G. V., 2010. Nanoparticle aggregation: Challenges to understanding transport and reactivity in the environment. J. Environ. Qual. 39, 1909–1924. https://doi.org/10.2134/jeq2009.0462

Houtman, C.J., 2010. Emerging contaminants in surface waters and their relevance for the production of drinking water in Europe. J. Integr. Environ. Sci. 7, 271–295. https://doi.org/10.1080/1943815X.2010.511648

Howard, A.G., 2010. On the challenge of quantifying man-made nanoparticles in the aquatic environment. J. Environ. Monit. 12, 135–142. https://doi.org/10.1039/b913681a

Huang, X., Wan, Y., Shi, B., Shi, J., 2020. Effects of powdered activated carbon on the coagulation-flocculation process in humic acid and humic acid-kaolin water treatment. Chemosphere 238, 124637. https://doi.org/10.1016/j.chemosphere.2019.124637

Inshakova, E., Inshakov, O., 2017. World market for nanomaterials: structure and trends. MATEC Web Conf. 129, 02013. https://doi.org/10.1051/matecconf/201712902013

Israelachvili, J., 1992. Intermolecular and Surface Forces, 2nd ed. Academic Press, London.

Jahan, S., Yusoff, I. Bin, Alias, Y.B., Bakar, A.F.B.A., 2017. Reviews of the toxicity behavior of five potential engineered nanomaterials (ENMs) into the aquatic ecosystem. Toxicol. Reports 4, 211–220. https://doi.org/10.1016/j.toxrep.2017.04.001

Jeevanandam, J., Barhoum, A., Chan, Y.S., Dufresne, A., Danquah, M.K., 2018. Review on

nanoparticles and nanostructured materials: History, sources, toxicity and regulations. Beilstein J. Nanotechnol. 9, 1050–1074. https://doi.org/10.3762/bjnano.9.98

Jiang, J.-Q., 2015. The role of coagulation in water treatment. Curr. Opin. Chem. Eng. 8, 36–44. https://doi.org/10.1016/j.coche.2015.01.008

Jiang, J., Oberdörster, G., Biswas, P., 2009. Characterization of size, surface charge, and agglomeration state of nanoparticle dispersions for toxicological studies. J. Nanoparticle Res. 11, 77–89. https://doi.org/10.1007/s11051-008-9446-4

Johnson, A.C., Bowes, M.J., Crossley, A., Jarvie, H.P., Jurkschat, K., Jürgens, M.D., Lawlor, A.J., Park, B., Rowland, P., Spurgeon, D., Svendsen, C., Thompson, I.P., Barnes, R.J., Williams, R.J., Xu, N., 2011. An assessment of the fate, behaviour and environmental risk associated with sunscreen TiO2 nanoparticles in UK field scenarios. Sci. Total Environ. 409, 2503–2510. https://doi.org/10.1016/j.scitotenv.2011.03.040

Joseph, L., Flora, J.R.V., Park, Y.-G., Badawy, M., Saleh, H., Yoon, Y., 2012. Removal of natural organic matter from potential drinking water sources by combined coagulation and adsorption using carbon nanomaterials. Sep. Purif. Technol. 95, 64–72. https://doi.org/10.1016/j.seppur.2012.04.033

Jung, C., Phal, N., Oh, J., Chu, K.H., Jang, M., Yoon, Y., 2015. Removal of humic and tannic acids by adsorption–coagulation combined systems with activated biochar. J. Hazard. Mater. 300, 808–814. https://doi.org/10.1016/J.JHAZMAT.2015.08.025

Kaegi, R., Englert, A., Gondikas, A., Sinnet, B., von der Kammer, F., Burkhardt, M., 2017. Release of TiO2 – (Nano) particles from construction and demolition landfills. NanoImpact 8, 73–79. https://doi.org/10.1016/J.IMPACT.2017.07.004

Kaegi, R., Voegelin, A., Ort, C., Sinnet, B., Thalmann, B., Krismer, J., Hagendorfer, H., Elumelu, M., Mueller, E., 2013. Fate and transformation of silver nanoparticles in urban wastewater systems. Water Res. 47, 3866–3877. https://doi.org/10.1016/j.watres.2012.11.060

Karlsson, H.L., Gustafsson, J., Cronholm, P., Möller, L., 2009. Size-dependent toxicity of metal oxide particles--a comparison between nano- and micrometer size. Toxicol. Lett. 188, 112–118. https://doi.org/10.1016/j.toxlet.2009.03.014

Kavcar, P., Sofuoglu, A., Sofuoglu, S.C., 2009. A health risk assessment for exposure to trace metals via drinking water ingestion pathway. Int. J. Hyg. Environ. Health 212, 216–227. https://doi.org/10.1016/J.IJHEH.2008.05.002

Kawata, K., Osawa, M., Okabe, S., 2009. In vitro toxicity of silver nanoparticles at noncytotoxic

doses to HepG2 human hepatoma cells. Environ. Sci. Technol. 43, 6046–6051.

Keller, A. a., McFerran, S., Lazareva, A., Suh, S., 2013. Global life cycle releases of engineered nanomaterials. J. Nanoparticle Res. 15, 1692–1719. https://doi.org/10.1007/s11051-013-1692-4

Keller, A. a, Wang, H., Zhou, D., Lenihan, H.S., Cherr, G., Cardinale, B.J., Miller, R., Ji, Z., 2010. Stability and aggregation of metal oxide nanoparticles in natural aqueous matrices. Environ. Sci. Technol. 44, 1962–1967. https://doi.org/10.1021/es902987d

Kent, R.D., Vikesland, P.J., 2012. Controlled evaluation of silver nanoparticle dissolution using atomic force microscopy. Environ. Sci. Technol. 46, 6977–6984. https://doi.org/10.1021/es203475a

Khan, Ibrahim, Saeed, K., Khan, Idrees, 2019. Nanoparticles: Properties, applications and toxicities. Arab. J. Chem. 12, 908–931. https://doi.org/10.1016/J.ARABJC.2017.05.011

Kim, S., Choi, J.E., Choi, J., Chung, K.-H., Park, K., Yi, J., Ryu, D.-Y., 2009. Oxidative stress-dependent toxicity of silver nanoparticles in human hepatoma cells. Toxicol. In Vitro 23, 1076–1084. https://doi.org/10.1016/j.tiv.2009.06.001

Kinsinger, N., Honda, R., Keene, V., Walker, S.L., 2015. Titanium Dioxide Nanoparticle Removal in Primary Prefiltration Stages of Water Treatment: Role of Coating, Natural Organic Matter, Source Water, and Solution Chemistry. Environ. Eng. Sci. 32, 1–9. https://doi.org/10.1089/ees.2014.0288

Klaine, S.J., Alvarez, P.J.J., Batley, G., Fernandes, T.F., Handy, R.D., Lyon, D.Y., Mahendra, S., McLaughlin, M.J., Lead, J.R., 2008. Nanomaterials in the environment: behaviour, fate, bioavailability and effects. Environ. Toxicol. Chem. 27, 1825–1851. https://doi.org/10.1002/etc.4147

Krystek, P., 2012. A review on approaches to bio distribution studies about gold and silver engineered nanoparticles by inductively coupled plasma mass spectrometry. Microchem. J. 105, 39–43. https://doi.org/10.1016/J.MICROC.2012.02.008

Krystek, P., Ulrich, A., Garcia, C.C., Manohar, S., Ritsema, R., 2011. Application of plasma spectrometry for the analysis of engineered nanoparticles in suspensions and products. J. Anal. At. Spectrom. 26, 1701–1721. https://doi.org/10.1039/c1ja10071h

Kumbıçak, U., Cavaş, T., Cinkılıç, N., Kumbıçak, Z., Vatan, O., Yılmaz, D., 2014. Evaluation of in vitro cytotoxicity and genotoxicity of copper-zinc alloy nanoparticles in human lung epithelial cells. Food Chem. Toxicol. 73C, 105–112. https://doi.org/10.1016/j.fct.2014.07.040

Laborda, F., Bolea, E., Cepriá, G., Gómez, M.T., Jiménez, M.S., Pérez-Arantegui, J., Castillo, J.R., 2016. Detection, characterization and quantification of inorganic engineered nanomaterials: A review of techniques and methodological approaches for the analysis of complex samples. Anal. Chim. Acta 904, 10–32. https://doi.org/10.1016/j.aca.2015.11.008

Laborda, F., Jiménez-Lamana, J., Bolea, E., Castillo, J.R., 2013. Critical considerations for the determination of nanoparticle number concentrations, size and number size distributions by single particle ICP-MS. J. Anal. At. Spectrom. 28, 1220–1232. https://doi.org/10.1039/c3ja50100k

Ladner, D.A., Steele, M., Weir, A., Hristovski, K., Westerhoff, P., 2012. Functionalized nanoparticle interactions with polymeric membranes. J. Hazard. Mater. 211–212, 288–295. https://doi.org/10.1016/J.JHAZMAT.2011.11.051

Lapresta-Fernández, A., Salinas-Castillo, A., Anderson De La Llana, S., Costa-Fernández, J.M., Domínguez-Meister, S., Cecchini, R., Capitán-Vallvey, L.F., Moreno-Bondi, M.C., Marco, M.P., Sánchez-López, J.C., Anderson, I.S., 2014. A general perspective of the characterization and quantification of nanoparticles: Imaging, spectroscopic, and separation techniques. Crit. Rev. Solid State Mater. Sci. 39, 423–458. https://doi.org/10.1080/10408436.2014.899890

Le Hir, M., Wyart, Y., Georges, G., Siozade Lamoine, L., Sauvade, P., Moulin, P., 2018. Effect of salinity and nanoparticle polydispersity on UF membrane retention fouling. J. Memb. Sci. 563, 405–418. https://doi.org/10.1016/J.MEMSCI.2018.05.077

Lead, J.R., Batley, G.E., Alvarez, P.J.J., Croteau, M.N., Handy, R.D., McLaughlin, M.J., Judy, J.D., Schirmer, K., 2018. Nanomaterials in the environment: Behavior, fate, bioavailability, and effects—An updated review. Environ. Toxicol. Chem. 37, 2029–2063. https://doi.org/10.1002/etc.4147

Lee, S., Bi, X., Reed, R.B., Ranville, J.F., Herckes, P., Westerhoff, P., 2014. Nanoparticle size detection limits by single particle ICP-MS for 40 elements. Environ. Sci. Technol. 48, 10291–10300. https://doi.org/10.1021/es502422v

Li, Q., Mahendra, S., Lyon, D.Y., Brunet, L., Liga, M. V., Li, D., Alvarez, P.J.J., 2008. Antimicrobial nanomaterials for water disinfection and microbial control: Potential applications and implications. Water Res. 42, 4591–4602. https://doi.org/10.1016/J.WATRES.2008.08.015

Li, S., Sun, W., 2011. A comparative study on aggregation/sedimentation of TiO 2

nanoparticles in mono- and binary systems of fulvic acids and Fe(III). J. Hazard. Mater. 197, 70–79. https://doi.org/10.1016/j.jhazmat.2011.09.059

Li, X., Lenhart, J.J., 2012. Aggregation and dissolution of silver nanoparticles in natural surface water. Environ. Sci. Technol. 46, 5378–5386. https://doi.org/10.1021/es204531y

Li, Z., Aly Hassan, A., Sahle-Demessie, E., Sorial, G.A., 2013. Transport of nanoparticles with dispersant through biofilm coated drinking water sand filters. Water Res. 47, 6457–6466. https://doi.org/10.1016/J.WATRES.2013.08.026

Lin, Y.L., Chiang, P.C., Chang, E.E., 2007. Removal of small trihalomethane precursors from aqueous solution by nanofiltration. J. Hazard. Mater. 146, 20–29. https://doi.org/10.1016/j.jhazmat.2006.11.050

Liu, H.H., Cohen, Y., 2014. Multimedia environmental distribution of engineered nanomaterials. Environ. Sci. Technol. 48, 3281–3292. https://doi.org/10.1021/es405132z

Liu, J., He, K., Tang, S., Wang, T., Zhang, Z., 2019. A comparative study of ferrous, ferric and ferrate pretreatment for ceramic membrane fouling alleviation in reclaimed water treatment. Sep. Purif. Technol. 217, 118–127. https://doi.org/10.1016/J.SEPPUR.2019.01.040

Liu, J.Y., Hurt, R.H., 2010. Ion release kinetics and particle persistance in aqueous nano-silver colloids. Environ. Sci. Technol. 44, 2169–2175.

Liu, N., Liu, C., Zhang, J., Lin, D., 2012. Removal of dispersant-stabilized carbon nanotubes by regular coagulants. J. Environ. Sci. 24, 1364–1370. https://doi.org/10.1016/S1001-0742(11)60933-9

Liu, Y., Tourbin, M., Lachaize, S., Guiraud, P., 2014. Nanoparticles in wastewaters: Hazards, fate and remediation. Powder Technol. 255, 149–156. https://doi.org/10.1016/j.powtec.2013.08.025

Lompe, K.M., Vo Duy, S., Peldszus, S., Sauvé, S., Barbeau, B., 2018. Removal of micropollutants by fresh and colonized magnetic powdered activated carbon. J. Hazard. Mater. 360, 349–355. https://doi.org/10.1016/J.JHAZMAT.2018.07.072

Long, T.C., Saleh, N., Tilton, R.D., Gregory, V., 2006. Titanium Dioxide (P25) Produces Reactive Oxygen Species in Implications for Nanoparticle. Environ. Sci. Technol. 40, 4346–4352. https://doi.org/10.1021/es060589n

Loosli, F., Le Coustumer, P., Stoll, S., 2013. TiO2 nanoparticles aggregation and disaggregation in presence of alginate and Suwannee River humic acids. pH and concentration effects on nanoparticle stability. Water Res. 47, 6052–6063.

https://doi.org/10.1016/j.watres.2013.07.021

Loosli, F., Vitorazi, L., Berret, J.-F., Stoll, S., 2015. Towards a better understanding on agglomeration mechanisms and thermodynamic properties of TiO_2 nanoparticles interacting with natural organic matter. Water Res. 80, 139–148. https://doi.org/10.1016/j.watres.2015.05.009

Loosli, F., Wang, J., Rothenberg, S., Bizimis, M., Winkler, C., Borovinskaya, O., Flamigni, L., Baalousha, M., 2019. Sewage spills are a major source of titanium dioxide engineered (nano)-particle release into the environment. Environ. Sci. Nano 6, 763–777. https://doi.org/10.1039/c8en01376d

Lowry, G. V., Gregory, K.B., Apte, S.C., Lead, J.R., 2012. Transformations of Nanomaterials in the Environment. Environ. Sci. Technol. 46, 6893–6899. https://doi.org/10.1016/B978-0-08-099408-6.00002-5

Lu, H., Wang, J., Stoller, M., Wang, T., Bao, Y., Hao, H., 2016. An overview of nanomaterials for water technology. Adv. Mater. Sci. Eng. 2016, 1–12. https://doi.org/110.1155/2016/4964828

Maguire, C.M., Rösslein, M., Wick, P., Prina-Mello, A., 2018. Characterisation of particles in solution–a perspective on light scattering and comparative technologies. Sci. Technol. Adv. Mater. 19, 732–745. https://doi.org/10.1080/14686996.2018.1517587

Maisano, M., Cappello, T., Catanese, E., Vitale, V., Natalotto, A., Giannetto, A., Barreca, D., Brunelli, E., Mauceri, A., Fasulo, S., 2015. Developmental abnormalities and neurotoxicological effects of CuO NPs on the black sea urchin Arbacia lixula by embryotoxicity assay. Mar. Environ. Res. 111, 121–127. https://doi.org/10.1016/J.MARENVRES.2015.05.010

Malvern, 2009. Zetasizer Nano Series - User Manual. Malvern Instruments Ltd., United Kingdom.

Markus, A.A., Krystek, P., Tromp, P.C., Parsons, J.R., Roex, E.W.M., Voogt, P. de, Laane, R.W.P.M., 2018. Determination of metal-based nanoparticles in the river Dommel in the Netherlands via ultrafiltration, HR-ICP-MS and SEM. Sci. Total Environ. 631, 485–495. https://doi.org/10.1016/j.scitotenv.2018.03.007

Mashayekhi, H., Ghosh, S., Du, P., Xing, B., 2012. Effect of natural organic matter on aggregation behavior of C 60 fullerene in water. J. Colloid Interface Sci. 374, 111–117. https://doi.org/10.1016/j.jcis.2012.01.061

Matilainen, A., Vepsäläinen, M., Sillanpää, M., 2010. Natural organic matter removal by

coagulation during drinking water treatment: A review. Adv. Colloid Interface Sci. 159, 189–197. https://doi.org/10.1016/j.cis.2010.06.007

Matthews, J.N.A., 2014. Taking stock of the nanotechnology consumer products market. Phys. Today 67, 22–24. https://doi.org/10.1063/pt.3.2273

Menard, A., Drobne, D., Jemec, A., 2011. Ecotoxicity of nanosized TiO2. Review of in vivo data. Environ. Pollut. 159, 677–684. https://doi.org/10.1016/j.envpol.2010.11.027

Merdzan, V., Domingos, R.F., Monteiro, C.E., Hadioui, M., Wilkinson, K.J., 2014. The effects of different coatings on zinc oxide nanoparticles and their influence on dissolution and bioaccumulation by the green alga, C. reinhardtii. Sci. Total Environ. 488–489, 316–324. https://doi.org/10.1016/J.SCITOTENV.2014.04.094

Merrifield, R.C., Stephan, C., Lead, J., 2017. Determining the Concentration Dependent Transformations of Ag Nanoparticles in Complex Media: Using SP-ICP-MS and Au@Ag Core-Shell Nanoparticles as Tracers. Environ. Sci. Technol. 51, 3206–3213. https://doi.org/10.1021/acs.est.6b05178

Missaoui, W.N., Arnold, R.D., Cummings, B.S., 2018. Toxicological status of nanoparticles: What we know and what we don't know. Chem. Biol. Interact. 295, 1–12. https://doi.org/10.1016/J.CBI.2018.07.015

Mitrano, D.M., Lesher, E.K., Bednar, A., Monserud, J., Higgins, C.P., Ranville, J.F., 2012. Detecting nanoparticulate silver using single-particle inductively coupled plasma-mass spectrometry. Environ. Toxicol. Chem. 31, 115–121. https://doi.org/10.1002/etc.719

Mitrano, D.M., Ranville, J.F., Bednar, A., Kazor, K., Hering, A.S., Higgins, C.P., 2014. Tracking dissolution of silver nanoparticles at environmentally relevant concentrations in laboratory, natural, and processed waters using single particle ICP-MS (spICP-MS). Environ. Sci. Nano 1, 248–259. https://doi.org/10.1039/c3en00108c

Mittelman, A.M., Fortner, J.D., Pennell, K.D., 2015. Effects of ultraviolet light on silver nanoparticle mobility and dissolution. Environ. Sci. Nano 2, 683–691. https://doi.org/10.1039/c5en00145e

Mohd Omar, F., Abdul Aziz, H., Stoll, S., 2014. Aggregation and disaggregation of ZnO nanoparticles: influence of pH and adsorption of Suwannee River humic acid. Sci. Total Environ. 468–469, 195–201. https://doi.org/10.1016/j.scitotenv.2013.08.044

Montaño, M.D., Badiei, H.R., Bazargan, S., Ranville, J.F., 2014. Improvements in the detection and characterization of engineered nanoparticles using spICP-MS with microsecond dwell times. Environ. Sci. Nano 1, 338–346. https://doi.org/10.1039/c4en00058g

Moore, M.N., 2006. Do nanoparticles present ecotoxicological risks for the health of the aquatic environment? Environ. Int. 32, 967–976. https://doi.org/10.1016/j.envint.2006.06.014

Morgeneyer, M., Aguerre-Chariol, O., Bressot, C., 2018. STEM imaging to characterize nanoparticle emissions and help to design nanosafer paints. Chem. Eng. Res. Des. 136, 663–674. https://doi.org/10.1016/J.CHERD.2018.06.013

Mudunkotuwa, I. a, Grassian, V.H., 2011. The devil is in the details (or the surface): impact of surface structure and surface energetics on understanding the behavior of nanomaterials in the environment. J. Environ. Monit. 13, 1135–1144. https://doi.org/10.1039/c1em00002k

Mueller, N., Nowack, B., 2008. Exposure modeling of engineered nanoparticles in the environment. Environ. Sci. Technol. 41, 4447–4453. https://doi.org/10.1021/es7029637

Narong, P., James, a. E., 2006. Effect of pH on the ??-potential and turbidity of yeast suspensions. Colloids Surfaces A Physicochem. Eng. Asp. 274, 130–137. https://doi.org/10.1016/j.colsurfa.2005.08.042

Navarro, E., Piccapietra, F., Wagner, B., Marconi, F., Kaegi, R., Odzak, N., Sigg, L., Behra, R., 2008. Toxicity of silver nanoparticles to Chlamydomonas reinhardtii. Environ. Sci. Technol. 42, 8959–8964.

Neal, C., Jarvie, H., Rowland, P., Lawler, A., Sleep, D., Scholefield, P., 2011. Titanium in UK rural, agricultural and urban/industrial rivers: Geogenic and anthropogenic colloidal/sub-colloidal sources and the significance of within-river retention. Sci. Total Environ. 409, 1843–1853. https://doi.org/10.1016/J.SCITOTENV.2010.12.021

Nel, A.E., Mädler, L., Velegol, D., Xia, T., Hoek, E.M.V., Somasundaran, P., Klaessig, F., Castranova, V., Thompson, M., 2009. Understanding biophysicochemical interactions at the nano-bio interface. Nat. Mater. 8, 543–557. https://doi.org/10.1038/nmat2442

Ng, H.Y., Elimelech, M., 2004. Influence of colloidal fouling on rejection of trace organic contaminants by reverse osmosis. J. Memb. Sci. 244, 215–226. https://doi.org/10.1016/J.MEMSCI.2004.06.054

Nowack, B., 2017. Evaluation of environmental exposure models for engineered nanomaterials in a regulatory context. NanoImpact 8, 38–47. https://doi.org/10.1016/J.IMPACT.2017.06.005

Nowack, B., Boldrin, A., Caballero, A., Hansen, S.F., Gottschalk, F., Heggelund, L., Hennig, M., Mackevica, A., Maes, H., Navratilova, J., Neubauer, N., Peters, R., Rose, J., Schäffer, A., Scifo, L., Stefan Van, L., Von Der Kammer, F., Wohlleben, W., Wyrwoll, A., Hristozov, D., 2016. Meeting the Needs for Released Nanomaterials Required for Further

Testing - The SUN Approach. Environ. Sci. Technol. 50, 2747–2753. https://doi.org/10.1021/acs.est.5b04472

Nowack, B., Bornhöft, N., Ding, Y., Riediker, M., Jiménez, A., Sun, T., van Tongeren, M., Wohlleben, W., 2015. The flows of engineered nanomaterials from production, use and disposal to the environment, in: Viana, M. (Ed.), Indoor and Outdoor Nanoparticles. The Handbook of Environmental Chemistry. Springer, pp. 209–231. https://doi.org/10.1007/698

Nowack, B., Bucheli, T.D., 2007. Occurrence, behavior and effects of nanoparticles in the environment. Environ. Pollut. 150, 5–22. https://doi.org/10.1016/j.envpol.2007.06.006

Nowack, B., Ranville, J.F., Diamond, S., Gallego-Urrea, J.A., Metcalfe, C., Rose, J., Horne, N., Koelmans, A.A., Klaine, S.J., 2012. Potential scenarios for nanomaterial release and subsequent alteration in the environment. Environ. Toxicol. Chem. 31, 50–59. https://doi.org/10.1002/etc.726

O'Brien, N., Cummins, E., 2010. Nano-scale pollutants: Fate in irish surface and drinking water regulatory systems. Hum. Ecol. Risk Assess. 16, 847–872. https://doi.org/10.1080/10807039.2010.501270

Odzak, N., Kistler, D., Sigg, L., 2017. Influence of daylight on the fate of silver and zinc oxide nanoparticles in natural aquatic environments. Environ. Pollut. 226, 1–11. https://doi.org/10.1016/J.ENVPOL.2017.04.006

Oomen, A.G., Steinhäuser, K.G., Bleeker, E.A.J., van Broekhuizen, F., Sips, A., Dekkers, S., Wijnhoven, S.W.P., Sayre, P.G., 2018. Risk assessment frameworks for nanomaterials: Scope, link to regulations, applicability, and outline for future directions in view of needed increase in efficiency. NanoImpact 9, 1–13. https://doi.org/10.1016/j.impact.2017.09.001

Ottofuelling, S., Von Der Kammer, F., Hofmann, T., 2011. Commercial titanium dioxide nanoparticles in both natural and synthetic water: Comprehensive multidimensional testing and prediction of aggregation behavior. Environ. Sci. Technol. 45, 10045–10052. https://doi.org/10.1021/es2023225

Pang, C., Selck, H., Misra, S.K., Berhanu, D., Dybowska, A., Valsami-Jones, E., Forbes, V.E., 2012. Effects of sediment-associated copper to the deposit-feeding snail, Potamopyrgus antipodarum: a comparison of Cu added in aqueous form or as nano- and micro-CuO particles. Aquat. Toxicol. 106–107, 114–122. https://doi.org/10.1016/j.aquatox.2011.10.005

Park, C.M., Chu, K.H., Her, N., Jang, M., Baalousha, M., Heo, J., Yoon, Y., 2017. Occurrence

and Removal of Engineered Nanoparticles in Drinking Water Treatment and Wastewater Treatment Processes. Sep. Purif. Rev. 46, 255–272. https://doi.org/10.1080/15422119.2016.1260588

Park, E.-J., Bae, E., Yi, J., Kim, Y., Choi, K., Lee, S.H., Yoon, J., Lee, B.C., Park, K., 2010. Repeated-dose toxicity and inflammatory responses in mice by oral administration of silver nanoparticles. Environ. Toxicol. Pharmacol. 30, 162–168. https://doi.org/10.1016/j.etap.2010.05.004

Peeters, J.M.M., Boom, J.P., Mulder, M.H. V, Strathmann, H., 1998. Retention measurements of nano ® ltration membranes with electrolyte solutions 145, 199–209.

Peijnenburg, W.J.G.M., Baalousha, M., Chen, J., Chaudry, Q., Von Der Kammer, F., Kuhlbusch, T. a. J., Lead, J., Nickel, C., Quik, J.T.K., Renker, M., Wang, Z., Koelmans, A. a., 2015. A review of the properties and processes determining the fate of engineered nanomaterials in the aquatic environment. Crit. Rev. Environ. Sci. Technol. 45, 2084–2134. https://doi.org/10.1080/10643389.2015.1010430

Peng, Y.-H., Tsai, Y.-C., Hsiung, C.-E., Lin, Y.-H., Shih, Y., 2017. Influence of water chemistry on the environmental behaviors of commercial ZnO nanoparticles in various water and wastewater samples. J. Hazard. Mater. 322, 348–356. https://doi.org/10.1016/J.JHAZMAT.2016.10.003

Peralta-Videa, J.R., Zhao, L., Lopez-Moreno, M.L., de la Rosa, G., Hong, J., Gardea-Torresdey, J.L., 2011. Nanomaterials and the environment: a review for the biennium 2008-2010. J. Hazard. Mater. 186, 1–15. https://doi.org/10.1016/j.jhazmat.2010.11.020

Peters, R.J.B., van Bemmel, G., Milani, N.B.L., den Hertog, G.C.T., Undas, A.K., van der Lee, M., Bouwmeester, H., 2018. Detection of nanoparticles in Dutch surface waters. Sci. Total Environ. 621, 210–218. https://doi.org/10.1016/J.SCITOTENV.2017.11.238

Phenrat, T., Saleh, N., Sirk, K., Tilton, R.D., Lowry, G. V., 2007. Aggregation and sedimentation of aqueous nanoscale zerovalent iron dispersions. Environ. Sci. Technol. 41, 284–290. https://doi.org/10.1021/es061349a

Piccinno, F., Gottschalk, F., Seeger, S., Nowack, B., 2012. Industrial production quantities and uses of ten engineered nanomaterials in Europe and the world. J. Nanoparticle Res. 14, 1109–1120. https://doi.org/10.1007/s11051-012-1109-9

Pietroiusti, A., Stockmann-Juvala, H., Lucaroni, F., Savolainen, K., 2018. Nanomaterial exposure, toxicity, and impact on human health. Wiley Interdiscip. Rev. Nanomedicine Nanobiotechnology 10, 1–21. https://doi.org/10.1002/wnan.1513

Pike, J., Chan, S.W., Zhang, F., Wang, X., Hanson, J., 2006. Formation of stable Cu2O from reduction of CuO nanoparticles. Appl. Catal. A Gen. 303, 273–277. https://doi.org/10.1016/j.apcata.2006.02.008

Pinotti, A., Zaritzky, N., 2001. Effect of aluminum sulfate and cationic polyelectrolytes on the destabilization of emulsified wastes. Waste Manag. 21, 535–542. https://doi.org/10.1016/S0956-053X(00)00110-0

Piplai, T., Kumar, A., Alappat, B.J., 2017. Removal of mixture of ZnO and CuO nanoparticles (NPs) from water using activated carbon in batch kinetic studies. Water Sci. Technol. 75, 928–943. https://doi.org/10.2166/wst.2016.521

Plakas, K. V., Karabelas, A.J., 2009. Triazine retention by nanofiltration in the presence of organic matter: The role of humic substance characteristics. J. Memb. Sci. 336, 86–100. https://doi.org/10.1016/j.memsci.2009.03.020

Popowich, A., Zhang, Q., Le, X.C., 2015. Removal of nanoparticles by coagulation. J. Environ. Sci. (China) 38, 168–171. https://doi.org/10.1016/j.jes.2015.10.001

Portuguese Government, 2007. Decree-Law n.306/2007 Water Quality for Human Consumption.

Prajitha, N., Athira, S.S., Mohanan, P.V., 2019. Bio-interactions and risks of engineered nanoparticles. Environ. Res. 172, 98–108. https://doi.org/10.1016/J.ENVRES.2019.02.003

Quik, J.T.K., Stuart, M.C., Wouterse, M., Peijnenburg, W., Hendriks, A.J., van de Meent, D., 2012. Natural colloids are the dominant factor in the sedimentation of nanoparticles. Environ. Toxicol. Chem. 31, 1019–1022. https://doi.org/10.1002/etc.1783

Rasouli, Y., Abbasi, M., Hashemifard, S.A., 2017. Investigation of in-line coagulation-MF hybrid process for oily wastewater treatment by using novel ceramic membranes. J. Clean. Prod. 161, 545–559. https://doi.org/10.1016/J.JCLEPRO.2017.05.134

Ribau Teixeira, M., Sousa, V., Rosa, M.J., 2010. Investigating dissolved air flotation performance with cyanobacterial cells and filaments. Water Res. 44, 3337–3344. https://doi.org/10.1016/j.watres.2010.03.012

Ricardo Energy & Environment, Milieu Consulting, Danish Technical University, 2016. Support for 3rd regulatory review on nanomaterials -environmental legislation, Project Report, Publications Office of the European Union. Luxembourg. https://doi.org/10.2779/49879

Rocha, T.L., Gomes, T., Sousa, V.S., Mestre, N.C., Bebianno, M.J., 2015. Ecotoxicological

impact of engineered nanomaterials in bivalve molluscs: An overview. Mar. Environ. Res. 111, 74–88. https://doi.org/10.1016/j.marenvres.2015.06.013

Romanello, M.B., Fidalgo de Cortalezzi, M.M., 2013. An experimental study on the aggregation of TiO2 nanoparticles under environmentally relevant conditions. Water Res. 47, 3887–3898. https://doi.org/10.1016/j.watres.2012.11.061

Sahu, M., Suttiponparnit, K., Suvachittanont, S., Charinpanitkul, T., Biswas, P., 2011. Characterization of doped TiO2 nanoparticle dispersions. Chem. Eng. Sci. 66, 3482–3490. https://doi.org/10.1016/j.ces.2011.04.003

Sajid, M., Ilyas, M., Basheer, C., Tariq, M., Daud, M., Baig, N., Shehzad, F., 2015. Impact of nanoparticles on human and environment: review of toxicity factors, exposures, control strategies, and future prospects. Environ. Sci. Pollut. Res. 22, 4122–4143. https://doi.org/10.1007/s11356-014-3994-1

Sauvé, S., Desrosiers, M., 2014. A review of what is an emerging contaminant. Chem. Cent. J. 8, 1–7. https://doi.org/10.1186/1752-153X-8-15

Savage, N., Thomas, T. a, Duncan, J.S., 2007. Nanotechnology applications and implications research supported by the US Environmental Protection Agency STAR grants program. J. Environ. Monit. 9, 1046–1054. https://doi.org/10.1039/b704002d

Saveyn, H., De Baets, B., Thas, O., Hole, P., Smith, J., Van der Meeren, P., 2010. Accurate particle size distribution determination by nanoparticle tracking analysis based on 2-D Brownian dynamics simulation. J. Colloid Interface Sci. 352, 593–600. https://doi.org/10.1016/j.jcis.2010.09.006

Sendra, M., Yeste, M.P., Gatica, J.M., Moreno-Garrido, I., Blasco, J., 2017. Homoagglomeration and heteroagglomeration of TiO2, in nanoparticle and bulk form, onto freshwater and marine microalgae. Sci. Total Environ. 592, 403–411. https://doi.org/10.1016/J.SCITOTENV.2017.03.127

Serrão Sousa, V., Corniciuc, C., Ribau Teixeira, M., 2017. The effect of TiO2 nanoparticles removal on drinking water quality produced by conventional treatment C/F/S. Water Res. 109, 1–12. https://doi.org/10.1016/J.WATRES.2016.11.030

Serrão Sousa, V., Ribau Teixeira, M., 2015. Silver nanoparticles separation from the water using nanofiltration membranes: The role of mono- divalent salts and NOM. Sep. Purif. Technol. 149, 165–173. https://doi.org/10.1016/J.SEPPUR.2015.05.036

Serrão Sousa, V., Ribau Teixeira, M., 2013. Aggregation kinetics and surface charge of CuO nanoparticles: the influence of pH, ionic strength and humic acids. Environ. Chem. 10,

313–322.

Serrão Sousa, V., Teixeira, M.R., 2015. Silver nanoparticles separation from the water using nanofiltration membranes: The role of mono- divalent salts and NOM. Sep. Purif. Technol. 149, 165–173. https://doi.org/10.1016/j.seppur.2015.05.036

Shandilya, N., Le Bihan, O., Bressot, C., Morgeneyer, M., 2015. Emission of titanium dioxide nanoparticles from building materials to the environment by wear and weather. Environ. Sci. Technol. 49, 2163–2170. https://doi.org/10.1021/es504710p

Shao, S., Liang, H., Qu, F., Yu, H., Li, K., Li, G., 2014. Fluorescent natural organic matter fractions responsible for ultrafiltration membrane fouling: Identification by adsorption pretreatment coupled with parallel factor analysis of excitation–emission matrices. J. Memb. Sci. 464, 33–42. https://doi.org/10.1016/J.MEMSCI.2014.03.071

Sharma, S. (Ed.), 2015. Heavy Metals in Water. Presence, removal and safety. Royal Society of Chemistry, Cambridge.

Sharp, E., Jarvis, P., Parsons, S., Jefferson, B., 2006a. Impact of fractional character on the coagulation of NOM. Colloids Surfaces A Physicochem. Eng. Asp. 286, 104–111. https://doi.org/10.1016/j.colsurfa.2006.03.009

Sharp, E., Parsons, S., Jefferson, B., 2006b. The impact of seasonal variations in DOC arising from a moorland peat catchment on coagulation with iron and aluminium salts. Environ. Pollut. 140, 436–443. https://doi.org/10.1016/j.envpol.2005.08.001

Sharp, E., Parsons, S., Jefferson, B., 2006c. Coagulation of NOM: linking character to treatment. Water Sci. Technol. 53, 67–76.

Shen, X., Gao, B., Guo, K., Yue, Q., 2020. Characterization and influence of floc under different coagulation systems on ultrafiltration membrane fouling. Chemosphere 238, 124659. https://doi.org/10.1016/J.CHEMOSPHERE.2019.124659

Shi, X., Li, Z., Chen, W., Qiang, L., Xia, J., Chen, M., Zhu, L., Alvarez, P.J.J., 2016. Fate of TiO2 nanoparticles entering sewage treatment plants and bioaccumulation in fish in the receiving streams. NanoImpact 3–4, 96–103. https://doi.org/10.1016/j.impact.2016.09.002

Shih, Y.H., Liu, W.S., Su, Y.F., 2012. Aggregation of stabilized TiO 2 nanoparticle suspensions in the presence of inorganic ions. Environ. Toxicol. Chem. 31, 1693–1698. https://doi.org/10.1002/etc.1898

Shon, H.K., Vigneswaran, S., Kim, I.S., Cho, J., Kim, G.J., Kim, J.B., Kim, J.-H., 2007. Preparation of Titanium Dioxide (TiO 2) from Sludge Produced by Titanium

Tetrachloride (TiCl 4) Flocculation of Wastewater. Environ. Sci. Technol. 41, 1372–1377. https://doi.org/10.1021/es062062g

Shvedova, A.A., Pietroiusti, A., Fadeel, B., Kagan, V.E., 2012. Mechanisms of carbon nanotube-induced toxicity: Focus on oxidative stress. Toxicol. Appl. Pharmacol. 261, 121–133. https://doi.org/10.1016/J.TAAP.2012.03.023

Sillanpää, M., Ncibi, M.C., Matilainen, A., Vepsäläinen, M., 2018. Removal of natural organic matter in drinking water treatment by coagulation: A comprehensive review. Chemosphere 190, 54–71. https://doi.org/10.1016/J.CHEMOSPHERE.2017.09.113

Snow, D., Cassada, D., Larsen, M., Mware, N., Li, X., DÁlessio, M., Zhang, Y., Brett Sallach, J., 2017. Detection, occurrence and fate of emerging cntaminants in agricultural environments. Water Environ. Res. 89, 897–920. https://doi.org/10.1002/cncr.27633.Percutaneous

Som, C., Wick, P., Krug, H., Nowack, B., 2011. Environmental and health effects of nanomaterials in nanotextiles and façade coatings. Environ. Int. 37, 1131–1142. https://doi.org/10.1016/J.ENVINT.2011.02.013

Springer, F., Laborie, S., Guigui, C., 2013. Removal of SiO2 nanoparticles from industry wastewaters and subsurface waters by ultrafiltration: Investigation of process efficiency, deposit properties and fouling mechanism. Sep. Purif. Technol. 108, 6–14. https://doi.org/10.1016/J.SEPPUR.2013.01.043

Stetefeld, J., McKenna, S.A., Patel, T.R., 2016. Dynamic light scattering: a practical guide and applications in biomedical sciences. Biophys. Rev. 8, 409–427. https://doi.org/10.1007/s12551-016-0218-6

Sun, H., Jiao, R., Xu, H., An, G., Wang, D., 2019. The influence of particle size and concentration combined with pH on coagulation mechanisms. J. Environ. Sci. (China) 82, 39–46. https://doi.org/10.1016/j.jes.2019.02.021

Sun, Q., Li, Y., Tang, T., Yuan, Z., Yu, C.-P., 2013. Removal of silver nanoparticles by coagulation processes. J. Hazard. Mater. 261, 414–420. https://doi.org/10.1016/j.jhazmat.2013.07.066

Sun, T.Y., Bornhöft, N.A., Hungerbühler, K., Nowack, B., 2016. Dynamic Probabilistic Modeling of Environmental Emissions of Engineered Nanomaterials. Environ. Sci. Technol. 50, 4701–4711. https://doi.org/10.1021/acs.est.5b05828

Sun, T.Y., Gottschalk, F., Hungerbühler, K., Nowack, B., 2014. Comprehensive probabilistic modelling of environmental emissions of engineered nanomaterials. Environ. Pollut. 185,

69–76. https://doi.org/10.1016/j.envpol.2013.10.004

Sun, T.Y., Mitrano, D.M., Bornhöft, N.A., Scheringer, M., Hungerbühler, K., Nowack, B., 2017. Envisioning Nano Release Dynamics in a Changing World: Using Dynamic Probabilistic Modeling to Assess Future Environmental Emissions of Engineered Nanomaterials. Environ. Sci. Technol. 51, 2854–2863. https://doi.org/10.1021/acs.est.6b05702

Suttiponparnit, K., Jiang, J., Sahu, M., Suvachittanont, S., Charinpanitkul, T., Biswas, P., 2010. Role of Surface Area, Primary Particle Size, and Crystal Phase on Titanium Dioxide Nanoparticle Dispersion Properties. Nanoscale Res. Lett. 6, 27–35. https://doi.org/10.1007/s11671-010-9772-1

Syafiuddin, A., Salmiati, S., Hadibarata, T., Kueh, A.B.H., Salim, M.R., Zaini, M.A.A., 2018. Silver Nanoparticles in the Water Environment in Malaysia: Inspection, characterization, removal, modeling, and future perspective. Sci. Rep. 8, 1–15. https://doi.org/10.1038/s41598-018-19375-1

Tang, S.C.N., Lo, I.M.C., 2013. Magnetic nanoparticles: essential factors for sustainable environmental applications. Water Res. 47, 2613–2632. https://doi.org/10.1016/j.watres.2013.02.039

Teixeira, M.R., Rosa, M.J., 2006. Comparing dissolved air flotation and conventional sedimentation to remove cyanobacterial cells of Microcystis aeruginosa. Sep. Purif. Technol. 52, 84–94. https://doi.org/10.1016/j.seppur.2006.03.017

Teodosiu, C., Gilca, A.F., Barjoveanu, G., Fiore, S., 2018. Emerging pollutants removal through advanced drinking water treatment: A review on processes and environmental performances assessment. J. Clean. Prod. 197, 1210–1221. https://doi.org/10.1016/j.jclepro.2018.06.247

Tercero Espinoza, L.A., Frimmel, F.H., 2008. Formation of brominated products in irradiated titanium dioxide suspensions containing bromide and dissolved organic carbon. Water Res. 42, 1778–1784. https://doi.org/10.1016/j.watres.2007.11.002

The Royal Society, Royal Academy of Engineering, 2004. Nanoscience and nanotechnologies: opportunities and uncertainties, Nanoscience and nanotechnologies: opportunities and uncertainties. London. https://doi.org/10.1007/s00234-004-1255-6

Tian, J., Ernst, M., Cui, F., Jekel, M., 2013. Effect of particle size and concentration on the synergistic UF membrane fouling by particles and NOM fractions. J. Memb. Sci. 446, 1–9. https://doi.org/10.1016/J.MEMSCI.2013.06.016

Tiede, K., Hanssen, S.F., Westerhoff, P., Fern, G.J., Hankin, S.M., Aitken, R.J., Chaudhry, Q., Boxall, A.B.A., 2015. How important is drinking water exposure for the risks of engineered nanoparticles to consumers? Nanotoxicology 10, 102–110. https://doi.org/10.3109/17435390.2015.1022888

Tolaymat, T.M., El Badawy, A.M., Genaidy, A., Scheckel, K.G., Luxton, T.P., Suidan, M., 2010. An evidence-based environmental perspective of manufactured silver nanoparticle in syntheses and applications: A systematic review and critical appraisal of peer-reviewed scientific papers. Sci. Total Environ. 408, 999–1006. https://doi.org/10.1016/J.SCITOTENV.2009.11.003

Tomaszewska, M., Mozia, S., Morawski, A.W., 2004. Removal of organic matter by coagulation enhanced with adsorption on PAC. Desalination 161, 79–87. https://doi.org/10.1016/S0011-9164(04)90042-2

Toncelli, C., Mylona, K., Kalantzi, I., Tsiola, A., Pitta, P., Tsapakis, M., Pergantis, S.A., 2017. Silver nanoparticles in seawater: A dynamic mass balance at part per trillion silver concentrations. Sci. Total Environ. 601–602, 15–21. https://doi.org/10.1016/J.SCITOTENV.2017.05.148

Tosco, T., Sethi, R., 2018. Human health risk assessment for nanoparticle-contaminated aquifer systems. Environ. Pollut. 239, 242–252. https://doi.org/10.1016/j.envpol.2018.03.041

Troester, M., Brauch, H.J., Hofmann, T., 2016. Vulnerability of drinking water supplies to engineered nanoparticles. Water Res. 96, 255–279. https://doi.org/10.1016/j.watres.2016.03.038

Trouiller, B., Reliene, R., Westbrook, A., Solaimani, P., Schiestl, R.H., 2009. Titanium dioxide nanoparticles induce DNA damage and genetic instability in vivo in mice. Cancer Res. 69, 8784–8789. https://doi.org/10.1158/0008-5472.CAN-09-2496

Tsiola, A., Pitta, P., Callol, A.J., Kagiorgi, M., Kalantzi, I., Mylona, K., Santi, I., Toncelli, C., Pergantis, S., Tsapakis, M., 2017. The impact of silver nanoparticles on marine plankton dynamics: Dependence on coating, size and concentration. Sci. Total Environ. 601–602, 1838–1848. https://doi.org/10.1016/J.SCITOTENV.2017.06.042

Tuoriniemi, J., Cornelis, G., Hassellöv, M., 2012. Size discrimination and detection capabilities of single-particle ICPMS for environmental analysis of silver nanoparticles. Anal. Chem. 84, 3965–3972. https://doi.org/10.1021/ac203005r

US EPA, 2017a. Secondary Drinking Water Standards: Guidance for Nuisance Chemicals [WWW Document]. US Environ. Prot. Agency. URL

https://www.epa.gov/dwstandardsregulations/secondary-drinking-water-standards-guidance-nuisance-chemicals#table-of-secondary

US EPA, 2017b. Drinking Water Treatability Database [WWW Document]. US Environ. Prot. Agency. URL https://iaspub.epa.gov/tdb/pages/treatment/treatmentOverview.do?treatmentProcessId=2109700949

Vahter, M., Berglund, M., Åkesson, A., Lidén, C., 2002. Metals and Women's Health. Environ. Res. Sect. A 88, 145–155. https://doi.org/10.1006/ENRS.2002.4338

Van Koetsem, F., Geremew, T.T., Wallaert, E., Verbeken, K., Van der Meeren, P., Du Laing, G., 2015. Fate of engineered nanomaterials in surface water: Factors affecting interactions of Ag and CeO2 nanoparticles with (re)suspended sediments. Ecol. Eng. 80, 140–150. https://doi.org/10.1016/j.ecoleng.2014.07.024

Varenne, F., Botton, J., Merlet, C., Vachon, J.-J., Geiger, S., Infante, I.C., Chehimi, M.M., Vauthier, C., 2015. Standardization and validation of a protocol of zeta potential measurements by electrophoretic light scattering for nanomaterial characterization. Colloids Surfaces A Physicochem. Eng. Asp. 486, 218–231. https://doi.org/10.1016/J.COLSURFA.2015.08.044

Verliefde, a. R.D., Cornelissen, E.R., Heijman, S.G.J., Verberk, J.Q.J.C., Amy, G.L., Van der Bruggen, B., van Dijk, J.C., 2008. The role of electrostatic interactions on the rejection of organic solutes in aqueous solutions with nanofiltration. J. Memb. Sci. 322, 52–66. https://doi.org/10.1016/j.memsci.2008.05.022

Von Der Kammer, F., Ottofuelling, S., Hofmann, T., 2010. Assessment of the physico-chemical behavior of titanium dioxide nanoparticles in aquatic environments using multi-dimensional parameter testing. Environ. Pollut. 158, 3472–3481. https://doi.org/10.1016/j.envpol.2010.05.007

Wang, H., Dong, Y. nan, Zhu, M., Li, X., Keller, A.A., Wang, T., Li, F., 2015. Heteroaggregation of engineered nanoparticles and kaolin clays in aqueous environments. Water Res. 80, 130–138. https://doi.org/10.1016/j.watres.2015.05.023

Wang, H.T., Ye, Y.Y., Qi, J., Li, F.T., Tang, Y.L., 2013. Removal of titanium dioxide nanoparticles by coagulation: effects of coagulants , typical ions , alkalinity and natural organic matters. Water Sci. Technol. 68, 1137–1143. https://doi.org/10.2166/wst.2013.356

Wang, Y., Xue, N., Chu, Y., Sun, Y., Yan, H., Han, Q., 2015. CuO nanoparticle–humic acid

(CuONP–HA) composite contaminant removal by coagulation/ultrafiltration process: The application of sodium alginate as coagulant aid. Desalination 367, 265–271. https://doi.org/10.1016/j.desal.2015.04.018

Wasmuth, C., Rüdel, H., Düring, R.-A., Klawonn, T., 2016. Assessing the suitability of the OECD 29 guidance document to investigate the transformation and dissolution of silver nanoparticles in aqueous media. Chemosphere 144, 2018–2023. https://doi.org/10.1016/J.CHEMOSPHERE.2015.10.101

Weinberg, H., Galyean, A., Leopold, M., 2011. Evaluating engineered nanoparticles in natural waters. TrAC - Trends Anal. Chem. 30, 72–83. https://doi.org/10.1016/j.trac.2010.09.006

Weir, A., Westerhoff, P., Fabricius, L., Hristovski, K., Von Goetz, N., 2012. Titanium dioxide nanoparticles in food and personal care products. Environ. Sci. Technol. 46, 2242–2250. https://doi.org/10.1021/es204168d

Weishaar, J.L., Aiken, G.R., Bergamaschi, B.A., Fram, M.S., Fujii, R., Mopper, K., 2003. Evaluation of specific ultraviolet absorbance as an indicator of the chemical composition and reactivity of dissolved organic carbon. Environ. Sci. Technol. 37, 4702–4708. https://doi.org/10.1021/es030360x

Westerhoff, P., Atkinson, A., Fortner, J., Wong, M.S., Zimmerman, J., Gardea-Torresdey, J., Ranville, J., Herckes, P., 2018. Low risk posed by engineered and incidental nanoparticles in drinking water. Nat. Nanotechnol. 13, 661–669. https://doi.org/10.1038/s41565-018-0217-9

Westerhoff, P., Song, G., Hristovski, K., Kiser, M.A., 2011. Occurrence and removal of titanium at full scale wastewater treatment plants: implications for TiO2 nanomaterials. J. Environ. Monit. 13, 1195–1203. https://doi.org/10.1039/c1em10017c

Wiesner, M., Lowry, G. V, Jones, K., Hochella, M., Di Giulio, R., Casman, E., Bernhardt, E., 2009. Decreasing uncertainties in assessing environmental exposure, risk, and ecological implications of nanomaterials. Environ. Sci. Technol. 43, 6453–6457. https://doi.org/10.1021/es8034544

Williams, R.J., Harrison, S., Keller, V., Kuenen, J., Lofts, S., Praetorius, A., Svendsen, C., Vermeulen, L.C., van Wijnen, J., 2019. Models for assessing engineered nanomaterial fate and behaviour in the aquatic environment. Curr. Opin. Environ. Sustain. 36, 105–115. https://doi.org/10.1016/j.cosust.2018.11.002

Windler, L., Height, M., Nowack, B., 2013. Comparative evaluation of antimicrobials for textile applications. Environ. Int. 53, 62–73.

https://doi.org/10.1016/J.ENVINT.2012.12.010

Wodka, D., Bielaníska, E., Socha, R.P., Elzbieciak-Wodka, M., Gurgul, J., Nowak, P., Warszyníski, P., Kumakiri, I., 2010. Photocatalytic activity of titanium dioxide modified by silver nanoparticles. ACS Appl. Mater. Interfaces 2, 1945–1953. https://doi.org/10.1021/am1002684

Woodrow Wilson International Center, 2005. Nanotechnology Consumer Product Inventory (CPI) [WWW Document]. URL http://www.nanotechproject.org/cpi/ (accessed 6.19.19).

World Health Organization, 2017. WATER QUALITY AND HEALTH - REVIEW OF TURBIDITY: Information for regulators and water suppliers, Who/Fwc/Wsh/17.01.

Wu, N., Wyart, Y., Siozade, L., Georges, G., Moulin, P., 2014. Characterization of ultrafiltration membranes fouled by quantum dots by confocal laser scanning microscopy. J. Memb. Sci. 470, 40–51. https://doi.org/10.1016/J.MEMSCI.2014.07.001

Xiao, Y., Vijver, M.G., Peijnenburg, W.J.G.M., 2018. Impact of water chemistry on the behavior and fate of copper nanoparticles. Environ. Pollut. 234, 684–691. https://doi.org/10.1016/J.ENVPOL.2017.12.015

Yang, X., Wang, Q., Qu, X., Jiang, W., 2017. Bound and unbound humic acids perform different roles in the aggregation and deposition of multi-walled carbon nanotubes. Sci. Total Environ. 586, 738–745. https://doi.org/10.1016/J.SCITOTENV.2017.02.050

Yang, Y., Quensen, J., Mathieu, J., Wang, Q., Wang, J., Li, M., Tiedje, J.M., Alvarez, P.J.J., 2014. Pyrosequencing reveals higher impact of silver nanoparticles than Ag+ on the microbial community structure of activated sludge. Water Res. 48, 317–325. https://doi.org/10.1016/J.WATRES.2013.09.046

Yang, Y., Westerhoff, P., 2014. Presence in, and Release of, Nanomaterials from Consumer Products, in: Capco, D., Chen, Y. (Eds.), Nanomaterial - Impacts on Cell Biology and Medicine. Springer, pp. 1–16. https://doi.org/10.1007/978-94-017-8739-0

Yu, C., Gao, B., Wang, W., Xu, X., Yue, Q., 2019. Alleviating membrane fouling of modified polysulfone membrane via coagulation pretreatment/ultrafiltration hybrid process. Chemosphere 235, 58–69. https://doi.org/10.1016/j.chemosphere.2019.06.146

Yu, K.-N., Yoon, T.-J., Minai-Tehrani, A., Kim, J.-E., Park, S.J., Jeong, M.S., Ha, S.-W., Lee, J.-K., Kim, J.S., Cho, M.-H., 2013. Zinc oxide nanoparticle induced autophagic cell death and mitochondrial damage via reactive oxygen species generation. Toxicol. In Vitro 27, 1187–1195. https://doi.org/10.1016/j.tiv.2013.02.010

Yu, S., Liu, J., Yin, Y., Shen, M., 2018. Interactions between engineered nanoparticles and

dissolved organic matter: A review on mechanisms and environmental effects. J. Environ. Sci. (China) 63, 198–217. https://doi.org/10.1016/j.jes.2017.06.021

Zhang, C., Hu, Z., Deng, B., 2016. Silver nanoparticles in aquatic environments: Physiochemical behavior and antimicrobial mechanisms. Water Res. 88, 403–427. https://doi.org/10.1016/J.WATRES.2015.10.025

Zhang, L., Mao, J., Zhao, Q., He, S., Ma, J., 2015. Effect of AlCl3 concentration on nanoparticle removal by coagulation. J. Environ. Sci. 38, 103–109. https://doi.org/10.1016/j.jes.2015.04.014

Zhang, Y., Chen, Y., Westerhoff, P., Crittenden, J., 2009. Impact of natural organic matter and divalent cations on the stability of aqueous nanoparticles. Water Res. 43, 4249–4257. https://doi.org/10.1016/j.watres.2009.06.005

Zhang, Y., Chen, Y., Westerhoff, P., Hristovski, K., Crittenden, J.C., 2008. Stability of commercial metal oxide nanoparticles in water. Water Res. 42, 2204–2212. https://doi.org/10.1016/j.watres.2007.11.036

Zhao, Y.X., Gao, B.Y., Zhang, G.Z., Phuntsho, S., Shon, H.K., 2014. Coagulation by titanium tetrachloride for fulvic acid removal: Factors influencing coagulation efficiency and floc characteristics. Desalination 335, 70–77. https://doi.org/10.1016/j.desal.2013.12.016

Zheng, Q., Zhou, M., Deng, W., Chris Le, X., 2015. Is there a silver lining? Aggregation and photo-transformation of silver nanoparticles in environmental waters. J. Environ. Sci. 34, 259–262. https://doi.org/10.1016/j.jes.2015.07.002

Zheng, X., Ernst, M., Jekel, M., 2009. Identification and quantification of major organic foulants in treated domestic wastewater affecting filterability in dead-end ultrafiltration. Water Res. 43, 238–244. https://doi.org/10.1016/J.WATRES.2008.10.011

Zouboulis, A.I., Moussas, P., Tzoupanos, N., 2009. Coagulation-flocculation processes applied in water or wastewater treatment, in: Samuelson, J. (Ed.), Industrial Waste: Environmental Impact, Disposal and Treatment. Nova Science Publishers, Inc., Hauppauge, pp. 289–324.

APPENDICES

APPENDIX A

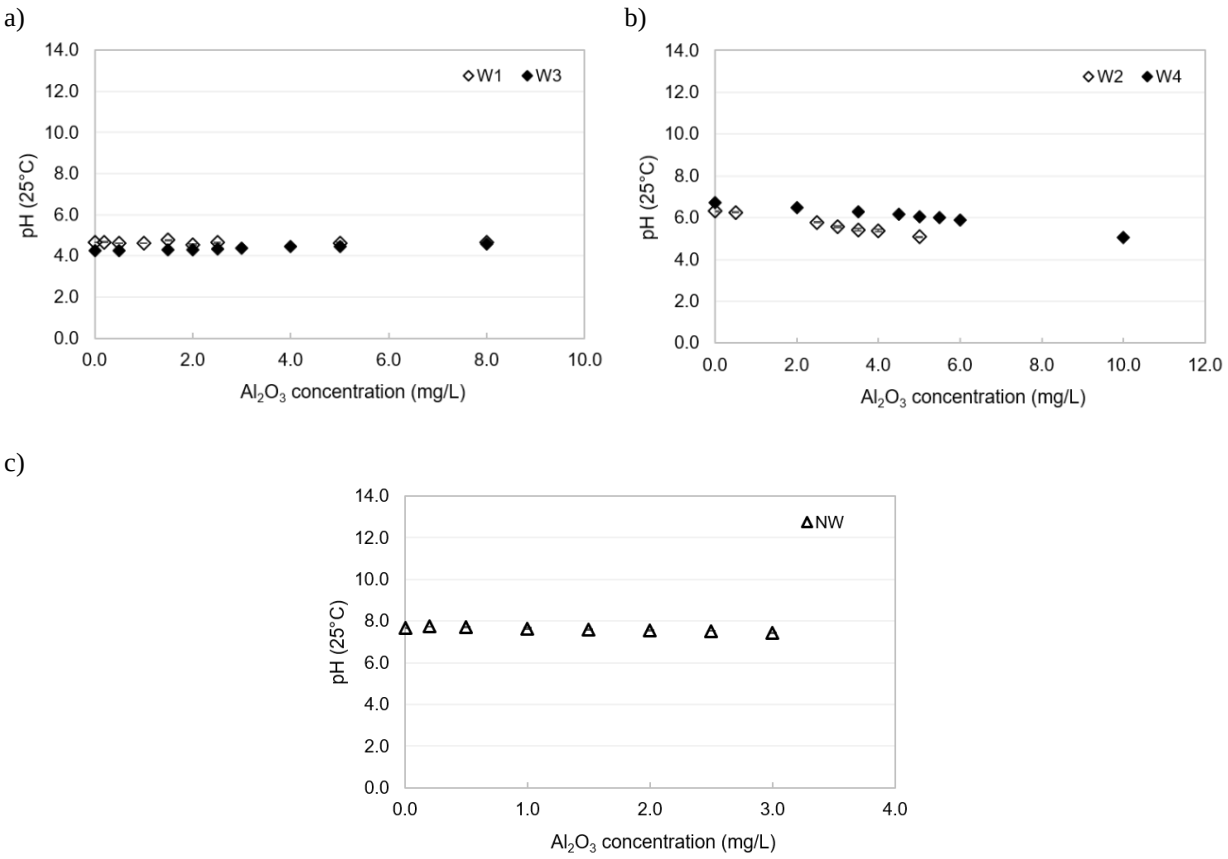

Figure A 1. Variation of water pH with added coagulant for a) hydrophilic, b) hydrophobic and c) natural waters.

APPENDIX B

Figure B 1 shows the FTIR images of virgin PAC as-received. The FTIR spectra described a broad band between 3600 and 3200 1/cm which was indicative of the presence of both free and hydrogen-bonded OH groups on the PAC surface. This stretching was due to of O-H bonds in hydrogen bonded hydroxyl groups of phenols and secondary alcohols. The strong band between 1600 and 1390 1/cm is due to COO- stretching in carboxylate groups, graphite C=C stretching, and methylene C-H and phenol and alcohol O-H bending. The FTIR spectra also indicated transmittance around 1200 and 1100 1/cm showing the stretching of C-O and C-O-C bonds in alcohols, phenols and ethers.

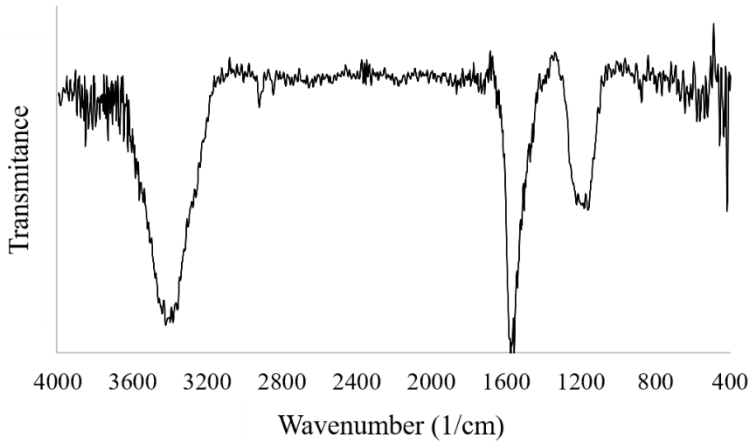

Figure B 1. FTIR images of PAC used in the experiments.

APPENDIX C

The Derjaguin–Landau–Verwey–Overbeek (DLVO) theory was used to estimate the net particle interaction energy. In this theory, the total interaction energy (V) is the sum of van der Waals attractive forces (V_{VDW}) and repulsive electrostatic interactions between particles (V_{EDL}). V_{VDW} and V_{EDL} were determined as already presented in (Serrão Sousa and Ribau Teixeira, 2013). Brieflty, V_{VDW} was calculated using the approximate expression of (Gregory, 1981) Gregory, 1981 and V_{EDL} (in J) was calculated as proposed by French et al. (2009):

$$V = V_{VDW} + V_{EDL} \quad (1)$$

$$V_{VDW} = -\frac{Aa}{6h\,(1+14\,{}^{h}/_{\lambda})} \quad (2)$$

$$V_{EDL} = 2\pi\varepsilon a\zeta^2 \ln\,(1 + e^{-\kappa h}) \quad (3)$$

where A is the Hamaker constant of $2.82\text{x}10^{-20}$ J suggested by (Israelachvili, 1992) for AgNPs in water, a is the particle radius measured by DLS, h is the separation distance, and λ is the dielectric wavelength for water (100 nm, (Shih et al., 2012)), $\varepsilon=\varepsilon_r\varepsilon_0$ is the dielectric constant, where ε_r (78.54) is the dielectric constant of water and ε_0 ($8.85\text{x}10^{-12}$ CV^{-1} m^{-1}) is the permittivity of vacuum, ζ is the zeta potential obtained from the measured electrophoresis mobility, and κ is the inverse Debye length estimated for each ionic strength as suggested by French et al. (2009).

DLVO interaction energy between particles variation with ionic strength and NOM type and concentration are presented in Figure C 1.

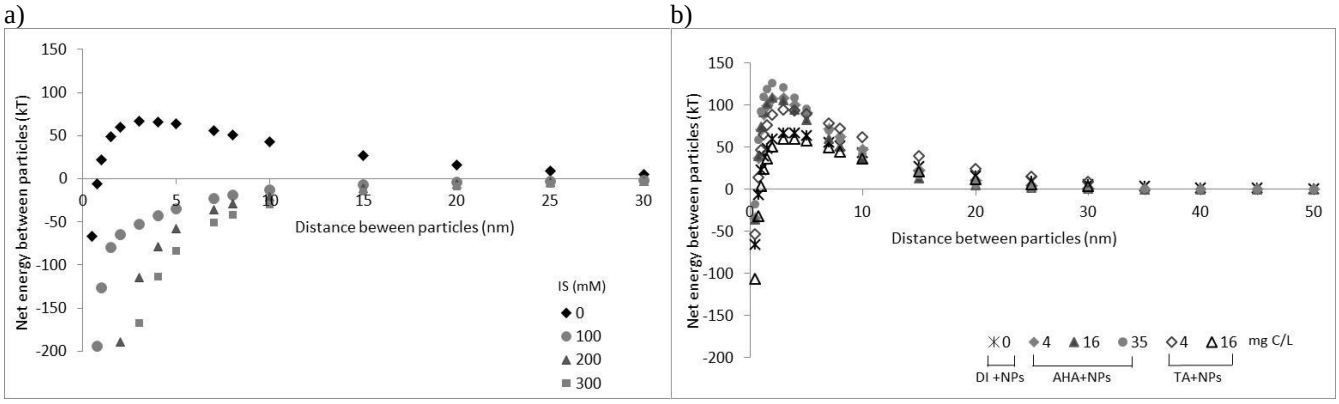

Figure C 1. DLVO interaction energy profiles for suspensions of AgNPs at different: (a) ionic strengths, and (b) NOM type and concentration.